



PhD-FSTM-2021-035
The Faculty of Science, Technology and Medicine

DISSERTATION

Presented on 01/06/2021 in Esch-sur-Alzette

to obtain the degree of

DOCTEUR DE L'UNIVERSITÉ DU LUXEMBOURG

EN BIOLOGIE

by

Mohamad SARMINI

Born on 19 July 1987 in Damascus (Syria)

**FUNCTIONAL ANALYSIS OF LONG NONCODING
RNAs IN GLIOBLASTOMA AND
CHEMORESISTANCE**



Dissertation Supervisor

Prof. Dr. Simone Niclou

Dissertation Defense Committee

Dr. Iris Behrmann, Chairman
University of Luxembourg (Luxembourg)

Dr. Lasse Sinkkonen, vice-chairman
University of Luxembourg (Luxembourg)

Dr. Simone Niclou, dissertation supervisor and jury member
Luxembourg Institute of Health (Luxembourg)

Dr. Sabrina Fritah, jury member
Luxembourg Institute of Health (Luxembourg)

Dr. André Verdel, jury member
Institute for Advanced Biosciences (France)



The work presented in this thesis was conducted at the:

Norlux Neuro-oncology Laboratory
Luxembourg Institute of Health



The work presented in this thesis was supported by:

Télévie – FNRS (Belgium)
Grant Reference:



Doctoral School in Systems and Molecular Biomedecine (DS_SMB)
University of Luxembourg



Fondation du Pélican de Mie et Pierre Hippert-Faber
Under the aegis of the Fondation de Luxembourg



Fondation Cancer



AFFIDAVIT

I Mohamad Sarmini hereby confirm that the PhD Thesis entitled “FUNCTIONAL ANALYSIS OF LONG NONCODING RNAs IN GLIOBLASTOMA AND CHEMORESISTANCE” has been written independently and without any other sources than cited.

Name: MOHAMAD SARMINI

Luxembourg, the 1st June 2021

CONFIDENTIALITY DISCLAIMER

All the information contained in this thesis entitled “FUNCTIONAL ANALYSIS OF LONG NONCODING RNAs IN GLIOBLASTOMA AND CHEMORESISTANCE” is confidential and/or contains privileged information and/or information protected by intellectual property rights. All information exchanged between the parties may not be used, disclosed or revealed as a result of the thesis examination until the thesis become part of the public domain.

ACKNOWLEDGMENTS

The work of this thesis comprises a summary of a lot of hard work and dedication in the last four years. Passion towards finding answers to scientific questions and unknown biological mechanisms was always my motivation to follow the path in molecular biology research and doing a PhD, which has been always an idea to pursue since the early days of my life. With this thesis, I completed another big challenge in my career. However, throughout this journey I came across several people who I would like to thank for their contribution to this work and help in achieving this important step of my life.

First and foremost I am grateful to my co-supervisor Sabrina for her daily help, support, invaluable advices, guidance and patience during my PhD study. I thank you for your confidence in me and our long discussions (as long as lncRNA) on both sides scientifically and personally. Research on lncRNA is challenging, but you were always there to cheer me up and give your valuable feedback on the project. I would like also to thank you for being always pushing me to produce the best science that I could and have the best outcome. I know that this PhD thesis would not be accomplished and have this final shape without your guidance. I wish you all the best for the future projects you do.

I would like also to extend my gratitude to my supervisor Simone for giving me the opportunity to do my PhD in her lab. Thank you for supporting this project and I very much appreciate your advices, feedbacks and the time taken by you for correcting this thesis.

Many thanks to the NorLux team for the time spent together and the good lab environment, I really learnt a lot from all of you. Special warm and big thanks to Monika for her massive help in this project and efforts in correcting the first drafts of this thesis. I would like also to acknowledge your assistance and constructive criticisms, which helped in consolidating our data. I wish that you would be able to make your trip to Uzbekistan so I can get your feedback about this place. Special thanks also go to Maggie for taking part also in reviewing the first drafts of this thesis, feedback on experiments, and overall nice way of being. I wish you all the best for your project and future career. Many thanks also to Anaïs and Virginie for their training and helping me out in doing animal experiments and MRI.

Doing my PhD was much easier with the help and support of several people in the administration departments. Special thanks to Siu-Thinh in LIH for her professional organization to our lab meetings and the swift actions in placing lab orders. I would like also to acknowledge the role of Malou -PhD Training Coordinator in LIH- for answering any doubts and concerns related to our PhD in LIH, organizing our annual PhD retreats, courses and training sessions that helped a lot in the progression of our PhD.

I would like to extend my thanks also to the people outside the Norlux team with whom I worked together in LIH. Eric, thanks for your valuable feedbacks, discussions, and providing us the tools we needed for this project. Thank you Bassam for being as a big brother to me. Victoria as well, very warm thanks to your friendly attitude with me and the nice conversations we had. Not to forget, the people who left Norlux to join other groups in- or outside LIH. Special thanks to Vanessa for her help in this project. Leaving NorLux team was sad for us because you are such a friendly person with a nice spirit. *ça va !!?* Was my only way to begin a very long and funny conversation with you (but sure in English). Huge thanks to Matthieu-former PhD student in LIH, it was a great pleasure to meet you and have this friendship with you. I really appreciate your tips on how to aim and shoot one drop from 2 meters height on the middle of a slide to get a nice chromosome spread. Many thanks for the scientific discussions and sharing together nice moments here in Luxembourg, nature exploration ideas, climbing training, and car oil replacement (although the car didn't last till the end of my PhD, I managed 45,000 Km around Europe). I was also glad to meet Sara and be part of the torture you got in your COVID19-special Bachelor party, I hope for you and Sara beautiful and lovely days and all the best for your future life.

To my colleagues at the office: Carina, Yolanda, Yahaya, Lara, and Hugo. Big thanks to you for being such wonderful colleagues and friends; it was really a pleasure to know you. Thanks for being there for a chat, cup of tea, scientific discussions, and support throughout these four years. Carina, don't give up on what you do and I am sure one day you will find the way to get a nice story as you find your way to scare the s**t out of me. Yolanda, keep the persistence and motivation, you are almost there as well (N.B: talking to me is not as difficult as you think, it is just you have to know how to break into it). Yahaya, you are such a wonderful and peaceful person and I really respect your efforts in managing both the PhD and family life. Lara, it was a real surprise to know recently that you are studying Chinese (再見), and keep always in mind that "shu maa'lem" can be used for anything. Not to forget to mention also to thank all the other PhDs in LIH, who contributed to a nice and fresh environment in the lab. Andrés, you are among the first people who I got to know in the lab. It was really nice to meet you and share with you the accommodation in Glesener (Do you remember the maximum level we reached in killing the Zombies!!? Was as hard as doing a PhD). Lia, our next MMA champion, you gotta the challenger spirit and I wish for you the best of luck together with Matthew (I hope I can make it in November). Ernesto, eeeh vabbe, thanks for the time spent together, I am gonna really miss the supply of Porcini and our conversations (we should though plan an expedition maybe to Greenland). Special thanks to Mohaned, I am really happy to have a friend like you in my life. I appreciate all your help, support, nice advice, and listening to me during the critical stages of my PhD. It was really nice to have a person who I can finally use my mother tongue

with (but please use proper Arabic because “keef” means “HOW not NOW” and you can’t use “whale” to refer simply to a “FISH”). In addition, you have to admit that I am better than you in “CRASH”, I have better driving skills, but you were winning just because you are lucky with trophies. You are a hard worker and wish you all the good luck for the rest of your PhD.

The work of this thesis will not be done without the generous help from the funding bodies. Special thanks to Télévie-FNRS for funding this project. Also thanks to the University of Luxembourg and Pelican Foundation for their awards, which helped me to travel abroad and meet scientists from the field to develop my knowledge, expertise, and complete my PhD study. I am also grateful to our collaborators for providing us the help, expertise, and experiments needed. In particular, Dr. Ross Carruthers from the University of Glasgow for his great work on DNA fiber assay and supplying us with results during the pandemic. Dr. Alena Shkumatava from Institute Curie for providing us the protocol and reagents to identify the lncRNA-protein partners. Dr. Yong-Jun Kwon from the Early Drug Discovery Platform in LIH for providing us the automated microplate washer and dispenser. I would like also to acknowledge Dr. Coralie Guerin- former head of National Cytometry Platform in LIH for her efforts in helping us setting up the high-throughput immuno-FISH by imaging flow cytometry technique.

I would like to express my deepest appreciation to my PhD thesis Jury and committee members for taking the time reading my thesis. In particular, special thanks to Dr. Lasse Sinkkonen for being present in each yearly PhD meeting and provided valuable comments, suggestions, and feedback which helped a lot in developing the work and quality of this project.

Very warm and massive thanks to all my old and long-life friends from outside the work environment, who were always present when I needed them and provided support from different places in the world. Beshar and Mazhar in Germany, Ahmad in Austria, Obaida in USA, and Mamdouh in Turkey. I love you boys and I know that I can count on you. We all passed through terrifying moments and life-threatening conditions. However, when I look now at each single one of you, I feel so proud of what you have all done and achieved so far after a lot of sacrifices. I wish we could meet like the old times, laugh, and stay till late night chatting.

I am deeply indebted to my Mom, Dad, and Sisters for all their love and encouragements. I know I always have my family to count on when times are rough, and I sincerely thank them for accepting my decision to pursue my career in research abroad, which so far costed us 7 years of separation. My hard-working parents have sacrificed their lives for my sisters and myself and provided unconditional love and care. I love you so much, and I would not have made this far without you. My Mom is the greatest person I have ever met; she sacrificed her life to bring the happiness and success for my sisters and myself in each stage of our lives. I

hope to be able to give her a little thing from what she made for me, even I know I could spend my whole life and it would not be enough to reward her. Thanks to my Dad, who treated me not only as a son but also as a friend. I have been his companion since the early days of my life, which I can now understand his way for raising me up in real life situations, know-how to deal with predicaments, and be honest no matter how much troubles I have. I am sorry if I complained for not getting what I asked for, but I really appreciate now that you wanted to produce a real and tough man able to depend on himself. I hope that I made you and my Mom proud. My sisters have been my best friends all my life and I love them dearly and thank them for all their advices and support from far away distance. Reem and Rasha you also sacrificed a lot and I know that life for you is so hard, I'm extremely grateful to your support and smiles from behind the camera, which they gave me enough charge to go on as I know nothing can be compared to what you are experiencing.

There is no way to finish without mentioning my deepest gratitude to my girlfriend, soulmate, and life-companion Giulia. Giulia was the first and still my true and great supporter. Thanks for being present in my life, listening, and motivating me during the hard times. I know that we took a huge decision to do our PhDs in different countries and I thank you dearly for your understanding and patience. Being separated for 4 years was not an easy ride for both of us, but it was another challenge and we managed not only to do our PhDs, but also to do what we like in travelling into 10 different countries and exploring more than 150 places. Yes, we made it, and I am really proud of your success and what you have achieved. I am sorry for pushing you to climb with me till the summit of each mountain or sail in small inflatable kayak to an isolated island. But, because I know that reaching our final goals together has an awesome feeling and I know how much you are competitive and you can do a lot (No worries, we will not die one day as you say). Giulia, we still have a lot to do and accomplish and I am sure that hand-by-hand we can reach one day what we planned together.

I am also deeply indebted to Giulia's family for being my second family here in Europe and I am really thankful to their kindness, support, and unconditional love. Giulia's Mom and Dad treated me as a son, and her brothers Simone and Marco as a brother. They let me feel when I am with them home, where I was away from home. There is no way to express how much I love you and I thank you so much for what you did to me.

I finally thank life hardships, frustrations, failures, rejections, sleepless nights, and who did not believe in my capacity. Because, they were all the fuel that kept me always pushing to go harder on myself to achieve my dreams.

TABLE OF CONTENTS

LIST OF ABBREVIATIONS.....	iv
LIST OF FIGURES	vi
LIST OF TABLES	vii
SUMMARY	viii

CHAPTER 1

INTRODUCTION.....	1
1. The noncoding genome.....	2
1.1. The revolution of noncoding RNAs	2
1.2. Regulatory RNAs and pervasive transcription	2
2. Long noncoding RNAs (lncRNAs).....	3
2.1. Definitions and biotypes of lncRNA	4
2.2. LncRNAs molecular features and biogenesis	4
2.2.1. Circular RNAs: unique products of RNA processing	5
2.3. Molecular functions of lncRNAs.....	7
2.3.1. Nuclear functions.....	7
<i>I. Recruitment of chromatin modifying and remodeling complexes.....</i>	<i>8</i>
<i>II. Interactions with transcription factors (TFs) and R-loop formation.....</i>	<i>9</i>
<i>III. Role in local modulation of chromatin state and gene silencing</i>	<i>10</i>
<i>IV. Role in facilitating chromosomal and enhancer-promoter interactions....</i>	<i>11</i>
<i>V. LncRNAs in nuclear bodies formation and function.....</i>	<i>11</i>
2.3.2. Cytoplasmic functions.....	12
<i>I. Regulation of mRNA stability</i>	<i>12</i>
<i>II. Regulation of mRNA translation.....</i>	<i>13</i>
<i>III. Regulation of post-translational modification.....</i>	<i>13</i>
2.4. LncRNA role in biological processes	13
2.4.1. Overview of the cell cycle	13
2.4.2. DNA synthesis and mitosis.....	15
2.4.3. LncRNAs in the regulation of the cell cycle and DNA damage response	17
2.5. LncRNA in cancer and chemo-resistance.....	20
3. Malignant brain tumors	23
3.1. General overview	23

3.2. IDH-mutant gliomas.....	25
3.3. IDH-wild type gliomas.....	26
3.3.1. Glioblastoma (GBM).....	27
<i>I. Genetic alterations</i>	27
<i>II. Clinical management</i>	29
3.4. Mechanisms of resistance to chemotherapy.....	29
3.4.1. Temozolomide pharmacology and mechanism of action	30
3.4.2. The DDR and the major TMZ-induced lesions repair pathways	30
<i>I. Temozolomide-direct repair (DR) by MGMT</i>	33
<i>II. Temozolomide-indirect DNA repair by mismatch repair (MMR)</i>	34
3.4.3. LncRNA in GBM and the regulation of GBM resistance to chemotherapy... 35	
CHAPTER 2	
SCOPE AND AIM OF THE THESIS.....	38
CHAPTER 3	
MATERIALS AND METHODS.....	40
Key resources table.....	41
Experimental models and subject details.....	46
CHAPTER 4	
RESULTS.....	61
RATIONALE.....	62
Temozolomide-Induced RNA Interactome Uncovers Novel LncRNA Regulatory Loops in Glioblastoma.....	63
EXTENDED DATA.....	87
CHAPTER 5	
RESULTS.....	89
RATIONALE.....	90
RADAR, a novel long noncoding RNA, regulates S-Phase DNA Damage, DNA Replication and Impairs Chromosome Segregation in Glioblastoma	92
EXTENDED DATA.....	123

CHAPTER 6	
DISCUSSION.....	136
CONCLUSIONS.....	151
CHAPTER 7	
REFERENCES	152
CHAPTER 8	
APPENDICES.....	174

LIST OF ABBREVIATIONS

A

α -KG α -ketoglutarate

A Adenine

ASOs Antisense oligonucleotides

B

BBB Blood brain barrier

BER Base excision repair

C

C Cytosine

CDK Cyclin-dependent kinases

ceRNAs Competitive endogenous RNAs

CGGA Chinese Glioma Genome Atlas

Chk Checkpoint

circRNA Circular RNA

CNS Central nervous system

D

3D Three-dimensional

DDR DNA damage response

dilncRNAs Damage-induced lncRNAs

DR direct damage repair

DSB Double strand break

E

ENCODE Encyclopedia of DNA elements

eRNA Enhancer RNA

ecDNA Extrachromosomal circular DNA

F

FA Fanconi anemia

FACS Fluorescence Activated Cell Sorting

FDA Food and drug administration

G

G Guanine

GBM Glioblastoma

GSC Glioblastoma stem cell

H

2-HG 2-hydroxyglutarate

HGP Human genome project

HR Homologous recombination

I

ICGC International Cancer Genome Consortium

IR Ionizing radiation

IRES Internal ribosome entry site

L

LncRNA Long noncoding RNA

M

miRNA Micro RNA

MMR Mismatch repair

MRI Magnetic resonance imaging

mRNA Messenger RNA

N

ncRNA Noncoding RNA

NER Nucleotide excision repair

NGS Next generation sequencing

NHEJ Non-homologous endjoining

O

O6-BG O6-Benzylguanine

O6-meG O-6-methylguanine

ORF Open reading frame

P

PCR Polymerase chain reaction

PRC Polycomb repressive complex

Q

qRT-PCR Quantitative real-time PCR

R

rDNA Ribosomal DNA

RNAi RNA interference
RNA-Seq RNA sequencing
ROS Reactive oxygen species
RTK Receptor tyrosine kinase
RT-PCR Real-time PCR

S

SINEs Short interspersed nuclear elements
snRNAs Small nuclear RNAs
snoRNA Small nucleolar RNAs
SSB Single strand break

T

T Thymine
TCGA The cancer genome atlas
TE Transposable element
TF Transcription factor
TME Tumor microenvironment
TMZ Temozolomide
tRNA Transfer RNA
TSS Transcription start site

U

UV Ultra violet
UTR Untranslated region

W

WHO World health organization

LIST OF FIGURES

Figure 1. Classification of lncRNAs based on their genomic localization to protein-coding genes

Figure 2. Circular RNA biogenesis, detection and biological function

Figure 3. lncRNAs regulate gene expression at transcriptional and post-transcriptional levels

Figure 4. lncRNA-mediated control of gene expression via TF interaction and R-loop formation

Figure 5. The different phases of the cell cycle

Figure 6. Representative images of the DNA fiber assay output and the analysis method of replication dynamics

Figure 7. lncRNAs regulation of cell cycle and DNA damage response

Figure 8. A selected lncRNAs involved in different cancer types

Figure 9. The current algorithm for the classification of diffuse gliomas

Figure 10. Glioblastoma; an aggressive, invasive and angiogenic tumor

Figure 11. Overview of molecular and signaling pathways alterations in GBM

Figure 12. Glioblastoma treatment protocol

Figure 13. The biological fate of temozolomide and its major cytotoxic lesions on the DNA bases

Figure 14. Overview of DNA lesions and most common repair pathways

Figure 15. The DNA damage response and its downstream signaling pathway

Figure 16. The two main DNA repair mechanisms involved in the c of TMZ toxic lesions

Figure 17. Model of the transcription activation of *RADAR*

Figure 18. *RADAR*'s cellular function hypothesis in normal cells and physiological condition

Figure 19. incPRINT method for the identification of *RADAR*-proteins partners

Figure 20. The proposed molecular mechanisms of *RADAR* regulation of DNA damage and its consequences on genome instability

***The figures in this thesis were created using www.biorender.com**

LIST OF TABLES

Table 1. List of several lncRNAs that can be used as biomarker for cancer diagnosis, prognosis and therapeutic response

Table 2. A list of the recommended 2016 WHO system and cIMPACT-NOW molecular markers for the diagnosis and classification of diffuse gliomas

Table 3. Key Resources Table

Table S1. List of oligonucleotides

SUMMARY

Advances in next generation sequencing shed light on the expression of long noncoding RNAs (lncRNAs) in health and disease. lncRNAs regulate gene expression and thereby, participate in fundamental biological processes such as cell cycle and DNA damage response (DDR). lncRNAs are deregulated in different cancer types including glioblastoma (GBM). GBM is one of the most common and aggressive malignant brain tumors in adults with the median survival rate not exceeding 15 months. First line therapy, after surgery, includes radio- and chemotherapy using Temozolomide (TMZ). Despite this multimodal therapy approach, resistance to therapy is inevitable. The function of lncRNAs in GBM and resistance to therapy is not fully understood. Therefore, the aim of this thesis was to investigate the molecular mechanism of lncRNAs in GBM chemosensitivity to TMZ.

We investigated how TMZ treatment can affect global transcription of coding and regulatory RNAs in several GBM stem-like cells compared with neural stem cells. We identified hundreds of dysregulated lncRNAs upon TMZ treatment in sensitive cells, and extracted cell specific gene regulatory networks involving mRNAs, miRNAs, and lncRNAs. We isolated 22 key lncRNAs involved in TMZ-regulatory loops and found a subset with prognostic value for overall GBM-patient survival. These lncRNAs are thought to function in chromosome organization, cell cycle, and DDR pathways. Next, we selected a lncRNA candidate for further characterization in GBM and response to TMZ. We found that this novel transcript, reported here as *RADAR* (RNA Associated with DNA DAmage and Replication) is localized in the nucleus and closely associates with chromatin. *RADAR* is upregulated upon TMZ treatment and other DNA damaging agents. *RADAR* overexpressing GBM cells displayed a decreased sphere growth, which is enhanced after the treatment with TMZ and other genotoxic drugs. *RADAR* overexpression promotes DNA breaks and potentiates the recruitment of DNA repair proteins such as γ H2AX, 53BP1, and RPA. *RADAR* expression is cell cycle regulated, with peaks in late G1/ early S phase. We showed that *RADAR* overexpression reduces DNA replication velocity while increasing stalled replication forks, resulting in premature S-phase exit. The molecular consequences of *RADAR* in DNA damage amplification and alteration of DNA replication are carried into M phase leading to mitotic abnormalities and sister chromatid cohesion loss.

In conclusion, our results provide insight into a new layer in the regulation of GBM response to chemotherapy, mediated by lncRNAs. By uncovering an RNA acting as cell cycle checkpoint regulator and chemosensitizer, our work opens up the possibility of future lncRNA-based therapeutic research and highlights the potential targeting of DNA replication against tumors, especially in organs with low proliferation activity, such as the brain.

CHAPTER 1

INTRODUCTION

1. The non-coding genome

1.1. The revolution of non-coding RNAs

For a long time, the basic principle in molecular biology stated that DNA carries the genetic cipher that is transcribed into mRNA and then translated into proteins which carry the biological functions. However, advances in next generation sequencing (NGS) and efforts of international consortia such as the Functional ANnotation Of the Mammalian genome (FANTOM), the Human Genome Project (HGP), and the Encyclopedia of DNA Elements (ENCODE) helped to reveal that ~75% of the human DNA is actively transcribed into different classes of RNA transcripts with less than 2% of the total genome size being occupied by protein-coding genes (Consortium, 2012; de Hoon et al., 2015; Djebali et al., 2012; Koboldt et al., 2013; Maston et al., 2006; Venter et al., 2001). The non-protein coding region of the genome was considered as “junk DNA” and its transcription was thought to be a byproduct or “transcriptional noise” from the genome without valuable biological function. However, a landmark paper revealed a correlation between organism complexity and the quantity and size of noncoding RNAs (ncRNAs) (Mattick, 2001; Mattick et al., 2010). Since then, the presence of different classes of ncRNA transcripts and their involvement in various biological and regulatory functions is progressively elucidated.

1.2. Regulatory RNAs and Pervasive transcription

The phenomenon by which eukaryotic and prokaryotic genomes are transcribed through the generalized presence of RNA polymerases without necessarily producing stable RNA molecules has been described as “pervasive transcription” (Consortium et al., 2007; Jensen et al., 2013; Wade and Grainger, 2014). Yet, stable and diverse ncRNAs are produced, which can be distinguished in two main classes: small noncoding RNAs and long noncoding RNAs. Transfer RNAs (tRNAs) and ribosomal RNAs (rRNAs) are among the functionally important ncRNA transcripts that are required for protein translation. Short ncRNAs including small interfering RNAs (siRNAs), piwi-interacting RNAs (piRNAs), small nucleolar RNAs (snoRNAs), and small nuclear RNAs (snRNAs) have regulatory functions in gene expression regulation, silencing of transposable elements, chemical modifications of other RNA transcripts, and processing of pre-mRNAs (Jensen et al., 2013). Additionally, earlier studies revealed another class of short ncRNAs known as microRNAs (miRNAs), which interact and degrade their mRNA targets to regulate the level of gene expression, with important functions in normal cellular processes as well as in pathophysiological conditions such as cancer (Calin and Croce, 2006). Recently, FANTOM and GENCODE projects successfully characterized the functional elements in the genome and introduce a new class of ncRNA transcripts, which is the long

noncoding RNA class (lncRNA) (de Hoon et al., 2015; Harrow et al., 2012; Kawai et al., 2001; Ramilowski et al., 2020).

2. Long noncoding RNAs (lncRNAs)

lncRNAs are now considered the most diverse and heterogeneous class of ncRNAs. They are highly abundant, display a tissue-specific expression pattern, and possess diverse physiological and biological functions (Derrien et al., 2012; Kung et al., 2013; Wapinski and Chang, 2011). The number of lncRNA transcripts is still rising with approximately a total of 270,044 human annotated lncRNA transcripts in 2019 (Ma et al., 2019). The existence of lncRNAs as a separate ncRNA entity was confirmed by evidence of chromatin signatures and histone chemical modifications on DNA intergenic regions supporting the conservation and active transcription of lncRNAs (Consortium, 2012; Guttman et al., 2009; Johnsson et al., 2014). The involvement of lncRNAs in biological function and epigenetics were first described with the early discovery of lncRNAs, such as *H19* in early development and embryogenesis, cell proliferation, and tumorigenesis (Ariel et al., 2000; Brannan et al., 1990; Kurukuti et al., 2006), the direct participation of *XIST* (X-inactive-specific transcript) in X chromosome inactivation (Borsani et al., 1991; Brockdorff et al., 1992; Brown et al., 1992; Chaumeil et al., 2006), and the involvement of *MALAT1* (Metastasis Associated Lung Adenocarcinoma Transcript 1) in mRNA splicing, genome organization, and modulation of gene expression (Ji et al., 2003; Tripathi et al., 2010; Tripathi et al., 2013). These studies refuted the general idea of lncRNA as transcriptional noise, and established lncRNAs as an actively transcribed RNA class, under-tightly regulated processes which enabled their function as important regulators of gene expression, at both transcriptional and post-transcriptional levels (Kapranov et al., 2007).

Compared to mRNAs, lncRNAs have a higher index of tissue-specific expression and subcellular localization (Carlevaro-Fita and Johnson, 2019; Derrien et al., 2012; Mercer et al., 2008; Ransohoff et al., 2018). Studies showed that lncRNAs could be expressed in correlation with other mRNAs, as part of co-expression networks, to participate in processes such as differentiation, development, and cell fate decision (Fatica and Bozzoni, 2014; Lopez-Urrutia et al., 2019). lncRNAs can also be used as markers correlating with human disease due to their specific expression pattern and the ability to interact with enhancers, chromatin modifiers, transcription factors (TF), other coding and noncoding RNAs (Flynn and Chang, 2014; Szczesniak and Makalowska, 2016; Wapinski and Chang, 2011).

2.1. Definition and biotypes of lncRNAs

lncRNAs are defined based on their length of at least 200 nt and limited protein coding potential (Kapranov et al., 2007). Total RNA sequencing showed that lncRNA transcripts could reach 50 kb or even up to 1 Mb (St Laurent et al., 2013). The most widely used method for the classification of lncRNAs is based on their genomic localization in respect to the protein-coding genes at a given locus (**Figure 1**) (Carninci et al., 2005; Harrow et al., 2012; Kung et al., 2013). Thus, a lncRNA which lies next to a protein coding gene on the same strand and/ or overlapping with some of its exonic sequences is considered a “sense lncRNA”. When the lncRNA gene is completely located within the intronic region of the protein-coding gene, it is known as “intronic lncRNA”. Conversely, a lncRNA gene present on the antisense strand of a protein-coding gene is an “antisense lncRNA”. “Intergenic lncRNAs” are those located between two protein-coding genes, regardless whether they are on the sense or antisense strand.

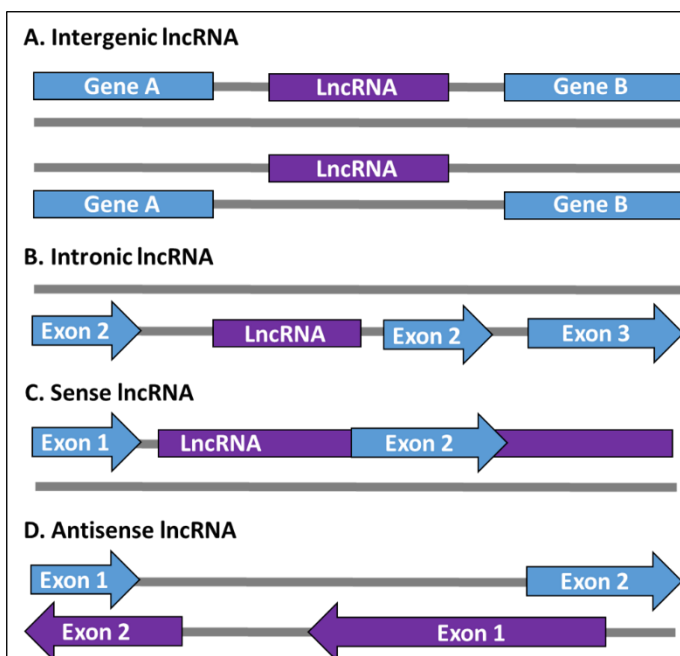


Figure 1. Classification of lncRNAs (violet) based on their genomic localization to protein-coding genes (blue). A) an intergenic lncRNA is located between two protein-coding genes either on the sense or antisense strands. B) An intronic lncRNA is transcribed within the intronic region of a protein-coding gene. C) A lncRNA gene, which is located on the same strand of a protein-coding gene or overlapping partially with its sequence is a sense lncRNA. D) An antisense lncRNA is located and transcribed from the opposite strand of a protein-coding gene and overlaps with its intronic or exonic sequence. Adapted from (Ma et al., 2013).

2.2. lncRNA molecular features and biogenesis

The nucleotide sequence and the three-dimensional structure of lncRNAs are the primary determinants of their subcellular localization and molecular function. While lncRNAs often contain repetitive elements mostly as transposable elements (TEs), these repeats tend to hybridize and base-pair between the complementary bases to form a stable complex secondary structure, enabling lncRNAs to perform their functions, either by binding to DNA, RNA, or proteins (Fort et al., 2021; Johnson and Guigo, 2014; Lee et al., 2019). Additionally, enrichment of *cis* elements such as C-rich sequence derived from *Alu* repeats (short interspersed nuclear elements (SINEs)) in lncRNAs enables their nuclear retention and their

attachment to the nuclear matrix protein hnRNP K (Lubelsky and Ulitsky, 2018; Shukla et al., 2018). LncRNAs can contain distinct motifs such as the pentamer sequence “AGCCC”, which also contributes to their nuclear localization (Zhang et al., 2014).

Given that TEs are mobile sequences which make up about one-half to two-thirds of the entire human genomic sequence (de Koning et al., 2011; Lander et al., 2001), they are considered one of the primary source in the evolution of genetic novelty, genome structure and function (Cordaux and Batzer, 2009; de Souza et al., 2013). TEs constitute a major group of repeated sequence within lncRNAs (up to 41% of lncRNA nucleotides). Therefore, mammalian lncRNAs have less invertebrate orthologues and have undergone rapid evolution between species (Kelley and Rinn, 2012; Ulitsky and Bartel, 2013). However, despite the low lncRNA sequence identity across different species, the physical structure and localization of their genomic loci more often remain stable within species (synteny), suggesting that these conserved lncRNAs are biologically relevant (Hezroni et al., 2015; Ulitsky and Bartel, 2013; Ulitsky et al., 2011).

An obvious feature among most lncRNAs is the lack of an open reading frame (ORF), which prevents their translation into proteins. However, recent findings suggest that at a subset of lncRNAs may exhibit active ORFs encoding for small peptides (Banfai et al., 2012; Gascoigne et al., 2012; Grelet et al., 2017). LncRNAs are mostly transcribed by RNA Pol II, then processed by undergoing 5' capping, 3' polyadenylation, and splicing. While most eukaryotes have bidirectional promoters (divergent: drive DNA transcription in both sense and antisense directions), it has been estimated that 13% of the total annotated lncRNAs are produced as a result of bidirectional transcription (Cabili et al., 2011). Whereas mRNAs are more likely to be co-transcriptionally spliced, lncRNAs are more often spliced after the transcription termination with an average of 2.3 isoforms (Cabili et al., 2011). Among the proteins that participate in lncRNA processing is the RNase P ribonucleoprotein complex which produces stable structures, mature ends, and different isoforms that exert roles in several cellular compartments (Marvin et al., 2011; Quinn and Chang, 2016).

2.2.1. Circular RNAs (circRNAs): unique products of RNA processing

High-throughput RNA sequencing (RNA-seq) and sophisticated bioinformatics algorithms identified an extensive array of RNA transcripts with circular structure, which added another level of complexity to the RNA world (Ivanov et al., 2015). CircRNAs can be processed from lncRNAs or mRNAs, through non-canonical splicing (back splicing) of their introns in which, the 3' sequence of one exon is back-spliced and fused with the 5' sequence of the same or other exon (**Figure 2**) (Chen, 2016a). The production of circRNAs is regulated by several splicing proteins among which is the alternative splicing factor (QKI) (Conn et al., 2015; Yu and

Kuo, 2019). Additionally, the presence of *Alu* repeats with complementary sequences flanking the circRNA has been suggested to facilitate the linear RNA circularization and the production of circRNAs (**Figure 2**) (Chen, 2016a).

Although circRNAs are classified as ncRNAs (Qu et al., 2015), this classification is under debate since some circRNAs can be translated into small peptides. This occurs in a cap-independent mechanism known as rolling circle translation based on the presence of active ORF and IRES-like structures for the assembly of ribosomes (Abe et al., 2015; Pamudurti et al., 2017; Schneider and Bindereif, 2017).

CircRNAs have a stable structure due to the closed ring form that protects them from the exonuclease-mediated degradation including RNase R (Kristensen et al., 2018). Therefore, most methods that are used for the detection and validation of circRNAs are performed after treatment with RNase R to ensure the degradation of all linear RNAs and avoid false-positive results. Methods for large-scale circRNA detection relies on microarrays and sequencing of rRNA-depleted total RNA (Glazar et al., 2014; Li et al., 2019). However, the quantification of circRNAs requires sufficient read length of at least 100 bp, and should include reads spanning the back-spliced exonic junction. Detection and profiling of a locus-specific circRNA is often performed by using northern blotting and PCR. Detection by northern blot requires the use of a probe, which overlaps with the back-spliced exonic junction. When the detection is done by PCR amplification, strategies include the use of either divergent primers or the usual convergent primers, provided one of these primers (forward or reverse) spans the back-spliced exonic junction (**Figure 2**) (Jeck and Sharpless, 2014).

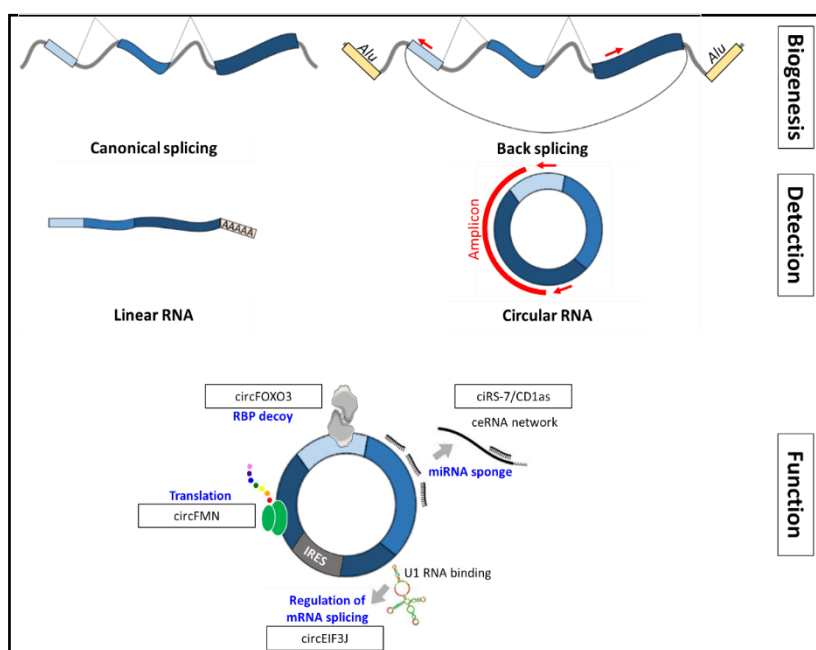


Figure 2. Circular RNA biogenesis, detection and biological function. Back-splicing refers to tail-to-head fusion of 3' end with 5' end of a linear RNA transcript to produce circRNA. The presence of repetitive elements such *Alu* repeats (yellow) facilitates the circularization of linear RNA. PCR can be used to detect the presence of circRNA using divergent primers (red) that would amplify in opposite directions with respect to gDNA and become properly inward facing and produce amplicons when a back-splice connects outside sequences. CircRNAs has multiple functions such as competitive endogenous RNAs (ceRNAs), protein sponges, regulation of splicing, or they can be translated into small peptides. Adapted from (Guarnerio et al., 2016; Ivanov et al., 2015; Quinn and Chang, 2016).

regulation of splicing, or they can be translated into small peptides. Adapted from (Guarnerio et al., 2016; Ivanov et al., 2015; Quinn and Chang, 2016).

CircRNAs are abundant in eukaryotes, have tissue-specific expression pattern and are mostly enriched in the brain. (Chen and Schuman, 2016; Salzman et al., 2013; Wang et al., 2014b). They participate in several biological processes including brain development (Piwecka et al., 2017), differentiation (Kristensen et al., 2018), and oncogenicity (Hsiao et al., 2017) by acting as competitive endogenous RNAs (ceRNAs), protein sponges, scaffolds or decoys (**Figure 2**) (Chen, 2016a; Yu and Kuo, 2019).

2.3. Molecular functions of lncRNAs

lncRNA sequence plays an important role for the determination of secondary structures due to the base-pairing between the complementary nucleotides that can be structured in motifs such as: stem-loops, hairpins, and G-quadruplex for specific interactions with DNA, RNA, and/ or proteins (Jayaraj et al., 2012; Zampetaki et al., 2018).

lncRNAs are essential regulators of gene expression at both transcriptional and post-transcriptional level (**Figure 3**). lncRNAs act either locally at their locus (*cis*-acting lncRNA) (**Figure 3, A**) or away from their transcription site (*trans*-acting lncRNA) (**Figure 3, B**) to regulate gene expression. Moreover, lncRNAs have the ability to act as scaffold for enhancers/ repressors (**Figure 3, C**) or recruit different protein components such chromatin remodelling complexes (**Figure 3, D**) to modulate its structure for gene transcription regulation. lncRNAs can also have other functions, including the modulation of enzymatic activity, as well as signaling pathways including DNA repair processes and cell cycle fate. For example, *MALAT1* controls cyclin A2 and B1 phosphorylation to regulate G1 and G2/M transitions (Tripathi et al., 2013). The mitochondrial lncRNA *MalL1* regulates the immune response to pathogens by acting as a structural component to the Toll-like receptor 4 (TLR4) immune signal transduction pathway (Aznaourova et al., 2020). The lncRNAs *lncND5*, *lncND6* and *lncCytB* are transcribed from mitochondrial DNA and regulate the expression of their sense complementary mRNAs (Rackham et al., 2011). Reports also showed that some lncRNAs such as *HOTTIP* and *NEAT1* can be loaded into extracellular vesicles (exosomes) and exported to function in cell-cell communication and to regulate the recipient cell functions (Kenneweg et al., 2019; O'Brien et al., 2020). Since lncRNAs can be present in both nuclear and cytoplasmic compartments, the following subsections will focus on their roles based on subcellular localization.

2.3.1. Nuclear functions

The three-dimensional (3D) conformation of the genome is highly organized into topologically associated domains which enables effective transcriptional regulation in active “euchromatin” or inactive “heterochromatin” states (Pombo and Dillon, 2015). During interphase, the chromosome structure is highly organized in space so gene expression is accurately controlled. Genes that are actively transcribed are present at the interior region of

the nucleus as euchromatin, while inactive regions are localized at the nuclear periphery in close relationship to the nuclear envelope, as densely compacted heterochromatin (Quinodoz et al., 2018). Several studies revealed that nuclear lncRNAs participate in 3D genome organization and play an essential role in the activation or silencing of genes through different molecular mechanisms that will be discussed in details below (Akhade et al., 2017; Quinodoz et al., 2018; Rinn and Guttman, 2014).

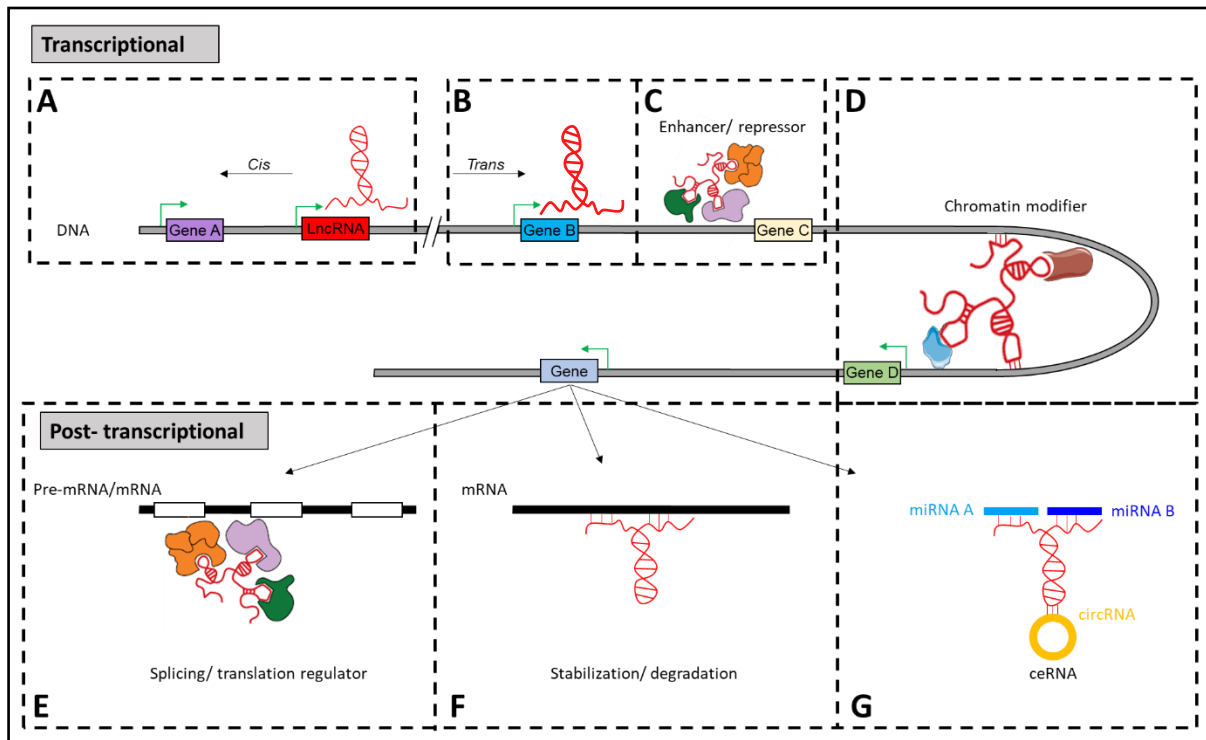


Figure 3. LncRNAs regulate gene expression at transcriptional and post-transcriptional levels. After the transcription of a lncRNA gene, the transcript localizes in the nucleus and regulates gene expression either in (A) *cis* or (B) *trans*. (C) LncRNAs can bind to and regulate the activity of enhancer, repressor proteins, and/or transcription factors to initiate or suppress gene transcription. (D) LncRNAs act as scaffold to bind and recruit chromatin modifiers, allowing them to change chromosome structure and control gene expression. Cytoplasmic lncRNAs control gene expression by regulating (E) mRNA splicing or its translation, (F) stability, or (G) serve as competitive endogenous RNA (ceRNA) through interactions with miRNAs and/ or circRNAs. Adapted from (Quinn and Chang, 2016; Rinn and Guttman, 2014).

I. Recruitment of chromatin modifying and remodeling complexes

A large number of lncRNAs bind to chromatin modifying complexes and recruit them at specific genomic loci to regulate gene expression. The polycomb repressive complexes (PRC1 and PRC2) are among the main protein complexes known to remodel chromatin structure and regulate gene expression, especially during development. Interestingly, sequencing analysis showed that around 20% of lncRNAs are co-immunoprecipitated with the polycomb-group proteins (Khalil et al., 2009).

The lncRNA *Xist* interacts with the polycomb repressive complexes (PRC1 and 2) components (SMRT, SHARP and HDAC3) to allow the deposition of the histone H3 lysine 27 trimethylation (H3K27me3) mark across the entire inactive X chromosome, as an integral part of X-chromosome inactivation process (McHugh et al., 2015; Zhao et al., 2008). Additionally, lncRNAs such as *Airn* (antisense of IGF2R non-protein coding RNA) and *HOTAIR* (HOX transcript antisense RNA) bind to PRCs and mediate PRC-dependent chromatin modifications of a wide range of genomic regions (Schertzer et al., 2019).

The BAF complex (SWI/SNF) is a well-known ATP-dependent chromatin remodeling complex, where its catalytic subunit (BRG1) interacts with enzymes (HDAC and PARP) to modulate the chromatin structure and activate gene expression. For example, the lncRNA *Mhrt* (myosin heavy-chain-associated RNA transcripts) protects against cardiac hypertrophy by acting as decoy to the ATP-dependent chromatin remodeler (BRG1). This lncRNA-protein interaction influence chromatin structure and the expression of genes associated with cardiac hypertrophy (Han et al., 2014).

The lncRNA *Kcnq1ot1* regulates the methylation status of certain genomic loci through its direct interaction and recruitment of the DNA Methyltransferase 1 protein (DNMT1) to specific regions on the DNA and control gene expression (Mohammad et al., 2010).

II. Interactions with transcription factors (TFs) and R-loop formation

lncRNAs affect gene transcription at the DNA level through direct or indirect interaction with transcription factors (TFs) and activate gene expression through DNA:RNA:protein interactions. Such interactions tether TFs to the promoter region of target genes via lncRNA interaction with the DNA through base pairing and forming a structure called (R-loop). An R-loop is a triplex nucleic acid structure composed of DNA:RNA hybrid. R-loops can be formed in a variety of circumstances. R-loop formation mainly depends on complementary sequences of the RNA to allow base-pairing with the DNA. A significant number of lncRNAs are reported to hybridize with the DNA alone, or in cooperation with protein complexes. These interactions modulate phase separation, nuclear compartment formation, and contribute to the regulation of gene expression and genomic instability (Guh et al., 2020). For instance, the *RMST* (rhabdomyosarcoma 2-associated transcript) lncRNA interacts with the transcription factor SOX2 to promote neuronal differentiation via the regulation of expression of SOX2-targeted genes (Ng et al., 2013).

Moreover, antisense lncRNAs such as *Khps1* participate in the activation of their sense mRNA (*SPHK1*) by allowing a higher accessibility to the E2F1 transcription factor to initiate gene transcription. This is achieved by *Khps1* direct interaction with both the coactivator proteins (p300/CBP) and DNA through base pairing with complementary sequence to form R-

loop structure, resulting in chromatin relaxation and the initiation of transcription (**Figure 4**) (Postepska-Igielska et al., 2015). Similarly, the direct interaction of the antisense lncRNA (*VIM-AS1*) with the transcription start site (TSS) of its sense transcript (*VIM*) through sequence homology, leads to R-loop formation and chromatin relaxation, which facilitates NF- κ B binding at the promoter region (Boque-Sastre et al., 2015). In contrast, the *Gas5* (growth arrest-specific 5) lncRNA acts as a tumor suppressor lncRNA by holding the glucocorticoid receptor (GR) away from its target genes and induces its degradation (Kino et al., 2010).

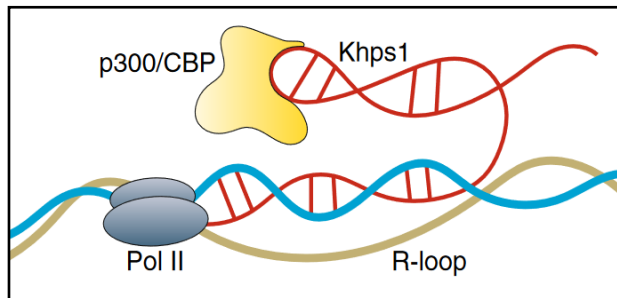


Figure 4. LncRNA-mediated control of gene expression via TF interaction and R-loop formation. *Khps1* drives the coactivator protein p300/CBP into proximity of *SPHK1* promoter via its direct interaction with the DNA complementary sequence at this region to cause chromatin relaxation and higher accessibility of E2F1 transcription factor. Adapted from (Yao et al., 2019).

III. Role in local modulation of chromatin state and gene silencing

The *XIST* lncRNA plays an essential role in the long term silencing of one of the two female X-chromosomes as part of the X-chromosome inactivation process for dosage compensation in female (Chaumeil et al., 2006; Galupa et al., 2020; Heard, 2004; Jegu et al., 2017). During early embryonic stage, *XIST* is transcribed from both X chromosomes. One of the X chromosomes will be inactivated through tight localization of *XIST* along the inactivated X chromosome and modulate its remodeling and condensation into highly compacted heterochromatin (Barr body). Through interaction with chromatin repressor complex, *XIST* represses global gene expression at the inactive X chromosome (Hall and Lawrence, 2010; Heard et al., 1997). *XIST* is able to bind with the scaffold attachment factor A (SAF-A) and this interaction is required for its loading on the inactivated chromosome and lamin B receptor (LBR) protein, and for keeping the chromosome highly condensed near the nuclear lamina (Chen et al., 2016; Creamer and Lawrence, 2017).

Another example of the regulatory role of lncRNAs in the modulation of local gene expression near their site of transcription was discovered in fission yeast. The transcription termination of nascent lncRNAs from either euchromatin or heterochromatin chromosomal regions promotes sexual differentiation or the formation and maintenance of heterochromatin in yeast respectively (Touat-Todeschini et al., 2017). In euchromatin state, the co-transcriptional interaction of the YTH domain of the RNA-binding protein Mmi1 with the lncRNA *nam1* facilitates the recruitment of the exosome, which results in the degradation of *nam1* and terminates its transcription. As a consequence, the transcription termination leads to the

repression of expression of *byr2* gene that is located downstream to *nam1* and responsible for the regulation of the entry into sexual differentiation (Touat-Todeschini et al., 2017). The heterochromatin gene silencing as well as the maintenance of heterochromatin state in fission yeast at centromeres is also achieved through the Mmi1-mediated termination of the nascent lncRNA transcription at pericentromeric regions together with RNA interference (RNAi) mechanism (Motamedi et al., 2004; Touat-Todeschini et al., 2017; Verdel et al., 2004).

IV. Role in facilitating chromosomal and enhancer-promoter interactions

In contrast to *XIST*'s function in local chromosome condensation, the lncRNA *Firre* (intergenic repeating RNA element) is localized near its transcription region and accumulates in other chromosomal sites, thereby allowing inter-chromosomal interactions via binding to hnRNPU, influencing nuclear architecture, and regulating *Slc25a12*, *Ypel4* and *Ppp1r10* gene expression (Hacisuleyman et al., 2014). Some genes at a given genomic locus are transcriptionally silent and become active through conformational changes by bringing nearby enhancer element close to the gene promoter region (Schoenfelder and Fraser, 2019). Studies showed that active enhancers drive the transcription of ncRNAs, referred to as enhancer RNAs (eRNAs), which in turn mediate the interaction between enhancers and promoters (Higgs, 2020; Kim et al., 2015). The *CCAT1-L* (Colorectal cancer associated transcript 1, long isoform) is a type of eRNA which is involved in intra-chromosomal interactions, which binds to the transcriptional repressor (CTCF) resulting in a chromatin loop between the *Myc* gene and its enhancer.

V. LncRNAs in nuclear bodies formation and function

Nuclear bodies such as the nucleoli, PML bodies, Polycomb bodies, and paraspeckles are nuclear structures that function in coordination with lncRNAs to respond to conditions such as cellular stress and participate in the 3D genome organization (Guh et al., 2020; Mao et al., 2011).

The transcription of ribosomal DNAs (rDNAs) occurs in the nucleolus, which can be activated by the physical interaction of the lncRNA (*SLERT*) with the nucleolar RNA helicase 2 (DDX21) resulting in DDX21 conformational change and activation (Xing et al., 2017). Paraspeckles are specialized ribonucleoprotein bodies that also regulate gene expression (Bond and Fox, 2009). They are composed of proteins such as PSF/SFPQ, P54NRB/NONO, PSPC1, and the serine/arginine (SR) splicing factors together with two major RNA transcripts: *NEAT1* (nuclear enriched abundant transcript 1) and *MALAT1* (Bond and Fox, 2009). Notably, under stress conditions *NEAT1* transcription is enhanced, and the processed transcript acts as a scaffold for the formation and maintenance of paraspeckles (Chujo et al., 2016; Clemson et al., 2009). *MALAT1*, on the other hand is not required for paraspeckles formation. However

following its transcription, processing, and export to the paraspeckles, it binds to SR proteins to regulate pre-mRNAs processing and splicing (Tripathi et al., 2010).

2.3.2. Cytoplasmic functions

A number of lncRNAs are exported to the cytoplasm where they regulate gene expression post-transcriptionally (**Figure 3**) through different mechanisms including regulation of mRNAs stability, translation, and/ or post-translational modifications (Rashid et al., 2016).

I. Regulation of mRNA stability

lncRNAs can affect mRNAs fate in the cytoplasm through different mechanisms. lncRNAs can function as competitive endogenous RNAs (ceRNAs) preventing miRNAs from binding to their target mRNAs, and thereby increasing the stability of mRNAs and translation (**Figure 3, G**) (Rashid et al., 2016). Recent studies also added another level of complexity for lncRNAs-mediated control of mRNA stability through a crosstalk mechanism involving lncRNA-circRNA-miRNA network that regulates mRNA translation (Kleaveland et al., 2018). For example, the circRNA *Cdr1as* (cerebellar degeneration-related protein 1 antisense transcript) is a potent sponge for miR-7. Thus, *Cdr1as* enrichment protects against the degradation of mRNAs targeted by miR-7 (Xu et al., 2015). However, the lncRNA (*Cyran*) also contains miR-7 binding sites, which leads to a higher enrichment and availability of *Cdr1as*, which is further targeted by miR-671 (Kleaveland et al., 2018). Thus, the amount of lncRNA can regulate the dosage compensation of mRNA-lncRNA-circRNA regulatory loops.

Anti-sense lncRNAs hybridize with their sense mRNA transcripts (RNA:RNA duplex) and act as positive or negative modulators of their stability (**Figure 3, F**) (Faghihi and Wahlestedt, 2009). The *BACE1-AS* lncRNA increases the stability of BACE1 mRNA through RNA:RNA hybridization between complementary sequences, thereby regulating the formation of β -amyloid plaques in neurodegenerative disease and enhancing BACE1 translation (Faghihi et al., 2008).

Another important role of the lncRNAs in controlling mRNA stability is the function of *NORAD* in regulating cellular mitosis. The expression of *NORAD* increases in response to cellular stress and DNA damage, and it helps maintain the genetic information as cells divide. *NORAD* regulates mitosis by increasing the stability of mRNAs involved in cell growth and division. *NORAD*-mediated regulation of mitosis is due to its functions as a decoy for the cytoplasmic Pumilio proteins (PUM1 and PUM2) that are involved in mRNA degradation (Tichon et al., 2016). Interestingly, *NORAD* loss of expression was also associated with accelerated aging in mice, due to increased PUM1 and PUM2 activities (Kopp et al., 2019).

II. Regulation of mRNA translation

LncRNAs can also regulate mRNA translation process. One mechanism of regulation was identified through ribosome profiling experiments, in which nuclear lncRNAs such as *MALAT1*, *H19*, and, *TUG1* were occupied by ribosomes but not translated (Ingolia et al., 2014). One mechanistic theory for ribosome-bound lncRNAs is their possible involvement in the regulation of translation machinery by occupying ribosomes when translation is not needed (Ingolia et al., 2014).

Another mechanism of lncRNA regulation of mRNA translation includes the role of the lncRNA (*lincRNA-p21*) that acts as a scaffold for the translation repressor protein (Rck) and recruits it to JUNB and CTNNB1 mRNAs to impair their translation (**Figure 3, E**) (Yoon et al., 2012).

III. Regulation of post-translation modification

The secondary structure of lncRNAs allows specific binding with specific proteins and impacts post-translational modifications. The lncRNA (*Lnc-DC*) whose expression is restricted to dendritic cells binds specifically to STAT3 and masks its binding site to the protein tyrosine phosphatase SHP1. Thus, *Lnc-DC* interaction with STAT3 prevents its dephosphorylation by SHP1 and therefore facilitates STAT3 activation (Wang et al., 2014a).

2.4. LncRNA role in biological processes

The presence of a large population of lncRNA transcripts in the cell indicates that these molecules have a more diverse role in biological processes than initially anticipated. Over the years, reports showed that lncRNAs have functions in several pathways including cell cycle (Kitagawa et al., 2013), DNA damage and repair (Su et al., 2018), cellular metabolism (Lin, 2020), cell development and differentiation (Flynn and Chang, 2014), and immune response (Hadjicharalambous and Lindsay, 2019). With the aims and scope of this thesis in mind, the regulatory roles and functions of lncRNAs in cell cycle and DNA damage are explored further.

2.4.1. Overview of the cell cycle

The cell cycle is a tightly regulated process which ensures faithful DNA replication and production of two daughter cells. The cell cycle is divided into 4 main phases: G1 (gap1), S (DNA synthesis), G2 (gap2), and M (mitosis) (**Figure 5**). Cells grow in size and duplicate their protein content and organelles during gap phases (G1 and G2). DNA replication takes place in S phase. Finally, in M phase, the chromosomes segregate and the cell cycle ends with cytokinesis which produces two identical daughter cells.

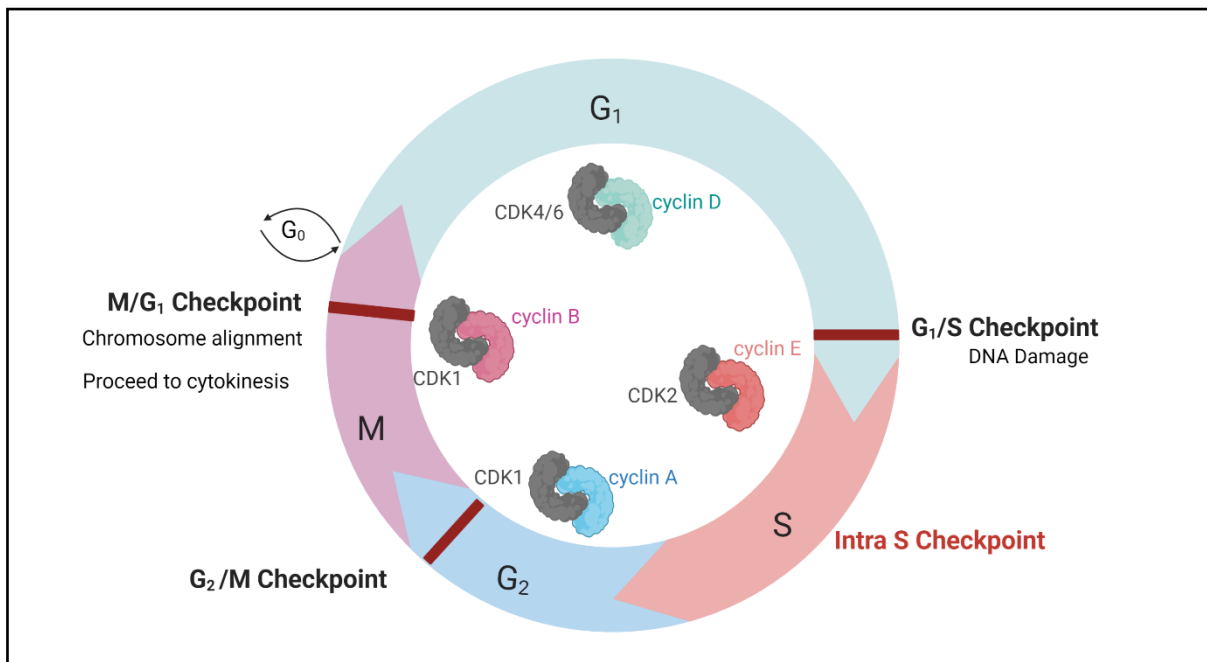


Figure 5. The different phases of the cell cycle. G₁ and G₂ (gap) phases provide time for the cell to grow and check for internal and external conditions. DNA replication occurs during S phase (DNA synthesis). Chromosomes segregation and cell division take place during M phase (mitosis). Different Cdk/cyclin complexes and checkpoints regulate cell cycle phase transition. Adapted from (Alberts, 2015).

The cell cycle is controlled by the presence of internal surveillance mechanisms known as “checkpoints” to control cell growth and division (**Figure 5**). However, when the cell starts to divide without control in repetitive cell cycles this can lead to cancer. For example, in case of DNA replication errors, the S phase checkpoint sends signals to delay phase progression into M phase, allowing sufficient time for the DNA repair machinery to correct replication mistakes and DNA damage, which if not repaired, may be deleterious and lead to unfaithful chromosome segregation (Mankouri et al., 2013). The cell cycle control system has three main regulatory checkpoints (**Figure 5**) (Barnum and O’Connell, 2014). The most critical is the late G₁/early S restriction point where the cells check for the availability of nutrients and DNA damage and commits cell cycle initiation and DNA replication. The G₂/M checkpoint controls for the complete and error-free DNA replication, as well as the correct alignment of the duplicated chromosomes on the mitotic spindle. The final checkpoint is during M-phase (metaphase to anaphase transition) where the two sister chromatids are monitored for equal distribution to the daughter cells and the completion of mitosis. Any perturbation in one of the cell cycle events will be detected at one of these checkpoints and lead to cell cycle arrest. Yet, bypassing the surveillance system may lead to genomic instability, mutations, chromosomal rearrangements, and contribute to oncogenic cell initiation (Molinari, 2000).

The cyclins and cyclin-dependent kinases (CDKs) are the main regulatory components of the cell cycle (**Figure 5**) (Lim and Kaldis, 2013). Upon the activation of CDK4 and CDK6 by G1-cyclins (D-type), CDK4/6-cyclin complexes regulate the cell cycle transition from G1 to S by controlling the level of phosphorylation of the Retinoblastoma protein (Malumbres and Barbacid, 2001). Then, the cyclin E activates CDK2, which is involved in the phosphorylation of downstream proteins such as the replication factors (RPA and RFC) to counteract G1/S restriction point and proceed to DNA replication (Lim and Kaldis, 2013). Once the DNA replication is completed, cyclin A replaces cyclin E and forms a complex with CDK2, phosphorylating both CDC6 and E2F for the termination of S phase and G2 entry. G2 to M transition occurs when cyclin A interacts with CDK1 (De Boer et al., 2008; Lim and Kaldis, 2013). During mitosis, condensation of chromosomes and alignment on microtubules is achieved via the cyclin B-CDK1 complex. Finally, the transition from metaphase to anaphase is done by inactivating the cyclin B-CDK1 complex via the anaphase-promoting complex (APC/C), and followed by chromosome segregation (Alfieri et al., 2017; Gavet and Pines, 2010).

2.4.2. DNA synthesis and mitosis

DNA replication and cell division are the most critical processes in the cell cycle as the cell has to overcome several obstacles and challenges including DNA damage and the correct alignment of sister chromatids on the microtubules. If these events are not properly repaired and completed successfully, they are considered the main source of chromosome breakage and genome instability (Ghosal and Chen, 2013; Tubbs and Nussenzweig, 2017). In addition, the use of chemotherapy for cancer treatment depends mainly on the production of genotoxic lesions which block DNA replication and trigger cell cycle arrest. However, cancer cells can evade these regulatory mechanisms due to aberrant signaling which facilitate resistance mechanisms to chemotherapy-induced genotoxic stress (Kitao et al., 2018; Langston and O'Donnell, 2006). Therefore, the understanding of DNA replication and mitosis processes provide knowledge on tumor resistance mechanisms.

In higher eukaryotes, DNA replication starts at several sites on the DNA known as the origins recognition complex (ORC). The progression from late G1 to early S requires the transformation of the pre-replication complex (CDC6, CDT1, MCM2-7) into a replication fork (Labib et al., 2000). DNA strands start to unwind and single stranded DNA becomes protected from degradation by the coating of RPA protein that also helps in replication origin unwinding and fork progression (Walter and Newport, 2000). After DNA unwinding and the binding of RPA, the DNA polymerases (α , δ , and ϵ) synthesize new strands of DNA (Stillman, 2008). Because of the antiparallel orientation of the two DNA strands, one daughter strand has to be

polymerized in the 5'- to -3' direction and the other in the 3'- to -5' direction. However, all DNA polymerases have proofreading activities only in the 5'- to -3' direction. Thus, the new strand which moves 5'- to -3' direction towards the replication fork is called the leading strand and is made continuously. Whereas, the antiparallel strand is called the lagging strand and synthesized by making pieces of DNA that are 1000-2000 nucleotides in length, known as Okazaki fragments. This mechanism requires Pol α , which makes a short RNA oligonucleotides that serve as primers on the lagging strand then can be elongated by the DNA polymerases δ , and ϵ . The final production of continuous DNA strand is achieved by a special DNA repair mechanism to eliminate the RNA primer and substitutes it with DNA, followed by joining the 3' end of the new DNA fragment to the 5' end of the previous Okazaki piece by the DNA ligase to complete the DNA synthesis process. At the end of S phase, the two copies of each chromosome are tightly connected together via the cohesin complex. Following the last stage of mitosis and the completion of the nuclear envelop structure, chromosomes start to decondense and a contractile ring structure appears at the middle of the cytoplasmic membrane to cleave the mother cell into two daughter cells, genetically identical to each other in a process known as cytokinesis (Guertin et al., 2002).

Of note, the presence of DNA damage can affect faithful DNA replication and if damage persisted it causes replication stress and stalled replication fork, which are the main source of genome instability, chromosomal rearrangement, sister chromatid missegregation, and chromosome breakage (Burrell et al., 2013; Lamm et al., 2016; Zeman and Cimprich, 2014). Therefore, studying the DNA replication dynamics is essential to assess the cellular response to replication stress. The DNA fiber assay is the gold standard technique to study DNA replication dynamics at single-molecule resolution. The assay depends on the sequential pulse (20 min) labeling of two fluorescent thymidine analogs (chlorodeoxyuridine (CldU) and iododeoxyuridine (IdU)), which are incorporated into the DNA during replication, then measured to evaluate several replication parameters including the length of DNA fiber, the replication fork speed and symmetry, the percentage of stalled replication fork, as well as the number of new replication origins and bidirectional replication forks. The analyses and calculations depend on the desired parameter that needs to be assessed, which are summarized in (**Figure 6**).

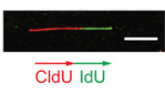
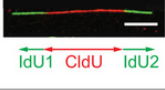
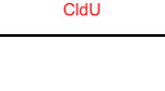
Representative image	Replication event	Calculation
A 	Ongoing fork	Length = CldU + IdU Fork Speed = $\frac{\text{Average (CldU + IdU)}}{20 \text{ minutes}}$
B 	Bi-directional replication fork	Fork symmetry = IdU1 : IdU2
C 	Double replication origins	Inter-origin distance = Ori 1 to Ori 2
D 	Replication fork termination	
E 	New replication origin	
F 	Stalled or terminated fork	

Figure 6. Representative images of the DNA fiber assay output and the analysis method of replication dynamics.

2.4.3. LncRNA in the regulation of the cell cycle and DNA damage response

In addition to the well-known proteins described above, lncRNAs also actively participate in cell cycle and DDR processes (**Figure 7**) (Guiducci and Stojic, 2021; Khanduja et al., 2016; Kitagawa et al., 2013; Schmitt et al., 2016; Yang and Qi, 2015). Hence, understanding the molecular role of lncRNAs in these pathways will bring novel insights to human diseases such as cancer.

At the G1/S restriction point, the cell checks for the level of DNA damage. In case of damaged DNA, G1 cell cycle arrest occurs primarily via decreasing the levels of cyclin D1. For example, the lncRNA *pncRNA* is transcribed upon DNA damage and involved in G1 cell cycle arrest by decreasing the expression of *CCND1*. *pncRNA* prevents CBP/p300 transcription factor from binding to *CCND1* promoter region by masking these binding sites through the recruitment of TLS complex to *CCND1* promoter leading to a decrease in cyclin D1 levels (Wang et al., 2008).

The expression of other lncRNAs such as *Gadd7*, *lincRNA p21*, *DINO*, and *PANDA* is induced in response to DNA damage and genotoxic stress and these lncRNAs regulate cell cycle progression and cell fate. *Gadd7* responds to damages caused by UV radiation and intra-strand crosslinks of platinum adducts. It regulates G1/S progression and cell cycle arrest through the modulation of the CDK6 mRNA at the post-transcriptional level (Liu et al., 2012).

The stability of CDK6 mRNA depends on its 3'-UTR hybridization with TDP-43 protein. However, in response to DNA damage, *Gadd7* competes with CDK6-mRNA in binding to TDP-43 protein, resulting in CDK6-mRNA degradation and G1/S transition block (**Figure 6**) (Liu et al., 2012).

The cyclin-dependent kinase inhibitor 1A (*CDKN1A*) gene has a major role as tumor suppressor in response to DNA damage by reducing cell proliferation in a *P53*-dependent manner (Harper et al., 1993; LaBaer et al., 1997). Surprisingly, the lncRNAs *lincRNA p21*, *DINO*, and *PANDA* are located at the same genomic locus of *CDKN1A* and are transcribed in response to genotoxic stress, and modulates DDR via the regulation of *CDKN1A* expression. DNA damage induces *P53* protein expression, which controls several cellular pathways and gene transcription including the transcriptional activation of both *lincRNA p21* and *DINO*. *LincRNA p21* acts as transcriptional repressor in a *P53*-dependent manner through its direct binding with hnRNP-K that is known to interact with other repressive complexes like the Histone H1.2 or PRCs (Huarte et al., 2010). On the other hand, *DINO* facilitates efficient DDR by directly interacting with *P53* protein and maintaining its stability, to arrest cell cycle and induce apoptosis (Schmitt et al., 2016). In contrast, *PANDA* regulates cell fate via its interaction with PRCs and NF-YA transcription factor to control gene expression and senescence (Puvvula et al., 2014).

MALAT1 is an oncogenic lncRNA with several functions including the regulation of expression of several genes involved in G1/S and mitotic phases. Cells depleted from *MALAT1* are arrested in G1 and/ or more prone to undergo apoptosis due to higher expression level of *P53* and *P21* genes. In addition, *MALAT1* depleted cells have lower proliferation index due to reduced *Myb12* expression that is responsible for G2/M progression (Tripathi et al., 2013). In another study, *MALAT1* depletion leads to the formation of fragmented nuclei as a result of chromosome missegregation which leads to cell cycle arrest at the G2/M boundary because of *MALAT1*'s ability to modulate the splicing of pre-mRNAs related to mitosis through the regulation of phosphorylated SR proteins levels (**Figure 7**) (Tripathi et al., 2010).

During S phase, lncRNAs have very important functions in the control of phase progression and DNA replication. A recent study showed that about 900 lncRNAs are enriched during S phase. Among them, three lncRNAs (LINC00704, LUCAT1, and MIAT) were confirmed to have an essential role in the transition through S phase. Antisense oligonucleotides (ASOs) mediated depletion of these lncRNAs revealed a slower progression and release from S phase together with a higher percentage of cells arrested in G1 (Yildirim et al., 2020). lncRNAs can also act directly to affect the efficiency of the DNA replication machinery such as the lncRNA *CONCR* (**Figure 7**). *CONCR* expression is cell cycle dependent during S phase and controlled

by the oncogenic TF MYC. *CONCR* is transcribed in an antisense orientation to the ATP-dependent DNA helicase (*DDX11*). Although *CONCR* does not affect *DDX11* transcription in *cis* or its mRNA levels, it is required to enhance the DNA binding and ATPase activity of *DDX11* protein. *CONCR* loss results in sister chromatid cohesion defects (**Figure 7**) (Marchese et al., 2016).

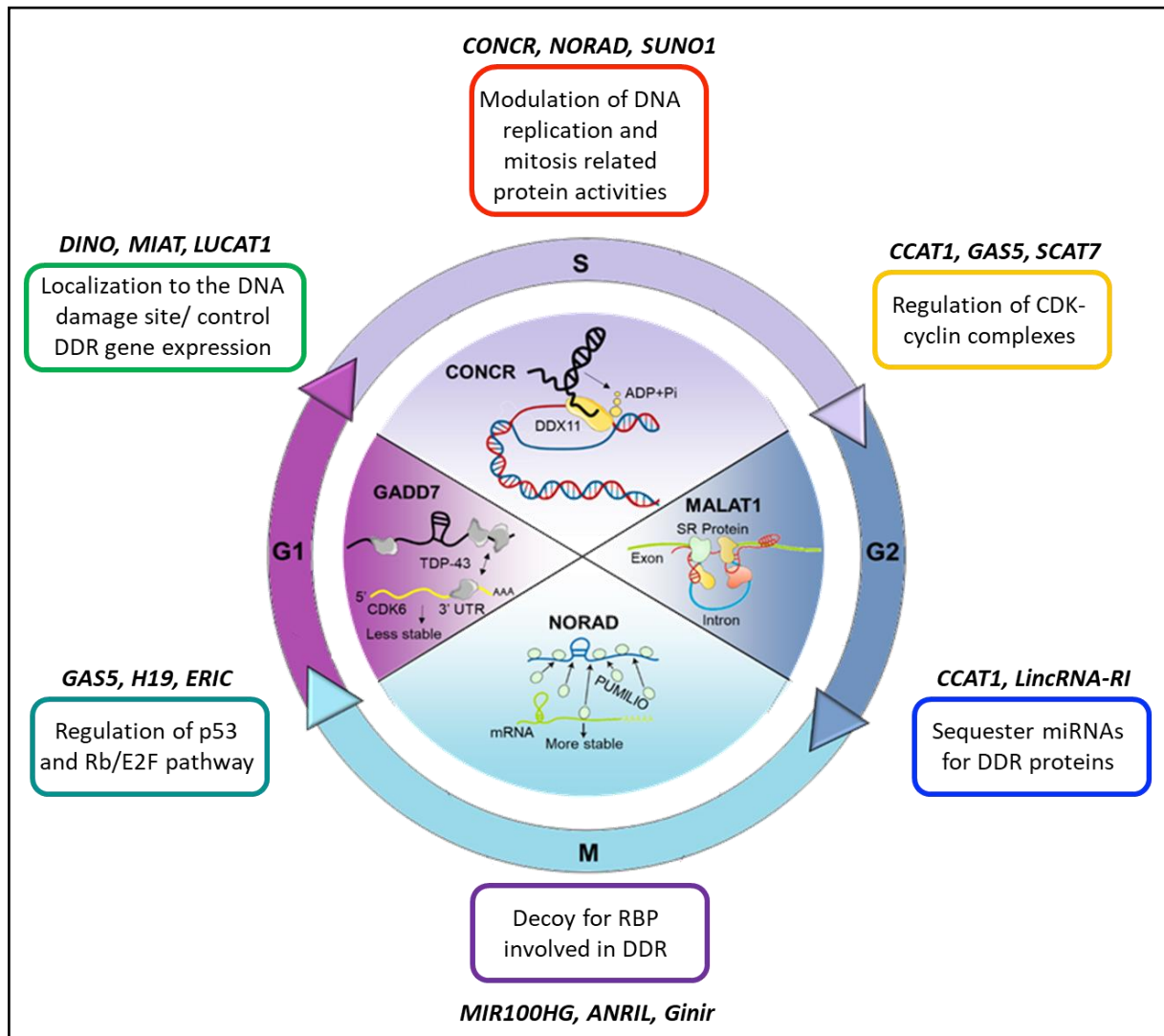


Figure 7. LncRNAs regulation of cell cycle and DNA damage response. A snapshot of the role of some lncRNAs in the regulation of cell cycle progression, DNA damage and fate decision. Adapted from (Guiducci and Stojic, 2021; Kitagawa et al., 2013; Yao et al., 2019; Yildirim et al., 2020; Zhu et al., 2019).

LncRNAs are also fundamental regulators of DNA damage during cell cycle with roles in controlling homologous recombination (HR). The transcription of the lncRNA *TERRA* occurs at the telomeres and promotes HR in *cis* via DNA:RNA hybridization and R-loop formation, to maintain genome stability and regulates gene transcription (Azzalin et al., 2007; Graf et al., 2017). The lncRNA *GUARDIN* also maintains genome stability by preventing telomere (end-to-end) fusion from different chromosomes. In response to DNA damage, *GUARDIN* acts as

ceRNA to sequester miRNA-23a and prevent the degradation of TRF2 mRNA, which has a role in telomere maintenance fusion of chromosomes (Hu et al., 2018). *NORAD* (non-coding RNA activated by DNA damage) is another lncRNA, expressed upon DNA damage and replication stress. It interacts with RBMX, a component of DDR, to facilitate the assembly of the topoisomerase genome instability inhibitory complex. Interestingly, *NORAD* downregulation causes reduced replication fork velocity and defects in sister chromatid segregation during M phase (Munschauer et al., 2018). The regulation of HR and DNA end resection also include the involvement of *DDSR1* lncRNA through ATM/NF- κ B-dependent mechanism. *DDSR1* interacts with hnRNPUL1 and regulates BRCA1 and RAP80 recruitment at the DNA damage sites (Sharma et al., 2015). Additionally, upon DNA double strand breaks, a number of lncRNAs termed as “damage-induced lncRNAs (dilncRNAs)” are transcribed from the damaged locus and localized to DSB ends where they interact with both small non-coding RNAs known as “DNA damage RNAs (DDRNA)” and the DNA repair protein 53BP1 to allow efficient repair of DNA breaks (Michellini et al., 2017).

2.5. LncRNA in cancer and chemo-resistance

LncRNAs play a very important role in human diseases including cancer (**Figure 8**), and are implicated in almost all the hallmarks of cancer (Bhan et al., 2017; Schmitt and Chang, 2016). LncRNAs can be either oncogenes that promote tumorigenesis, cell proliferation, and resistance to treatment, or tumor suppressive genes that impair cancer development and promote apoptosis. Oncogenic lncRNAs such as *ANRIL*, *H19*, *HOTAIR*, and *UCA1* are aberrantly overexpressed in cancer tissues. In contrast, examples of tumor suppressive lncRNAs include *MEG3*, *LincRNA-p21*, and *CASC15-S*.

LncRNAs, in large part due to their tissue- and disease specific expression are powerful tools as clinical biomarkers for cancer prognosis and response to treatment (Schmitt and Chang, 2016) (**Table 1**). Of note, the detection of the lncRNA *PCA3* (prostate cancer antigen 3) in urine is the first successful example of a lncRNA-based biomarker approved for prostate cancer diagnosis. *PCA3* is specifically expressed in prostate cancer and plays a role in cell survival by modulating androgen receptor signaling (Bussemakers et al., 1999). *PCA3* is not the only lncRNA used in clinical decision making. For instance, *HOTAIR* detection in surgically extracted breast cancer is considered complementary to the histological examination for the prediction of metastasis (Gupta et al., 2010). Moreover, *HOTAIR* detection is of value for the determination of patient outcome in response to platinum-based chemotherapy (Teschendorff et al., 2015).

MYC is a proto-oncogene commonly overexpressed in many cancer types (Dang, 2012). Several lncRNAs were reported to regulate *MYC* expression. The *PVT1* lncRNA is a key driver

for aberrant *MYC* expression in a mechanism involving *PVT1*-mediated control of interaction between the human immunoglobulin enhancer with *MYC* promoter (Tseng et al., 2014). Additionally, *CCAT1* lncRNA drives colon cancer progression via *cis* regulation of *Myc* promoter with its enhancer elements (Xiang et al., 2014). lncRNAs act also as tumor suppressor, such as the lncRNA *TARID* which binds GADD45a and guiding it to *TCF21* promoter and activates its transcription via GADD45a-mediated promoter demethylation (Arab et al., 2014).

lncRNAs can also play a role in cancer transcriptional reprogramming. For example, the lncRNA *Paupar* is strictly expressed in CNS. In neuroblastoma, *Paupar* can interact with local and distal promoter regions to regulate cell cycle progression and maintain a dedifferentiated phenotype of the disease (Vance et al., 2014). Another example is the lncRNA *NEAT1*, which is associated with higher risk of progression and metastasis of prostate cancer by regulating the expression of estrogen receptor alpha (Lin, 2016).

Studies showed that lncRNAs can also regulate resistance and response to therapy through different mechanisms. The activation of PI3K/AKT/mTOR pathway is directly linked to chemoresistance, due to the upregulation of anti-apoptotic proteins such as Bcl2 family members (Rebucci and Michiels, 2013). *PVT1* upregulation in gastric cancer leads to increased levels of the mTOR targets-multidrug resistance proteins, resulting in decreased apoptosis and resistance to cisplatin (Zhang et al., 2015b). Another example is *H19*, which serves as a decoy for miR-141 and activates the β -catenin pathway, responsible for tumor development and chemoresistance (Ren et al., 2018).

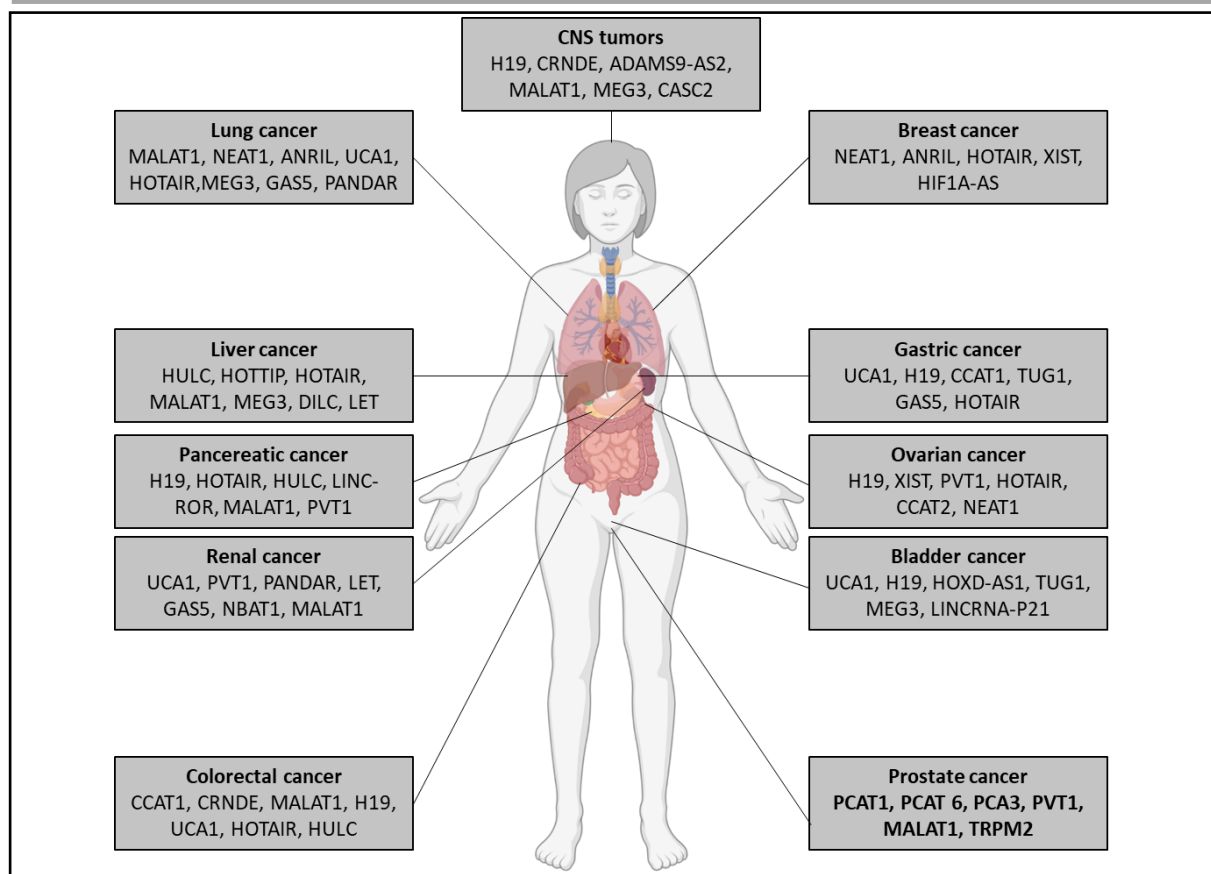


Figure 8. A selected lncRNAs involved in different cancer types. Adapted from (Bhan et al., 2017).

LncRNAs in Cancer Diagnosis and Monitoring

LncRNA	Cancer Type	Bioavailability of LncRNA
H19	Gastric	Blood
HULC	Hepatocellular	Blood
AA174084	Gastric	Gastric secretions
PCA3	Prostate	Urine
SeCATs	Sezary	Tumor
SPRY4-IT1	Melanoma	Tumor

Prognostic LncRNAs

LncRNA	Cancer Type	Prognostic Information
FAL1	Ovarian	Poor prognosis
HOTAIR	Breast	Increased risk of metastasis
HOTTIP	Hepatocellular	Increased risk of progression
MEG3	Meningioma	Associated with tumor grade and risk of progression
NBAT-1	Neuroblastoma	Good prognosis
NKILA	Breast	Decreased risk of metastasis
SCHLAP1	Prostate	Increased risk of metastasis

Table 1. List of several lncRNAs that can be used as biomarker for cancer diagnosis, prognosis and therapeutic response. Adapted from (Schmitt and Chang, 2016).

3. Malignant brain tumors

3.1. General overview

Malignant brain tumors are among the deadliest types of cancers. “Diffuse glioma” is the medical terminology used to describe the central nervous system (CNS) tumors, which resemble the astrocytic or oligo-dendroglial morphologies (Ellison et al., 2019). Worldwide, gliomas occur in approximately 6 individuals per 100,000 (Ostrom et al., 2019). Most of the cases of gliomas are sporadic without major known risk factors. However, there are some exogenous risk factors such as exposure to radiation which is associated with increased risk of brain tumor development (Ohgaki and Kleihues, 2005).

While signs and symptoms can vary in their manifestation, they mainly depend on which part of the CNS the tumor develops. Neurological symptoms such as headache, confusion, memory loss, seizures, speech and balance difficulties are generally observed in patients with gliomas (Posti et al., 2015). Magnetic Resonance Imaging (MRI) is the recommended modality for diagnosing brain tumors. Post-operative examination of the tumor tissue through histological staining and molecular genetic profiling is performed to ensure precise diagnosis and tumor classification.

The World Health Organization (WHO) classification of CNS tumors is the reference for the diagnostic classes, grading and criteria (Louis et al., 2016). Based on continuous improvement of molecular profiling methods and large-scale omics analyses, the 2016 WHO classification has undergone extensive updates and refinement. Therefore, the Consortium to Inform Molecular and Practical Approaches to CNS Tumor Taxonomy-Not Officially WHO (cIMPACT-NOW) regularly proposes newly updated guidelines (Louis et al., 2017a; Louis et al., 2017b). cIMPACT-NOW criteria are not only based on histological features (proliferation activity, necrosis, and angiogenesis), but also encompass molecular signatures present in brain tumors (Brat et al., 2020; Brat et al., 2018; Ellison et al., 2019; Louis et al., 2020). The molecular markers which are recommended by the 2016 WHO system together with cIMPACT-NOW are essential for the classification and grading of diffuse gliomas (**Figure 9** and **Table 2**).

Molecular Marker	Biological Function	Diagnostic Role
IDH1 R132 or IDH2 R172 mutation	Gain- of- function mutation	Distinguishes diffuse gliomas with IDH mutation from IDH- wild- type GBM and other IDH- wild- type gliomas
1p/19q codeletion	Inactivation of tumor suppressor genes such as FUBP1 and CIC	Distinguishes oligodendroglioma, IDH- mutant and 1p/19q- codeleted from astrocytoma, IDH- mutant
Loss of nuclear ATRX	Role in proliferation and alternative lengthening of telomere	Loss of nuclear ATRX in an IDH- mutant glioma is diagnostic for astrocytic lineage tumors
Histone H3 K27M mutation	H3F3A or HIST1H3B/C missense mutation to affect gene expression	Defining molecular feature of diffuse midline glioma, H3 K27M- mutant
Histone H3.3 G34R/V mutation	Affecting gene expression	Defining molecular feature of diffuse hemispheric glioma, H3.3 G34- mutant
MGMT promoter methylation	DNA repair	None, but is a predictive biomarker of benefit from TMZ in patients with IDH- wild- type GBM
Homozygous deletion of CDKN2A/CDKN2B	Regulators of Rb1 and p53- dependent signaling	A marker of poor outcome and WHO grade 4 disease in IDH- mutant astrocytomas
EGFR amplification	Cell proliferation, invasion and resistance to induction of apoptosis	EGFR amplification occurs in ~40–50% of GBM, IDH wild type. Molecular marker of GBM, IDH wild type.
TERT promotor mutation	Cell proliferation; increasing TERT expression	TERT promotor mutation occurs in ~70% of GBM, IDH wild type and >95% of oligodendroglioma, IDH- mutant and 1p/19q- codeleted. Molecular marker of GBM, IDH wild type.
+7/–10 cytogenetic signature	Gain of chromosome 7 combined with loss of chromosome 10	Molecular marker of GBM, IDH wild type.
BRAF^{V600E} mutation	Oncogenic driver mutation leading to MAPK pathway activation	Rare in adult diffuse gliomas but amenable to pharmacological intervention

Table 2. A list of the recommended 2016 WHO system and cIMPACT-NOW molecular markers for the diagnosis and classification of diffuse gliomas. Adapted from (Weller et al., 2020).

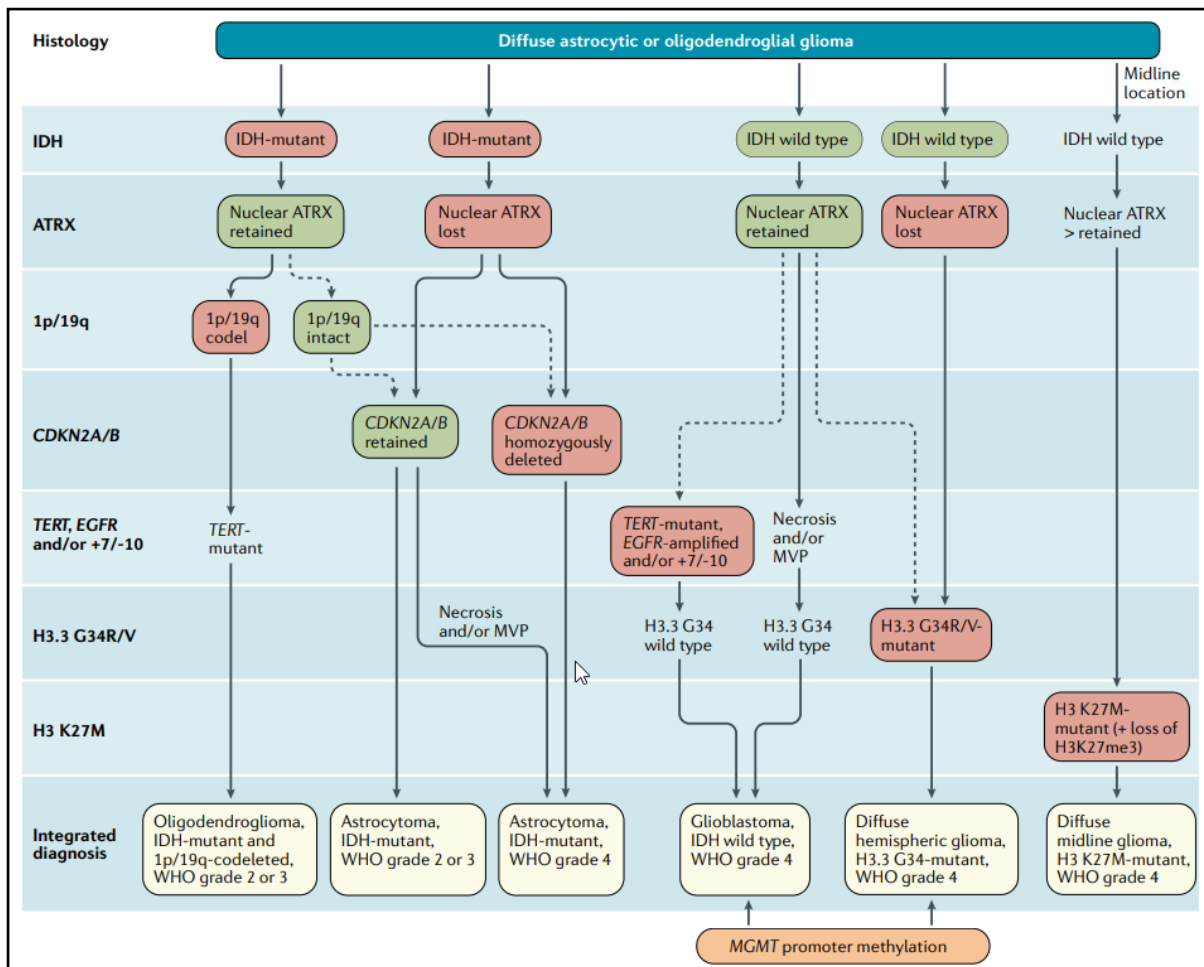


Figure 9. The current algorithm for the classification of diffuse gliomas. Diagnosis and classification of diffuse gliomas should combine the evaluation of both histological features and molecular signatures presented by the tumor. MVP, microvascular proliferation. Adapted from (Weller et al., 2020).

3.2. IDH-mutant gliomas

Heterozygous point mutations resulting from the substitution of the amino acid arginine (R) in codon 132 of IDH1 or codon 172 of IDH2 are the molecular signatures defining IDH-mutant astrocytomas and oligodendrogliomas.

The *IDH* genes (*IDH1*, *IDH2*, and *IDH3*) encode the Isocitrate Dehydrogenase isoenzymes that play an important role in cellular metabolism by catalyzing the oxidative decarboxylation of isocitrate to α -ketoglutarate (α -KG) and the production of NADPH. IDH mutation leads to a gain of function enzyme that produces the oncometabolite 2-hydroxyglutarate (2-HG) (Dang et al., 2009). The oncogenic effect of 2-HG comes from its competitive inhibition of α -KG dependent enzymes such as TET2 (myeloid tumor suppressor ten-eleven-translocation 2) and JmJc (jumonji C domain-containing histone demethylases) (Xu et al., 2011). These enzymes play critical roles in the regulation of DNA methylation and the alteration of their function has been associated with glioma CpG island hypermethylator phenotype known as (G-CIMP). This

phenotype is characterized by the downregulation of genes involved in cell differentiation and programmed cell death (Duncan et al., 2012; Figueroa et al., 2010; Turcan et al., 2012). In addition, 2-HG is associated with a reduced NADPH pool, which is the source for reduced glutathione regeneration that has important function to protect against oxidative damage (Pramono et al., 2020; Tedeschi et al., 2015).

Astrocytomas and oligodendrogliomas are usually classified as WHO grade 2 or 3. However, loss of *ATRX* and homozygous deletion of *CDKN2A/B* genes are usually found in astrocytomas, leads to a more aggressive tumor classified as WHO grade 4 astrocytoma. The characteristics of these tumors include necrosis, high microvascular proliferation and low levels of global DNA methylation (G-CIMP-low), which are associated with poor prognosis in patients (Brat et al., 2020; Louis et al., 2020). When *ATRX* is retained, it is necessary to evaluate the 1p/19q status to differentiate astrocytoma from oligodendroglioma, where 1p/19q codeletion remains exclusive to this latter subtype (Louis et al., 2016). Other molecular characteristics present in astrocytomas include *CDK4* amplification and homozygous deletion of *RB1* which can be considered together as strong predictors of poor patient prognosis (Aoki et al., 2018; Brat et al., 2020).

3.3.IDH-wild type gliomas

Gliomas with wild type IDH status are classified as WHO grade 4. Subtypes are defined based on the assessment of *ATRX* and histone H3 status. IDH-wild type hemispheric glioma is mostly seen in pediatric and young adult patients exhibiting *ATRX* and *OLIG2* loss (90% of cases) together with the histone variant H3.3-G34 mutation (missense mutations substituting glycine (G) with arginine (R) or valine (V) at position 34 of H3 histone family 3 (H3.3) encoded by *H3F3A*) (Louis et al., 2020). Diffuse midline gliomas display WT *ATRX* with H3 K27M-mutation (replacing lysine (K) to methionine (M) at position 27 of H3 histone family 3 (H3.3) encoded by *H3F3A*) (Louis et al., 2016). These tumors appear in midline structures such as in the spinal cord and are characterized by an aggressive phenotype (Louis et al., 2020). Gliomas with IDH, *ATRX* and histone H3 wild type status are classified as WHO grade 4 glioblastomas (GBM) (Louis et al., 2016). Of note, MGMT promoter is frequently found methylated in ~ 60% of WHO grade 4 GBM and hemispheric glioma. Although, MGMT promoter methylation status has minimal value for classification, it is a major predictor of patient response to chemotherapy with alkylating agents.

As the work of this thesis investigates the role of lncRNAs in glioblastoma and the regulation of chemoresistance, I will describe in details the WHO grade 4 glioblastoma (GBM).

3.3.1. Glioblastoma

I. Genetic alterations

Glioblastoma (GBM) is the most common and aggressive malignant brain tumor in adults with very poor prognosis and an average overall survival not exceeding 12-15 months. GBM has an incidence rate of approximately 3.2/ 100,000 cases per year, predominantly in patients over 55 years of age (Tamimi and Juweid, 2017).

Histologically, GBM cells are characterized by their polygonal shape with nuclear pleomorphism and a high nuclear/ cytoplasmic ratio. As GBM develops rapidly, the growing tumor shows very high vascularization resulting in aberrant blood vessels, red blood cell extravasation, and necrotic foci within the central zone of the tumor, due to insufficient blood supply (**Figure 10**) (Urbanska et al., 2014).

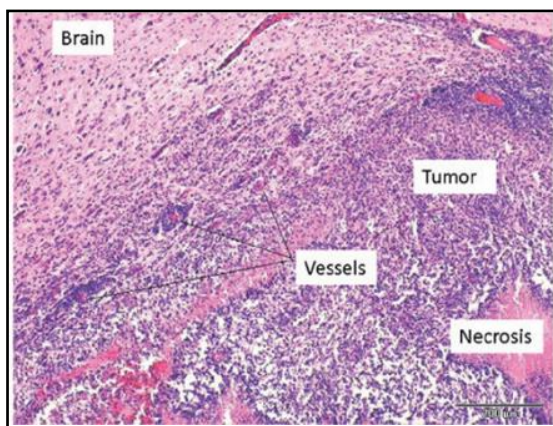


Figure 10. Glioblastoma; an aggressive, invasive and angiogenic tumor. Representative micrograph for hematoxylin-eosin staining highlighting GBM features: dense tumor cells, abnormal blood vessels, and necrotic area. Adapted from (Linsenmann et al., 2019).

The Cancer Genome Atlas (TCGA), the Chinese Glioma Genome Atlas (CGGA), and the International Cancer Genome Consortium (ICGC) led intensive research efforts to identify key genetic drivers and aberrations in GBM (Brennan et al., 2013; Cancer Genome Atlas Research, 2008; Verhaak et al., 2010; Yan et al., 2012; Zhang et al., 2011). This covered dysregulated gene expression, promoter methylation status, mutations, copy number variations, and key molecular markers in GBM.

GBM frequently show unique molecular signatures such as *EGFR* gene amplification, *TERT* promoter mutations, and gain of chromosome 7 and loss of chromosome 10 (+7/-10) (Brat et al., 2018; Louis et al., 2020). Alterations in at least one of the Receptor Tyrosine Kinase (RTK) pathways occur in >80% of GBMs (**Figure 11**). These alterations could result either in a loss of function in genes such as: *PTEN* (40%) and *NF1* (10%) or gain of function in genes predominantly occurring in: *EGFR* (57%) and *PDGFRA* (10%) and their downstream signaling pathways like *PIK(3)K* (25%) (**Figure 11**) (Brennan et al., 2013).

GBM cells are also characterized by carrying circular extrachromosomal DNA elements (ecDNA). ecDNA are minute chromatin bodies that carry amplifications of several oncogenes such as *MYC*, *EGFR*, and the *CDK4-MDM2* gene cluster which in turn are highly expressed and lead to increased tumorigenic capacity of GBM as well as poor therapy response (deCarvalho et al., 2018; Sanborn et al., 2013; Turner et al., 2017). Genes regulating cell cycle and apoptotic pathways also appear inactivated or mutated. For instance, the tumor suppressor gene *TP53* is mutated in 30% of primary GBMs (Brennan et al., 2013) (**Figure 11**).

Furthermore, the Retinoblastoma (RB) signaling pathway is deregulated in ~80% of GBMs through the inactivation or deletion of the *CDKN2A/B* locus (80%) or the amplification of *CDK4/6* (15%) (Brennan et al., 2013) (**Figure 11**). *CDK4* and *CDK6* proteins play a critical role in enhancing cell proliferation through cell cycle regulation. Thus, *CDK4/6* promote G1/S phase progression by inhibiting *RB1* protein. This provides a rationale for the development of *CDK4/6* inhibitors to arrest the cell cycle in G1 such as Palbociclib (Romero-Pozuelo et al., 2020; Sherr et al., 2016).

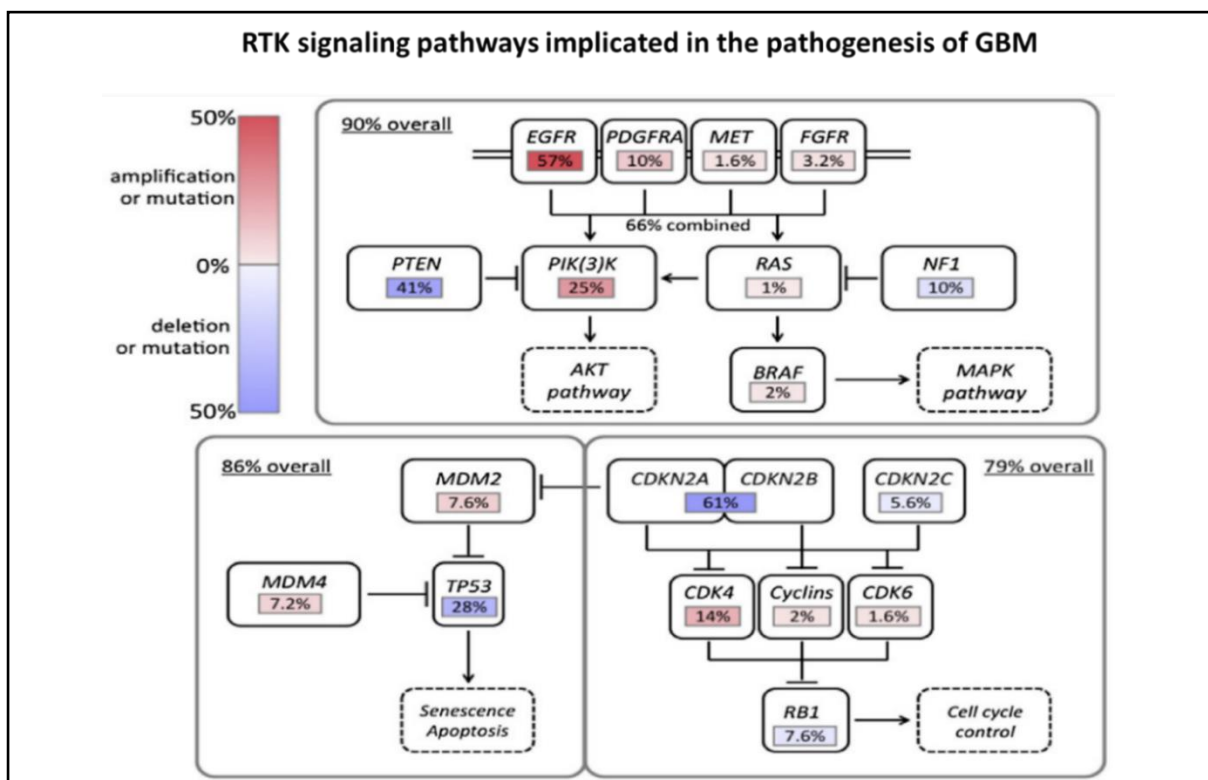


Figure 11. Overview of molecular and signaling pathways alterations in GBM. Receptor Tyrosine Kinases (RTKs) and their downstream pathways are important oncogenic mediators in the pathogenesis of GBM. Abnormalities in tumor suppressor genes such as *TP53* and *RB* are also indicated. The color scale indicates the frequency and the type of genetic alteration. Red: activating mutation and gene amplification, Blue: inactivation mutation and gene deletion. Adapted from (Brennan et al., 2013).

II. Clinical management

Surgical resection of the tumor from the brain is the first line approach for the management of GBM to extract as much tumor tissue as possible without affecting neurological functions. GBM is characterized by its ability to infiltrate the brain parenchyma, so the complete extraction of the tumor mass is impossible. Therefore, combined radio- and chemotherapy are the standard treatment protocol following tumor resection (Stupp et al., 2005). Radiotherapy usually begins 3-5 weeks post-surgery with dosage between 50-60 Gy in 1.8-2 Gy daily fractions (Press et al., 2020). Escalating radiotherapy dosage above 60 Gy showed an increased neurotoxicity without adding additional survival benefits to the patients (Breen et al., 2020; Cabrera et al., 2016).

The current standard GBM chemotherapy includes daily doses of 75 mg/m² (75 mg per square meter of body surface area) of the alkylating agent Temozolomide (TMZ). The treatment regimen follows a 6 week protocol of focal radiotherapy with concomitant chemotherapy given once daily, followed by 6 cycles of TMZ (150-200 mg/m²) for 5 days every 28 days (**Figure 12**) (Stupp et al., 2005).

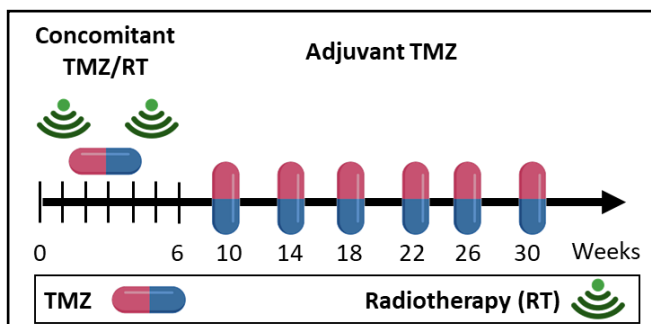


Figure 12. Glioblastoma treatment protocol. Treatment scheme recommended by (Stupp et al., 2005). Daily radiotherapy (50-60 Gy in 1.8-2 Gy daily fractions) and concomitant TMZ doses (75 mg/m²), followed by adjuvant interval chemotherapy. Modified from (Omuro et al., 2014).

3.4. Mechanisms of resistance to chemotherapy

In spite of advances in neurosurgical technologies and the intensive course of radio- and chemotherapy, patient survival is still limited and patients quickly develop resistance to treatment. Development of novel therapeutics is challenging also due to the presence of the blood brain barrier (BBB), which limits the penetration and access of certain drugs to the tumor mass. In addition, the brain tumor microenvironment (TME) plays a role in chemoresistance, as excessive tumor growth results in hypoxic and necrotic niches. This stimulates the production of several factors including Hypoxia Induced Factor-1 (HIF-1) which contributes to increased vascularization and more resistance to therapy. Moreover, our laboratory and others demonstrated that GBM cells have stem-like properties displaying high plasticity, allowing them to adapt to a changing microenvironment (Bradshaw et al., 2016; Dirkse et al., 2019; Lathia et al., 2015).

Resistance to TMZ in large part is due to efficient DNA repair mechanisms which overcome toxic lesions induced by TMZ. Therefore, I will first present the mechanism of TMZ-induced DNA damage followed by the major DNA repair pathways of TMZ-induced lesions. Finally, I will highlight novel mechanisms of lncRNAs in GBM and the regulation of chemoresistance.

3.4.1. Temozolomide pharmacology and mechanism of action

TMZ belongs to the second generation of DNA alkylating agents. It is an imidazotetrazine derivative with lipophilic properties and is small prodrug size (MW= 194 Da) making it readily absorbed by the intestine and able to penetrate the BBB. Like other prodrugs, TMZ is spontaneously hydrolyzed into the active form 3-methyl-(triazen-1-yl) imidazole-4-carboxamide (MTIC) and quickly degrades to form 5-aminoimidazole-4-carboxamide (AIC) and Methyl diazonium, a highly reactive cation (Newlands et al., 1997) (**Figure 13**). The therapeutic effect of TMZ is based on its ability to methylate guanine (N7 and O6 positions) and adenine residues (N3 position). The “O-6-methylguanine adduct (O6-meG)” is the most genotoxic lesion produced by TMZ treatment although it corresponds to only 8% of its activity. The O6-meG modification induces a nucleotide mismatch pairing with thymine (T) instead of cytosine (C) during DNA replication process (Zhang et al., 2012a) (**Figure 13**). This activates DDR pathways to repair the genotoxic adducts. However, if not properly repaired, this results in single- and double-strand DNA breaks (SSB and DSB) and induces cell cycle arrest during G2/M phase leading to apoptosis and cell death (Zhang et al., 2012a). TMZ triggers apoptosis via Fas/CD95/Apo-1 receptor activation in glioma cells that have wild type P53. In P53-mutated glioma cell death results from the activation of the mitochondrial apoptotic pathway (Roos et al., 2007).

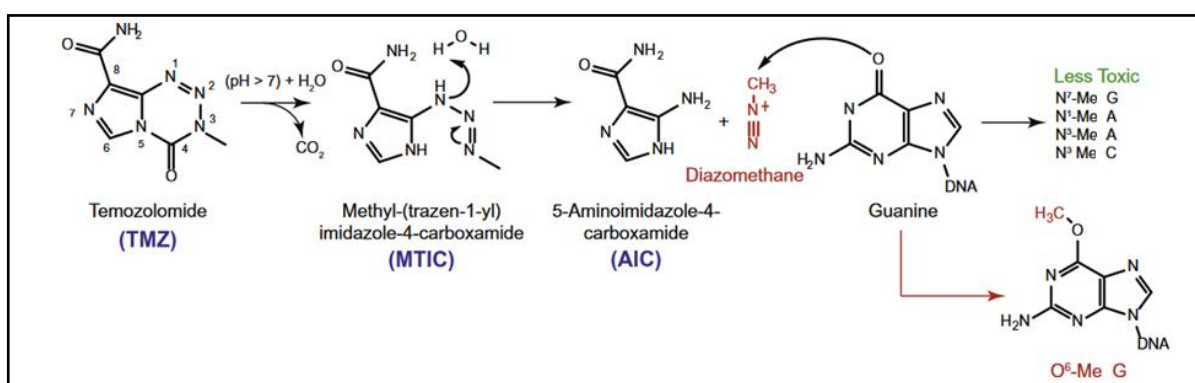


Figure 13. The biological fate of temozolomide and its major cytotoxic lesions on the DNA bases. TMZ is a prodrug hydrolyzed to yield MTIC, which degrades into AIC and Methyl diazonium (diazomethane), the highly reactive cation that methylates A, C, G on the DNA. Adapted from (Rai et al., 2016).

3.4.2. The DNA damage response and the major TMZ-induced lesion repair pathways

DNA damage can arise through exogenous factors or during naturally occurring endogenous biological processes. Endogenous damages can occur due to DNA replication

errors. Additionally, internal DNA damage can originate from processes such as the incorporation of incorrect nucleotides by DNA polymerases, hydrolytic and non-enzymatic methylation reactions that generate abasic sites, and the deamination of DNA bases. Moreover, reactive oxygen species (ROS) generated by cellular metabolic processes such as mitochondrial respiration or through redox-cycling events are another cause of endogenous DNA damage (Tubbs and Nussenzweig, 2017). On the other hand, exogenous DNA damage results from exposure to externally encountered or applied DNA-damaging agents. Examples include ultraviolet light (UV), exposure to X-ray, Ionizing radiation (IR), and chemical substances administered as part of cancer chemotherapy.

All of these processes result in various DNA lesions, which can lead to SSB and DSB. In order to avoid lethal consequences, cells activate the DDR. DDR is a network of cellular pathways that recognize genotoxic lesions, carry efficient DNA repair, and transmit signals which determine cell-fate decisions. There are several DDR factors responsible for controlling DNA integrity that can activate cell cycle checkpoints in the case of DNA damage and initiate DNA repair pathways.

The major DNA repair pathways include, direct damage repair (DR), base excision repair (BER), mismatch repair (MMR), nucleotide excision repair (NER), DNA cross-link damage repair, the Fanconi Anemia (FA) pathway, and finally the DSB repair, including 2 pathways: homologous recombination (HR) and non-homologous end joining (NHEJ) (Lord and Ashworth, 2012) (**Figure 14**).

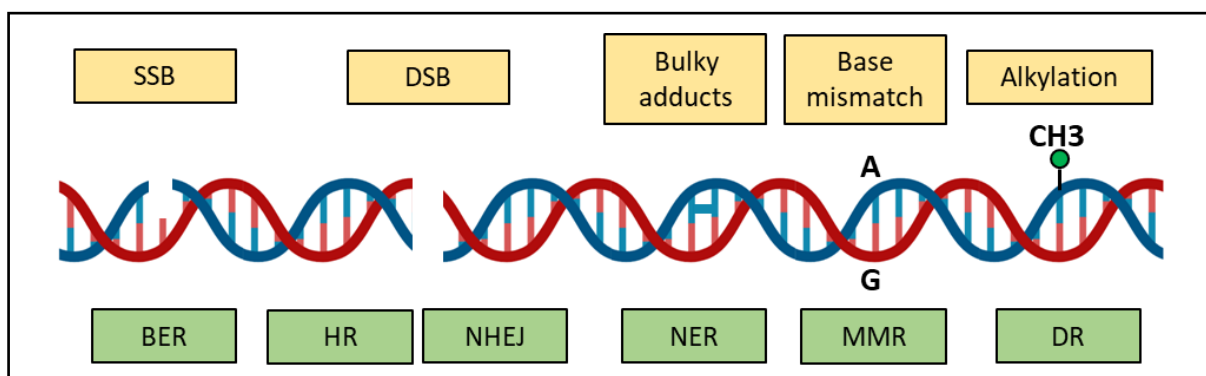


Figure 14. Overview of DNA lesions and most common repair pathways. See text for details. SSB: single strand break, DSB: double strand break, BER: base excision repair, HR: homologous recombination, NHEJ: non-homologous endjoining, NER: nucleotide excision repair, MMR: mismatch repair, DR: direct damage repair, A: adenine, G: guanine, CH3: methyl group. Adapted from (Lord and Ashworth, 2012).

For instance, DSB activates the DDR pathway (**Figure 15**), which starts by the recognition of a DNA break by the MRN complex (MRE11-RAD50-NBS1) which in turn activates Ataxia Telangiectasia mutated (ATM) kinase to control the phosphorylation status of several downstream DNA repair proteins (Scully et al., 2019; Sulli et al., 2012). SSB at the collapsed

replication fork are characterized by the accumulation of RPA and ATRIP on the stretches of ssDNA, and are recognized by the 9-1-1 sensor (RAD9-RAD1-HUS1) which activates the Ataxia Telangiectasia and Rad3-related (ATR) kinase (**Figure 15**).

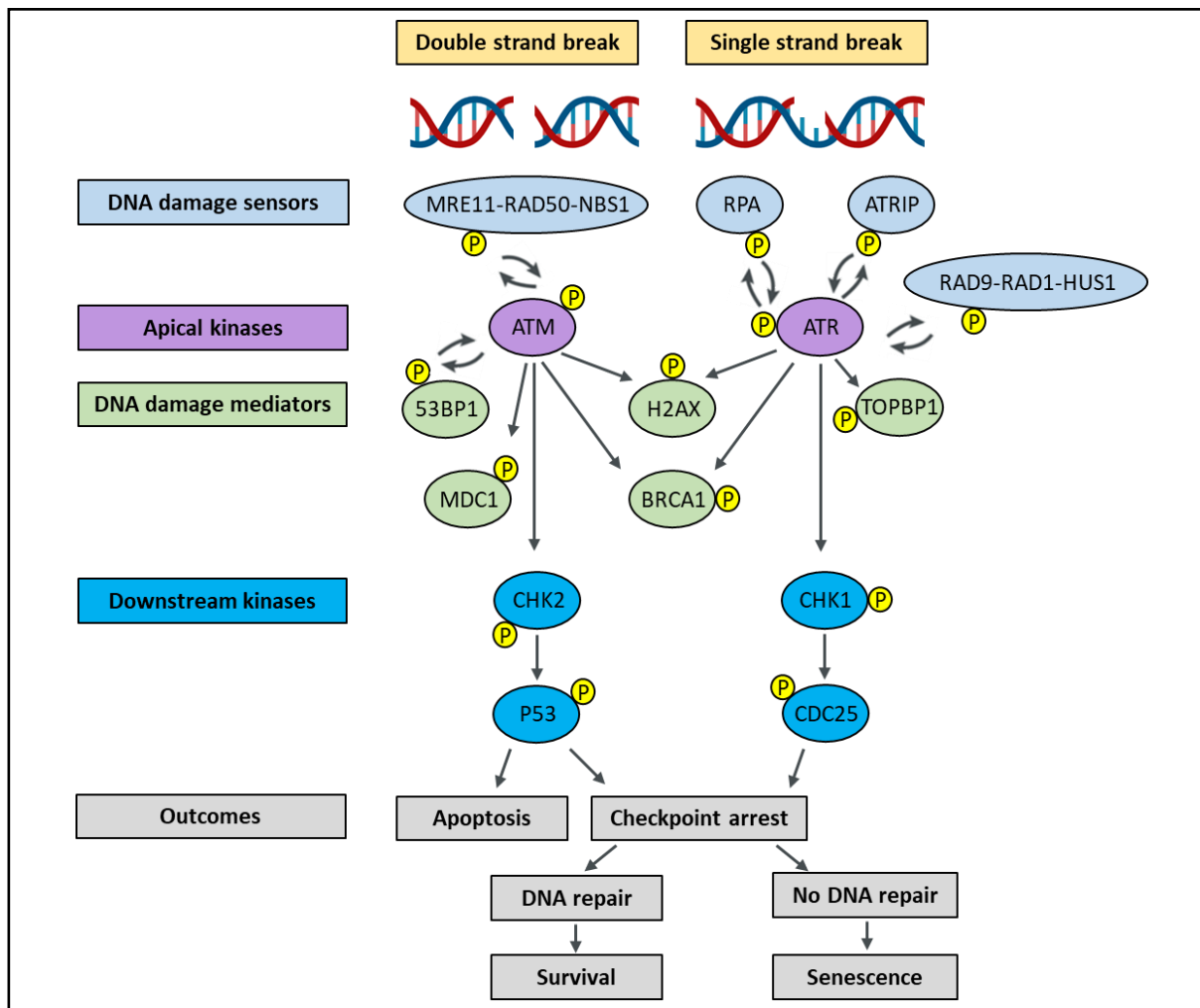


Figure 15. The DNA damage response and its downstream signaling pathway. The DNA damage response (DDR) has two principal sensors: MRE11-RAD50-NBS1 and RAD9-RAD1-HUS1/ RPA complex that recognize DSB and SSB respectively. These sensors recruit ATM and ATR kinases at the site of the DNA lesion which in turn phosphorylate γ H2AX (H2A variant) in the region proximal to the DNA lesion. While ATM responds to lesions that cause DSBs, ATR predominantly is activated to events related to DNA replication stress. Several downstream mediators of DNA repair factors are thus activated for the execution of essential cellular programs such as cell cycle arrest to allow efficient DNA damage repair and the continuation of cell division. However, when the damage is not efficiently or correctly repaired this leads to cellular senescence or the activation of programmed cell death. Adapted from (Sulli et al., 2012).

Both kinases ATM and ATR become active upon their phosphorylation and further trigger phosphorylation events of downstream effectors (Delacroix et al., 2007; Sulli et al., 2012) (**Figure 15**). DNA damage mediators such as 53BP1 and CHK2 control G1 to S cell cycle progression. TOPBP1 together with CHK1 regulate DNA replication, and lastly CDC25 control G2/M checkpoint for monitoring chromosome segregation (Jackson and Bartek, 2009). In

addition, both kinases (ATM and ATR) phosphorylate the histone variant H2AX which can be found in around 10-15% of the nucleosomes (Iacovoni et al., 2010). One of the most common phosphorylation site of H2AX is the serine 139 (S139), a post-translational modification known as γ H2AX that spreads over large chromatin domains, serving as scaffold for the recruitment of the DSB machinery.

I. Temozolomide-direct repair (DR) by MGMT

The primary mechanism of TMZ resistance is the direct removal of the O6-meG adduct by the methylguanine-DNA methyltransferase (MGMT) protein. MGMT acts through a suicidal reaction via a stoichiometric transfer of the alkyl group “O6-meG adduct” on the DNA to the cysteine 145, which is located within the catalytic pocket of MGMT and leads to its degradation (Fang et al., 2005) (**Figure 16a**).

The expression of *MGMT* is epigenetically regulated through the methylation of CpG islands located in its promoter region. The *MGMT* promoter is unmethylated in ~55% of GBMs resulting in stable MGMT protein expression which may result in fruitful DNA repair of TMZ lesions and resistance to therapy. Interestingly, high levels of MGMT are reported in gliomas and correlate with resistance to TMZ (Cai et al., 2005; Kitange et al., 2009). Thus, patients with unmethylated *MGMT* promoter harbor little benefit from TMZ. Indeed, the *MGMT*-promoter methylation status is a predictive marker of patient clinical benefit of TMZ treatment (Hegi et al., 2005; Wick et al., 2013).

Due to the importance of MGMT-mediated control of TMZ resistance, novel approaches are therefore under investigation to target and inhibit MGMT in an attempt to increase GBM sensitivity to TMZ. For example, O6-Benzylguanine (O6-BG) is a guanine synthetic derivative that acts as MGMT inhibitor. However, combining TMZ therapy with O6-BG was found to be toxic with severe myelo-suppression without adding significant benefit over TMZ alone (Quinn et al., 2005; Schilsky et al., 2000). To overcome the side effects, strategies have been developed for the local O6-BG delivery or the use of folate conjugates in order to specifically target the tumor cells. These efforts have so far not been fruitful (Quinn et al., 2009; Ranson et al., 2006). Other strategies to manipulate MGMT levels use epigenetic drugs such as histone deacetylase inhibitors (levetiracetam and valproic acid) to downregulate *MGMT* expression (Nakada et al., 2012), or by manipulating MGMT-promoter methylation using decitabine and 5-azacytidine (Moen et al., 2014). Such drugs are however unspecific and may affect multiple pathways and have unwanted effects in patients.

II. Temozolomide-indirect DNA repair by mismatch repair (MMR)

Other DNA repair mechanisms are involved in the correction of TMZ lesions (O6-meG), such as the detection and correction of misincorporated nucleotides during DNA replication through a conserved process called MMR (**Figure 16b**).

In the absence of MGMT or when O6-meG lesions are not repaired, the mismatch of guanine and thymine triggers the MMR pathway. Activation of MSH2 and MSH6 recognize mismatches through heterodimerization at the site of incorrectly paired bases (Acharya et al., 1996). Then, MLH1 and PMS2 form a tertiary complex to carry out the excision and replacement of the wrong base (Prolla et al., 1998) (**Figure 16b**).

Of note, TMZ treatment may induce a hypermutated phenotype involving MMR proteins in recurrent gliomas (Daniel et al., 2019; van Thuijl et al., 2015). Mutations in *MSH6* post-TMZ treatment have been reported, suggesting an acquired mechanism of GBM resistance to TMZ. (Cahill et al., 2007; Hunter et al., 2006). Moreover, the downregulation or loss of the *MSH2* gene also occurs in recurrent GBM after TMZ treatment, which greatly decreased its efficacy (McFaline-Figueroa et al., 2015).

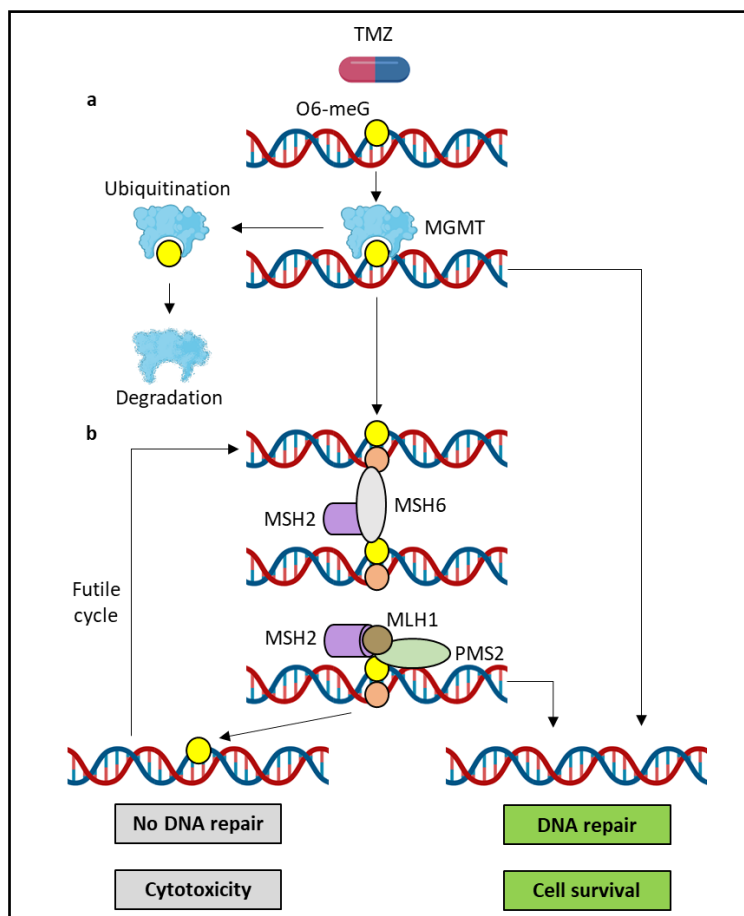


Figure 16. The two main DNA repair mechanisms involved in the correction of TMZ toxic lesions. A) MGMT-mediated direct DNA repair of TMZ major toxic lesion “O6-meG”. The alkyl group (orange circle) transferred to cysteine 145 that is present in the MGMT catalytic pocket followed by its degradation. **B)** O6-meG adduct is recognized by MSH2, MSH6, MLH1, and PMS2 complexes. Adapted from (Wick et al., 2014).

3.4.3. LncRNA in GBM and the regulation of resistance to chemotherapy

Long noncoding RNAs (lncRNAs) are now recognized as essential players in cancer biology as they actively participate in almost all the hallmarks of cancer described by Hanahan and Weinberg in 2000 (Di Gesualdo et al., 2014; Hanahan and Weinberg, 2000; Schmitt and Chang, 2016). However, the number of studies focusing on lncRNA mechanisms that drive oncogenicity in the brain GBM is still limited.

The polycomb repressive complex (PRC) can modulate cancer development (Chan and Morey, 2019). Several lncRNAs including *XIST*, *HOTAIR*, and *TUG1* are able to interact with PRCs, modulate their activities, and affect cancer development (Davidovich and Cech, 2015). In neuroblastoma, the lncRNA *NBAT-1* (neuroblastoma associated transcript-1) is a tumor suppressor. *NBAT-1* interacts directly with EZH2 (enzymatic subunit of the PRC2 complex) and regulates the deposition of H3K27me3 histone mark on EZH2 target genes that are involved in neuronal differentiation, cellular proliferation, and invasion (Pandey et al., 2014). In GBM, *NBAT-1* expression is downregulated compared to healthy tissue whilst the exogenous introduction of *NBAT-1* in GBM cells decreases cell proliferation through downregulation of *AKT* expression (Liu et al., 2018). *NEAT1* physically interacts with EZH2 to mediate H3K27me3 in the promoter region of WNT/ β -catenin (*CTNBB1*) leading to pathway activation and GBM progression (Chen et al., 2018).

The *MEG3* (Maternally Expressed 3) lncRNA has a tumor suppressor function and its expression is downregulated or lost in many cancers (Zhou et al., 2012). *MEG3* promotes apoptosis by enhancing the transcription and stability of P53 through its direct interaction with P53 protein thus regulating the expression of some P53 target genes such as *GADD45A*, *EGR1*, and *SESN2* (Zhu et al., 2015). *MEG3* overexpression in GBM cell lines results in decreased proliferation, while increased expression of *MEG3* is associated with better patient outcomes (Wang et al., 2012; Zhang et al., 2012b). *MEG3* knockdown in GBM leads to increased angiogenesis due to an elevated expression of the genes involved in VEGF angiogenic pathway such as *VEGFA* and *VEGFR1* (Gordon et al., 2010). Other mechanisms of *MEG3*-mediated suppression of GBM cell proliferation include its role acting as a ceRNA and sequestering miR-6088 thus protecting against *SMARCB1*-mRNA degradation which is a repressor of *GLI* (glioma-associated oncogene homologue) transcription (Gong and Huang, 2020). *MEG3* also binds miR-96-5p preventing the degradation of *MTSS1*-mRNA and suppressing tumor growth (Zhang and Guo, 2019).

The lncRNA *CRNDE* is highly upregulated in glioma and controls gene expression related to neuronal differentiation through binding with PRC2 and CoREST (Ellis et al., 2012). *CRNDE* acts also as a sponge for miR-384, thereby increasing PIWIL4 and STAT3 proteins levels.

Thus, *CRNDE* enhances cell proliferation and inhibits apoptosis in GBM cells (Wang et al., 2015).

Several other lncRNAs are highly expressed in GBM with suggested functions in controlling cell stemness and neuronal differentiation (Zhang et al., 2015a). Examples include *MIAT*, *H19*, and *XIST* which exhibit multiple CTCF-specific binding domains, allowing them to physically interact with CTCF to modulate chromatin looping and regulate cell differentiation and development (Kurukuti et al., 2006; Plasschaert et al., 2014; Zhang et al., 2015a). *XIST* in GBM also promotes angiogenesis by acting as sponge of miR-429 (Cheng et al., 2017).

Additionally, studies correlated the differential expression of lncRNA with glioma progression and recurrence (Chen et al., 2017; Murat et al., 2008; Zhang et al., 2012b). Moreover, the downregulation or loss of the *MSH2* gene also occurs in recurrent GBM after TMZ treatment, which greatly decreased its efficacy (Han et al., 2012). Another study of lncRNA expression in conjunction with data analysis of the TCGA cohort correlated patient survival with specific lncRNAs. This study found nearly 500 lncRNAs associated with poor GBM prognosis (Reon et al., 2016). These studies reveal the potential of lncRNA signatures in glioma as biomarkers for better disease prognostication and determining clinical outcomes (Zhang et al., 2012b).

The differential expression of lncRNAs between treated glioma versus untreated samples, as well as between primary and secondary gliomas suggests that lncRNAs may play a role in resistance to chemotherapy. Based on data extracted from the Chinese Glioma Genome Atlas (CGGA), the lncRNA *SNHG12* was highly expressed in GBM cells resistant to TMZ, and *SNHG12* knockdown resulted in higher response to therapy. Interestingly, *SNHG12* has a role in resistance to TMZ by regulating caspase-3 and the cleavage of its substrate PARP to control the cell cycle via G1/S arrest. The direct mechanism of *SNHG12* mediated control of GBM response to TMZ involves miR-129-5p decoy, which enhances *MAPK1* and *E2F5* mRNA translation (Lu et al., 2020). The lncRNA *KCNQ1OT1* also contributes to TMZ resistance by acting as ceRNA and sequesters miR-761 leading to increased levels of multiple drug resistance proteins (Wang et al., 2020).

The SOX2 transcription factor is highly expressed in TMZ-resistant GBM cells and controls the development of early embryonic tissue by maintaining pluripotency of stem cells (Annovazzi et al., 2011; Kamachi and Kondoh, 2013; Wang et al., 2013b). The lncRNA *SOX2OT* is located at the same genomic locus of *SOX2* and its expression is elevated in TMZ-resistant cells as well as in recurrent GBM. Furthermore, its high expression was correlated with high risk of relapse and poor prognosis (Liu et al., 2020). lncRNAs can either positively or negatively regulate their neighboring gene expression in *cis*. *SOX2OT* regulates GBM

response to TMZ by enhancing *SOX2* expression through binding and recruitment of ALKBH5 to *SOX2*-mRNA, which leads to *SOX2* transcript demethylation and increased expression (Liu et al., 2020).

The lncRNA *TP73-AS1* contributes to higher aggressiveness and TMZ-resistance in GSCs through its ability to regulate the expression of *ALDH1A1*, which promotes drug resistance through the detoxification of aldehyde substrates via NAD(P)⁺ oxidation mechanism (Mazor et al., 2019). The lncRNA *ADAMTS9-AS2* is also overexpressed in TMZ-resistant GBM cells and *ADAMTS9-AS2* knockdown resulted in decreased GBM cell proliferation and TMZ sensitivity due to the downregulation of FUS protein expression. Functional analysis showed that *ADAMTS9-AS2* directly interacts with RRM and Znf_RanBP2 domains of FUS, resulting in enhanced FUS protein stability and increased expression by protecting it from ubiquitin-mediated degradation (Yan et al., 2019). Altogether, these studies highlight the potential of novel lncRNAs in GBM and response to TMZ.

CHAPTER 2

SCOPE AND AIM OF THE THESIS

Glioblastoma (GBM) is still considered one of the most common and aggressive malignant brain tumor in adults. Despite an intensive therapeutic regimen, GBM recurrence is inevitable due to resistance to treatment resulting in dismal outcomes for patients who only survive between 12-14 months.

As discussed in (**chapter 1**), resistance to treatment arises from several factors, which is in large part due to the inherited genetic ability to efficiently engage the DDR and repair the DNA damage in cancer cells. Therefore, novel approaches based on targeting DNA repair pathways in order to maximize the damage induced by genotoxic agents in malignant cells are gaining importance (O'Connor, 2015). So far, most research for novel therapies focused on protein-coding genes including DDR proteins involved in the response of GBM to TMZ with very limited success. Since more than 97% of total RNA transcripts are considered as non-coding RNAs (ncRNAs) with the vast majority belonging to long noncoding RNAs (lncRNAs), it could rationally be argued that some research effort in this field may lead to a shift in our understanding of the biology of human disease and drug discovery.

Thus, the main aim of this PhD thesis was to investigate the role of lncRNAs in GBM chemoresistance to TMZ. The project was based on a small and total RNA-Seq profiling previously performed in the lab to isolate TMZ-induced lncRNA transcripts in GBM cells to determine GBM transcriptional reprogramming induced by TMZ. We aimed to identify regulatory loops composed of lncRNAs:miRNAs:TFs:mRNAs controlling the transcriptional TMZ response in GBM. In addition, the TMZ-induced lncRNA candidates were prioritized based on their clinical relevance for GBM patient survival, and potential involvement in biological processes related to DNA damage, cell cycle, and apoptosis. Based on these criteria we focused on one particular lncRNA for detailed characterization, functional studies, and the molecular mechanism in regulating GBM response to TMZ. Therefore, my PhD thesis largely focuses on this novel lncRNA candidate gene and includes:

- The characterization of its isoforms and localization within cellular compartments.
- The investigation of its biological effect on GBM cells and response to chemotherapy.
- Uncovering its molecular mechanism of action in GBM biology and chemosensitivity to TMZ and other DNA damaging agents.

CHAPTER 3

MATERIALS AND METHODS

Table 3: Key Resources Table

REAGENT or RESOURCE	SOURCE	IDENTIFIER
Bacterial and Virus Strains		
Escherichia coli DH5alpha	New England Biolabs (NEB)	Cat# C2987
Antibodies		
Mouse monoclonal anti-MGMT	Chemicon	Cat# MAB16200, RRID: AB_2281919
Rabbit monoclonal anti- β Actin	Cell Singalling Technology	Cat# 4970S, RRID: AB_2223172
Rat monoclonal anti-Cisplatin modified DNA	Abcam	Cat# ab103261, RRID: AB_10715243
Rabbit monoclonal anti- P-Histone H2A.X (Ser139)	Cell Singalling Technology	Cat# 9718, RRID: AB_2118009
Rat monoclonal anti-RPA32/RPA2	Cell Singalling Technology	Cat# 2208, RRID: AB_2238543
Rabbit monoclonal anti-53BP1	Abcam	Cat# ab36823, RRID: AB_722497
Mouse monoclonal anti- β Tubulin III	Millipore	Cat# MAB1637, RRID: AB_2210524
BV510 Mouse Anti-Human CD90	BD Biosciences	Cat# 563070, RRID: AB_2737987
V510 Rat IgG2b, κ Isotype Control	BD Biosciences	Cat# 562951, RRID: AB_2869437
Mouse anti H2AX-Phospho Ser139-Alexa Fluor 647	BD Biosciences	Cat# 560447, RRID: AB_1645414
Mouse anti ATM-PhosphoSer1981-PE	Millipore	Cat# FCMAB110P, RRID: AB_10562803
Rat monoclonal anti-BrdU	Abcam	Cat# ab6326, RRID: AB_305426
Mouse monoclonal anti- BrdU	BD Biosciences	Cat# 347580, RRID: AB_10015219
Sheep Anti-Mouse IgG - Horseradish Peroxidase secondary antibody	Amersham	Cat# NA931, RRID: AB_772210
Goat Anti-Rabbit IgG - Horseradish Peroxidase secondary antibody	Jackson Labratoriy	Cat# 111-035-003, RRID: AB_2313567
Goat anti-Rat IgG secondary antibody, Alexa Fluor 555	Invitrogen	Cat# A-21434, RRID:AB_2535855
Goat anti-Mouse IgG secondary antibody, Alexa Fluor 488	Invitrogen	Cat# A-11017, RRID:AB_143160
Goat anti-Rabbit IgG secondary antibody, Alexa Fluor 647	Invitrogen	Cat# A-21244, RRID:AB_2535812

PerCP-Cy 5.5 Mouse anti-BrdU	BD Biosciences	Cat# 560809, RRID: AB_2033929
IRDye 800CW Goat anti-Rat IgG secondary antibody	LI-COR Biosciences	Cat# 925-32219, RRID:AB_2721932
Chemicals, Peptides, and Recombinant Proteins		
Temozolomide	Sigma-Aldrich	Cat# T2577
Cytarabine	Merck	Cat# C3350000
Cisplatin	Sigma-Aldrich	Cat# P4394
Thymidine	Sigma-Aldrich	Cat# T9250
Giemsa's azur eosin methylene blue	Merck	Cat# 109204
Puromycin dihydrochloride	Sigma-Aldrich	Cat# P8833
G418 (Geneticin)	Invivogen	Cat# ant-gn-1
Nocodazole	Sigma-Aldrich	Cat# SML1665
Colchicine	Sigma-Aldrich	Cat# C9754
TRIzol	Invitrogen	Cat# 15596
TURBO DNase	Invitrogen	Cat# AM2238
RNase R	Epicenter	Cat# RNR07250
UltraPure Glycogen	Invitrogen	Cat# 10814-10
RNaseOUT	Invitrogen	Cat# 10777019
RNase, DNase-free	Roche	Cat# 11119915001
DMEM	Lonza	Cat# BE12-604F
Opti-MEM I Reduced Serum Medium	Gibco	Cat# 31985070
DMEM:F-12 Medium	Lonza	Cat# BW12-719F
Neurobasal Medium	Gibco	Cat# 21103049
BIT-100 Supplement	Provitro	Cat# 2043100
B-27 Supplement	Gibco	Cat# 17504044
Ultra Glutamine	Lonza	Cat# BE17-605E/U1
Sodium acetate buffer solution	Sigma-Aldrich	Cat# S7899
Heparin sodium salt	Sigma-Aldrich	Cat# H3149-25KU
X-tremeGENE HP DNA Transfection Reagent	Roche	Cat# 6366236001
SuperSignal West Pico PLUS Chemiluminescent Substrate	Thermo Fisher Scientific	Cat# 34580
RIPA Lysis Buffer, 10X	Millipore	Cat# 20-188

PhosSTOP	Roche	Cat# 04906837001
cOmplete Protease Inhibitor Cocktail	Roche	Cat# 04693116001
EGF (Epidermal Growth Factor)	Provitro	Cat# 1325950499
Human FGF-2, premium grade	Miltenyi	Cat# 130-093-841
Bovine Serum Albumin	Sigma-Aldrich	Cat# A7906
Triton X 100	Carl Roth	Cat# 3051
Propidium Iodide	Invitrogen	Cat# P3566
ECM Gel	Sigma-Aldrich	Cat# E1270
VECTASHIELD Antifade Mounting Media	Vector Laboratories	Cat# H-1200
Eukitt Quick-hardening mounting medium	Sigma-Aldrich	Cat# 03989
Critical Commercial Assays		
PrimeFlow RNA Assay Kit	Thermo Fisher Scientific	Cat# EB16488
Comet Assay Kit	Abcam	Cat# Ab238544
SMARTer RACE 5'/3' Kit	Takara	Cat# 634858
Superscript III Reverse Transcriptase kit	Invitrogen	Cat# 18080044
Fast SYBR Green Master Mix kit	Thermo Fisher Scientific	Cat# 4385612
Agilent RNA 6000 Pico Kit	Agilent Technologies	Cat# G2938-90049
DNeasy Blood & Tissue Kits	Qiagen	Cat# 69504
NucleoSpin Gel and PCR Clean-up	Macherey-Nagel	Cat# 740609.250
Phusion Hot Start II DNA Polymerase	Thermo Fisher Scientific	Cat# F-549L
NEBuilder HiFi DNA Assembly Master Mix	New England Biolabs (NEB)	Cat# E2621S
LIVE/DEAD Fixable Near-IR Dead Cell Stain Kit	Thermo Fisher Scientific	Cat# L34975
Zombie NIR Fixable Viability Kit	Biolegend	Cat# 423105
BD PharmingenT BrdU Flow Kit	BD Bioscience	Cat# 559619
CloneJET PCR Cloning Kit	Thermo Fisher Scientific	Cat# K1231
Experimental Models: Cell Lines		
HEK293T	ATCC	Cat# CRL-11268; RRID:CVCL_1926

U251	NCI-DTP	Cat# U-251; RRID:CVCL_0021
LN229	ATCC	Cat# CRL-2611; RRID:CVCL_0393
Human: NCH601	Dr. Christel Herold-Mende	(Campos et al., 2010)
Human: NCH421k	Dr. Christel Herold-Mende	(Campos et al., 2010)
Human: NCH644	Dr. Christel Herold-Mende	(Campos et al., 2010)
Human: NCH465	Dr. Christel Herold-Mende	(Campos et al., 2010)
Human: hNSC100	NsGene	(Villa et al., 2000)
Experimental Models: Organisms/Strains		
Female Swiss Nude MOUSE (42-48 days)	Charles River Laboratories	Cat# 620SWISSNUDE; RRID: MGI:5649767
Oligonucleotides		
Primers for real time PCR, PCR, and RACE-PCR assays	This study	Table S1
sgRNAs	This study	Table S1
shRNAs	This study	Table S1
UBR5-AS1 (RADAR) PrimeFlow Probe Set	Thermo Fisher Scientific	Cat# PF-204, Assay ID: VA1-3024684-PF
EF1 α PrimeFlow Probe Set	Thermo Fisher Scientific	Cat# PF-204, Assay ID: VA1-10418-PF
Other		
PrimeSurface 3D culture: Ultra-low Attachment 384 well Plate	S-BIO	Cat# #MS-9384UZ
NuPAGE 4 to 12%, Bis-Tris, 1.0 mm, Mini Protein Gel, 12-well	Invitrogen	Cat# NP0322BOX
iBlot 2 Transfer Stacks, nitrocellulose	Invitrogen	Cat# IB23002
Thermo Scientific SuperFrost Plus Adhesion slides	Thermo Fisher Scientific	Cat# J1800AMNZ
96-well Bio-Dot Microfiltration Apparatus	Bio-Rad	Cat# 1706545
Bioruptor sonication system	Diagenode	Cat# UCD-200
Recombinant DNA		
pLKO.1neo	Addgene	Cat# 13425
pcDNA3.1(-)	Invitrogen	Cat# V79520
pMD2.G	Addgene	Cat# 12259

pCMVR8.74	Addgene	Cat# 22036
pCDH-CB-IRES-copGFP-T2A-Puro	Addgene	Cat# 72299
pCW57-MCS1-2A-MCS2	Addgene	Cat# 71782
pCDH-EF1 α -MCS-IRES-Puro	Systems Biosciences	Cat# CD532A_2
lenti MS2-P65-HSF1_Hygro	Addgene	Cat# 61426
lenti dCAS-VP64_Blast	Addgene	Cat# 61425
lenti sgRNA(MS2)_zeo backbone	Addgene	Cat# 61427
lentiGuide-Puro	Addgene	Cat# 52963
pHR-SFFV-KRAB-dCas9-P2A-mCherry	Addgene	Cat# 60954
pCDH-EF1-MCS-BGH-PGK-copGFP-T2A-Puro	This study	N/A
pCDH-EF1-RADAR-BGH-PGK-copGFP-T2A-Puro	This study	N/A
pCDH-EF1-RADAR*1-BGH-PGK-copGFP-T2A-Puro	This study	N/A
pCDH-EF1-RADAR*2-BGH-PGK-copGFP-T2A-Puro	This study	N/A
lenti sgRNA(MS2)-puro	This study	N/A
pCDH-EF1-Krab-dCas9-P2A-Blast	This study	N/A
Software and Algorithms		
ImageJ	NIH	Version 1.52a https://imagej.nih.gov/ij/
Prism	GraphPad Software Inc.	Version 8.0.1
QuantStudio 5 Real-Time PCR System Software	Applied Biosystems	Version 1.5.0
Comet Assay IV	Instem	Version 4.3
ZEN 2.3 SP1 (Black)	ZEISS	Version 14.0.0.201
IncuCyte ZOOM	EssenBioScience	Version 2018A/ 6.2.9200.0
Image Studio Lite	LI-COR Biosciences	Version 5.2
IDEAS Softwar	EMD Millipore	Version 6.2

Experimental Model and Subject Details

3D GBM Stem-like Cells (GSCs) Cultures

The 3D GBM stem-like cells (GSCs) NCH601, NCH421k, and NCH465 were cultured in DMEM-F12 medium (Lonza, Switzerland) supplemented with 1x BIT-100 (Provitro, Germany), 2 mM Ultra Glutamine (Lonza, Switzerland), 1 U/ml Heparin (Sigma-Aldrich, USA), 20 ng/ml FGF (Miltenyi, Germany), 20 ng/ml EGF (Provitro, Germany), and 30 U/ml Pen-Strep. Whereas, the NCH644 and hNSC 100 cells were cultured in Neurobasal medium (Gibco, USA) supplemented with 2% (v/v) B-27 (Gibco, USA), 4 mM Ultra Glutamine (Lonza, Switzerland), 1 U/ml Heparin (Sigma-Aldrich, USA), 20 ng/ml FGF (Miltenyi, Germany), 20 ng/ml EGF (Provitro, Germany), and 30 U/ml Pen-Strep. GSCs were mechanically dissociated and then passaged when sphere size reached 200-300 μm .

Plasmids Construction

Plasmids for RADAR Overexpression

RADAR overexpression or control plasmids were constructed from (pCDH-CB-IRES-copGFP-T2A-Puro) empty backbone (Addgene, USA). Briefly, the BGH terminator was amplified from pcDNA3.1(-) vector (Invitrogen, USA) and the human PGK promoter was amplified from (pCW57-MCS1-2A-MCS2) plasmid (Addgene, USA). The IRES element of the plasmid (pCDH-CB-IRES-copGFP-T2A-Puro) was replaced with the BGH terminator followed by the human PGK promoter using the NEBuilder HiFi DNA Assembly Master Mix (NEB, USA) to create pCDH-CB-MCS-BGH-PGK-copGFP-T2A-Puro. The CB promoter was exchanged with the EF1 promoter from (pCDH-EF1 α -MCS-IRES-Puro) plasmid (System Biosciences, USA) to create pCDH-EF1-MCS-BGH-PGK-copGFP-T2A-Puro using Clal and NotI restriction enzymes. The RACE product for RADAR (**Appendix 1**) was then cloned 5' of the EF1 promoter to obtain pCDH-EF1-RADAR-BGH-PGK-copGFP-T2A-Puro plasmid that is used in this study. Plasmid constructs were sequenced by Sanger sequencing (LGC genomics, Germany). Oligos used are listed in (**Table S1**).

Plasmids for RADAR Deletion Constructs

RADAR*1 "third exon only" (**Appendix 4**) and RADAR*2 "3' deletion" (**Appendix 5**) constructs were prepared from pCDH-EF1-RADAR-BGH-PGK-copGFP-T2A-Puro plasmid. The third exon of RADAR was amplified using primers (**Table S1**), and the 3' deletion plasmid of RADAR was amplified using primers (**Table S1**). pCDH-EF1-RADAR-BGH-PGK-copGFP-T2A-Puro plasmid and PCR fragments were digested with NheI and BamHI restriction enzymes and ligated to obtain pCDH-EF1-RADAR*1-BGH-PGK-copGFP-T2A-Puro and pCDH-EF1-RADAR*2-BGH-PGK-copGFP-T2A-Puro plasmids respectively.

Plasmids for MGMT Knockdown

pLKO.1neo plasmid (Addgene, USA) with neomycin resistance gene was used for expressing MGMT-targeting shRNA or SCR-shRNA as control. DNA sequences (**Table S1**) as reported by (Viel et al., 2013) were cloned between Age I and EcoR I sites followed by ligation.

Plasmids for CRISPR/dCas9 Synergistic Activation Mediator (SAM) system (CRISPRa)

The three plasmid based on CRISPR/dCas9 Synergistic Activation Mediator (SAM) system described by (Konermann et al., 2015) were used for CRISPR activation (CRISPRa). plenti MS2-P65-HSF1_Hygro plasmid (Addgene, USA) and plenti dCAS-VP64_Blast plasmid (Addgene, USA) were used as described. The guide plasmid was modified by ligating the 2.5 kbp U6 promoter sgRNA(MS) NotI+XhoI fragment from lenti sgRNA(MS2)_zeo backbone (Addgene, USA) into lentiGuide-Puro (Addgene, USA) to obtain lenti sgRNA(MS2)-puro.

Plasmids for CRISPR/dCas9 Transcription Repression system (CRISPRi)

KRAB-dCAS9_P2As-mCherry fragment was excised from HR-SFFV-KRAB-dCas9-P2A-mCherry plasmid (Addgene, USA) via EcoRI and Sall restriction sites and cloned into pCDH-EF1-MCS-IRES-Neo (System Biosciences, USA) to obtain plasmid pCDH_KRAB-dCAS9-P2A-mCherry. P2A-Blast fragment was amplified using specific primers (**Table S1**) from plenti dCAS-VP64_Blast plasmid (Addgene, USA) and cloned via BamHI and NotI restriction enzyme sites into pCDH_KRAB-dCAS9-P2A-mCherry plasmid to obtain pCDH-EF1-P2ABlast. KRAB-dCAS9 plasmid was excised from pCDH_KRAB-dCAS9-P2A-mCherry via BamHI restriction sites and ligated into pCDH-EF1-P2ABlast to obtain pCDH-EF1-Krab-dCas9-P2A-Blast that is used in this study.

Plasmids for sgRNA Expression

sgRNA Oligonucleotides (**Table S1**) were annealed and ligated into guide plasmids lentiGuide-Puro (Addgene, USA) or lenti sgRNA(MS2)-puro (This study, see above), which were digested with BsmBI restriction enzyme.

Lenti viral Vector (LV) Production and Transduction

HEK293 cells were used for LV production. Briefly, at day 1 (5×10^5) cells were seeded in DMEM medium (Lonza, Switzerland) supplemented with 10% FBS, 2 mM Ultra Glutamine (Lonza, Switzerland), and 30 U/ml Pen-Strep and incubated in a tissue culture incubator at 37 °C for 24 h. At day 2, the medium was removed and replaced with DMEM medium (Lonza, Switzerland) supplemented with 2 mM Ultra Glutamine (Lonza, Switzerland) and 2% FBS followed by adding the transfection mix solution containing 125 μ l Optimem medium (Gibco, USA), 0.4 μ g of pMD2.G plasmid expressing the lentiviral VSV-G envelope (Addgene, USA),

0.73 µg of the lentiviral pack pCMVR8.74 plasmid (Addgene, USA), 1.1 µg of the purified plasmid of interest, and 2.5 µl of X-tremeGENE HP DNA transfection reagent (Roche, Switzerland). At day 3 the medium was removed and replaced with DMEM medium (Lonza, Switzerland) supplemented with 2 mM Ultra Glutamine (Lonza, Switzerland) and 2% FBS. At day 4, viral particles were harvested by collecting the medium, centrifuged, and filtered through 0.45 µm cellulose filter. GSCs were transduced by adding 500 µl of lentivirus on previously seeded GSCs in a T25 flask at the density of 2×10^5 cells/well at day 1. Medium was refreshed at day 2, and the selection with antibiotics Puromycin (Sigma-Aldrich, USA) for *RADAR* overexpression and G418 (Invivogen, USA) for MGMT knockdown started at day 5 for 7 days.

Transient cell Transfection

U251 and LN229 adherent GBM cells were seeded (1×10^4 cells/ well) in 6-well plate in DMEM medium (Lonza, Switzerland) supplemented with 10% (v/v) FBS, 2 mM Ultra Glutamine (Lonza, Switzerland), and 30 U/ml Pen-Strep and incubated in a tissue culture incubator at 37 °C for 24 h. At day 2, the medium was removed and replaced by 1 ml DMEM medium (Lonza, Switzerland) supplemented with 2 mM Ultra Glutamine (Lonza, Switzerland) and 2% FBS followed by adding the transfection mix solution which was prepared and incubated previously for 20-30 minutes at RT and containing 250 µl Optimem medium (Gibco, USA), 2.5 µl of X-tremeGENE HP DNA transfection reagent (Roche, Switzerland), and 2 µg of the purified plasmid of interest. After 3 h, the medium was completed by adding 2 ml of DMEM medium (Lonza, Switzerland) supplemented with 10% (v/v) FBS, 2 mM Ultra Glutamine (Lonza, Switzerland), and 30 U/ml Pen-Strep.

3D GBM Stem-like Cells (GSCs) Drug Treatment

GSCs were seeded and kept in culture for 72 h before starting the treatment. Temozolomide (TMZ) (Sigma-Aldrich, USA) and Cytarabine (ARA-C) (Merck, USA) were dissolved in DMSO to prepare a stock solution of 0.1 M TMZ and 0.01 M ARA-C. TMZ and ARA-C were added to GSCs for a final concentration of (500 µM) TMZ and (0.1-10 µM) ARA-C then incubated for 24 h except elsewhere specified. Cisplatin (Sigma-Aldrich, USA) was prepared extemporaneously in 0.9% NaCl to prepare a stock solution of 0.05 M, and cells were treated for a final concentration of (25 µM) for 4 h except elsewhere specified. GSCs were then mechanically dissociated and washed twice in cold PBS before subsequent assays.

Single 3D GBM-Spheroid Assay

GSCs were mechanically dissociated for single-cell suspension seeding in PrimeSurface 3D culture 384 well plate (S-BIO, Singapore) of 250 cells/well. Plate was then centrifuged at 300 g and incubated at 37 °C for 24 h to facilitate single sphere formation. At day 2, TMZ (Sigma-Aldrich, USA) was added to the wells and the plate transferred to the IncuCyte live-cell imaging

instrument. Images for each well were recorded with both phase contrast and GFP fluorescence every 4 h for a total duration of time up to 60 h using 10x magnification. The total fluorescent area ($\mu\text{m}^2/\text{well}$) of each formed GBM-Sphere at a given time point was used to calculate spheroid growth over time (at least 3 spheres per biological replicate).

Multi-color flow cytometry

TMZ or vehicle were added 24 h or 6 h prior analysis. For proliferation assay, BrdU incorporation was performed for 6 h before the end of the experiment. Prior to fixation, cells were dissociated and incubated with the IR-LIVE/DEAD Fixable Dead Cell Stain (ThermoFisher scientific; 1 $\mu\text{g}/\text{ml}$, USA). Cells were fixed, permeabilised and stained with the BD Pharmingen BrdU Flow Kit (BD Bioscience) according to the manufacturer's instructions. The following conjugated antibodies were used: anti H2AX-Phospho Ser139-Alexa Fluor 647 (BD Biosciences, 560447), anti-ATM-PhosphoSer1981-PE (Millipore, FCMAB110P). DNA was counterstained with DAPI (1 $\mu\text{g}/\text{ml}$) and anti-BrDU-PerCP-Cy5.5 (BD, 560809 kit). Data were acquired on a on a FACS Aria™ SORP cytometer (BD Biosciences) and analysed with Diva (BD Biosciences) and FlowJo software.

Cell Cycle Analysis by Flow Cytometry

Cells ($2-3 \times 10^6$) were seeded and cultured at 37 °C for 48 h. Distinct cell cycle populations were obtained by double-thymidine block and release method. To this end, 2 mM thymidine (Sigma-Aldrich, USA) was added to the cells for 18 h. Cells were washed with pre-warmed PBS and then fresh media was added to release the cells for 9 h. A second round of 2 mM thymidine was performed for 18 h then cells were released as before and were collected at different time points for cell cycle analysis, RNA extraction, and gene expression analysis. For the discrimination of early-mid-late from each cell cycle phases, cells were cultured for 24 h in the presence of 2.5 mM thymidine, for 12 h in normal medium, and blocked again for 24 h in the presence of 2.5 mM thymidine. Normal medium was then used for the release and Nocodazol (Sigma-Aldrich, USA) was added to the medium for a final concentration of 40 ng/ml to enrich for G2/M population and cells were collected at different time points for cell cycle analysis. Flow cytometry cell cycle analysis was done using the BD FACSCanto instrument (BD Biosciences, USA). Cells from each collected time point were taken and resuspended in PBS, stained with Zombie NIR dye (Biolegend, USA) to differentiate live/ dead cells, then fixed with cold 70% ethanol for at least 30 min at -20 °C. Fixed cells were collected by centrifugation and the DNA was stained using 1 ml of PBS solution containing 1 $\mu\text{g}/\text{ml}$ PI (Invitrogen, USA) in 0.1% Triton X-100 (Carl Roth, Germany) and 200 μg of DNase-free RNase A (Roche, Switzerland) for 30 min at RT in the dark prior analysis.

High Through-put Immuno FISH by Imaging Flow Cytometry

RNA imaging flow cytometry was performed using PrimeFlow RNA Assay Kit (Thermo Fisher Scientific, USA) according to the manufacturer's protocol and as described in (Soh and Wallace, 2018). Cells were stained with BV510 mouse anti-human CD90 cell surface marker antibody (RRID: AB_2737987, BD Biosciences, USA) and V510 rat IgG2b, κ isotype (RRID: AB_2869437, BD Biosciences, USA) as control then fixed, permeabilized, and stained with PrimeFlow RNA probes Alexa Fluor 647 targeting *RADAR* (VA1-3024684-PF, Thermo Fisher Scientific, USA) or *EF1 α* (VA1-10418-PF, Thermo Fisher Scientific, USA) as control. The DNA was stained using PBS solution containing 1 μ g/ml PI (Invitrogen, USA). Events were recorded using Amnis ImageStream instrument (Luminex, USA) at 60x magnification. Unstained, single-stained, and Fluorescence Minus One (FMO) stained samples were collected for each experiment as controls. Analysis was performed using IDEAS software (EMD Millipore, USA) to measure the RNA intensity in the cell. For the determination of cellular localization, features on IDEAS software were used to create and design masks on the basis of DNA and RNA fluorescence images to calculate the overlap of signals between them.

Immunofluorescence Microscopy

ECM gel (Sigma-Aldrich, USA) 1:10 dilution in medium was used to coat glass coverslips by applying 80 μ l on the top surface of the coverslip and incubating at 37 °C for 4h. 5×10^3 to 10×10^3 of non-adherent GSCs were then seeded on the precoated glass coverslips and grown at 37 °C for 72h. Cells were fixed with 4% paraformaldehyde for 15 minutes at RT and permeabilized with 0.5% Triton X-100 (Carl Roth, Germany) in PBS for 15 minutes at RT. Non-specific sites were blocked by 1h incubation using (10% FBS, 0.3% Triton X-100) in PBS, and then stained for 2-3h with rabbit monoclonal anti- P-Histone H2A.X (Ser139) antibody (1:400 dilution, RRID:AB_2118009, Cell Signalling Technology, USA), rat monoclonal anti-RPA32/RPA2 antibody (1:200 dilution, RRID: AB_2238543, Cell Signalling Technology, USA), rabbit monoclonal anti-53BP1 antibody (1:100 dilution, RRID:AB_722497, Abcam, UK), or mouse monoclonal anti- β Tubulin III antibody (1:100 dilution, RRID: AB_2210524, Millipore, USA) diluted in PBS containing (2% FBS, 0.3% Triton X-100). After washing the coverslips with 0.3% Triton X-100 in PBS, cells were incubated for 2h with goat anti-rabbit IgG secondary antibody, Alexa Fluor 647 (1:500 dilution, RRID: AB_2535812, Invitrogen, USA), or goat anti-rat IgG secondary antibody, Alexa Fluor 555 (1:500 dilution, RRID: AB_2535855, Invitrogen, USA) diluted in PBS containing (2% FBS, 0.3% Triton X-100). Coverslips were washed with 0.3% Triton X-100 in PBS, dried and embedded in Vectashield *mounting* medium (Vector Laboratories, USA) containing DAPI for nuclei staining. Images were recorded on a laser scanning confocal microscope (LSM880 FastAiry, Carl Zeiss) equipped with a x63/1.4 numerical aperture (NA) oil immersion Plan-Apochromat objective for cell imaging. All pictures

were acquired with multitrack configuration with a confocal optical slice set at 1 μm thickness and quantified with ImageJ software.

Comet Assay

Neutral comet assay was performed using the Comet Assay Kit (Abcam, UK). 500×10^3 GSCs were seeded and grown at 37 °C for 72 h before being treated for 24 h with 500 μM TMZ or DMSO as a control. After centrifugation at 4 °C at 500 g for 3 min, cell pellets were washed twice with cold PBS then resuspended in cold PBS at 100×10^3 cells/ml and kept on ice in the dark. Low melting agarose gel was heated in a water bath at 95 °C for 20 min then cooled to a 37 °C in a water bath for 20 min. Slides were prepared in duplicates for each condition by adding 70 μL of comet agarose per well onto the slide to create a base layer then transferred to 4 °C for 15 min. Samples were combined with comet agarose at 1/10 ratio (v/v), mixed and 75 μL / well was immediately added onto the top of comet agarose base layer and left at 4 °C in the dark for 15 min. Slides were immersed in lysis buffer for 30-60 min at 4 °C in the dark then transferred to an alkaline solution for 30 min at 4 °C in the dark and washed twice with TBE electrophoresis solution. Slides were submitted to gel electrophoresis by immersing them in TBE solution for 10-15 min at 30 V power. Slides were then washed 3 times with deionized H_2O followed by 70% ice-cold ethanol wash for 5 min. After drying, slides were stained by adding 100 μL / well of 1x vista green DNA dye (Abcam, UK) at RT for 15 min then visualized at 10x magnification by epifluorescence microscope. DNA damage was quantified in at least 50 comets/ each biological replicate ($n=3$) by measuring the displacement between the comet head and the resulting tail. Comet assay analysis was performed using Comet Assay IV software (Instem, UK). All buffers kept cold in ice before use.

Dot blot Measurement of 1,2-Pt-(GpG) Adducts

After 4 hours of Cisplatin treatment, cells were harvested then washed twice in cold PBS followed by genomic DNA extraction using the DNeasy Blood & Tissue Kit (Qiagen, Germany) according to manufacturer's instruction. DNA concentration was quantified by NanoDrop and DNA samples were denatured by adding 2x DNA denaturing Buffer (200 mM NaOH, 20 mM EDTA) and incubating at 95°C for 10 min. 20x Saline-sodium citrate (SSC) buffer (3.0 M NaCl, 0.3 M Sodium Citrate, pH to 7.0) was then added to the DNA samples, which are applied onto a nitrocellulose membrane pre-wetted with 10x SSC buffer using a 96-well Bio-Dot Microfiltration Apparatus (Bio-Rad, USA). The membrane was then baked for 2h at 80°C, blocked with 5% non-fat milk in TBS containing 0.1% Tween-20 (TBS-T), and incubated with rat monoclonal anti-Cisplatin modified DNA antibody (1:1000, RRID:AB_10715243, Abcam, UK) diluted in TBS-T with 5% (w/v) BSA overnight at 4°C. The membrane was washed three times with TBS-T and incubated for 1h with IRDye 800CW Goat anti-Rat IgG secondary antibody (1:5000, RRID:AB_2721932, LI-COR Biosciences, USA) diluted in blocking buffer.

Visualization of signals was done using Odyssey CLx Imaging system (LI-COR Biosciences, USA) at 800 nm and then quantitatively assessed using Image Studio Lite software (LI-COR Biosciences, USA).

Metaphase Chromosome Spread

GSCs were seeded (750×10^3) and kept at 37 °C for 48h before adding 0.5 µg/ml of colchicine (Sigma-Aldrich, USA) for 24h. Cells were then mechanically dissociated, harvested, and resuspended in a pre-warmed hypotonic solution (KCl 0.075M) for 20 min at 37 °C. Cells were subsequently fixed twice with freshly made Carnoy's buffer (1:3 acetic acid:methanol), each time for 10 min at room temperature (RT) and pelleted. Pellets were resuspended in 1 ml of cold Carnoy's buffer before being dropped onto a tilted clean slide from a distance. Slides were then submitted to the steam of a water bath pre-warmed into 65 °C. Slides were air dried and stained for 20 min with Giemsa's azur eosin methylene blue (Merck, USA) (1:20 dilution in H₂O). Slides were rinsed with water and air dried. Slides were then mounted in Eukitt mounting medium (Sigma-Aldrich, USA). Chromosome spreads from individual cells were imaged by light microscopy. At least 50 metaphases per biological replicate were blindly scored.

Western Blot

Cell pellets were washed twice in cold PBS and lysed in RIPA buffer (Millipore, USA) supplemented with PhosSTOP and cOmplete Protease Inhibitor Cocktail as phosphatases and proteases inhibitors (Roche, Switzerland). Samples were sonicated using Bioruptor sonication system (Diagenode, Belgium) at 160 W power for 10 min at 4 °C in intermittent pulses (30 sec on, 30 sec off), and centrifuged at 16.000g for 15 min to remove debris. 20 µg of total protein extract were loaded per lane, separated using precast 4-12% NuPAGE Bis-Tris gels (Invitrogen, USA) and transferred to iBlot nitrocellulose membrane (Invitrogen, USA) according to standard protocols. Membranes were blocked with 5% non-fat milk in Tris-buffered saline containing 0.1% Tween-20 (TBS-T) for 1h at RT. Membranes were incubated with primary antibody against mouse monoclonal anti-MGMT (1:1000 dilution, RRID: AB_2281919, Chemicon, Germany) diluted in TBS-T with 5% (w/v) BSA overnight at 4°C. The rabbit monoclonal anti-β Actin (1:10,000 dilution, RRID: AB_2223172, Cell Signalling Technology, USA) was used as a loading control. Membranes were washed three times with TBS-T for 5 minutes, incubated for 1 h with mouse or rabbit secondary HRP conjugated antibodies diluted in TBS-T (1:10,000 dilution; RRID:AB_772210, RRID: AB_2313567), washed three times with TBS-T for 5 minutes, and developed using SuperSignal West Pico PLUS chemiluminescent substrate (Thermo Fisher Scientific, USA). The chemiluminescent signal was detected using a CCD imaging system (Image Quant LAS4000, GE Healthcare, USA).

RNA Extraction, qPCR, and Gene Expression Analysis

Cell pellets were washed twice in cold PBS and RNA extraction was performed using TRIzol (Invitrogen, USA) according to standard protocols. 10 µg of RNA was treated with TURBO DNase (Invitrogen, USA) for 30 min at 37 °C and precipitated using 3 M sodium acetate (Sigma-Aldrich, USA), 20 µg of glycogen (Invitrogen, USA), and 100% ethanol at -80 °C overnight. RNA sample quality was checked by on-chip electrophoresis on Agilent 2100 Bioanalyzer using Agilent RNA 6000 Pico kit (Agilent Technologies, USA) following manufacturer's protocol. RNAs were reverse transcribed (RT) using SuperScript III Reverse Transcriptase Kit (Invitrogen, USA) with oligo dT primers. RT-qPCR analyses were performed using Fast SYBR Green Master Mix kit (Thermo Fisher Scientific, USA) for 40 cycles using the QuantStudio 5 or Viiia 7 instruments and QuantStudio software (Applied Biosystems, USA). To determine gene expression, the difference (ΔC_t) between the threshold cycle (C_t) of each gene and that of the reference gene was calculated. Relative quantification values were calculated as the fold-change expression of the gene of interest over its expression in the reference sample, by the formula $2^{-\Delta\Delta C_t}$. *Ezrin* or *EF1 α* were used as housekeeping genes. RT-qPCR primers are listed in (Table S1).

Subcellular Fractionation

Subcellular fractionation was performed as described in (Gagnon et al., 2014). Briefly, cell pellets were gently resuspended in ice-cold Hypotonic Lysis Buffer (HLB) (10 mM Tris-HCl (pH 7.5), 10 mM NaCl, 3 mM MgCl₂, 0.3% (v/v) NP-40, and 10% (v/v) glycerol) supplemented with RNaseOUT (Invitrogen, USA), and incubated on ice for 10 min. After centrifugation at 1,000g for 3 min, the supernatant (cytoplasmic fraction) was gently transferred to a new tube and RNA Precipitation Solution (RPS) added immediately (0.5 ml of 3 M sodium acetate (pH 5.5) with 9.5 ml of ethanol) then stored at -20 °C. Pellets (semipure nuclei) from the previous step were washed 3 times with ice-cold HLB then Modified Wuarin-Schibler buffer (MWS) (10 mM Tris-HCl (pH 7.0), 4 mM EDTA, 0.3 M NaCl, 1 M urea, and 1% (v/v) NP-40) was added supplemented with RNaseOUT (Invitrogen, USA). Nuclei in MWS were vortexed and the mixture was set on ice for 5 min and then centrifuged at 200g for 2 min. Supernatant (nucleoplasmic fraction) was gently transferred to a new tube and RPS was added immediately and stored at -20 °C. Pellets (chromatin) from the previous step were washed 3 times with MWS and centrifuged at 1,000g for 3 min. TRIzol (Invitrogen, USA) was added to the chromatin pellets, vortexed and stored at -20 °C. Samples that have been incubated in RPS at -20 °C were centrifuged at 18,000g for 5 min, the pellets were washed with ice-cold 70% ethanol, and TRIzol (Invitrogen, USA) was added to the pellets. 10 µl of 0.5 M EDTA was added to the samples in Trizol and heated to 65 °C with vortexing until the pellet is dissolved. Chloroform:isoamyl alcohol (24:1) was added, then RNA was extracted as described before.

RNAs purified from nuclear and chromatin fractions were treated with TURBO DNase (Invitrogen, USA) as described before. cDNA was then generated and analyzed by RT-qPCR as described above. *MALAT1*, *NEAT1* and *GAPDH* were used as reference genes for the relative determination of RNA subcellular localization. Primers used in the study are listed in (Table S1).

5' and 3' RACE

Total RNA was isolated from hNSC100 using TRIzol (Invitrogen, USA) and treated with TURBO DNase (Invitrogen, USA) as described before. 5' and 3' RACE were performed with the SMARTer RACE 5'/3' Kit (Takara, Japan) using gene specific primers (Table S1) according to the instructions of the manufacturer. PCR products were separated on agarose gels. After gel extraction using the NucleoSpin Gel and PCR Clean-up kit (Macherey-Nagel, Germany) following manufacturer's protocol, PCR products were cloned using CloneJET PCR Cloning Kit (Thermo Fisher Scientific, USA) and subsequently sequenced by Sanger sequencing (LGC genomics, Germany).

Polymerase Chain Reaction (PCR) and Transcript Variant Detection

RNA extraction and cDNA synthesis were performed as described before. PCR amplification was done with isoform specific primers (Table S1) for 45 cycles using the Phusion Hot Start II DNA Polymerase (Thermo Fisher Scientific, USA) following manufacturer's protocol. Amplified products separated by agarose gel electrophoresis and visualized by ethidium bromide staining.

RNase R treatment and circRNA detection

Total RNA was extracted using TRIzol (Invitrogen, USA) as described before. Samples were then treated with RNase R (Lucigen, USA) 1U per 1µg of total RNA for 10 minutes at 37°C. After the validation of successful RNA degradation by on-chip electrophoresis on Agilent 2100 Bioanalyzer using Agilent RNA 6000 Pico kit (Agilent Technologies, USA), the RNA was reverse transcribed using SuperScript III Reverse Transcriptase Kit (Invitrogen, USA) with gene specific primer (Table S1). CircRADAR was amplified by PCR as described before using divergent primers (Table S1). Amplified products were loaded on 0.8% agarose gel and separated by electrophoresis then visualized by ethidium bromide staining.

Animal Experiments

GSCs (NCH421k or NCH644) (50×10^3 cells per mouse in DMEM medium) were implanted in the brain of Female Swiss Nude Mice (42-48 days) (Charles River Laboratories, France) using a Hamilton syringe (Hamilton, USA), then tumor development was monitored once (for NCH421k) or twice (for NCH644) a week by MRI. 8 mice were implanted with NCH421k cells

overexpressing *RADAR* and 8 mice were implanted with NCH421k cells containing an empty vector as control. To check *RADAR* effect *in-vivo* upon TMZ treatment, 8 mice were implanted with NCH644 cells overexpressing *RADAR* and 8 mice were implanted with NCH644 cells containing an empty vector as control and received 2 weeks post implantation a TMZ dose (40 mg/kg) via oral gavage 5 times a week. The control untreated group (7 mice were implanted with NCH644 cells overexpressing *RADAR* and 7 mice were implanted with NCH644 cells containing an empty vector as control) received DMSO as a vehicle only. Animals were housed under specific- pathogen-free (SPF) conditions and sacrificed via cervical dislocation at the appearance of neurological (locomotor problems, uncontrolled movements), or behavioral abnormalities (prostration, hyperactivity) and weight loss. The handling of animals and the surgical procedures were performed in accordance with the regulations of the European Directive on animal experimentation (2010/63/EU). The experimental protocols were approved by the local authorities and ethical committees for Animal Welfare Structure of the Luxembourg Institute of Health (protocols: LRNO-2017-02 and LUPA2019/94).

Magnetic Resonance Imaging (MRI)

MRI was performed as described in (Golebiewska et al., 2020). MRI images were acquired on a 3T MR Solutions with a quadratic mouse head transmitter/receiver coil. Animals were anesthetized with 2.5% isoflurane, and placed lying prone in a cradle equipped with a heating pad set to 37°C and constantly monitored for breathing values. A Fast Spin Echo T2-weighted MRI sequence was applied, with field of view of 25 mm, matrix size of 256 × 256, TE of 68 ms, TR of 3000 ms, and slice thickness of 1 mm. MRI data were analyzed by ImageJ.

Coding Potential Analysis

Prediction of putative protein translation was evaluated using Open Reading Frame (ORF) finder from NCBI (Nishikawa et al., 2000). Coding potential calculation was based on coding probability from Coding Potential Assessment Tool (CPAT) (Wang et al., 2013a), coding potential score from Coding Potential Calculator (CPC) (Kong et al., 2007), and pyloCSF score (Lin et al., 2011). We set a minimal ORF = 90 nt for transcripts < 4 kb and 300 nt for transcripts > 4 kb. In the raw phyloCSF track we considered regions in which most codons have a score greater than 0 are likely to be protein-coding. *MALAT1* and *NEAT1* were used as control noncoding genes whereas *GAPDH* and β -*actin* as control protein-coding genes.

TCGA data analysis

Prediction of lncRNAs as potential prognostic markers were reported in reference (Du et al., 2013) and analysed using GEPIA and GETX data were used for normal tissue expression. The MGMT promoter methylation status was from reference (Bady et al., 2012). Cohort was divided

in two groups based on expression median for each lncRNA. Group expression was represented using Graph Pad Prism or extracted from GEPIA.

Statistical Analysis

All statistical analyses were conducted with GraphPad Prism (V. 8.0.1). In all studies, values are expressed as mean \pm standard error of the mean (SEM) and n represent the number of biological repeats. Statistical comparisons were based on two-tailed Student's t-test between the corresponding groups, except where otherwise stated. The data results of the single sphere growth curve were analyzed by calculating the linear regression for each condition with 95% confidence of the best-fit line. Differences were considered statistically significant at * $p < 0.05$, ** $p < 0.01$, *** $p < 0.001$, **** $p < 0.0001$, "ns" represents non significance.

DNA Fiber Assay

DNA fiber assays were performed as previously described (Carruthers et al., 2018). Briefly, cultured cells were sequentially pulse labelled with media containing CldU (25uMol/L) and IdU (250uMol/L) for 20 minutes and cell suspensions were pipetted and lysed onto glass slides. Resulting DNA fibers were spread by inclining the slide and immunostaining was performed. CldU was detected using anti-BrdUrd (rat) primary antibody (Abcam, ab6326, 1:400) and anti-rat alexa fluorophore 555 (Invitrogen, A21434, 1:500) secondary. IdU was detected using anti BrdUrd (mouse) primary antibody (BD, 347580, 1:500) and anti-mouse alexa fluorophore 488 (Invitrogen, A11017, 1:500).

RNA Sequencing and Bioinformatic Analysis

Total and Small RNA Sequencing to Identify TMZ-Transcriptional Regulatory Loops

Total RNA was extracted with Trizol according to manufacturer's protocol and quantified using Nanodrop. The quality of RNA was checked using a bioanalyzer (Agilent, USA). Total RNAs were depleted from Ribosomal RNAs using RiboMinus technology (ThermoFisher scientific, USA). RNA-seq libraries were prepared using TruSeq Stranded RNA Kits (Illumina, USA). Small RNA-Seq libraries were generated from total RNA using TruSeq Small RNA Library Prep Kit (Illumina, USA). HiSeq2500 instrument (Illumina, United States) was used to obtain single stranded sequencing reads and base calling was performed with CASAVA 1.8.2 pipeline (Illumina, USA). The following steps were performed as described in (Fritah et al., 2020). Fastq data and processed counts of RNA-seq and small RNA-seq are available through Gene Expression Omnibus (GSE98128).

RNA Sequencing to Investigate gene expression regulation in cis/trans following RADAR Overexpression

Total RNA was extracted with Trizol according to manufacturer's protocol and quantified using Nanodrop. The quality of RNA was checked using a bioanalyzer (Agilent, USA). Fastq files from paired-end strand specific of 75 nucleotides length have been quality checked with *FastQC* (<https://www.bioinformatics.babraham.ac.uk/projects/fastqc/>) for overall QCs and *FastQScreen* for potential library contamination (https://www.bioinformatics.babraham.ac.uk/projects/fastq_screen/). Reads were mapped to human genome (GRCh38) using *TopHat* (v. 2.1.1) (Kim et al., 2013) leading to a mapping rate of concordant pairs higher than 90% for each sample. Sorted *bam* files were counted with *htseq-counts* on exon features. Analysis of significantly expressed genes were conducted under *R* with the package *EdgeR*. The normalization factor was evaluated using the *TMM* method and genes with a FDR < 0.05 were considered as significant.

Systems approaches

The associations of TFs with genes, miRNAs, or lncRNAs were obtained from ChipBase (Yang et al., 2013). Associations between miRNAs and genes were obtained from StarBase (Li et al., 2014). Because the number miRNAs-lncRNAs associations in StarBase was small, we also integrated the miRcode database (Jeggari et al., 2012). As a result, the background regulatory network consisted of 1145815 regulations, including 107 TFs, 1851 mature miRNAs, 10970 lncRNAs, and 18812 genes. Detailed information is shown in Fig. 4B. Next, we mapped the differentially expressed genes, miRNAs, and lncRNAs of each cell line into the background network separately. We constructed the cell line-specific subnetworks by extracting the edges (observed expression correlation) between the DE nodes. We focused on three types of 3-node FFLs containing lncRNAs or mRNAs, and which included a TF, a miRNA and a target lncRNAs or mRNAs (Figure 4a and Figure Supplementary S4 respectively). In the first type, a TF regulates miRNA and lncRNA, and a miRNA regulates lncRNA. We termed it TF-mediated FFL. In the second type, miRNA-mediated FFL, a miRNA regulates TF and lncRNA, and a TF regulates lncRNA. In the third type, a miRNA and a TF are mutually regulated, and both regulate a lncRNA. We extracted all FFLs from the cell line-specific subnetworks using R-language scripts.

Table S1: List of oligonucleotides

Primers for qPCR		
Gene Name	Sequence	
	Forward	Reverse
UBR5-AS1 "RADAR" (universal)	CAACATACAGAAGCATGGAA CTA	AACAACATCCCTCCCATAAAGA
UBR5-AS1 "RADAR" (Iso 1)	CCAGTCGCCCGGCTT	GTAGGCTAAGCAGTCCAGAG
UBR5-AS1 "RADAR"(Iso 3)	GATCTCAAGGAGTAAGAGGAT TCTG	TTAAGGGGAGGTGTATCCAAGT
UBR5-AS1 "RADAR" (Iso 4)	ATTGAAGGCACTTCCAACCAG C	CTGAGAGCCAAACCTTTCCTAC
UBR5-AS1 "RADAR" (Iso 5)	GCAATGGATGATGATGTTGC	GTTATCCCATGGCTACGATG
UBR5-AS1 "RADAR" (Iso 6)	GGCTGGCTGAAGGATGGTAA	ACGCTATGGCAGGTTTGAGA
MALAT1	GGTAACGATGGTGTGCGAGGTC	CCAGCATTACAGTTCTTGAACAT G
NEAT1	CTTCCTCCCTTTAACTTATCCA TTCAC	CTTTCCTCCACCATTACCAACA ATAC
UBR5	TTAGGCTTTTGGTAAATGGCTG CG	TGAGGGCATAGGCTGGAATCCT TC
RRM2B	TTGGGCCTTGCATGGATAG	AGTGAGTCCTGGCATAAGACC
EZRIN	TGCCCCACGTCTGAGAATC	CGGCGCATATACAACCTCATG
EF1 α	TTGTCGTCATTGGACACGTAG	TGCCACCGCATTATAGATCAG
β -Actin	AGAGCTACGAGCTGCCTGAC	AGCACTGGTGTGGCGTACAG
GAPDH	CATGAGAAGTATGACAACAGC CT	AGTCCTTCCACGATACCAAAGT
MGMT	TTTTCCAGCAAGAGTCGTTAC	GGGACAGGATTGCCTCTCAT
CDC25C	GACACCCAGAAGAGAATAATC ATC	CGACACCTCAGCAACTCAG
CCNA2	AAGACGAGACGGGTTGC	GGCTGTTTACTGTTTGCTTTCC
TFAP2A	CTCCGCCATCCCTATTAACAAG	GACCCGGAAGTGAACAGAAGA
RPRRML	ACCTGCTCATCAAGTCCGAG	CAGATGGCGCTCAGTACAGC
Primers for PCR		
Gene Name	Forward	Reverse
UBR5-AS1 "RADAR" (Iso 1)	CCAGTCGCCCGGCTT	GTAGGCTAAGCAGTCCAGAG
UBR5-AS1 "RADAR"(Iso 3)	GATCTCAAGGAGTAAGAGGAT TCTG	TTAAGGGGAGGTGTATCCAAGT
UBR5-AS1 "RADAR" (Iso 4)	ATTGAAGGCACTTCCAACCAG C	CTGAGAGCCAAACCTTTCCTAC
UBR5-AS1 "RADAR" (Iso 5)	GCAATGGATGATGATGTTGC	GTTATCCCATGGCTACGATG
UBR5-AS1 "RADAR" (Iso 6)	GGCTGGCTGAAGGATGGTAA	ACGCTATGGCAGGTTTGAGA
UBR5-AS1 "RADAR" (Iso 8)	GTGAATGCGGAGTCTCGCTC	CTGTAATCCCAGCTATTCGG

UBR5-AS1 "RADAR" (Iso 10)	GCTGGTTTTAGTCTCGCTC	CTGTAATCCCAGCTATTCGG
UBR5-AS1 "RADAR" (Exon 3) for RADAR*1	TCTAGAGCTAGCGAATT TGTTTCAGAATCACCTGGGAT G	GATCATGGATCCGAAGAAACAA TAGTTTTTATTTATGTAGTTGTAC
UBR5-AS1 "RADAR" (3' deletion) for RADAR*2	CTCCACGCTTTGCCTGACCCT GCTT	CGAATTCCTGCAGCCCCGGGGAT CCTGCTACTACTATTTTTTTCCC TAAATCATCTGG
P2A-Blast fragment	GATCGGATCCGGCAGTGGAGA GGGCAGAG	GATCTAGCGGCCGCTTAGCCCT CCCACACATAACCAG
Primers for RACE PCR		
Gene Name	Sequence	Purpose
UBR5-AS1 "RADAR"	CCGGGCTCTAGCCACTTG	3' RACE GSP1
	CAGGCCGGCTCGAGATTC	3' RACE GSP2
	GCATTCCTCATCCTCTTGCCCTC CTTTCTGA	5' RACE GSP1
	TTCTGATTCAGTAAGTCTTTGG TGGAGGC	5' RACE GSP2
Primers for the detection of circRADAR		
Gene Name	Sequence	Purpose
UBR5-AS1 "RADAR"	AGGAGAAGGGTAAGGGGGAG GAAG	circRNA detection
	TTGTCATTCTCTGGCAAGCTTA TGGCATGG	circRNA detection
	TTGTCATTCTCTGGCAAGCTTA TGGCATGG	circRNA gene specific primer (GSP)
sgRNAs		
Gene Name	Sequence	Purpose
Control	GCTGAAAAAGGAAGGAGTTGA	Non targeting control 1 (NT1) (Konermann et al., 2015)
	GAAGATGAAAGGAAAGGCGTT	Non targeting control 2 (NT2) (Konermann et al., 2015)
UBR5-AS1 "RADAR"	GAGCTATCCCAGAGTCCGCG	sgRNA1 for CRISPRa
	GCAGTGGAAAGCCGGGCGAC T	sgRNA2 for CRISPRa
	GGGAGAAACCCTTAGGCCGC	sgRNA3 for CRISPRa
	GGGATCCCTTAGGCCGCAGT	sgRNA4 for CRISPRa
	GGAGACAGGGATAATCCCTT	sgRNA5 for CRISPRa
	GAGGCGTGGCTGGCAGAGGT	sgRNA6 for CRISPRa
	GCGGAAGCAGGGAGATTTCC	sgRNA7 for CRISPRa
	GAGTGGCTAGAGCCCCGGGGA	sgRNA1 for CRISPRi
	GAGGAGTGGGCGCCCGGAGT	sgRNA2 for CRISPRi
	GTGGCCCCACCTCACCTCAT	sgRNA3 for CRISPRi
	GTGGGATAGCTCCTCAGGAGT	sgRNA4 for CRISPRi
	GCTCCTCAGGAGTGGGCGCC	sgRNA5 for CRISPRi
GCGAGGCGAGGTGGGACGAG G	sgRNA6 for CRISPRi	

	GACGAGGCGGGGTGGTGAGC	sgRNA7 for CRISPRi
shRNAs		
Gene Name	Sequence	Purpose
MGMT	CCGGAAGCTGGAGCTGTCTGG TTGTTCAAGAGAACAACCAGA CAGCTCCAGCTTTTTTTG	shMGMT 1 (sense)
	AATTCAAAAAAGCTGGAGCT GTCTGGTTGTTCTCTTGAAACA ACCAGACAGCTCCAGCTT	shMGMT 1 (antisense)
	CCGGAAGCTGCTGAAGGTTGT GAAATTCAAGAGATTCACAAC CTTCAGCAGCTTTTTTTG	shMGMT 2 (sense)
	AATTCAAAAAAGCTGCTGAAG GTTGTGAAATCTCTTGAATTC ACAACCTTCAGCAGCTT	shMGMT 2 (antisense)
Control	CCGGAAGCTACCGTTGTTATA GGTGTTCAGAGACACCTATA ACAACGGTAGTTTTTTTTG	shSCR 1 (sense)
	AATTCAAAAAAGCTACCGTTG TTATAGGTGTCTCTTGAACACC TATAACAACGGTAGTTT	shSCR 1 (antisense)
Oligos for Sanger sequencing		
Serial	Sequence	Purpose
1	TCGGGATCCGCTAGCGTTTAA ACGCGGCCCGCCTGTGCCTTCT AGTTGCCAGCCATCTGTTGTT GCC	BGH forward for cloning
2	CAACCCCAACCCCCATAGAG CCCACCGCAT	Bgh rev with hPGK for cloning
3	TGGGCTCTATGGGGGGTTGGG GTTGCGC	hPGK forward with bGH for cloning
4	TCGCTCTCCATGGTGGATCTT GTGGCCAGCTGGGGAGAGAG GTCGGTGATTCG	hPGK rev for cloning
5	agCTAGCGAATTCGCCGGCTT TCCACTGAG	RADAR forward with NheI and EcoRI sites
6	gatcatggatccGAAGAAACAATAG TTTTTATTTATGTAGTTGTAC	RADAR reverse with BAMHI site

CHAPTER 4

RESULTS

Temozolomide-Induced RNA Interactome Uncovers Novel Long non-coding RNA Regulatory Loops in Glioblastoma

Sabrina Fritah, Arnaud Muller, Wei Jiang, Ramkrishna Mitra, Mohamad Sarmini, Monika Dieterle, Anna Golebiewska, Tao Ye, Eric Van Dyck, Christel Herold-Mende, Zhongming Zhao, Francisco Azuaje and Simone P. Niclou

Cancers (Basel). 2020 Sep; 12(9): 2583

doi: 10.3390/cancers12092583

RATIONALE

The first part of the result section represents a manuscript which is considered the basis for my main experimental work presented in (**Chapter 5**). The work here aimed to assess:

1. How does TMZ treatment affect the transcriptional reprogramming in GBM?
2. Are lncRNAs regulated upon TMZ treatment in GBM?
3. Identify TMZ-transcriptional regulatory loops which could provide novel potential targets of TMZ resistance in GBM.

In this study, we identified 22 lncRNAs differentially expressed upon TMZ treatment between GBM-sensitive and resistant cells that are also involved in transcriptional regulatory loops with other mRNAs and miRNAs. Using bioinformatic analyses and data integration from TCGA and other public datasets on our results, we predicted lncRNA potential functions in GBM. Several lncRNAs could represent novel prognostic marker for GBM patient survival and response to therapy. Our manuscript thus provides a novelty at the level of transcriptomic changes upon TMZ treatment in GBM and shed light on novel lncRNA-based predictors of chemosensitivity in GBM.

Personal contribution:

- Maintaining GSCs culture, drug treatment, extraction and quality control of the RNA.
- Proofreading of the manuscript.
- Validation of key genes and lncRNAs from the RNA-Seq data and the interactions among the crucial regulatory loop networks revealed in the manuscript. This part of the work is listed and discussed in “EXTENDED DATA” section, as it was not integrated in the published manuscript.



Article

Temozolomide-Induced RNA Interactome Uncovers Novel LncRNA Regulatory Loops in Glioblastoma

Sabrina Fritah ¹, Arnaud Muller ², Wei Jiang ³, Ramkrishna Mitra ³, Mohamad Sarmini ^{1,4}, Monika Dieterle ¹, Anna Golebiewska ¹, Tao Ye ⁵, Eric Van Dyck ⁶, Christel Herold-Mende ⁷, Zhongming Zhao ^{3,8}, Francisco Azuaje ^{1,2} and Simone P. Niclou ^{1,9,*}

¹ NORLUX Neuro-Oncology Laboratory, Department of Oncology, Luxembourg Institute of Health, Luxembourg L-1526, Luxembourg; sabrina.fritah@lih.lu (S.F.); mohamad.sarmini@lih.lu (M.S.); monika.dieterle@lih.lu (M.D.); anna.golebiewska@lih.lu (A.G.); francisco.azuaje@ucb.com (F.A.)

² Quantitative Biology Unit, Luxembourg Institute of Health, Luxembourg L-1526, Luxembourg; arnaud.muller@lih.lu

³ Department of Biomedical Informatics, Vanderbilt University Medical Center, Nashville, TN 37203, USA; biocjw@yahoo.com (W.J.); santu.bioinf@gmail.com (R.M.); zhongming.zhao@uth.tmc.edu (Z.Z.)

⁴ Faculty of Science, Technology and Medicine, University of Luxembourg, L-4365 Esch-sur-Alzette, Luxembourg

⁵ Institut de Génétique et de Biologie Moléculaire et Cellulaire (IGBMC), Centre National de la Recherche Scientifique, UMR7104, Institut National de la Santé et de la Recherche Médicale, U964, Université de Strasbourg, 67404 Illkirch, France; yetao@igbmc.fr

⁶ DNA Repair and Chemoresistance, Department of Oncology, Luxembourg Institute of Health, Luxembourg L-1526, Luxembourg; eric.vandyck@lih.lu

⁷ Experimental Neurosurgery, Department of Neurosurgery, University of Heidelberg, 69120 Heidelberg, Germany; h.mende@med.uni-heidelberg.de

⁸ School of Biomedical Informatics, The University of Texas Health Science Center at Houston, Houston, TX 77030, USA

⁹ Department of Biomedicine, University of Bergen, N-5009 Bergen, Norway

* Correspondence: simone.niclou@lih.lu; Tel.: +352-26970-273; Fax: +352-26970-390

Received: 17 July 2020; Accepted: 8 September 2020; Published: 10 September 2020



Simple Summary: Glioblastoma (GBM) is the most aggressive brain tumor and most resistant to therapy. The identification of novel predictive biomarkers or targets to counteract chemoresistance, requires a better understanding of the GBM primary response to therapy. The aim of our study was to assess the molecular response of GBM to the standard of care chemotherapy by temozolomide (TMZ). We established a comprehensive map of gene expression changes after treatment and discovered that GBM cells elicit a coordinated gene expression program after chemotherapy that differs between sensitive and resistant cells. We found that a novel class of genes expressed as long non-coding RNAs (lncRNAs) is involved in gene regulatory circuits in GBM and could represent novel markers of GBM patient prognosis. By shedding light on the involvement of the non-coding genome in GBM, our results may provide new mechanistic insight on lncRNAs and their importance in chemoresistance.

Abstract: Resistance to chemotherapy by temozolomide (TMZ) is a major cause of glioblastoma (GBM) recurrence. So far, attempts to characterize factors that contribute to TMZ sensitivity have largely focused on protein-coding genes, and failed to provide effective therapeutic targets. Long noncoding RNAs (lncRNAs) are essential regulators of epigenetic-driven cell diversification, yet, their contribution to the transcriptional response to drugs is less understood. Here, we performed RNA-seq and small RNA-seq to provide a comprehensive map of transcriptome regulation upon TMZ in patient-derived GBM stem-like cells displaying different drug sensitivity. In a search for regulatory mechanisms, we integrated thousands of molecular associations stored in public databases to generate a background “RNA interactome”. Our systems-level analysis uncovered a coordinated program of TMZ response reflected by regulatory circuits that involve transcription factors, mRNAs,

miRNAs, and lncRNAs. We discovered 22 lncRNAs involved in regulatory loops and/or with functional relevance in drug response and prognostic value in gliomas. Thus, the investigation of TMZ-induced gene networks highlights novel RNA-based predictors of chemosensitivity in GBM. The computational modeling used to identify regulatory circuits underlying drug response and prioritizing gene candidates for functional validation is applicable to other datasets.

Keywords: glioblastoma; temozolomide; lncRNA; regulatory circuit; chemoresistance; transcriptome

1. Introduction

Since the introduction of temozolomide (TMZ) [1] in 2005 as standard chemotherapy against glioblastoma (GBM) [2], no additional drug has been identified to effectively slow down GBM progression. Unfortunately, however, median patient survival remains dismal and resistance to TMZ is inevitable. The epigenetic regulation of the O-6-methylguanine-DNA methyltransferase (MGMT) gene is the only known determinant of the clinical response to TMZ [3–6], eventually however, both MGMT methylated and unmethylated GBM develop resistance to TMZ. Additional resistance mechanisms are being investigated, including alternative DNA repair pathways, receptor tyrosine kinase or tumor suppressor (TP53, PTEN) signaling [7,8].

As studies of the transcriptional changes induced by TMZ mainly assessed long-term changes following the selection of resistant clones, the primary impact of TMZ on the GBM transcriptome remains elusive [9]. Moreover, available gene expression studies have traditionally been performed on classical adherent serum-dependent GBM cell lines [10,11], while it has been recognized that patient-derived tumor cells grown as three-dimensional spheres (commonly called glioma stem cells, GSCs) represent improved GBM models that display cellular and molecular gradients relevant for drug response studies [12,13].

Advances in next-generation sequencing (NGS) have revealed the importance of long non-coding RNAs (lncRNAs) as major components of the human transcriptome [14]. lncRNAs are pleiotropic regulators of transcription, acting as transcriptional enhancers [15] or scaffolds for chromatin remodeling complexes [16,17], while a subset of lncRNAs, known as competing endogenous RNAs (ceRNAs), can sequester miRNAs and prevent the binding of miRNAs to their mRNA targets [18,19]. lncRNAs are implicated in cancer [20,21], including GBM [22–24], yet few lncRNAs have been characterized at the functional level. Although a large number of lncRNAs are retrieved from sequencing data, the prioritization of lncRNAs for functional analysis remains a common challenge.

In this project, using sequencing of small and long RNAs, we established the transcriptomic changes induced by TMZ in patient-derived GBM stem-like cells [25], differing in drug sensitivity. We found that TMZ elicited different gene expression programs in sensitive versus resistant GBM cell lines and that the extent of transcriptomic alterations correlated with sensitivity to TMZ. In addition to mRNAs, TMZ induced a large number of regulatory RNAs, especially lncRNAs. We inferred and analyzed transcriptional regulatory circuits generated from the integration of small RNA-seq and RNA-seq datasets, which were further integrated with clinical and independent molecular data. We thus uncovered coordinated programs of drug response in GBM, i.e., regulatory circuits that involve transcription factors (TFs), mRNAs, miRNAs, and lncRNAs. Finally, we identified several lncRNAs that bear functional relevance for drug response whilst representing independent prognostic markers in GBM patients.

2. Results

2.1. Differential DNA Damage Responses in GBM Stem-Like Cells Treated with TMZ

We analyzed the response to TMZ of three patient-derived GBM stem-like cultures (NCH601, NCH421k, and NCH644, referred later as GSCs) [25,26] and of a human neural stem cell line (hNSC.100, referred later as NSCs) used as non-neoplastic control. We found that NCH644 GSCs, expressing the MGMT DNA repair enzyme, showed high resistance to TMZ (IC₅₀ (half maximal inhibitory concentration) = 2.2×10^8 nM vs. $2.7\text{--}3.7 \times 10^5$ nM for the MGMT negative NCH421k and NCH601) (Figure S1a). Since TMZ is rapidly converted to the short-lived active compound MTIC, we hypothesized that a brief TMZ exposure could activate DDR. Therefore, we monitored established DDR markers using multi-color flow cytometry: phosphorylation of the histone variant H2AX on serine 139 (γ -H2AX) present at double strand DNA breaks and phosphorylation of Ataxia telangiectasia mutated (ATM) on serine 1981 (P-ATM) (Figure 1a). The basal levels of γ -H2AX were heterogeneous already prior TMZ treatment (Figure 1b, dotted line discriminates low and high subpopulations). NCH421k showed a high basal level (40% γ -H2AX high, Figure 1b), whereas NCH601 and NCH644 were similar to NSCs (6–16% γ -H2AX high). TMZ induced DNA double-strand breaks (γ -H2AX) after 6 h in three cell lines and after 24 h treatment in all cells (Figure 1b and Figure S1b). DDR activation as measured by P-ATM labeling was relatively homogeneous at baseline, with NCH644 showing the lowest basal level (Figure 1b, black lines indicate median expression in control conditions for each cell type). Upon TMZ treatment, NCH421k and NCH644 displayed P-ATM induction and accumulated in the S/G2/M phases of the cell cycle (Figure 1b), while NCH601 and NSCs showed little to no induction of P-ATM. In this experimental setting, we could not observe the presence of a sub-G1 peak after 24 h TMZ treatment indicative of apoptotic cells (Figure 1b). As expected, BrdU+ proliferative cells exhibited higher levels of γ -H2AX and P-ATM (Figure S1c). Taken together, our experiments revealed different cellular behavior upon TMZ (Figure 1c) from highly responsive (NSCs and NCH601: low basal level and strong induction of γ -H2AX, no induction of P-ATM), mildly responsive (NCH421k, high basal level and mild induction of γ -H2AX, low induction of P-ATM) to low responsive (NCH644, low basal level and strong induction of γ -H2AX, strong induction of P-ATM and S/G2/M accumulation). These results are in line with previous literature demonstrating the role of ATM in G2-M cell cycle block and protection from cell death, thereby leading to TMZ resistance [27]. These responses may reflect GBM cell heterogeneity and demonstrate the drug impact at an early time point. As we observed a differential DDR activation between the cell lines at 24 h after TMZ treatment, we therefore used these experimental conditions to further assess the primary transcriptional response to TMZ and identify the associated regulatory circuits (Figure 1c).

2.2. lncRNAs Are a Major Component of the Transcriptional Response to TMZ

To determine the immediate transcriptional response of GBM to TMZ, we carried out RNA sequencing from cells treated for 24 h with TMZ or vehicle. From the same RNA samples, we performed small RNA sequencing, to allow the direct comparison of small RNA, mRNA and lncRNA expression levels, an essential experimental set-up for accurate data integration.

Principal component analysis (PCA) identified individual variations between the respective GBM lines as the main determinant of transcriptome variability (Figure S2a). In both datasets, the variability measured by PC2 distinguished NCH644 cells from the other three cell lines and TMZ had a limited effect on variability. We compared the expression of different RNA biotypes with or without TMZ treatment (Table S1) and defined differential gene expression using a false discovery rate (FDR) < 5% and an absolute fold change > 2 for mRNAs and > 1.5 for miRNAs and lncRNAs. The volcano plots in Figure 2a represent the differentially expressed genes (DEGs) for mRNAs, lncRNAs, and miRNAs. In addition to the regulation of mRNAs, we observed that regulatory RNAs (miRNAs and lncRNAs) represented a large component of the transcriptome response elicited by TMZ (Figure 2a).

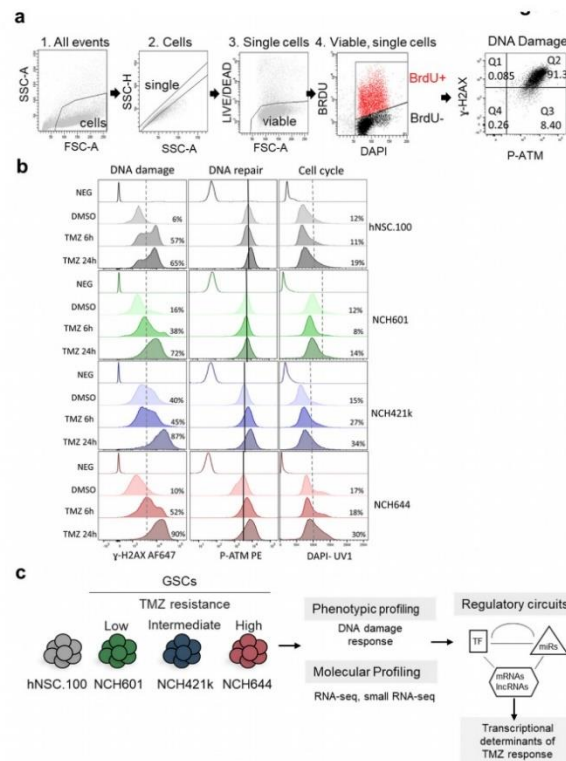


Figure 1. Glioblastoma (GBM) cells differentially activate DDR (DNA damage Response) in response to TMZ (temozolomide). **(a)** Gating strategy used for flow cytometry analysis. NCH644 GSCs (Glioblastoma stem-like cells) after 24 h TMZ treatment are shown as an example. (1) Cells were distinguished from debris using Forward Scatter (FSC) and Side Scatter (SSC). (2) Cell doublets and aggregates were gated out based on their properties displayed on the SSC area (SSC-A) versus height (SSC-H) dot plot. (3) Dead cells were recognized by their strong positivity for the dead cell discrimination marker. (4) Proliferating cells were distinguished as BrdU+ (Bromodeoxyuridine / 5-bromo-2'-deoxyuridine) events. DAPI (4',6-diamidino-2-phenylindole) staining shows cell cycle profile. (5) DNA damage was assessed by measuring the levels of γ -H2AX whereas P-ATM (phosphorylated Ataxia telangiectasia mutated) was used to measure the extent of DDR activation. The gating applied discriminates between P-ATM positive vs. negative cells, and γ -H2AX high vs. low cells. Percentage of cells in each quartile is presented. **(b)** Response to TMZ was analyzed in GSCs (NCH601, NCH421k, and NCH644). Neural stem cells (hNSC.100) were used as a non-neoplastic control. DNA damage (γ -H2AX), DNA repair (P-ATM), and cell cycle profiles (DAPI) after TMZ treatment (TMZ 6 h and TMZ 24 h) or DMSO as vehicle, are measured in the indicated cell lines. Isotype controls for antibody staining are shown for each cell (Neg). Dotted lines separate low and high γ -H2AX cells, or G0/G1 and S/G2/M cell cycle (DAPI graphs). Percentage of γ -H2AX high cells and cells in the S/G2/M cell cycle phases is presented. Black lines indicate median expression of P-ATM in DMSO treated cells. **(c)** GBM stem-like cells of different chemoresistance to TMZ: Low (NCH601), Intermediate (NCH421k), and High (NCH644), and neural stem cells (hNSC.100) were further used for transcriptional profiling and systems level analysis.

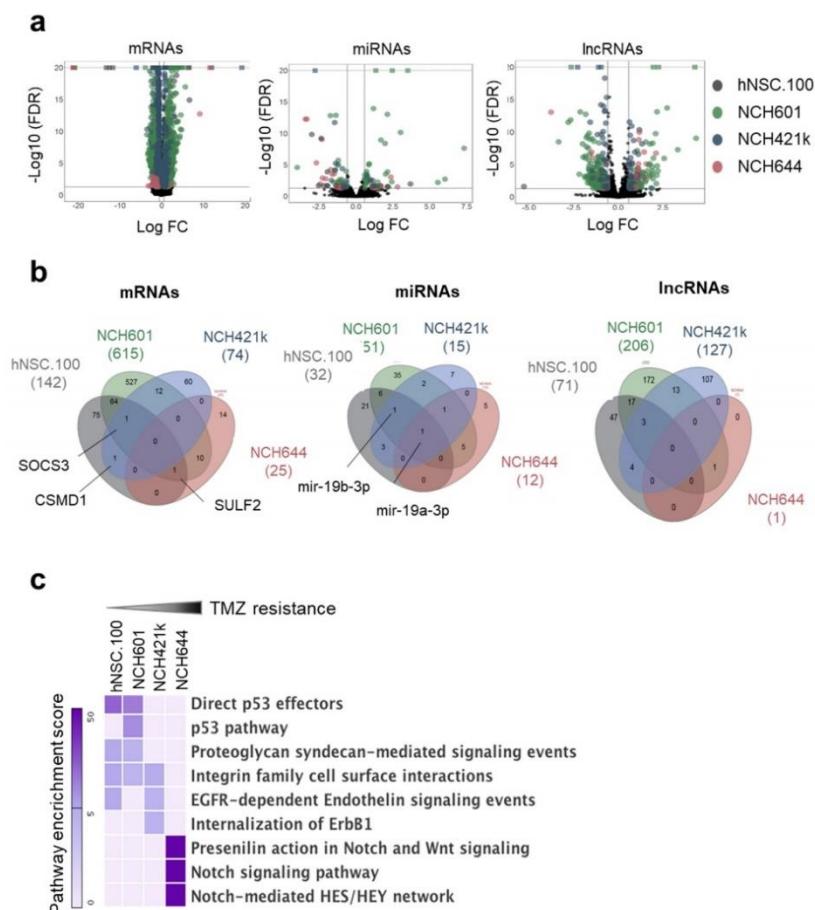


Figure 2. Genome-wide transcriptional changes induced by TMZ in GSCs. (a) Volcano plots representing the TMZ-regulated RNA subclasses in three GSCs (NCH601, NCH421k, NCH644) and one control neural stem cell line (hNSC.100): mRNAs (left panel), microRNAs (middle panel), lncRNAs (right panel). Each differentially expressed gene is represented by a dot and cell lines are indicated by different colors. Cut-offs for differential expression: FDR < 0.05 and absolute log FC > 2 for mRNAs, and FDR < 0.05 and absolute log FC > 1.5 for non-coding RNAs. Genes not satisfying these criteria are in black. For visualization purposes, the vertical axis has a limit of $-\log_{10}(\text{FDR}) = 20$. (b) Venn diagrams showing the intersection of RNAs regulated by TMZ from the four cell lines. (c) Heat map representing the enrichment score of the top three pathways associated with mRNAs regulated by TMZ in each cell line.

The extent of the transcriptional response of GBM cells to TMZ was very different in NCH644 in comparison with the other GSCs and NSCs (Figure 2b). NCH601 cells, the most sensitive GBM in our selection, displayed the largest number of differentially expressed mRNAs (614), miRNAs (51), and lncRNAs (206), whereas in NCH644, the most TMZ resistant cell line, only 25 mRNAs, 12 miRNAs, and 1 lncRNA were significantly deregulated (Figure 2b and Table S2). By comparing the overlap of DEGs we found that individual gene regulation was not conserved across GSCs except for a limited

number of genes e.g., *SOCS3*, *CSMD1*, and *SULF2* (Figure 2b). The same was true for miRNAs and lncRNAs. Interestingly, miR-19a-3p was the only common miRNA deregulated in all four cultures including NSCs, while miR-19b-3p regulation was observed in all cells except NCH644.

We then asked if there was a coordinated TMZ-regulation of coding genes leading to statistical functional pathway enrichment [28]. Although there was limited overlap of differentially expressed mRNAs between cell lines, we identified several commonly enriched pathways in cells with similar response to TMZ (Figure 2c). For example, the p53 pathway was shared in sensitive cells (hNSC.100 and NCH601) whereas enrichment of Notch/Wnt signaling was present in the resistant NCH644. As all GSCs are TP53 WT (Figure S2b–d), the absence of p53 pathway induction in NCH421k and NCH644 upon TMZ is not due to a mutation in *p53*. In hNSC.100 we detected a heterozygous mutation p.K132M which is a described cancer missense mutation. The differential pathway enrichment in sensitive versus resistant GSCs is in line with the known role of *p53* in drug sensitivity and the involvement of developmental pathways (Notch/Wnt) in chemoresistance [29,30].

2.3. TMZ-Regulated lncRNAs Are Prognostic Markers of Overall and Disease-Free Survival for Glioma Patients

A previous analysis of lncRNA expression on exon arrays from The Cancer Genome Atlas cohort (TCGA) revealed 133 lncRNAs as putative prognostic markers in GBM [31]. Four of our 364TMZ regulated lncRNAs were also found in this dataset: *ENSG00000224272*, *ENSG00000233230*, *ENSG00000233695* (or *GAS6-AS1*), and *ENSG00000246263* (Figure 3a). Using the webtool GEPIA [32], we calculated their prognostic capacity on glioma overall (Figure 3b) and disease-free survival (Figure S3a), and confirmed the positive prognostic value for *ENSG00000246263* and *ENSG00000224272* but not for *ENSG00000233230*. On the other hand, a high expression of *GAS6-AS1* was a negative prognostic factor in gliomas, as previously observed in gastric cancer [33]. We next compared the expression of these four lncRNAs in GBM, lower grade gliomas (LGG), and normal brain (GTEx). The median expression of each lncRNA was not significantly different between LGG and GBM or between brain tumors and normal brain, except for *ENSG00000224272*, which was more expressed in LGG than normal brain (Figure 3c). We then searched if the lncRNA expression differed in GBM subgroups of better prognosis, taking into account either the promoter methylation of MGMT (GBM patients who benefit from TMZ) or GBMs harboring a DNA hypermethylation gene signature (CIMP phenotype). Within the GBM cohort, we found that the expression of the four selected lncRNAs was independent of MGMT status (Figure S3b) and the CIMP phenotype (Figure S3c). In summary, we identified novel lncRNAs that are regulated by TMZ and display prognostic value in GBM, suggesting a role in tumor progression and response to therapy.

2.4. Computational Inference of TMZ-Associated RNA Interactome

A common challenge in noncoding RNA research is to predict the biological significance of newly identified molecules and select key genes for functional validation. As noncoding RNAs exert major functions in transcriptional regulation, we sought to uncover regulatory networks underlying the GBM response to TMZ. To this aim, we developed a pipeline based on available information on lncRNA and mRNA associations with transcription factors (TFs) and miRNAs.

To build such a global gene regulatory network of mRNAs, ncRNAs (miRNAs and lncRNAs), and TFs, we first retrieved molecular association data from several databases: ChipBase, StarBase, and miRcode databases (Figure 4a) [34–36]. TF-mRNA and TF-lncRNA associations from ChipBase were based on Chip-seq data of TF binding to promoters of mRNAs and lncRNAs. From Starbase, we extracted miRNA-mRNA/lncRNA associations from HITS-CLIP and PAR-CLIP experiments. Additional computationally predicted miRNA-lncRNA associations were added from miRcode. After gene annotation using Refseq for mRNAs, miRBase release 20 for miRNAs, and Ensembl for lncRNAs, the molecular associations described in Figure 4a were combined to obtain a global background network

that we named the “RNA interactome”. This exhaustive network contains regulatory interactions among 107 TFs, 1851 miRNAs, 10’970 lncRNAs, and 18’812 mRNAs (Table S3).

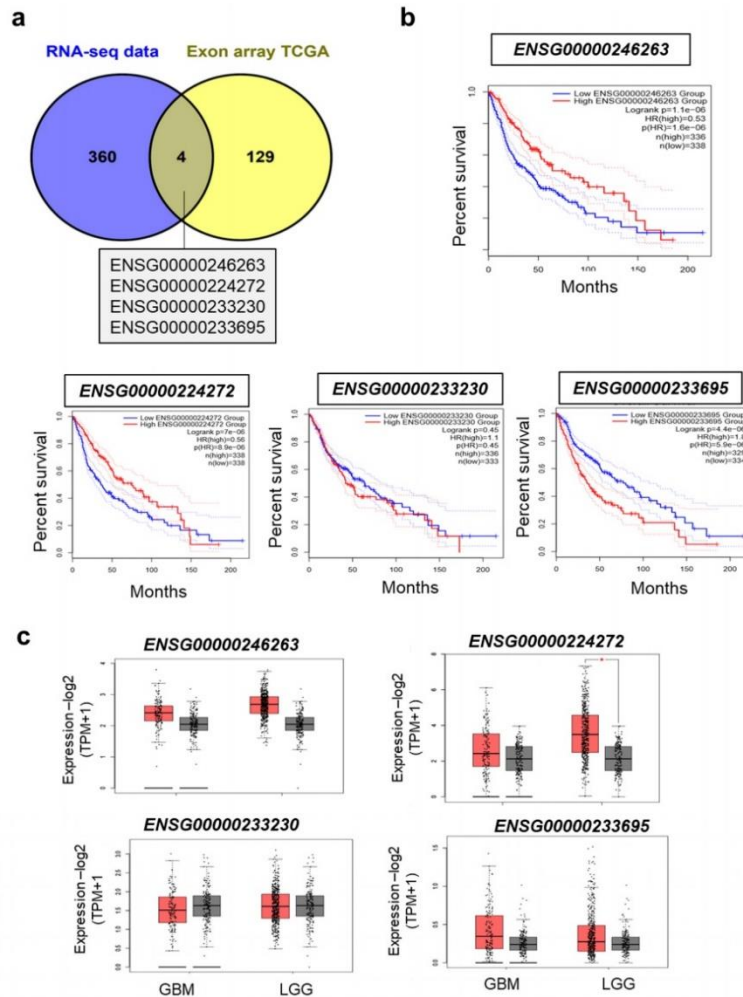


Figure 3. TMZ-regulated lncRNAs as novel independent GBM prognosis markers. (a) Overlap between the 360 TMZ-regulated lncRNAs and 133 lncRNAs proposed to correlate with GBM patient prognosis in the TCGA cohort [31]. (b) Kaplan Meier overall survival curves for the four overlapping lncRNAs in gliomas patients. The number of patients (*n*) analyzed for each group (high lncRNA expression group in red, low lncRNA expression group in blue) is indicated on the graphs. For each group *n* ≥ 329. Hazard ratios (H.R) and significance (log rank *p*-value) are indicated on the graphs. (c) Box plots of selected lncRNA median expression in GBM (*n* = 163) and lower grade gliomas (LGG, *n* = 518) (in red) compared to control brain tissue (grey, *n* = 207). Significant expression change is indicated by a red asterisk.

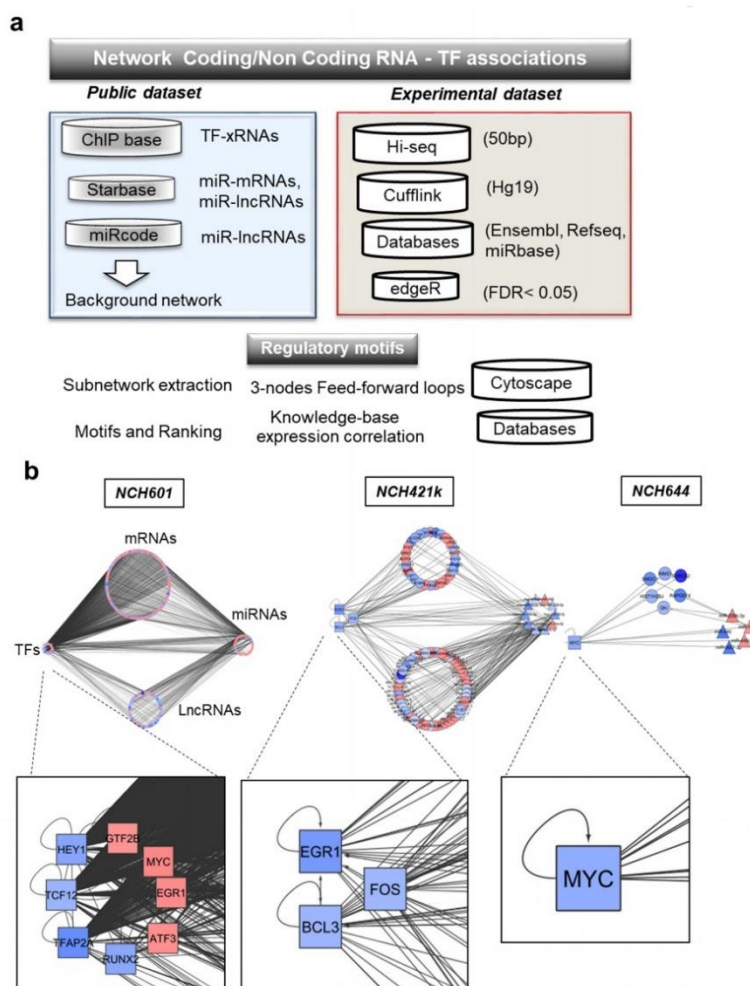


Figure 4. Systems approaches used for the generation of the RNA interactome and gene regulatory networks induced by TMZ in GBM. (a) Overview of the analysis pipeline, (b) gene regulatory networks representing the molecular associations between different RNA biotypes in different GSCs: mRNAs, miRNAs, lncRNAs, and transcription factors (TFs). Up- and downregulated RNAs are shown in red and blue, respectively. Different node shapes distinguish RNA biotypes: TF: square, miRNA: triangle, mRNA: circle, lncRNA: hexagon.

Next, we mapped our experimental dataset of TMZ-induced DEGs on the RNA interactome and extracted specific networks. In these networks, mRNAs coding for transcription factors were labeled as TFs. These analyses resulted in cell line-specific subnetworks composed of RNA-RNA and/or TF-RNA interactions. Cell line subnetworks were visualized as circular layouts (Figure 4b) using cytoscape, where each cluster represents the RNA biotype (TFs, mRNAs, lncRNAs, or miRNAs). Inside each cluster, nodes represent individual genes, with the sense of TMZ-induced deregulation indicated by a color code (increased expression in red; decreased expression in blue) (Figure 4b). We found that

some TMZ-regulated molecules appeared to organize in network hubs of highly connected genes (Table S4). Furthermore, transcriptional responses to TMZ involved a great number of TF-mRNAs and TF-lncRNAs interactions. These interactions involved the following transcription factors: MYC, TFAP2A, TCF12, HEY1 and EGR1, FOS and BCL3 (Table S4). Gene regulatory networks were largely composed by ncRNA interactions (miRNAs-mRNAs or miRNAs-lncRNAs) regulated by a specific subset of miRNAs. Several DEGs, as for example MYC and miR-19a-3p, showed opposite regulation by TMZ in the sensitive NCH601 and resistant NCH644 cell lines. This may indicate that the specific gene regulatory network contains key regulators of TMZ response.

We next analyzed the connectivity between the DEGs. We identified complex subnetworks in NCH601 and NCH421k that displayed a large number of DEGs. In contrast, only a small subnetwork was detected in NCH644, which displayed relatively few TMZ-associated DEGs, with some of its components being also present in NCH601 networks. We then measured the connectivity of each node (i.e., a gene) by calculating the in-degree (number of interactions that target a node) and out-degree of each node (number of out-going edges from a node). Notably, miR-19a-3p and miR-19b-3p displayed high out-degree values in almost all cells, suggesting a prominent regulatory role for these miRNAs in TMZ treatment response.

In parallel, we searched for putative promoter activities that may explain the observed transcriptional changes using ISMARA web tool [37]. The analysis of promoter motifs highlights TFs with different activity in response to TMZ without changes in their expression levels. We analyzed the top 10 transcription factor motifs sorted by activities (z-value) and identified common promoter motifs as for example YBX1, NRF1, and SP1 (Figure S4). Whereas this observation indicates that common transcriptional regulators can react in response to TMZ, it also suggests that they do so in opposite direction in resistant and sensitive cells: if they are activated/unchanged in responsive cells (NSC and NCH601), they tend to be repressed in resistant cells (NCH421k and NCH644). In summary, our genome-wide view of the transcriptional response to TMZ discerned sensitive and resistant behaviors.

Taken together, these data show that TMZ treatment impacts not only mRNA expression, but also miRNA and lncRNA levels, which may constitute regulatory networks with other RNA biotypes and TFs. Such regulatory networks, which were mostly observed in sensitive cell lines, may provide novel insight into chemosensitivity of GBM cells.

2.5. TMZ-Induced Transcriptional Regulatory Motifs Contain LncRNAs

To identify critical components of the transcriptional regulation elicited by TMZ, we analyzed cell line specific subnetworks at a higher systems level and extracted feed-forward loops (FFLs) involving TFs, miRNAs, mRNAs, or lncRNAs (Figure 5a). Such loops represent three-component interaction motifs consisting of miRNA-mediated loops, TF-mediated loops or mixed loops, i.e., those involving a dual interaction between TFs and miRNAs (Figure 5a). Transcriptional motifs were only present in the GBM cell lines, as no TF was regulated in NSC upon TMZ. Although the NCH644 network included a limited number of TMZ-regulated transcripts, we found two TF-mediated motifs with mRNAs involving MYC and miR-19a-3p. Conversely, in the TMZ sensitive cell line NCH601, we identified 308 miRNA-mediated loops, 559 TF-mediated loops, and 136 mixed loops regulated by TMZ (see Table S5 and Figure S5a). Strikingly, miR-19a-3p associated motifs were present in all GBM cell lines, although these associations involved different TFs, mRNAs, or lncRNAs depending on the cell line (Table S5).

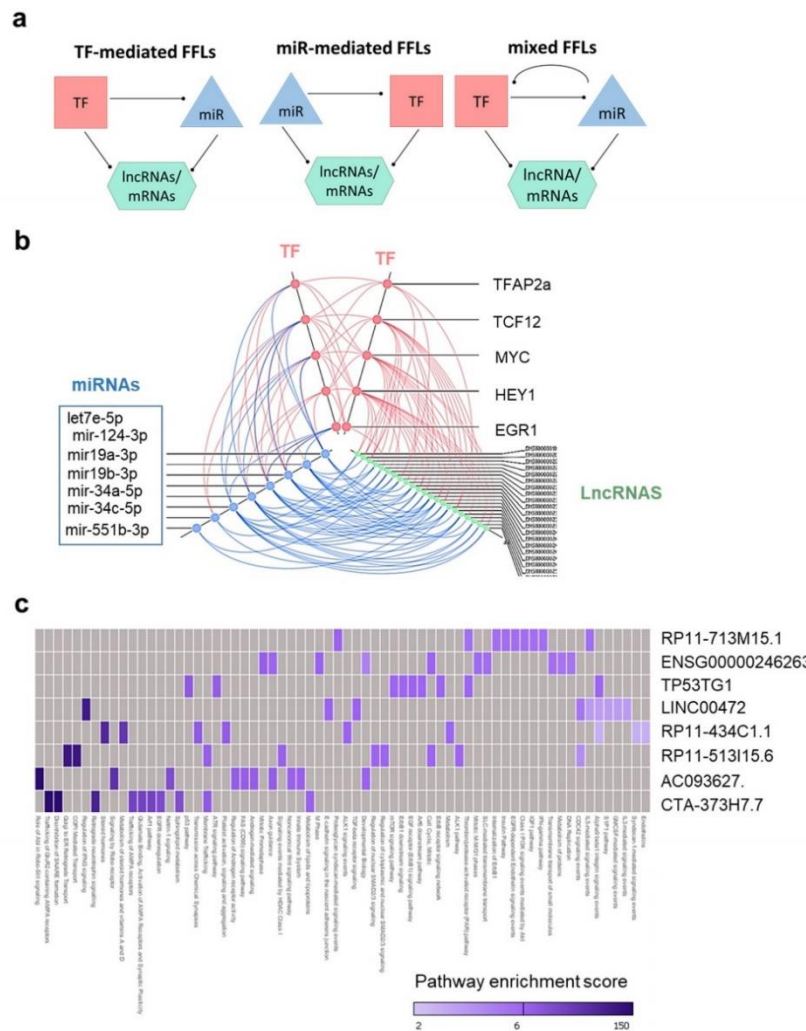


Figure 5. Identification of TMZ-associated transcriptional regulatory motifs involving lncRNAs. (a) Graphical representation of the motif structures where mRNAs or lncRNAs are the targets regulated by miRNA (miR) and TF associations. (b) Hive plot representing TMZ-regulated FFLs containing lncRNAs from NCH601. Axes indicate different RNA families, with each dot corresponding to a gene (TF, miRNA, or lncRNA) involved in lncRNA-containing loops. Molecular interactions are represented by a color code line (stimulatory interactions in red, inhibitory interactions in blue). (c) Heatmap showing enriched pathway for the indicated lncRNAs.

We focused on the composition of motifs involving lncRNAs, as such motifs were only present in the most sensitive GSCs (NCH601). The 22 lncRNAs formed 104 loops by interaction with a limited number of regulators (five TFs and six miRNAs, Figure 4b), as visualized by the hive plot in Figure 5b. Notably, a small number of key regulators such as miR-19a/b, MYC, EGR1, and HEY1 were consistently

present in most of the lncRNA-containing loops. To verify the non-coding identity of these 22 lncRNAs, we retrieved their sequences [38], calculated their coding potential probabilities [39], and compared them with those obtained from reference sets of known lncRNAs and mRNAs [40]. The lncRNAs involved in TMZ-associated regulatory loops had a low coding probability, similar to other known lncRNAs, suggesting that these lncRNAs are indeed noncoding (Figure S5b).

Among the 22 lncRNAs involved in loops, eight were expressed in all RNA-seq samples. By calculating the expression correlation coefficient between lncRNAs and mRNAs (Table S6) and pathway enrichment analysis using Webgestalt, we were able to associate these eight lncRNAs with putative biological functions. Analysis of the top 10 pathways identified for each lncRNA based on their statistical significance revealed that several pathways were shared (Figure 5c). Thus, five lncRNAs were associated with cell cycle regulation and DDR and six lncRNAs with EGFR signaling and/or developmental function (Figure 5c). As these functions were also enriched at the mRNA level (Figure 2c), our data collectively strengthen the notion that the motif-specific lncRNAs identified by our analysis are involved in biological functions relevant to drug response.

2.6. lncRNAs in TMZ Regulatory Loops May Function as CeRNAs

A subset of lncRNAs signal through binding of miRNAs, thereby acting as competing endogenous RNAs (ceRNAs) with mRNAs. We investigated the TMZ associated gene regulatory networks and selected mRNA-miRNA and miRNA-lncRNA pairs for the seven miRNAs involved in TMZ regulatory loops (Figure 5b): let7e-5p, miR-124-3p, miR-19a-3p, miR-19b-3p, miR-34a-5p, miR34c-5p, and miR-551b-3p. Interestingly, we found that except for miR-551b-3p (Figure S6), all miRNAs investigated shared molecular interactions with mRNAs and lncRNAs (Figure 6 and Figure S6). Taken together, these results suggest that these lncRNAs may act as sponges for miRNAs to fine tune the expression of mRNAs regulated by TMZ.

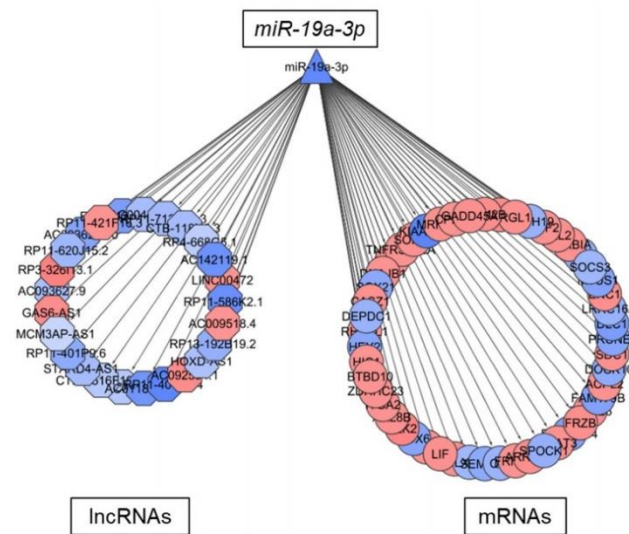


Figure 6. Putative ceRNA function of lncRNAs regulated by TMZ. Gene regulatory network representing the molecular associations between miR-19a-3p and mRNAs or lncRNAs in NCH601. Up- and downregulated RNAs are shown in red and blue, respectively. Different node shapes distinguish RNA families; TF: square, miRNA: triangle, mRNA: circle, lncRNA: hexagon.

3. Discussion

The transcriptional response to chemotherapeutic drugs has so far been mostly analyzed at the level of mRNAs, yet, a wealth of information is present in non-coding RNAs, making up more than 90% of the human genome [41]. Here, we report that GSCs elicit a heterogeneous cellular and transcriptional response to acute TMZ exposure. Although TMZ induced DNA damage in all cells, DDR activation was only observed in the TMZ-resistant MGMT positive GSC. Yet, this strong DDR activation was not associated with a major deregulation of the transcriptome in the resistant GSC, which is in line with our recent study where TMZ did not induce phenotypic changes in this cell line [42]. At present we cannot evaluate if and to what extent this is linked to MGMT expression in this cell line. In our experimental conditions, we showed that TMZ induces cell cycle block in some GSCs and we did not detect TMZ induction of apoptosis (subG1 peak) in GSCs, which is in line with previous report [43,44]. As other studies have evidenced apoptosis induction by TMZ in GBM cells, or more recently ferroptosis [6,45–47], it would be interesting to assess if the transcriptional changes and regulatory circuits identified here are involved in TMZ mediated apoptosis.

Our study provides a comprehensive overview of the RNA regulatory circuits induced by TMZ and lays the basis for exploring non-coding RNA function in GBM tumorigenesis and chemosensitivity. The analysis of regulatory network identified key TF-miRs molecular interactions, as the crosstalk between mir-19 and MYC [48]. Mir-19, a key oncogenic miRNA involved in glioma proliferation, invasion, and progression [49–51], appears to be a central regulator of the transcriptional response to TMZ. The upregulation of mir-19 in the resistant GSCs could participate in chemoresistance. Of note, it was reported that mir-19 targeting decreased the expression of MYC and delayed GBM tumor growth [52]. The systems-level characterization of lncRNAs and their inclusion in human-curated databases are still at an early stage. A study investigating a ceRNA network, which was built with co-expression measurements from paired genes (mRNAs and lncRNAs), proposed lncRNAs with potential clinical relevance in GBM [53]. The present approach expands on a network generation and analysis strategy that we previously reported in the context of miRNAs and GBM [54]. This strategy resulted in a comprehensive integration of datasets and regulatory associations, which is required to provide systems-level insights into specific cell models and treatment responses. An important challenge for such a strategy is the lack of tools for full integration of the different modeling and analysis steps. Another obstacle is the limitation imposed by the relatively poor consistency of ncRNA annotations between databases [55]. The reannotation of existing patient datasets with lncRNA expression [31] and sequencing of total RNAs could enhance the phenotypic studies of lncRNAs and the predictive potential of network-based discovery strategies. Nevertheless, the strategy presented here can be applied to multiple fields of cancer research investigating transcriptional programs (treatment resistance, cell invasion, immuno-oncology), whilst also contributing to the development of appropriate methodologies and analytical tools. In this regard, it is notable that the methodology we implemented to prioritize lncRNA candidates for functional validation resulted in the identification of a subset of lncRNAs with a putative role in DDR or developmental pathways. Among these novel lncRNAs, the lncRNAs TP53TG1 and ENSG000246263, were recently uncovered in a study using a machine-learning method to stratify cancer-related lncRNAs [56]. Furthermore, the documented roles of TP53TG1 in glioma cell proliferation [57] and response to chemotherapy in lung cancer [58] provide experimental support for our *in silico* prediction of a role for TP53TG1 in the response of GBM cells to TMZ.

Our work has revealed that a large number of lncRNAs are differentially regulated by TMZ in chemo-sensitive and resistant GSCs, as well as in non-malignant NSCs, and identified key lncRNAs that may be linked to the regulation of DDR, apoptosis, and EGFR signaling in GBM, as part of co-expression networks with mRNAs and other small RNAs. Although several DNA repair mechanisms are involved in the repair of TMZ-induced lesions, TMZ resistance in the clinic has so far been associated mainly with the activity of MGMT and the selection of resistant clones that account for tumor recurrence [8]. To date, albeit recent reports involve lncRNAs as regulators of drug sensitivity [59–61] and of GBM

pathogenesis [22,23], a genome-wide analysis of lncRNAs in the regulation of drug response in GBM has not been done. We expect that functional analyses of TMZ-associated lncRNAs will provide valuable insight into the mechanisms that govern drug response in GBM. Given the importance of lncRNAs in cellular lineage and as transcriptional enhancers, it is highly possible that some of the lncRNAs identified in this study operate through epigenetic mechanisms that drive selection of resistant cells, independently of MGMT. In this respect, we identify four lncRNAs with prognostic value in glioma patients that are involved in the transcriptional response to TMZ, independent of MGMT status. Although lncRNAs are generally expressed at low levels, it would be of interest to verify their prognostic value by RNA in situ hybridization on glioma tissue. Additionally, as lncRNAs play important roles in DNA damage signaling and chemoresistance, these molecules could have a functional role in TMZ response independently of MGMT as recently shown for the lncRNA TP73-AS1 [62]. If confirmed, targeting these molecules could be used to counteract chemoresistance in GBM.

4. Material and Methods

4.1. Cell Lines, Treatments, and Cytotoxicity Assay

The glioblastoma stem-like cell cultures NCH421k, NCH601 and NCH644 were generated in the lab of Dr Christel Herold-Mende (Department of Neurosurgery, University of Heidelberg) [63] and characterized previously [25]. Human fetal neural stem cells hNSC.100 were described previously [64]. All cell lines were grown as 3D neurospheres in serum-free medium. NCH421k and NCH601 were cultured as non-adherent spheres in DMEM-F12 medium (Lonza, Basel, Switzerland) containing 1xBIT100 (Provitro, Berlin, Germany), 2mM L-Glutamine, 30U/ml Pen-Step, 1U/ml Heparin (Sigma), 20ng/ml bFGF (Miltenyi, Bergisch Gladbach, Germany 130-093-841) and 20ng/ml EGF (Provitro, Berlin, Germany 1325950500). NCH644 and hNSC.100 grew as non-adherent spheres in Neurobasal@base medium (ThermoFischer Scientific, Waltham, Massachusetts, USA) supplemented with 1xB-27, 2mM L-Glutamine, 30U/ml Pen-Step, 1U/ml Heparin (Sigma), 20ng/ml bFGF and 20ng/ml EGF. Temozolomide (TMZ, Sigma Aldrich, Overijse, Belgium, 76899) sensitivity was measured by WST-1 assay (Roche, Basel, Switzerland, 5015944001) developed with Fluorostar Optima system. IC50 was determined using Graphpad Prism. Cell biomass was determined 72 h after TMZ treatment. Cells were treated with 500 μ M TMZ for 6 or 24 h for flow cytometry, and 24 h for RNA-seq experiments.

4.2. Multi-Color Flow Cytometry

TMZ or vehicle were added 24 or 6 h prior to analysis. For proliferation assay, BRDU (Bromodeoxyuridine / 5-bromo-2'-deoxyuridine) incorporation was performed for 6 h before the end of the experiment. Prior to fixation, cells were dissociated and incubated with the IR-LIVE/DEAD@Fixable Dead Cell Stain (ThermoFisher scientific; Waltham, MA, USA, 1 μ g/mL). Cells were fixed, permeabilized and stained with the BD Pharmingen™ BrdU Flow Kit (BD Bioscience, San Jose, CA, USA) according to the manufacturer's instructions. The following conjugated antibodies were used: anti H2AX-Phospho Ser139-Alexa Fluor 647 (BD Biosciences, 560447), anti-ATM-PhosphoSer1981-PE (Millipore, Burlington, MA, USA, FCMAB110P), Alexa Fluor@647 Mouse IgG1 κ Isotype Control (BD Bioscience, 565571), Mouse IgG1 Negative Control, clone Ci4, PE conjugate (Millipore, MABC002H). DNA was counterstained with DAPI (1 μ g/mL) and anti-BrDU-PerCP-Cy5.5 (BD, 560809 kit). Data were acquired on a FACS Aria™ SORP cytometer (BD Biosciences) and analyzed with Diva (BD Biosciences) and FlowJo software version v10.5.3.

4.3. RNA and Small RNA-Sequencing

Total RNA was extracted with Trizol and quantified using Nanodrop. Three biological replicates were used per experimental condition. RNA quality was checked using a bioanalyzer (Agilent, Santa Clara, CA, USA). Total RNAs were depleted from Ribosomal RNAs using RiboMinus™ technology. RNA-seq libraries were prepared according to the Illumina standard protocol using TruSeq Stranded

RNA Kits. Small RNA-Seq libraries were generated from total RNA using TruSeq Small RNA Library Prep Kit. Single stranded sequencing reads were performed on HiSeq2500 instrument (Illumina, San Diego, CA, United States). Base calling was performed with CASAVA 1.8.2 pipeline (Illumina). Fastq data and processed counts of RNA-seq (24 samples in total) and small RNA-seq (24 samples in total) are available through Gene Expression Omnibus (GSE98128).

4.4. Systems Approaches

The associations of TFs with genes, miRNAs, or lncRNAs were obtained from ChipBase [36]. Associations between miRNAs and genes were obtained from StarBase [35]. As the number miRNAs-lncRNAs associations in StarBase was small, we also integrated the miRcode database [34]. As a result, the background regulatory network consisted of 1,145,815 regulations, including 107 TFs, 1851 mature miRNAs, 10,970 lncRNAs, and 18,812 genes. Detailed information is shown in Figure 4B. Next, we mapped the DEGs (Differentially Expressed) genes, miRNAs, and lncRNAs of each cell line into the background network separately. We constructed the cell line-specific subnetworks by extracting the edges (observed expression correlation) between the DE nodes. We focused on three types of 3-node FFLs containing lncRNAs or mRNAs, and which included a TF, a miRNA, and a target lncRNAs or mRNAs (Figure 5a and Figure S5, respectively). In the first type, a TF regulates miRNA and lncRNA, and a miRNA regulates lncRNA. We termed it TF-mediated FFL. In the second type, miRNA-mediated FFL, a miRNA regulates TF and lncRNA, and a TF regulates lncRNA. In the third type, a miRNA and a TF are mutually regulated, and both regulate a lncRNA. We extracted all FFLs from the cell line-specific subnetworks using R-language scripts.

4.5. TCGA Data Analysis

Prediction of lncRNAs as potential prognostic markers were reported in [31], analyzed using GEPIA, and GETX data were used for normal tissue expression. The MGMT promoter methylation status was from [65]. Cohort was divided in two groups based on expression median for each lncRNA. Group expression was represented using Graph Pad Prism or extracted from GEPIA.

5. Conclusions

In conclusion, this study provided a comprehensive map of transcriptome regulation upon TMZ in GSCs displaying different drug sensitivity. The transcriptional response to TMZ is a coordinated program of coding and non-coding RNAs, orchestrated by regulatory loops, some of them being oppositely modulated in sensitive and resistant GBM cells. Importantly, we uncovered a subset of largely unknown lncRNAs potentially involved in essential pathways of tumorigenesis and drug resistance. Several TMZ regulated lncRNAs display prognostic value in GBM patients. This data resource, the systems approaches, and novel RNA targets identified in this study open the way for understanding lncRNA function in GBM.

Supplementary Materials: The following are available online at <http://www.mdpi.com/2072-6694/12/9/2583/s1>, Figure S1 TMZ sensitivity and DDR activation in GSCs, Figure S2: Principal Component analysis of all samples and TP53 genomic status of GSCs, Figure S3: TMZ-regulated lncRNAs as novel independent GBM prognosis markers of progression free survival, Figure S4: Selected examples of Top 10 transcription factor motifs sorted by activities (z-value) from ISMARA Figure S5: mRNA-containing regulatory loops and coding potential of selected lncRNAs, Figure S6: Gene regulatory networks representing the molecular associations between selected miRNAs and mRNAs or lncRNAs in NCH601, Table S1: All expression data, Table S2: Differentially expressed genes per biotype and cell line, Table S3: Regulatory background network, Table S4: Degree in subnetworks, Table S5: Transcriptional motifs summary, Table S6: Expression correlation calculation.

Author Contributions: Conceptualization, S.P.N. and S.F.; Methodology, S.F., A.M., W.J., R.M., M.S., M.D.; Software, T.Y., A.M., R.M., W.J., F.A.; Validation, M.S., M.D., S.F.; Formal Analysis, S.F., A.M., T.Y., A.G.; Investigation, S.F., F.A.; Resources, W.J., R.M., C.H.-M., E.V.D., Data Curation, T.Y., W.J., A.M., Writing—Original Draft Preparation, S.F.; Writing—Review and Editing, S.F., S.P.N.; Visualization, S.F., A.M., W.J., A.G.; Supervision, S.P.N., F.A., Z.Z., S.F.; Project Administration, S.P.N., S.F., F.A.; Funding Acquisition, S.P.N., S.F., F.A., Z.Z. All authors have read and agreed to the published version of the manuscript.

Funding: This work was supported by the Luxembourg Institute of Health (ADAPT project of SPN), the Fonds National de la Recherche (FNR) of Luxembourg (CIRCUITOMA, INTER/MOBILITY/13/6548771 grant to FA), the FNRS-Télévie (CREG n^o 7.4592.14, Link-GBM n^o 7.4570.16, grants to SPN, SF and MS), and the Fondation Cancer of Luxembourg (INCOMING, grant to SF). ZZ was partially supported by National Institutes of Health grants (R01LM012806) and the Cancer Prevention and Research Institute of Texas (CPRIT RP180734 and RP170668).

Acknowledgments: We thank Dr Laurent Vallar for advice in transcriptomics. Sequencing was performed by the IGBMC (Institut de génétique et de biologie moléculaire et cellulaire) GenomEast Platform, member of the France Genomic program.

Conflicts of Interest: The authors declare no conflict of interest.

References

1. Zhang, J.; Stevens, M.F.G.; Bradshaw, T.D. Temozolomide: Mechanisms of action, repair and resistance. *Curr. Mol. Pharmacol.* **2012**, *5*, 102–114. [[CrossRef](#)] [[PubMed](#)]
2. Stupp, R.; Mason, W.P.; van den Bent, M.J.; Weller, M.; Fisher, B.; Taphoorn, M.J.B.; Belanger, K.; Brandes, A.A.; Marosi, C.; Bogdahn, U.; et al. Radiotherapy plus concomitant and adjuvant temozolomide for glioblastoma. *N. Eng. J. Med.* **2005**, *352*, 987–996. [[CrossRef](#)] [[PubMed](#)]
3. Hegi, M.E.; Diserens, A.-C.; Gorlia, T.; Hamou, M.-F.; de Tribolet, N.; Weller, M.; Kros, J.M.; Hainfellner, J.A.; Mason, W.; Mariani, L.; et al. MGMT gene silencing and benefit from temozolomide in glioblastoma. *N. Eng. J. Med.* **2005**, *352*, 997–1003. [[CrossRef](#)] [[PubMed](#)]
4. Kaina, B.; Christmann, M.; Naumann, S.; Roos, W.P. MGMT: Key node in the battle against genotoxicity, carcinogenicity and apoptosis induced by alkylating agents. *DNA Repair* **2007**, *6*, 1079–1099. [[CrossRef](#)] [[PubMed](#)]
5. Weller, M.; Stupp, R.; Reifenberger, G.; Brandes, A.A.; van den Bent, M.J.; Wick, W.; Hegi, M.E. MGMT promoter methylation in malignant gliomas: Ready for personalized medicine? *Nat. Rev. Neurol.* **2010**, *6*, 39–51. [[CrossRef](#)] [[PubMed](#)]
6. Roos, W.P.; Batista, L.F.; Naumann, S.C.; Wick, W.; Weller, M.; Menck, C.F.; Kaina, B. Apoptosis in malignant glioma cells triggered by the temozolomide-induced DNA lesion O6-methylguanine. *Oncogene* **2007**, *26*, 186–197. [[CrossRef](#)]
7. Messaoudi, K.; Clavreul, A.; Lagarce, F. Toward an effective strategy in glioblastoma treatment. Part I: Resistance mechanisms and strategies to overcome resistance of glioblastoma to temozolomide. *Drug Discov. Today* **2015**, *20*, 899–905. [[CrossRef](#)]
8. Erasmus, H.; Gobin, M.; Niclou, S.; Van Dyck, E. DNA repair mechanisms and their clinical impact in glioblastoma. *Mutat. Res. Rev. Mutat. Res.* **2016**, *769*, 19–35. [[CrossRef](#)]
9. Hannen, R.; Selmansberger, M.; Hauswald, M.; Pagenstecher, A.; Nist, A.; Stiewe, T.; Acker, T.; Carl, B.; Nimsky, C.; Bartsch, J.W. Comparative Transcriptomic Analysis of Temozolomide Resistant Primary GBM Stem-Like Cells and Recurrent GBM Identifies Up-Regulation of the Carbonic Anhydrase CA2 Gene as Resistance Factor. *Cancers* **2019**, *11*, 921. [[CrossRef](#)]
10. Bektas, M.; Johnson, S.P.; Poe, W.E.; Bigner, D.D.; Friedman, H.S. A sphingosine kinase inhibitor induces cell death in temozolomide resistant glioblastoma cells. *Cancer Chemother. Pharmacol.* **2009**, *64*, 1053–1058. [[CrossRef](#)]
11. Huang, G.; Ho, B.; Conroy, J.; Liu, S.; Qiang, H.; Golubovskaya, V. The microarray gene profiling analysis of glioblastoma cancer cells reveals genes affected by FAK inhibitor Y15 and combination of Y15 and temozolomide. *Anti Cancer Agents Med. Chem.* **2014**, *14*, 9–17. [[CrossRef](#)] [[PubMed](#)]
12. Hirschhaeuser, F.; Menne, H.; Dittfeld, C.; West, J.; Mueller-Klieser, W.; Kunz-Schughart, L.A. Multicellular tumor spheroids: An underestimated tool is catching up again. *J. Biotechnol.* **2010**, *148*, 3–15. [[CrossRef](#)] [[PubMed](#)]
13. Kunz-Schughart, L.A.; Freyer, J.P.; Hofstaedter, F.; Ebner, R. The use of 3-D cultures for high-throughput screening: The multicellular spheroid model. *J. Biomol. Screen.* **2004**, *9*, 273–285. [[CrossRef](#)] [[PubMed](#)]
14. Bernstein, B.E.; Birney, E.; Dunham, I.; Green, E.D.; Gunter, C.; Snyder, M. An integrated encyclopedia of DNA elements in the human genome. *Nature* **2012**, *489*, 57–74.
15. Lam, M.T.; Li, W.; Rosenfeld, M.G.; Glass, C.K. Enhancer RNAs and regulated transcriptional programs. *Trends Biochem. Sci.* **2014**, *39*, 170–182. [[CrossRef](#)] [[PubMed](#)]

16. Meller, V.H.; Joshi, S.S.; Deshpande, N. Modulation of Chromatin by Noncoding RNA. *Annu. Rev. Genet.* **2015**, *49*, 673–695. [[CrossRef](#)]
17. Tsai, M.C.; Manor, O.; Wan, Y.; Mosammamaparast, N.; Wang, J.K.; Lan, F.; Shi, Y.; Segal, E.; Chang, H.Y. Long noncoding RNA as modular scaffold of histone modification complexes. *Science* **2010**, *329*, 689–693. [[CrossRef](#)]
18. Salmena, L.; Poliseno, L.; Tay, Y.; Kats, L.; Pandolfi, P.P. A ceRNA hypothesis: The Rosetta Stone of a hidden RNA language? *Cell* **2011**, *146*, 353–358. [[CrossRef](#)]
19. Qu, J.; Li, M.; Zhong, W.; Hu, C. Competing endogenous RNA in cancer: A new pattern of gene expression regulation. *Int. J. Clin. Exp. Med.* **2015**, *8*, 17110–17116.
20. Di Gesualdo, F.; Capaccioli, S.; Lulli, M. A pathophysiological view of the long non-coding RNA world. *Oncotarget* **2014**, *5*, 10976–10996. [[CrossRef](#)]
21. Isin, M.; Dalay, N. LncRNAs and neoplasia. *Clin. Chim. Acta Int. J. Clin. Chem.* **2015**, *444*, 280–288. [[CrossRef](#)] [[PubMed](#)]
22. Mineo, M.; Ricklefs, F.; Rooj, A.K.; Lyons, S.M.; Ivanov, P.; Ansari, K.I.; Nakano, I.; Chiocca, E.A.; Godlewski, J.; Bronisz, A. The Long Non-coding RNA HIF1A-AS2 Facilitates the Maintenance of Mesenchymal Glioblastoma Stem-like Cells in Hypoxic Niches. *Cell Rep.* **2016**. [[CrossRef](#)] [[PubMed](#)]
23. Pastori, C.; Kapranov, P.; Penas, C.; Peschansky, V.; Volmar, C.H.; Sarkaria, J.N.; Bregy, A.; Komotar, R.; St Laurent, G.; Ayad, N.G.; et al. The Bromodomain protein BRD4 controls HOTAIR, a long noncoding RNA essential for glioblastoma proliferation. *Proc. Natl. Acad. Sci. USA* **2015**, *112*, 8326–8331. [[CrossRef](#)] [[PubMed](#)]
24. Yao, Y.; Ma, J.; Xue, Y.; Wang, P.; Li, Z.; Liu, J.; Chen, L.; Xi, Z.; Teng, H.; Wang, Z.; et al. Knockdown of long non-coding RNA XIST exerts tumor-suppressive functions in human glioblastoma stem cells by up-regulating miR-152. *Cancer Lett.* **2015**, *359*, 75–86. [[CrossRef](#)] [[PubMed](#)]
25. Bougnaud, S.; Golebiewska, A.; Oudin, A.; Keunen, O.; Harter, P.N.; Mader, L.; Azuaje, F.; Fritah, S.; Stieber, D.; Kaoma, T.; et al. Molecular crosstalk between tumour and brain parenchyma instructs histopathological features in glioblastoma. *Oncotarget* **2016**, *7*, 31955–31971. [[CrossRef](#)]
26. Campos, B.; Zeng, L.; Daotrong, P.H.; Eckstein, V.; Unterberg, A.; Mairbäurl, H.; Herold-Mende, C. Expression and regulation of AC133 and CD133 in glioblastoma. *Glia* **2011**, *59*, 1974–1986. [[CrossRef](#)]
27. Eich, M.; Roos, W.P.; Nikolova, T.; Kaina, B. Contribution of ATM and ATR to the resistance of glioblastoma and malignant melanoma cells to the methylating anticancer drug temozolomide. *Mol. Cancer Ther.* **2013**, *12*, 2529–2540. [[CrossRef](#)]
28. Wang, J.; Duncan, D.; Shi, Z.; Zhang, B. WEB-based GENE SeT AnaLysis Toolkit (WebGestalt): Update 2013. *Nucleic Acids Res.* **2013**, *41*, W77–W83. [[CrossRef](#)]
29. Hirose, Y.; Berger, M.S.; Pieper, R.O. p53 effects both the duration of G2/M arrest and the fate of temozolomide-treated human glioblastoma cells. *Cancer Res.* **2001**, *61*, 1957–1963.
30. Ulasov, I.V.; Nandi, S.; Dey, M.; Sonabend, A.M.; Lesniak, M.S. Inhibition of Sonic hedgehog and Notch pathways enhances sensitivity of CD133(+) glioma stem cells to temozolomide therapy. *Mol. Med. (Camb. Mass.)* **2011**, *17*, 103–112. [[CrossRef](#)]
31. Du, Z.; Fei, T.; Verhaak, R.G.W.; Su, Z.; Zhang, Y.; Brown, M.; Chen, Y.; Liu, X.S. Integrative genomic analyses reveal clinically relevant long noncoding RNAs in human cancer. *Nat. Struct. Mol. Biol.* **2013**, *20*, 908–913. [[CrossRef](#)] [[PubMed](#)]
32. Tang, Z.; Li, C.; Kang, B.; Gao, G.; Li, C.; Zhang, Z. GEPIA: A web server for cancer and normal gene expression profiling and interactive analyses. *Nucleic Acids Res.* **2017**, *45*, W98–W102. [[CrossRef](#)] [[PubMed](#)]
33. Zhang, P.; Dong, Q.; Zhu, H.; Li, S.; Shi, L.; Chen, X. Long non-coding antisense RNA GAS6-AS1 supports gastric cancer progression via increasing GAS6 expression. *Gene* **2019**, *696*, 1–9. [[CrossRef](#)] [[PubMed](#)]
34. Jeggari, A.; Marks, D.S.; Larsson, E. miRcode: A map of putative microRNA target sites in the long non-coding transcriptome. *Bioinformatics* **2012**, *28*, 2062–2063. [[CrossRef](#)] [[PubMed](#)]
35. Li, J.-H.; Liu, S.; Zhou, H.; Qu, L.-H.; Yang, J.-H. starBase v2.0: Decoding miRNA-ceRNA, miRNA-ncRNA and protein-RNA interaction networks from large-scale CLIP-Seq data. *Nucleic Acids Res.* **2014**, *42*, D92–D97. [[CrossRef](#)]
36. Yang, J.-H.; Li, J.-H.; Jiang, S.; Zhou, H.; Qu, L.-H. ChIPBase: A database for decoding the transcriptional regulation of long non-coding RNA and microRNA genes from ChIP-Seq data. *Nucleic Acids Res.* **2013**, *41*, D177–D187. [[CrossRef](#)]

37. Balwierz, P.J.; Pachkov, M.; Arnold, P.; Gruber, A.J.; Zavolan, M.; van Nimwegen, E. ISMARA: Automated modeling of genomic signals as a democracy of regulatory motifs. *Genome Res.* **2014**, *24*, 869–884. [[CrossRef](#)]
38. Volders, P.-J.; Helsens, K.; Wang, X.; Menten, B.; Martens, L.; Gevaert, K.; Vandesompele, J.; Mestdagh, P. LNCipedia: A database for annotated human lncRNA transcript sequences and structures. *Nucleic Acids Res.* **2013**, *41*, D246–D251. [[CrossRef](#)]
39. Wang, L.; Park, H.J.; Dasari, S.; Wang, S.; Kocher, J.P.; Li, W. CPAT: Coding-Potential Assessment Tool using an alignment-free logistic regression model. *Nucleic Acids Res.* **2013**, *41*, e74. [[CrossRef](#)]
40. Cabili, M.N.; Trapnell, C.; Goff, L.; Koziol, M.; Tazon-Vega, B.; Regev, A.; Rinn, J.L. Integrative annotation of human large intergenic noncoding RNAs reveals global properties and specific subclasses. *Genes Dev.* **2011**, *25*, 1915–1927. [[CrossRef](#)]
41. Djebali, S.; Davis, C.A.; Merkel, A.; Dobin, A.; Lassmann, T.; Mortazavi, A.; Tanzer, A.; Lagarde, J.; Lin, W.; Schlesinger, F.; et al. Landscape of transcription in human cells. *Nature* **2012**, *489*, 101–108. [[CrossRef](#)] [[PubMed](#)]
42. Dirkse, A.; Golebiewska, A.; Buder, T.; Nazarov, P.V.; Muller, A.; Poovathingal, S.; Brons, N.H.C.; Leite, S.; Sauvageot, N.; Sarkisjan, D.; et al. Stem cell-associated heterogeneity in Glioblastoma results from intrinsic tumor plasticity shaped by the microenvironment. *Nat. Commun.* **2019**, *10*, 1787. [[CrossRef](#)] [[PubMed](#)]
43. Beier, D.; Röhl, S.; Pillai, D.R.; Schwarz, S.; Kunz-Schughart, L.A.; Leukel, P.; Proescholdt, M.; Brawanski, A.; Bogdahn, U.; Trampe-Kieslich, A.; et al. Temozolomide preferentially depletes cancer stem cells in glioblastoma. *Cancer Res.* **2008**, *68*, 5706–5715. [[CrossRef](#)] [[PubMed](#)]
44. Gong, X.; Schwartz, P.H.; Linskey, M.E.; Bota, D.A. Neural stem/progenitors and glioma stem-like cells have differential sensitivity to chemotherapy. *Neurology* **2011**, *76*, 1126–1134. [[CrossRef](#)]
45. Balvers, R.K.; Lamfers, M.L.; Kloezeman, J.J.; Kleijn, A.; Berghauer Pont, L.M.; Dirven, C.M.; Leenstra, S. ABT-888 enhances cytotoxic effects of temozolomide independent of MGMT status in serum free cultured glioma cells. *J. Transl. Med.* **2015**, *13*, 74. [[CrossRef](#)] [[PubMed](#)]
46. Buccarelli, M.; Marconi, M.; Pacioni, S.; De Pascalis, I.; D’Alessandris, Q.G.; Martini, M.; Ascione, B.; Malorni, W.; Larocca, L.M.; Pallini, R.; et al. Inhibition of autophagy increases susceptibility of glioblastoma stem cells to temozolomide by igniting ferroptosis. *Cell Death Dis.* **2018**, *9*, 841. [[CrossRef](#)] [[PubMed](#)]
47. Hombach-Klonisch, S.; Mehrpour, M.; Shojaei, S.; Harlos, C.; Pitz, M.; Hamai, A.; Siemianowicz, K.; Likus, W.; Wiechec, E.; Toyota, B.D.; et al. Glioblastoma and chemoresistance to alkylating agents: Involvement of apoptosis, autophagy, and unfolded protein response. *Pharmacol. Ther.* **2018**, *184*, 13–41. [[CrossRef](#)]
48. Anauate, A.C.; Leal, M.F.; Calcagno, D.Q.; Gigeck, C.O.; Karia, B.T.R.; Wisniewski, F.; Dos Santos, L.C.; Chen, E.S.; Burbano, R.R.; Smith, M.A.C. The Complex Network between MYC Oncogene and microRNAs in Gastric Cancer: An Overview. *Int. J. Mol. Sci.* **2020**, *21*, 1782. [[CrossRef](#)]
49. Chen, Q.; Guo, W.; Zhang, Y.; Wu, Y.; Xiang, J. MiR-19a promotes cell proliferation and invasion by targeting RhoB in human glioma cells. *Neurosci. Lett.* **2016**, *628*, 161–166. [[CrossRef](#)]
50. Olive, V.; Bennett, M.J.; Walker, J.C.; Ma, C.; Jiang, I.; Cordon-Cardo, C.; Li, Q.J.; Lowe, S.W.; Hannon, G.J.; He, L. miR-19 is a key oncogenic component of mir-17-92. *Genes Dev.* **2009**, *23*, 2839–2849. [[CrossRef](#)]
51. Wang, W.; Zhang, A.; Hao, Y.; Wang, G.; Jia, Z. The emerging role of miR-19 in glioma. *J. Cell Mol. Med.* **2018**, *22*, 4611–4616. [[CrossRef](#)] [[PubMed](#)]
52. Sun, J.; Jia, Z.; Li, B.; Zhang, A.; Wang, G.; Pu, P.; Chen, Z.; Wang, Z.; Yang, W. MiR-19 regulates the proliferation and invasion of glioma by RUNX3 via β -catenin/Tcf-4 signaling. *Oncotarget* **2017**, *8*, 110785–110796. [[CrossRef](#)] [[PubMed](#)]
53. Cao, Y.; Wang, P.; Ning, S.; Xiao, W.; Xiao, B.; Li, X. Identification of prognostic biomarkers in glioblastoma using a long non-coding RNA-mediated, competitive endogenous RNA network. *Oncotarget* **2016**. [[CrossRef](#)] [[PubMed](#)]
54. Sun, J.; Gong, X.; Purow, B.; Zhao, Z. Uncovering MicroRNA and Transcription Factor Mediated Regulatory Networks in Glioblastoma. *PLoS Comput. Biol.* **2012**, *8*, e1002488. [[CrossRef](#)] [[PubMed](#)]
55. Fritah, S.; Niclou, S.P.; Azuaje, F. Databases for lncRNAs: A comparative evaluation of emerging tools. *RNA* **2014**, *20*, 1655–1665. [[CrossRef](#)]
56. Zhang, X.; Wang, J.; Li, J.; Chen, W.; Liu, C. CRlncRC: A machine learning-based method for cancer-related long noncoding RNA identification using integrated features. *BMC Med. Genom.* **2018**, *11*, 120. [[CrossRef](#)]
57. Chen, X.; Gao, Y.; Li, D.; Cao, Y.; Hao, B. LncRNA-TP53TG1 Participated in the Stress Response Under Glucose Deprivation in Glioma. *J. Cell Biochem.* **2017**, *118*, 4897–4904. [[CrossRef](#)]

58. Xiao, H.; Liu, Y.; Liang, P.; Wang, B.; Tan, H.; Zhang, Y.; Gao, X.; Gao, J. TP53TG1 enhances cisplatin sensitivity of non-small cell lung cancer cells through regulating miR-18a/PTEN axis. *Cell Biosci.* **2018**, *8*, 23. [[CrossRef](#)]
59. Feldstein, O.; Nizri, T.; Doniger, T.; Jacob, J.; Rechavi, G.; Ginsberg, D. The long non-coding RNA ERIC is regulated by E2F and modulates the cellular response to DNA damage. *Mol. Cancer* **2013**, *12*, 131. [[CrossRef](#)]
60. Lee, S.; Kopp, F.; Chang, T.C.; Sataluri, A.; Chen, B.; Sivakumar, S.; Yu, H.; Xie, Y.; Mendell, J.T. Noncoding RNA NORAD Regulates Genomic Stability by Sequestering PUMILIO Proteins. *Cell* **2016**, *164*, 69–80. [[CrossRef](#)]
61. Prensner, J.R.; Chen, W.; Iyer, M.K.; Cao, Q.; Ma, T.; Han, S.; Sahu, A.; Malik, R.; Wilder-Romans, K.; Navone, N.; et al. PCAT-1, a long noncoding RNA, regulates BRCA2 and controls homologous recombination in cancer. *Cancer Res.* **2014**, *74*, 1651–1660. [[CrossRef](#)] [[PubMed](#)]
62. Mazor, G.; Levin, L.; Picard, D.; Ahmadov, U.; Carén, H.; Borkhardt, A.; Reifenberger, G.; Leprivier, G.; Remke, M.; Rotblat, B. The lncRNA TP73-AS1 is linked to aggressiveness in glioblastoma and promotes temozolomide resistance in glioblastoma cancer stem cells. *Cell Death Dis.* **2019**, *10*, 246. [[CrossRef](#)]
63. Campos, B.; Wan, F.; Farhadi, M.; Ernst, A.; Zeppernick, F.; Tagscherer, K.E.; Ahmadi, R.; Lohr, J.; Dictus, C.; Gdynia, G.; et al. Differentiation therapy exerts antitumor effects on stem-like glioma cells. *Clin. Cancer Res.* **2010**, *16*, 2715–2728. [[CrossRef](#)] [[PubMed](#)]
64. Villa, A.; Snyder, E.Y.; Vescovi, A.; Martinez-Serrano, A. Establishment and properties of a growth factor-dependent, perpetual neural stem cell line from the human CNS. *Exp. Neurol.* **2000**, *161*, 67–84. [[CrossRef](#)] [[PubMed](#)]
65. Bady, P.; Sciuscio, D.; Diserens, A.C.; Bloch, J.; van den Bent, M.J.; Marosi, C.; Dietrich, P.Y.; Weller, M.; Mariani, L.; Heppner, F.L.; et al. MGMT methylation analysis of glioblastoma on the Infinium methylation BeadChip identifies two distinct CpG regions associated with gene silencing and outcome, yielding a prediction model for comparisons across datasets, tumor grades, and CIMP-status. *Acta Neuropathol.* **2012**, *124*, 547–560. [[CrossRef](#)]



© 2020 by the authors. Licensee MDPI, Basel, Switzerland. This article is an open access article distributed under the terms and conditions of the Creative Commons Attribution (CC BY) license (<http://creativecommons.org/licenses/by/4.0/>).

Supplementary Materials:

Temozolomide-Induced RNA Interactome Uncovers Novel LncRNA Regulatory Loops in Glioblastoma

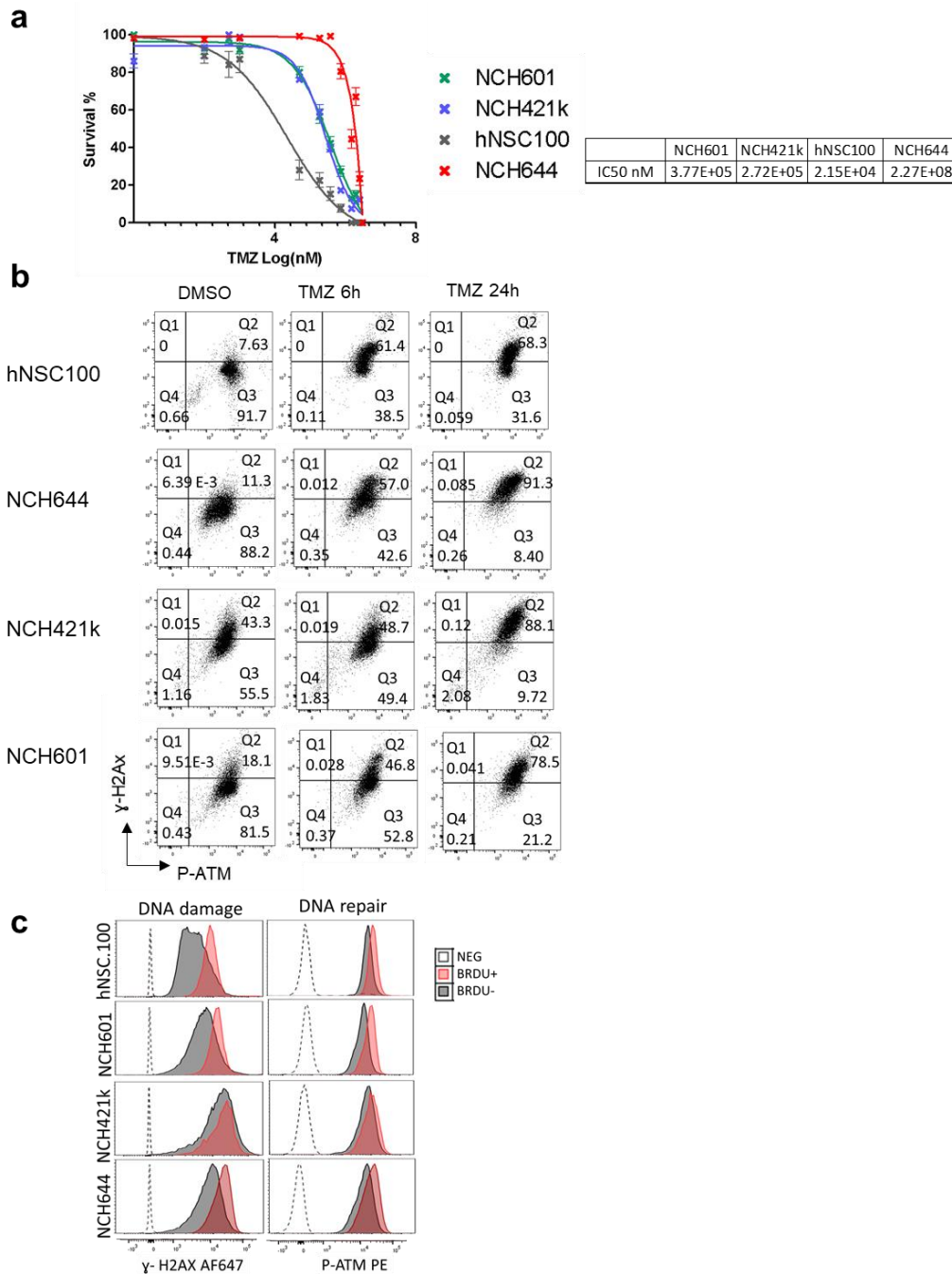


Figure S1. TMZ sensitivity and DDR activation in GSCs. **(a)** IC₅₀ after 72 h of TMZ treatment **(b)** Dot plots showing basal level and induction of DNA damage (γ -H2AX) and DNA repair (P-ATM) after 6 hours and 24 hours TMZ treatment, or 24 h DMSO. The gating applied discriminates between P-ATM positive vs. negative cells, and γ -H2AX high vs low cells. Percentage of cells in the four quartiles are shown. **(c)** Basal level of γ -H2AX and P-ATM is higher in BRDU+ cells than BRDU- cells. Isotype controls for antibody staining are shown for each cells (Neg).

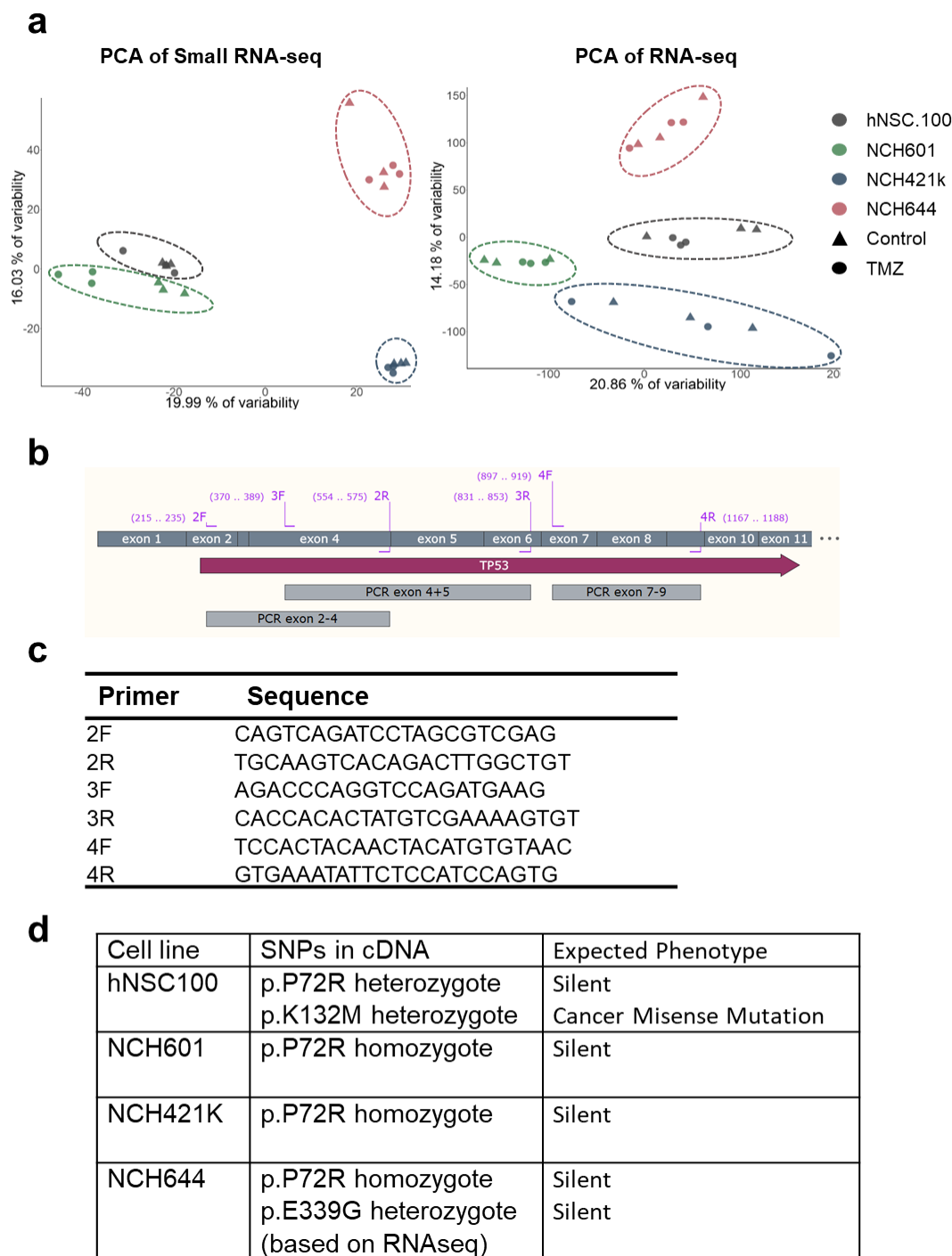


Figure S2. Principal Component analysis of all samples and TP53 genomic status of GSCs (a) Principal component analysis of Small RNA-seq and RNA-seq data: the cell line is the main source of transcriptome variation. Three biological replicate have been analysed per condition. Cell lines are shown as followed: hNSC100 are in grey, NCH601 in green, NCH421k in blue, NCH644 in pink; control samples are in triangle and treated samples as circles. (b) The scheme indicates the position of the primers used and the sequenced PCR fragments, (c) Table with primer sequences used for PCR, (d) Table with detected SNPs and related phenotype based on IARC database.

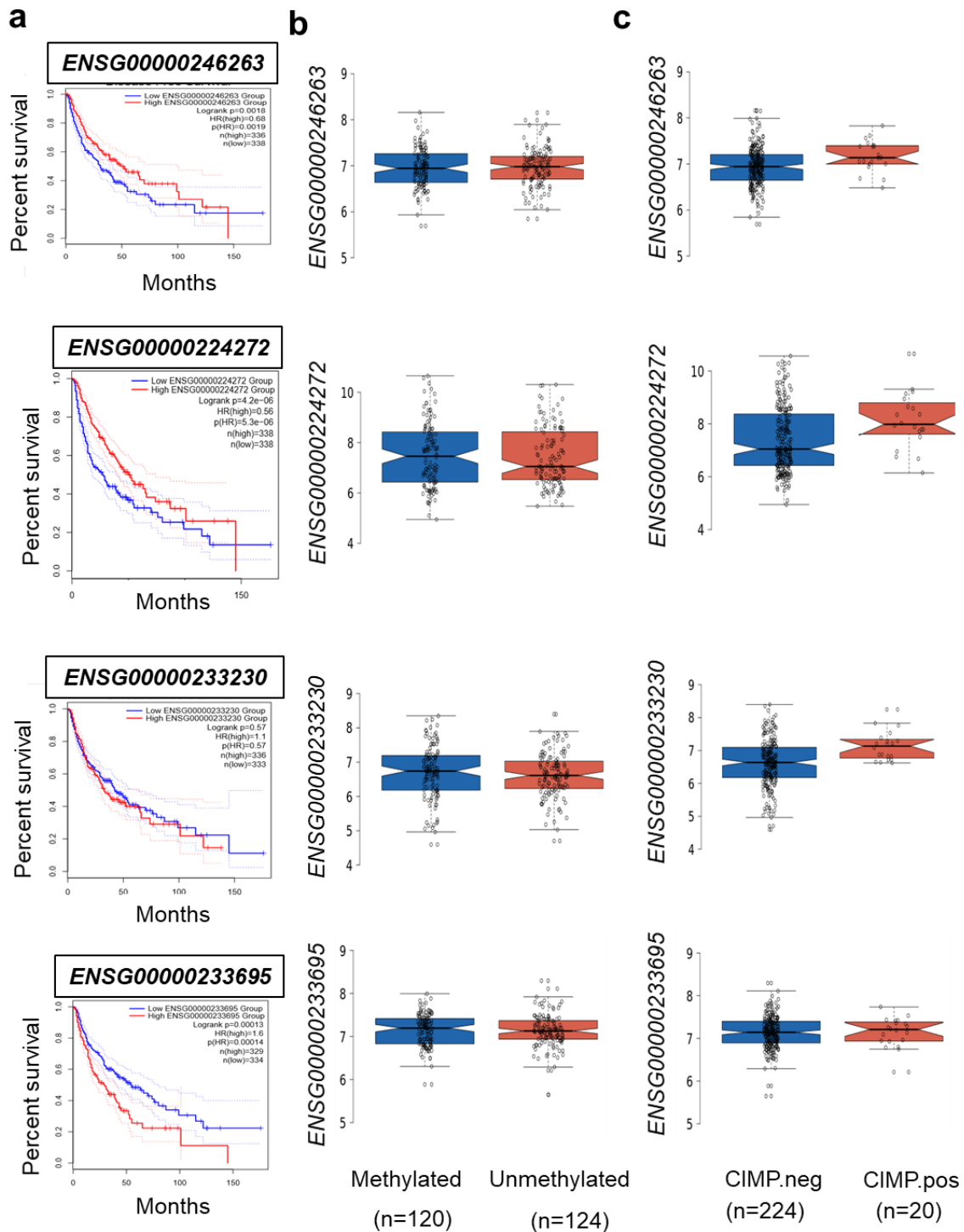


Figure S3. TMZ-regulated lncRNAs as novel independent GBM prognosis markers of progression free survival **(a)** Kaplan Meier disease-free survival curves for the 4 overlapping lncRNAs in gliomas patients. Significance is indicated by log rank p-value on the graphs **(b)** and **(c)** Box plots of lncRNAs in GBM patients with methylated ($n = 120$) or unmethylated MGMT ($n = 124$) in **(b)**, as well as GBM patients with positive ($n = 20$) or negative CIMP phenotypes ($n = 224$) in **(c)**. Significance is indicated by non-overlapping notches.

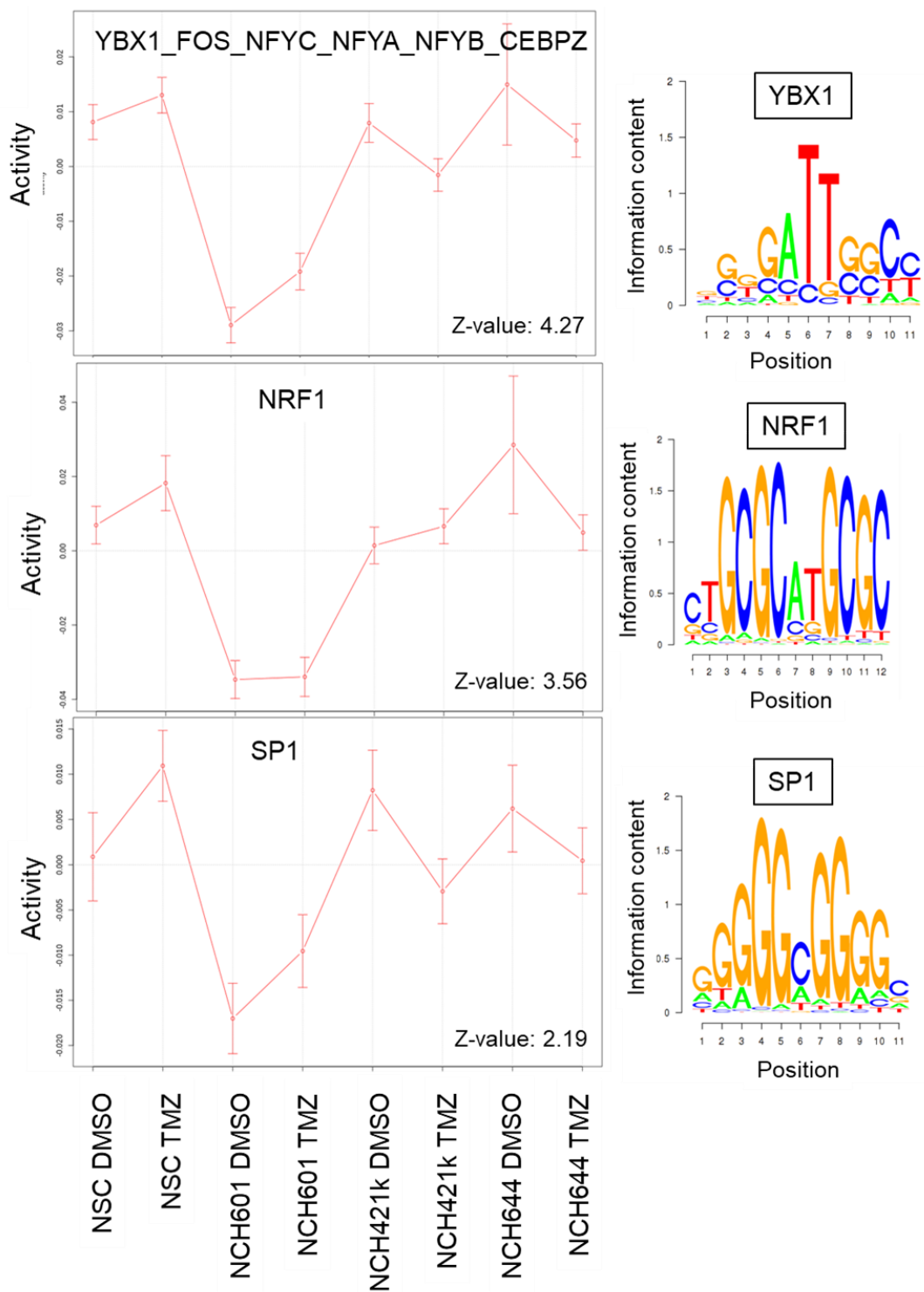


Figure S4. Selected examples of Top 10 transcription factor motifs sorted by activities (z-value) from ISMARA.

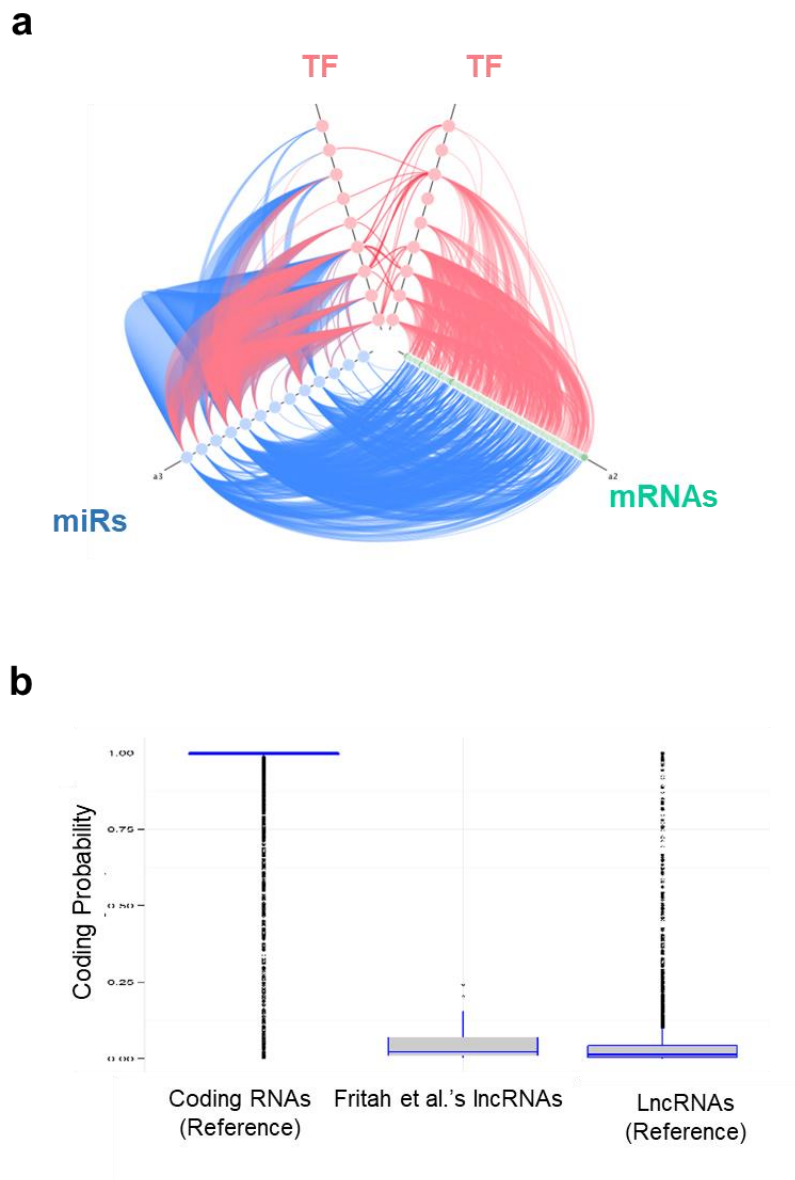


Figure S5. mRNA-containing regulatory loops and coding potential of selected lncRNAs (a) Hive plot representing TMZ-regulated FFLs containing mRNAs from NCH601. Axes indicate different RNA families, with each dot corresponding to a gene (TF, miRNA, or mRNA) involved in mRNA-containing loops. Molecular interactions are represented by a colour code line (stimulatory interactions in red, inhibitory interactions in blue), (b) Distribution of the coding potential of the 22 lncRNAs present in the TMZ- associated motifs predicted by CPAT.

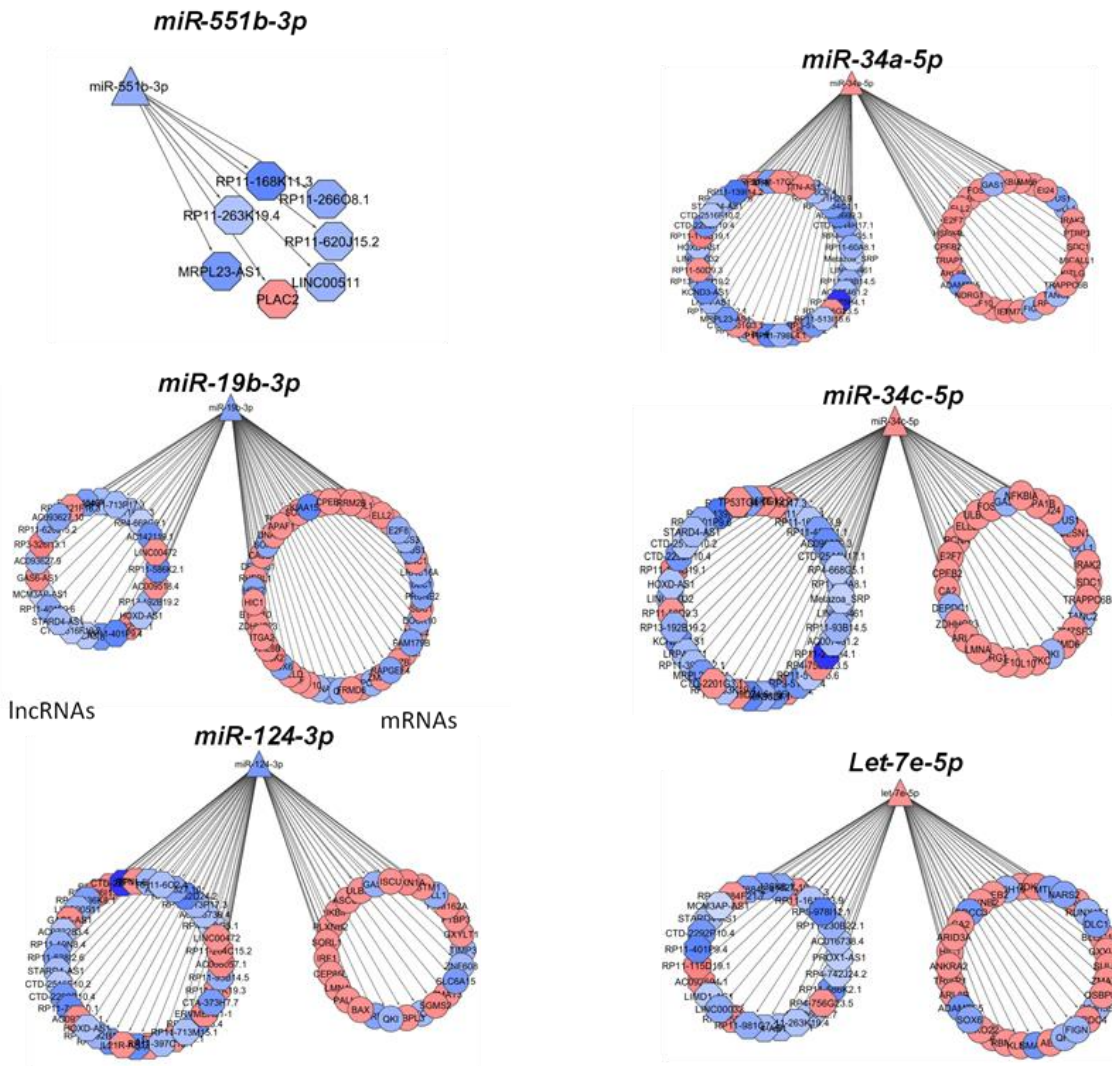
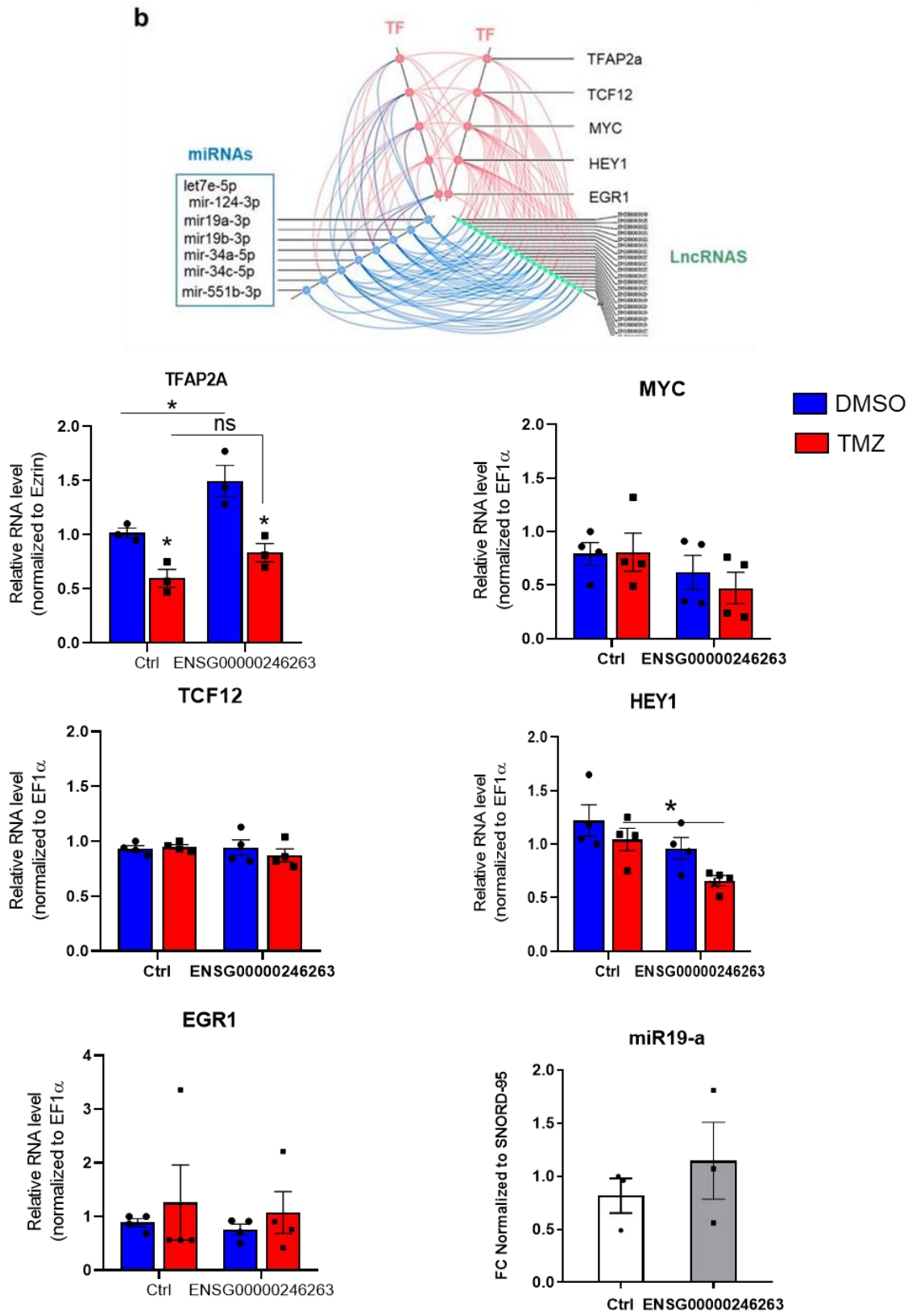


Figure S6. Gene regulatory networks representing the molecular associations between selected miRNAs and mRNAs or lncRNAs in NCH601. Up- and downregulated RNAs are shown in red and blue, respectively. Different node shapes distinguish RNA families; TF: square, miRNA: triangle, mRNA: circle, lncRNA: hexagon.

EXTENDED DATA**The validation of TMZ-induced transcriptional regulatory loop**

For the validation of the TMZ-induced regulatory circuit, we concentrated on regulators (transcription factors and miRNAs) present in most of the lncRNA-containing loops (Figure 5b). We selected key regulators including miR-19a, TCF12, TFAP2A, MYC, EGR1, and HEY1 and validated their expression by RT-qPCR in NCH601 cells treated or not with (500 μ M) TMZ. Moreover, we tested their expression regulation after the overexpression of one selected lncRNA candidate (ENSG00000246263) in NCH601 cells. RT-qPCR (Figure EX1) showed no statistical difference in gene expression regulation after TMZ treatment or upon ENSG00000246263 overexpression.

Extended_Figure 1



CHAPTER 5

RESULTS

RADAR, a novel long noncoding RNA, regulates S-Phase DNA Damage, DNA Replication and Impairs Chromosome Segregation in Glioblastoma

Mohamad Sarmini^{1,2}, Monika Dieterle¹, Ross D. Carruthers³, Coralie Guerin^{4,5}, Eliane Klein¹, Vanessa Barthelemy¹, Arnaud Muller⁶, Eric Van Dyck⁷, Simone Niclou^{1,8,*}, and Sabrina Fritah^{1*}

Submitted

RATIONAL

From the 22 lncRNAs described in (**Chapter 4**), we selected one lncRNA (*ENSG00000246263*) to investigate its role in GBM and TMZ-resistance. The selection was based on rational criteria that should match a prognostic value in glioma overall and disease free survival, differential expression in GBM compared to control brain tissue, induction upon TMZ treatment in sensitive GSCs compared to resistant cells, and enrichment in biological functions related to cell cycle regulation and DDR pathways.

Being a novel lncRNA gene, the results described in this chapter comprise my main work for this PhD thesis, which includes a full characterization of this gene, descriptive analysis of its biological role in the regulation of GBM response to TMZ, and uncovering its molecular mechanism of action. We named this novel lncRNA gene ***RADAR*** (***R******N******A*** ***A******s******s******o******c******i******a******t******e******d*** ***w******i******t******h*** ***D******A******m******a******g******e*** ***a******n******d*** ***R******e******p******l******i******c******a******t******i******o******n***) because our results indicate that *RADAR* is induced upon TMZ treatment and amplifies the DNA damage upon replication stress caused by DNA damaging agents. We found that *RADAR* reduces GBM sphere size and enhances the sensitivity to DNA damaging agents. Its expression is cell cycle dependent during G1/S and has a role during DNA replication which leads to a reduced DNA synthesis velocity and replication fork progression, causing premature S-phase exit, mitotic abnormalities, and sister chromatid cohesion loss. The results are presented here in the form of a manuscript.

Contribution:

The vast majority of experimental procedures, data analysis, figure production, and writing of the first manuscript draft for this study were done by me. Additional contributions were as follows:

- Simone Niclou:
 - ✓ Supervision and advice
 - ✓ Manuscript correction and proofreading
- Sabrina Fritah:
 - ✓ Supervision, advice, and experimental planning
 - ✓ Manuscript draft correction and proofreading
 - ✓ Figures (1A, 1G, S2D, and 6D)
 - ✓ High through-put immuno FISH experimental procedure
- Monika Dieterle:
 - ✓ Generation of cell lines (*RADAR* overexpression)
 - ✓ Figures (S1C and 2K)
- Ross D. Carruthers:

- ✓ DNA fiber assay experimental procedure, data analysis, and figures (6A-C and S8A-B)
- Eliane Klein:
 - ✓ Immunofluorescence in Figure 6A
- Coralie Guerin:
 - ✓ High through-put immune FISH experimental procedure
- Arnaud Muller:
 - ✓ Bioinformatic analysis for figure S4D and S4E
- Eric Van Dyck:
 - ✓ Molecular tools (NCH644 cells with MGMT knockdown)

Beside this manuscript, I will describe and discuss in “EXTENDED DATA” section additional results linked to:

- *RADAR* isoform characterization and the identification of a circular RNA isoform backspliced from *RADAR*.
- Experimental procedures and strategies in attempts to generate new molecular tools to manipulate *RADAR* expression and validate its function.
- *In-vivo* studies aiming to address *RADAR* function and effect in GBM orthotopic xenograft models

Title

RADAR, a novel long noncoding RNA, regulates S-Phase DNA Damage, DNA Replication and Impairs Chromosome Segregation in Glioblastoma

Authors

Mohamad Sarmini^{1,2}, Monika Dieterle¹, Ross D. Carruthers³, Coralie Guerin^{4,5}, Eliane Klein¹, Vanessa Barthelemy¹, Arnaud Muller⁶, Eric Van Dyck⁷, Simone Niclou^{1,8,*}, Sabrina Fritah^{1*}

Affiliations

¹NorLux Neuro-Oncology Laboratory, Department of Oncology, Luxembourg Institute of Health, Luxembourg, L-1526, Luxembourg

²Faculty of Science, Technology and Medicine, University of Luxembourg, L-4365 Esch-sur-Alzette, Luxembourg

³Institute of Cancer Sciences, Wolfson Wohl Cancer Research Centre, University of Glasgow, Glasgow, G61 1QH, UK

⁴Université de Paris, Innovative Therapies in Haemostasis, INSERM, 75006, Paris, France

⁵Cytometry Department, Curie Institute, 75006, Paris, France

⁶Quantitative Biology Unit, Luxembourg Institute of Health, Luxembourg, L-1445, Strassen, Luxembourg

⁷DNA Repair and Chemoresistance, Department of Oncology, Luxembourg Institute of Health, Luxembourg, L-1526

⁸Department of Biomedicine, University of Bergen, Bergen, N-5009, Norway.

*These authors share senior authorship

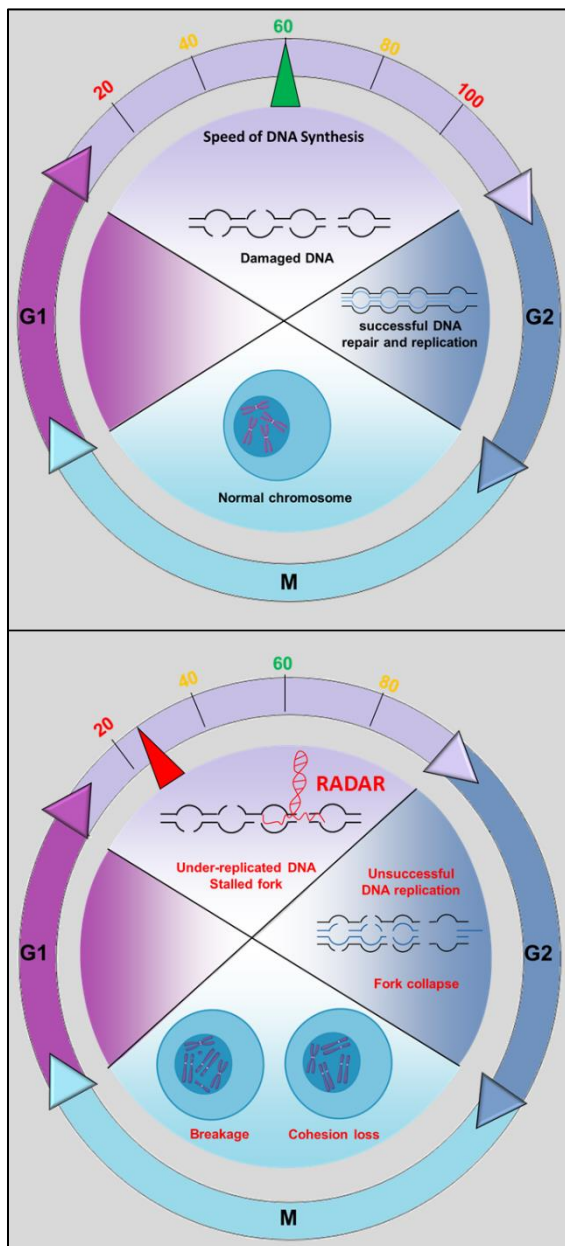
Correspondence

sabrina.fritah@lih.lu and simone.niclou@lih.lu

Key Words

Glioblastoma, lncRNA, Chemoresistance, Cell Cycle, DNA damage, DNA replication, sister chromatid

Graphical abstract



In Brief

Sarmini et al. show that *RADAR* is a novel diRNA modulating Glioblastoma sensitivity to genotoxic drugs. *RADAR* is expressed in G1/S phase and has a role during DNA replication. It exacerbates replication-associated DNA damage, leading to increased accumulation of the DNA damage markers γ -H2Ax, 53BP1 and RPA-coated ssDNA. *RADAR* enhances replication stress, impairs DNA replication, and triggers chromosome mis-segregation in mitosis.

Highlights

- *RADAR* is a novel chromatin-associated diRNA
- *RADAR* sensitizes Glioblastoma stem-like cells to TMZ *in vitro*
- *RADAR* increases DNA damage associated with DNA replication
- *RADAR* impairs the velocity of DNA replication forks and induces replication stress
- Overexpression of *RADAR* causes mitotic abnormalities and loss of chromosome cohesion

SUMMARY (193 words)

Resistance to therapy remains a major challenge to effective treatment for Glioblastoma (GBM). We recently found that long noncoding RNAs (lncRNAs) represent an underestimated component of the transcriptional response to the DNA alkylator Temozolomide (TMZ), the mainstay in chemotherapy against GBM. We hypothesized that the functional exploration of lncRNAs may shed light on novel mechanisms to overcome chemotherapeutic resistance in GBM. Here, we characterized a novel lncRNA, that we named *RADAR* (RNA Associated with DNA damage And Replication). We showed that *RADAR* is a nuclear dilncRNA (damage-induced lncRNAs), activated by TMZ and other alkylating agents, which sensitizes glioblastoma stem-like cells to chemotherapy in vitro. Upon genotoxic stress, *RADAR* overexpression resulted in accumulation of double stranded DNA breaks and RPA-coated single stranded DNA. Moreover, cell cycle synchronization experiments identified *RADAR* as a cell cycle-regulated lncRNA which acted during S-Phase. *RADAR* impaired replication fork velocity and increased replication stress, resulting in sister chromatid cohesion defects in mitosis. In conclusion, we provide a novel mechanism of cell cycle and DNA damage control by a lncRNA that could be further exploited to chemosensitize GBM to TMZ.

INTRODUCTION

Noncoding RNAs represent the vast majority of the human transcriptome, among which, long noncoding RNAs (lncRNAs) are a main class of potent regulatory and tissue-specific transcripts. lncRNAs are defined by a length > 200 nt with limited coding potential (Kung et al., 2013). A subclass of lncRNAs, named damage induced lncRNA (dilncRNA) are activated by exposure to genotoxic drugs and function in the initiation of DNA Damage response (DDR) and/or the regulation of its effectors (Su et al., 2018). When DNA damage occurs, several DDR factors are loaded on the site of the lesion for the detection of damage type, the choice of repair pathway(s) and cell fate decision (Jackson and Bartek, 2009). However, our knowledge still requires a deep understanding on how the DDR factors are guided to the site of DNA damage and how DNA repair pathways are orchestrated. Based on their complementary sequence and secondary structure, dilncRNAs expressed immediately after the DNA damage can guide DDR factors to the damaged locus and act as scaffold for the assembly of DDR complexes (Michelini et al., 2017). Another study described a dilncRNA named "*DINO*" as an essential DDR component that stabilizes the P53 protein, hence, promoting apoptosis after reaching a threshold of DNA damage (Schmitt et al., 2016).

Increasing evidence shows the importance of lncRNAs in hallmarks of cancer and more specifically, in glioblastoma (GBM) (Stackhouse et al., 2020; Zhang et al., 2015a). We and others showed that glioma progression and invasion are regulated by lncRNAs, predominately

through the regulation of signaling pathways and/or via lncRNAs-microRNAs interactions (Han et al., 2020; Li et al., 2018; Zhang et al., 2013). Resistance to therapy remains the main challenge to effectively treat GBM. Since 15 years, and despite large efforts in developing new therapeutic strategies, GBM patients are still treated, after surgery, with radio- and chemotherapy using the DNA alkylating agent Temozolomide (TMZ) (Stupp et al., 2005). Primary resistance to TMZ is largely due to the expression of the O⁶-methylguanine-DNA methyltransferase (MGMT), which directly removes the cytotoxic lesions induced by TMZ (Kitange et al., 2009), yet, other DNA repair mechanisms can contribute to primary and secondary GBM chemoresistance (Erasimus et al., 2016; Higuchi et al., 2020; Yi et al., 2019).

As lncRNAs display important roles in DNA damage signaling, we hypothesize that they could play a role in GBM response to TMZ. To do so, we performed RNA-seq and small RNAseq on Glioblastoma stem-like cells (GSCs) treated with TMZ and investigated gene networks in sensitive versus resistant cells (Fritah et al., 2020). This work highlighted lncRNAs as novel component of transcriptional regulatory circuits in GBM, among which the lncRNA (ENSG00000246263 or UBR5-AS1), that we named here, *RADAR* (*RNA Associated with DNA damage And Replication*), (Fritah et al., 2020). This lncRNA was selected for further investigation based on its prognostic value as biomarker of glioma patient overall survival.

Here, we describe and functionally characterize this novel transcript. RADAR is induced by cytotoxic agents, including TMZ, hence it belongs to the damage-induced lncRNA subclass (dilncRNA). We demonstrate that RADAR is a nuclear retained lncRNA which sensitize GBM cells to TMZ. Upon genotoxic stress, RADAR enhances the extent of DNA damage and promotes the recruitment of the DNA damage proteins RPA and 53BP1. Moreover, we found that RADAR expression is periodic in the cell cycle, with peaks in S-Phase. RADAR overexpression induces replication fork stalling and leads to replication stress, which results in mitotic abnormalities, displayed by loss of sister chromatid cohesion. In summary, we identify RADAR as a novel regulator of DNA damage and replication and shed new light on the critical function of lncRNAs as cell cycle checkpoints and regulators of chromosome stability.

RESULTS

RADAR Sensitizes GSCs to TMZ and Other DNA Damaging Drugs

We previously identified that RADAR was induced upon TMZ treatment in GSCs (Fritah et al., 2020). Using RT-qPCR, we validated that *RADAR* expression was activated only in sensitive cells (NCH601 and NCH421k) cells, but not in TMZ-resistant GSCs (NCH465 and NCH644) (Figure 1a), suggesting a role of *RADAR* in TMZ response. To investigate the biological function of *RADAR*, we generated 3 GSC models with stable *RADAR* overexpression. A

comparative level of overexpression, ranging from 15 to 25 fold enrichment of *RADAR* was achieved in the GSCs (Figure 1b). We measured sphere growth in the absence or presence of TMZ. While *RADAR* expressing cells displayed a small reduction in sphere size in NCH601 and NCH644 GSCs in untreated conditions (Figure 1c), GSC growth was significantly impaired in all *RADAR* GSCs, following TMZ treatment (Figure 1c).

The DNA repair protein MGMT is the main determinant of TMZ resistance in GBM (Kitange et al., 2009). Taken into consideration that *RADAR* expression was not induced following TMZ treatment in MGMT expressing cells (NCH644) (Figure 1a), we sought to investigate a putative relationship between *RADAR* and MGMT. To do so, we depleted MGMT in NCH644/*RADAR*⁺ cells using interference RNA. WT and *RADAR*⁺ NCH644 cells were transduced with two independent shRNAs targeting MGMT or scrambled oligonucleotide as control (Figure S1a and S1b). The depletion of MGMT did not rescue the induction of *RADAR* upon TMZ (Figure S1c), indicating that *RADAR* expression is independent of MGMT. We next monitored the growth ability of these cells. As expected, cells depleted from MGMT showed a significant reduction in sphere size upon TMZ (Figure S1d and S1e, light blue). Moreover, cells with concomitant MGMT depletion and *RADAR* overexpression displayed further significant reduction in GBM-sphere growth upon TMZ (Figure S1d and S1e, red). These results indicate that *RADAR* is a novel regulator of GBM chemosensitivity, and acts independently of MGMT.

Next, we tested the impact of other DNA damaging drugs in *RADAR* expressing cells. In NCH421k and NCH644 treated with cisplatin (10 μ M), a platinum-based antineoplastic drug which forms crosslink with purine DNA bases (Dasari and Tchounwou, 2014), we observed a significant reduction in sphere size of *RADAR* overexpressing cells (Figure 1d). TMZ is a genotoxic drug which induces multiple DNA lesions, which can lead, if not repaired, to replication stress (Yoshimoto et al., 2012). We next evaluated *RADAR* induction with Cytarabine (ARA-C) which blocks DNA replication (Richardson et al., 2004). *RADAR* expression was induced with increasing doses of ARA-C in the TMZ-sensitive NCH601 GSC. At high dose of ARA-C *RADAR* was also induced in the NCH644 TMZ resistant (Figure 1e and 1f). *RADAR* also impaired GBM cell growth *in vitro* upon ARA-C (0.1 μ M) treatment (Figure 1g). Altogether, we evidenced that *RADAR* is a novel lincRNA with potential role in GBM chemosensitivity to DNA damaging agents.

***RADAR* Is A Nuclear And Chromatin-Associated lincRNA**

RADAR (also termed *UBR5-AS1* or *ENSG00000246263*) is located on chr.8q22.3, in opposite orientation to the protein-coding genes *RRM2B* and *UBR5* (Figure 2a). The LNCipedia database (LNCipedia v4.1) reports nine isoforms of *RADAR* (Figure S2a), and, by variant specific RT-PCR, we detected seven of these isoforms, expressed in multiple patient-derived

GSCs (data not shown). Despite the large overlapping regions between most of *RADAR* isoforms, we were able to design isoform-specific probes for isoform 1/7, 3, 4, 5 and 6. We did not detect isoform-specific induction by TMZ, although isoform 3 had the highest tendency of induction among other *RADAR* transcripts detected by RT-qPCR (Figure S2b). Using 5' and 3' RACE-PCR, we found that *RADAR* is mainly expressed as a major transcript of 1.9 kb, composed of three exons (Figure S2a and S2c). We next evaluated the non-coding nature of *RADAR* using CPAT, CPC and PhyloCSF *in-silico* analysis tools (Figure S2d to S2f). Given that lncRNAs may contain small open reading frames (smORFs), we investigated the presence and length of putative smORFs, taking a threshold of 100 amino acids and a low level of phylogenetic conservation into consideration, both criteria being widely used to differentiate between protein-coding and non-coding eukaryotic transcripts (Clamp et al., 2007; Frith et al., 2006; Goffeau et al., 1996). We did not identify a conserved ORF in *RADAR*, indicating that this transcript is likely to act as a lncRNA (Figure S2g).

Despite limited overall sequence identity, functional lncRNA genes host relative evolutionary conservation among species (Quinn et al., 2016; Ulitsky et al., 2011). When analysing *RADAR* gene structure and nucleotide sequence we showed that *RADAR* is only conserved among higher primates with identities matching up to 98.92% for the transcript (*XR_001720343.2*) in Pan troglodytes (NCBI-BLAST). Moreover, we located a transcript (*Gm49085*) that resembles *RADAR* and is in antisense orientation to *Rrm2b* and *Ubr5* genes in the mouse genome (UCSC-GRCm38/mm10, Figure S3a), suggesting that this locus structure is retained during evolution, reinforcing its potential biological significance.

As lncRNAs accumulate in different cellular compartments, their subcellular localization may be indicative of their molecular functions (Carlevaro-Fita and Johnson, 2019; Chen, 2016b). Using publicly available data of the ENCODE project, on cytoplasmic and nuclear RNA expression in commonly used cell lines, we found that *RADAR* is predominantly in the nucleus, except in embryonic stem cells (Figure S3b). Subcellular fractionation of RNAs followed by RT-qPCR showed that *RADAR* is a nuclear lncRNA, also in GSCs (Figure 2b).

We further assessed *RADAR* expression by performing RNA-FISH combined with imaging flow cytometry. To do so, we used a specific probe targeting *RADAR* (or *EF1 α* as control) and measured the obtained RNA intensity signal using the Prime flow technology. In comparison to other available methods, RNA-FISH by imaging cytometry has the unique advantage to measure RNA expression and localization, at a single cell level, in a high-throughput manner, and can be combined with phenotypic markers. In addition to RNA, GSCs were stained with the following markers: CD90 as surface marker, DRR internal markers (γ -H2Ax and P-ATM) and propidium iodide for DNA. As shown in Figure 2c, *RADAR* signal was present in the nucleus whereas *EF1 α* transcripts were present in the cytoplasm. We quantified the overlap

between the fluorescent foci of *RADAR* with the nuclear staining (PI) (Figure 2e, upper histogram) compared to a probe targeting the cytoplasmic mRNA *EF1 α* as control (Figure 2e, lower). These results clearly indicate that *RADAR* is a nuclear retained lncRNA and its subcellular localization is not affected by TMZ treatment (Figure 2e and S3c). We next asked if the expression of *RADAR* and its induction upon TMZ were restricted to a subpopulation of GSCs. We found that *RADAR* is expressed in 70% of the cells and this proportion increased upon TMZ treatment (78%). In addition, a larger population of TMZ-treated cells displayed higher *RADAR* intensity compared to vehicle, used as a control (Figure 2f). As the resolution of imaging cytometry and fluorescence microscopy can differ we assessed the localization of *RADAR* by classical RNA-FISH and confirmed that *RADAR* accumulates in dotted nuclear structures (Figure 2h).

lncRNAs may regulate gene expression of neighboring genes in *Cis* and/or in *Trans* (Kopp and Mendell, 2018). Based on the nuclear localization of *RADAR*, we sought to identify if its overexpression affects gene expression in GSC. To test this (Figure S3d, we used our previously generated GBM cells with stable *RADAR* overexpression (Figure 1b). In all 3 tested GCSs, *RADAR* expression did not impact on either *RRM2B* or *UBR5* RNA levels (Figure S3e). We next assessed transcriptome changes by RNAseq in NCH601 cells and found a total of 129 differentially expressed genes in *RADAR* samples versus control cells (Table S1). Of note, there were 10 times more upregulated genes (118 genes) in *RADAR* overexpressing cells than downregulated (11 genes) (Figure S3f). Altogether, these results indicate that *RADAR* is not a *cis*-acting lncRNA but rather positively regulate gene expression *in trans*.

***RADAR* Potentiates DNA Damage Signaling and Triggers Single Strand Break (SSB)**

We evaluated the effect of *RADAR* on DNA damage formation. Hence, we performed neutral comet assay, where the length of the comet tail reflects the amount of single- and double-strand DNA breaks in a given cell (Collins, 2004; Olive and Banath, 2006). Even without genotoxic stress, *RADAR* overexpressing GSCs (NCH601 and NCH644) displayed longer comet tails, an effect dramatically enhanced upon TMZ (Figure 3a and 3b). The extent of DNA damage measured by the percentage of DNA in tail (Figure S4a and S4e), the tail migration (Figure S4b and S4f), the tail moment (Figure S4c and S4g), and the length: width DNA ratios (Figure S4d and S4h) indicate that *RADAR* overexpression: (1) induces DNA breaks in the absence of any treatment and (2) enhances the extent of DNA damage upon TMZ. Similarly, *RADAR* expression lead to higher accumulation of DNA platinum adducts when the cells were treated with 25 μ M Cisplatin (Figure 3C and 3D). To address the type of DNA damage present in *RADAR* expressing cells, we applied (1) the phosphorylation of Ser139 of the histone variant

H2Ax (γ H2Ax) as marker of DSBs (Valdiglesias et al., 2013), (2) RPA32/RPA2 to label single stranded DNA breaks (SSB) that forms during replication or upon DNA stress (Chen and Wold, 2014; Sleeth et al., 2007), (3) p53-binding protein 1 (53BP1) recruited to the sites of DNA strand breaks following DNA damage (Mirza-Aghazadeh-Attari et al., 2019).

By immunofluorescence staining of the aforementioned markers and quantification of foci, we showed that at basal level, *RADAR* cells showed a slightly higher number of γ H2Ax foci compared to the control (Figure 3e,3g and Figure S5a-c). As expected, the number of DSBs (γ H2Ax foci) and SSBs (RPA32/RPA2 foci) increased after TMZ treatment, especially in MGMT negative cells (NCH601 and NCH421k, Figure 3e, Figure S5a-c). Indeed, when TMZ-induced O6-meG lesions are not directly repaired by MGMT, other DNA repair pathways such as mismatch repair are involved, leading to stalled replication forks (Erasmus et al., 2016). Moreover, we quantified a higher number of 53BP1 foci, especially after TMZ treatment in *RADAR* cells (Figure 3F and 3i, S5d-f). In summary, these results show that *RADAR* directly induces DNA damage, specifically the accumulation of SSBs and DSBs and associated DNA repair signaling pathways, an effect that is significantly amplified by exposure to genotoxic stress.

RADAR Expression is Cell Cycle-Dependent and Impacts on DNA Replication

Using co-expression and pathway enrichment analysis from our RNAseq data on GSCs, we previously showed that *RADAR* (ENSG00000246263) could be linked to cell cycle regulation and DNA replication (Fritah et al., 2020). These bioinformatic predictions are in line with the observed phenotype in GSCs: (1) enhanced DNA damage in *RADAR* overexpressing cells, (2) the increase in RPA32/RPA2 foci in *RADAR* cells following TMZ treatment, (3) *RADAR* induction upon ARA-C, a drug that blocks S-phase. Hence, we sought to investigate the expression of *RADAR* during cell cycle progression. To this effect, we synchronized GSCs at the G1/S borders by double thymidine block and release. The quality of cell cycle synchronization was assessed by flow cytometry (Figure 4a and Figure S6a) and in parallel, *RADAR* expression was determined at each time point collected, by RT-qPCR. We found that *RADAR* is a cell cycle-regulated lncRNA with a peak of expression in late G1-early S (Figure 4b, red). As controls, we used the specific cell cycle genes *CDC25C* (M-phase peaks) and *CCNA2* (G2-phase peaks) (Figure 4b).

We next asked if *RADAR* expression impacts on cell cycle progression. Therefore, we synchronized *RADAR* overexpressing and control cells, similarly as above, except that we added time-points to subdivide each cell cycle phase into early-mid-late phase. After validating the synchronization of the cells (Figure S6b-d), we noticed that *RADAR* expressing cells displayed a comparative cell cycle profile in unsynchronized, at early (0.5h, 2.5h) and late time

points (24h) after synchronization (Figure 4c). Yet, clear differences were observed between RADAR expressing cells and control cells at 5.5h and 7h, reflected by a shift to the right in the DNA content curve at these specific time-points (Figure 4c). These results indicate that *RADAR* cells remain for a shorter period in mid and late S phase (Figure 4d) compared to control cells and exit faster from S-phase. At later time points, the cell cycle profile of RADAR expressing cells and control cells overlaps, implying that G2 phase and/or mitosis may be longer in RADAR expressing cells.

To monitor DNA replication in S-Phase, we performed the DNA fiber assay (Figure 4e) which is based on the sequential incorporation of fluorescent nucleotide analogues CldU (red) and IdU (green) to determine, the velocity of replication and the level of replication stress (Carruthers et al., 2018; Nieminuszczy et al., 2016). Quantitative analysis revealed that *RADAR* cells displayed a reduction in DNA replication velocity as well as an increase in replication forks stalling, indicating that RADAR enhances replication stress in GSCs (Figure 4f-g and S6e). Taken together, these results indicate that *RADAR* expression is tightly regulated across the cell cycle and its overexpression impairs S-phase completion.

RADAR Causes Mitotic Spindle Abnormalities and Sister Chromatid Loss of Cohesion

Despite the fact that *RADAR* impairs DNA replication, RADAR overexpressing cells were still able to enter mitosis and complete their cell cycle (Figure 4c). Since we have shown that RADAR increases S-Phase DNA damage, we hypothesized that RADAR may bypass DNA damage checkpoints and/or may induce cells to exit S-Phase with underreplicated/ unrepaired DNA. We therefore investigated the effect of *RADAR* in mitosis. *RADAR* expressing cells showed a dramatically impaired mitosis (Figure 5a) reflected by defects in mitotic spindle assembly and chromosome segregation. At the level of chromosome structure, *RADAR* overexpression resulted in severe loss of sister chromatid cohesion in metaphase spreads. Importantly, we noticed that *RADAR* overexpression induced chromosome breakage, and the loss of cohesion was observed generally across the entire chromosomes (Figure 5b and 5c). Hence, RADAR overexpression may increase genomic instability.

DISCUSSION and CONCLUSION

TMZ remains the only available drug against GBM, yet eventually recurrence is inevitable. Identifying mechanisms of TMZ resistance may enable novel combinatorial strategies. In this respect, we recently identified that TMZ elicits major transcriptomic changes, coordinated in regulatory loops and involving a large number of lncRNAs with unknown functions (Fritah et al., 2020). Here we characterized one of these lncRNAs, *ENSG00000246263*, here termed *RADAR* whose expression is indicative of glioma prognosis and independent of the MGMT

status of GBM patients (Fritah et al., 2020). We showed that (1) RADAR expression leads to DNA damage and increase in vitro sensitivity to cytotoxic drugs, including TMZ, (2) RADAR expression is cell cycle dependent and (3) its overexpression leads to chromosomal abnormalities and mitotic defects.

The classification and nomenclature of lncRNAs is evolving and database contents are not always concordant (Fritah et al., 2014). The gene described here, RADAR (RNA-associated with DNA damage and Replication) is indicated as *UBR5-AS1* in several databases and antisense lncRNAs were initially described to regulate sense mRNAs. However, we did not observe any effect of RADAR on the level of *RRM2B* and *UBR5* mRNAs in *cis*, indicating that RADAR does not act as an antisense lncRNA but rather regulate gene expression in *trans*. Nevertheless, to rule out any effect of RADAR on neighboring gene transcription, it would be important to inactivate RADAR expression. Yet, so far our attempts to knock-out RADAR by CRISPR or use CRISPRi failed to retrieve reliable clones. In addition, the targeting of antisense lncRNAs by gene knock-out is challenging due to the proximity of neighboring coding genes. Conversely, the functional activation of RADAR by CRISPRa resulted in *RRM2B* induction, as these genes probably share the same promoter (data not shown).

The cell cycle is a tightly regulated process in which each phase completion is orchestrated by the expression of cell-cycle proteins and DNA damage checkpoints. lncRNAs are novel critical regulators of cell proliferation, either by controlling the expression of cell cycle genes or by acting on DNA damage signaling during cell cycle (Kitagawa et al., 2013). Recently, an independent study identified >200 lncRNAs with peak expression occurring during S-phase. In line with our data, *RADAR* was among the cell cycle-regulated RNA candidates, confirming that RADAR is a S-Phase-enriched lncRNA in other cell types (Yildirim et al., 2020). As RADAR expression tends to be upregulated in gliomas compared to healthy brain, its increase may confer an advantage of cancer cells to bypass DNA damage checkpoints and increase genomic instability. Yet, investigating the role of RADAR in normal cells will be important to understand its precise function. In this respect, we have identified from ENCODE data that RADAR is in the nucleus in cell lines originating from different tissues, except in embryonic stem cells (ESCs), where it is enriched in the cytoplasm. If confirmed, as ESCs have a different cell cycle regulation, this could set up a basis for exploring a putative role of RADAR in lineage programming.

Our findings reinforce the importance of lncRNAs as critical modulators of DNA damage signaling, cycle progression and genomic instability (Guiducci and Stojic, 2021). This is in line with several pioneering studies: (1) the lncRNA CONCR (cohesion regulator noncoding RNA) regulates the activity of a DNA-dependent ATPase and helicase (*DDX11*) involved in DNA

replication and chromatid cohesion (Marchese et al., 2016), (2) the inactivation of the lncRNA NORAD "noncoding RNA activated by DNA damage" increases chromosome segregation defects and reduces replication-fork velocity (Lee et al., 2016) (3), the lncRNA SUNO1 (S-phase-Upregulated NON-coding-1) has been shown to promote cell proliferation by controlling YAP1/Hippo signaling pathway (Hao et al., 2020). In these studies, the phenotypes on DNA replication and genomic instability have been observed upon lncRNA depletion. To the best of our knowledge, RADAR is the first report of a lncRNA that directly induces DNA damage and loss of sister chromatid cohesion.

The precise molecular mechanism of *RADAR* on DNA replication and DNA damage remains to be elucidated. However, we propose that *RADAR* could form RNA:DNA hybrids during DNA replication and the formation of R-loop-mediated genomic instability. Indeed, R-loops can form obstacles to efficient DNA replication, leading to DNA damage, replicative stress and chromosomal alteration, that can result in chromosome rearrangements (Aguilera and García-Muse, 2012; Skourti-Stathaki and Proudfoot, 2014). lncRNAs can contain G-Quadruplex structural motifs to form R-loops. By *in-silico* prediction tool (Quadfinder) (Jayaraj et al., 2012), we identified 5 G-Quadruplex motifs in *RADAR* (data not shown). A mechanism involving the lncRNA NEAT1 G-quadruplex motifs recognition by NONO is essential for paraspeckle formation (Simko et al., 2020). In telomeric regions R-loop formation triggers telomere fragility and the lncRNA *TERRA* associates to telomeres through R-loop formation via a RAD51-dependent mechanism (Feretzaki et al., 2020). *RADAR*, through G-quadruplex, may form R-loops during replication and thereby causing DNA damage signaling. It has been shown that DNA damage and genome instability by G-quadruplex ligands are mediated by R-loops in human cancer cells (De Magis et al., 2019).

Another possible mechanism could involve a direct role of *RADAR* on chromatin structure. *RADAR* could enhance chromatin accessibility or DNA unwinding during DNA replication, which could explain the increase of DNA accessibility and DNA damage upon treatment with genotoxic drugs. *RADAR* may regulate the enzymatic activity of the DNA replication machinery or recruit or act as a scaffold for proteins involved in DNA replication or DDR.

Finally, targeting replication stress and enhancing levels of DNA damage with lncRNAs may represent a valuable approach, especially in low proliferative tissue such as healthy brain. This could be achieved by using drugs against lncRNA-associated proteins or by direct targeting of lncRNA by antisense nucleotides. It is tempting to speculate that exploiting such mechanism, as exemplified here with *RADAR*, which acts as a direct DNA damage amplifier and inducer of chromosome breaks in cancer cells, could pave the way for novel lncRNA-therapeutic research efforts in the future.

Figure 1

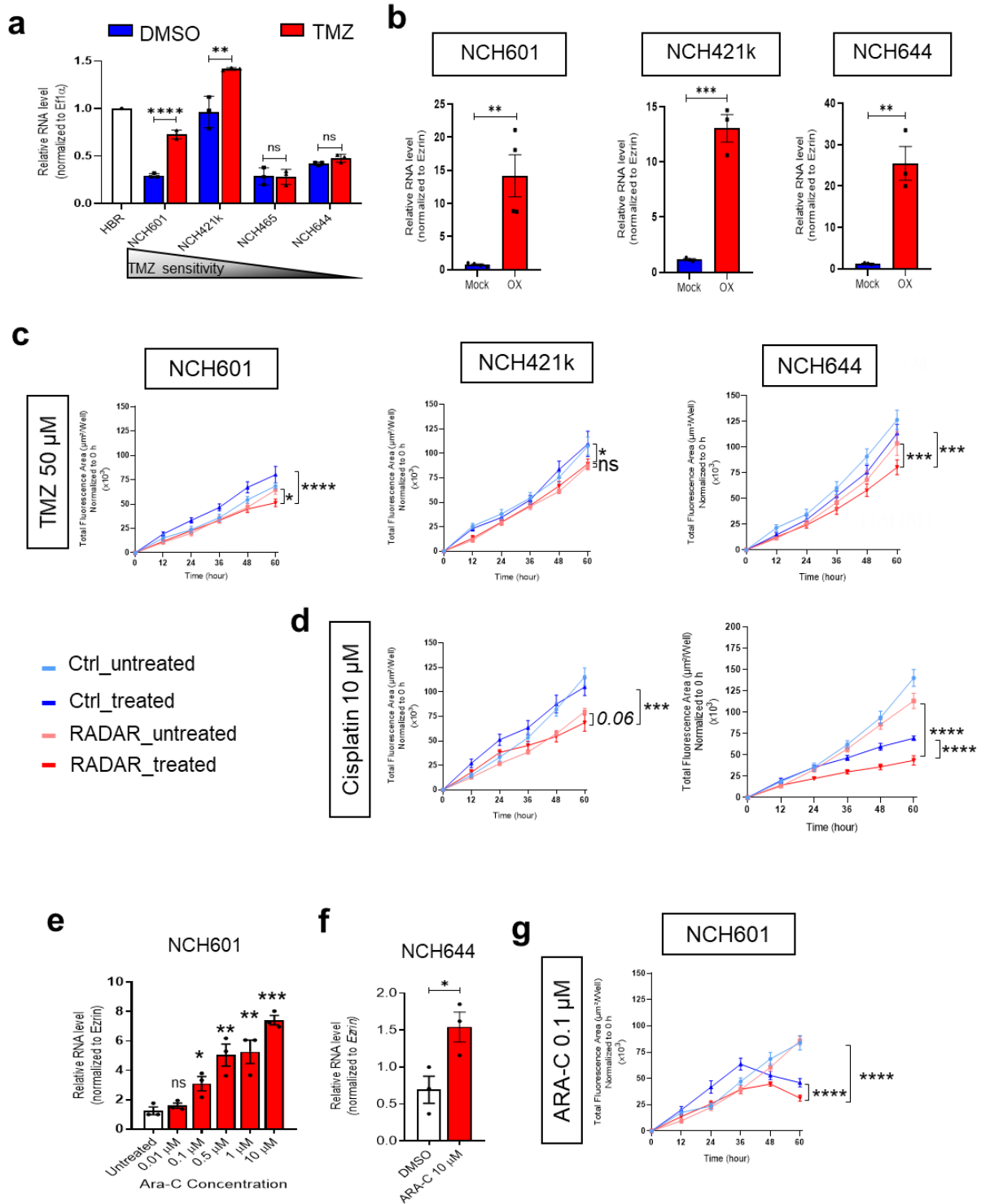
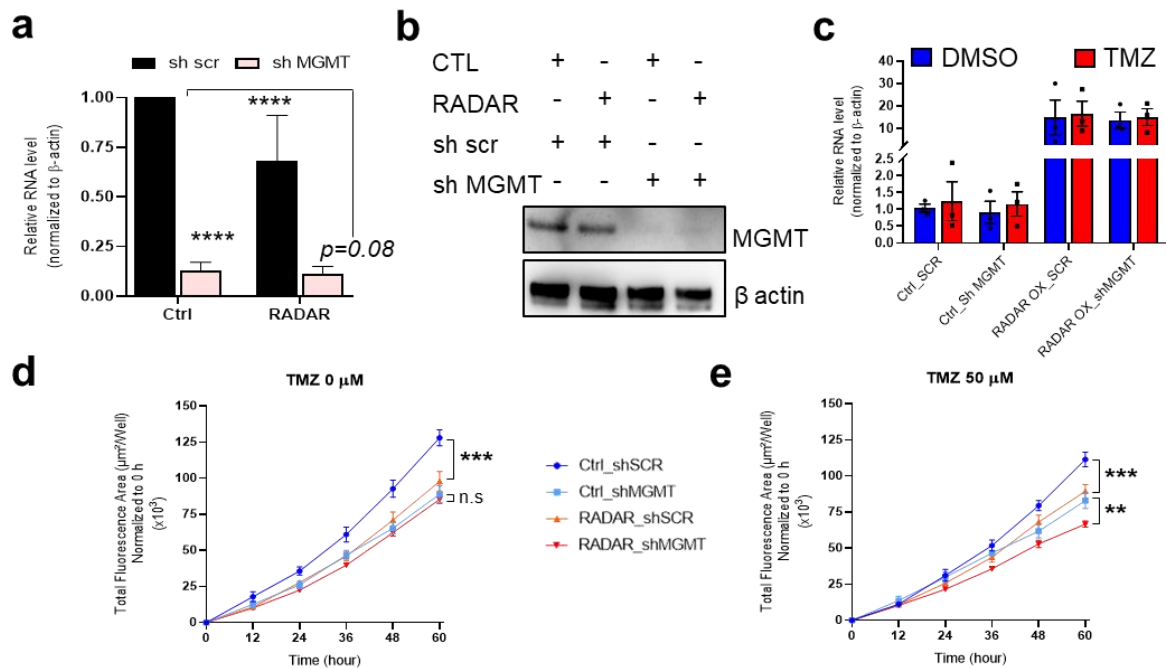


Figure 1. RADAR is a diIncRNA which increases sensitivity to genotoxic drugs in vitro

(a) *RADAR* relative RNA level across GBM cell lines treated or not with TMZ for 24 hr determined by qRT-PCR and normalized to Human Brain Reference (HBR) RNA. (b) *RADAR* overexpression in NCH601, NCH421k, and NCH644 GBM cells obtained through Lenti-viral infection (LV) of *RADAR* 5'-RACE and determined by qRT-PCR. (c,d,g) Real-time monitoring of single GBM-spheroid growth over 60 hr, untreated or treated with (50 μ M) TMZ (c), (10 μ M) Cisplatin (d) or (g) (0.1 μ M) ARA-C. Changes in GFP fluorescent object area measured every 12 hr. Single GBM-spheroid growth curves show mean \pm SEM of 3 independent experiments, where at least 3 spheres per biological replicate are used to calculate the fluorescent object area for each time point. The data results of the growth curve were analyzed by calculating the linear regression of each condition with 95% confidence of the best-fit line. (ns, not significant; *, $p < 0.05$; **, $p < 0.01$; ***, $p < 0.001$; ****, $p < 0.0001$). (e, f) *RADAR* relative RNA level upon ARA-C treatment in NCH601 and NCH644. Graphs show mean \pm SEM of three independent experiments. Two-tailed unpaired Student test was applied to determine statistical significance.

Suppl_Figure 1

**Supplementary Figure 1. RADAR effect on TMZ sensitivity is independent of MGMT**

(a) MGMT knockdown efficiency was determined by qRT-PCR and (b) western blot (c) *RADAR* relative RNA level in cells with MGMT knockdown treated or not with TMZ for 24 hr determined by qRT-PCR. (d,e) Single GBM-spheroid growth curves show mean \pm SEM of three independent experiments, where at least 3 spheres per biological replicate are used to calculate the fluorescent object area for each time point. The data results of the growth curve were analyzed by calculating the linear regression of each condition with 95% confidence of the best-fit line. (ns, not significant; *, $p < 0.05$; ***, $p < 0.001$; ****, $p < 0.0001$).

Figure 2

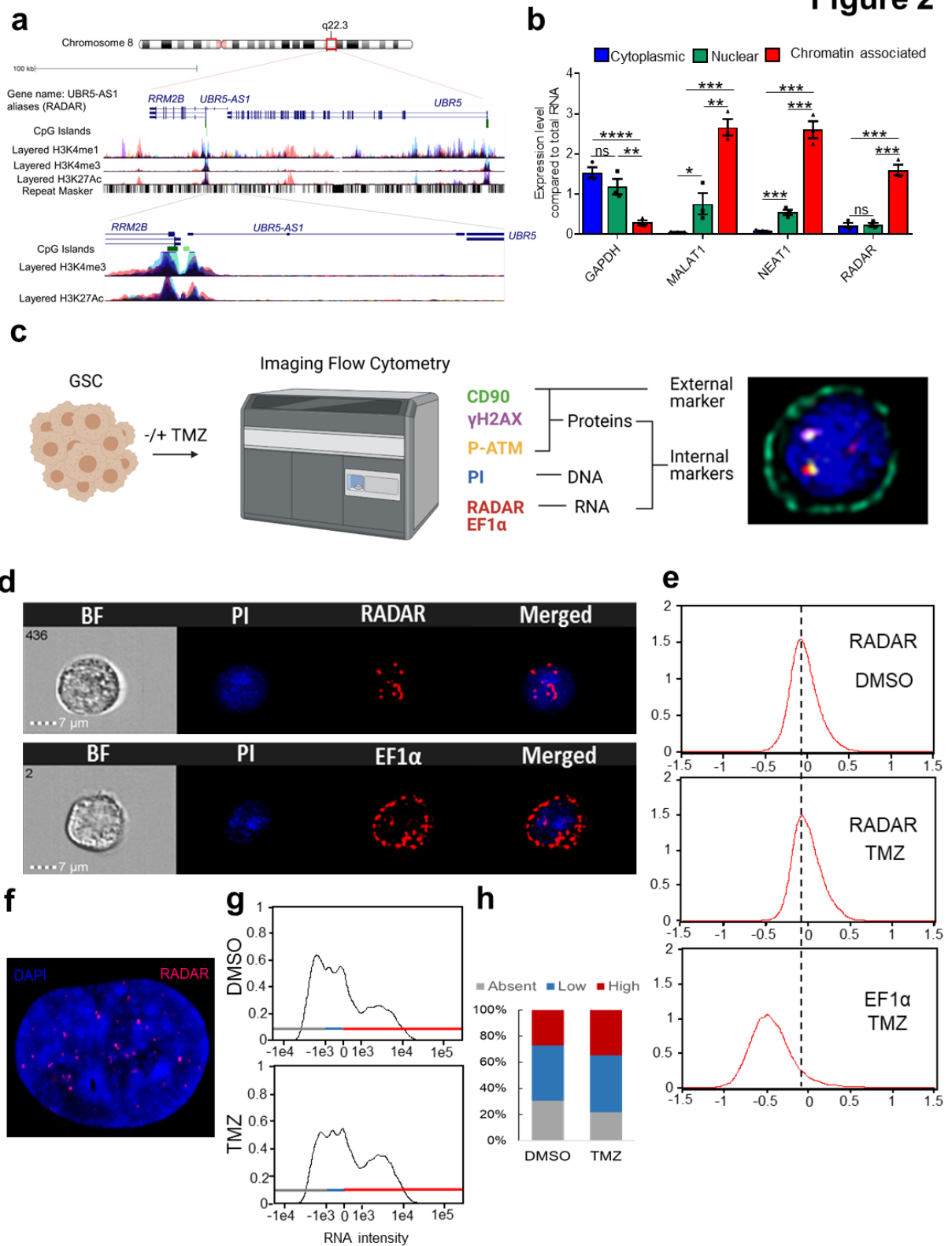
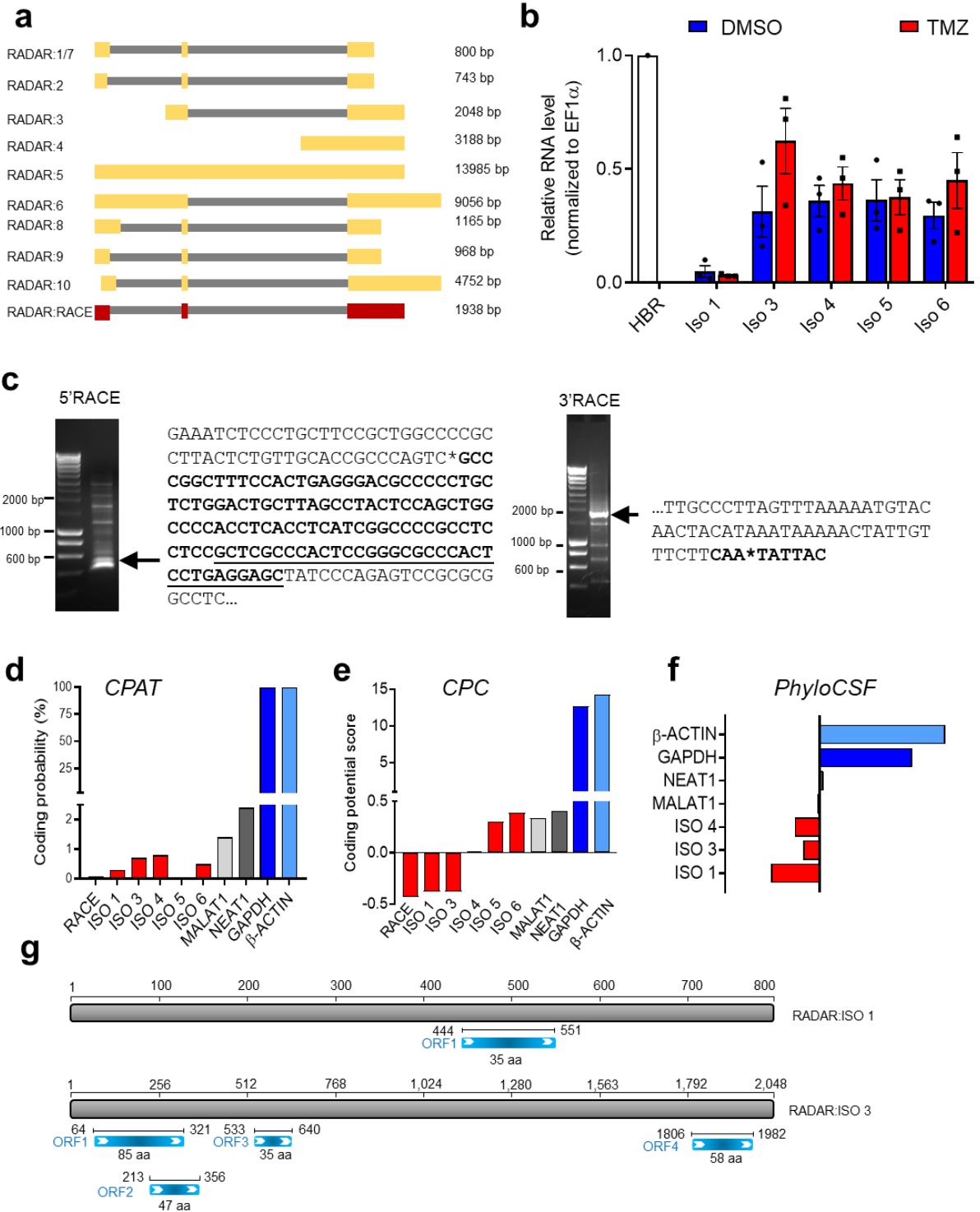


Figure 2. RADAR is a nuclear lncRNA

(a) Genomic locus of the lncRNA *RADAR*. Ideogram represents its location on the long arm of chromosome 8. The structure and orientation of *RADAR* and its neighboring genes *UBR5* and *RRM2B* as annotated in RefSeq. CpG island, H3K4me1, H3K4me3 and H3K27Ac marks on seven cell lines from ENCODE are indicative of active transcription, (b) *RADAR* relative RNA level in the cytoplasmic, nuclear and chromatin-associated fractions isolated from NCH601 using RNA-subcellular fractionation. *GAPDH* used as reference mRNA control whereas *MALAT1* and *NEAT1* used as reference lncRNAs controls, (c) Workflow of Immuno-RNA FISH by Imaging Flow Cytometry, (d) Representative images of NCH601 cells following RNA-target probe hybridization by imaging flow cytometry show the presence of distinct nuclear and cytoplasmic FISH signals (red dots) for *RADAR* (upper) and *EF1 α* (lower) respectively. BF=Bright Field; PI= Propidium Iodid (DNA). *EF1 α* used as reference cytoplasmic mRNA. Scale bar, 7 μ m. (e) Histogram of the nuclear localization of *RADAR* and *EF1 α* FISH signals calculated using the “co-localization” feature (Amnis[®] ImageStream) which measures the overlap of signals between the nuclear mask (PI) and the dotted mask (RNA-target probe), (f) Representative image of *RADAR*'s (magenta) dotted structure and localization in the nucleus (DAPI) using single molecule RNA-FISH using specific probe targeting *RADAR*, (g) Gating and quantification of the percentage of the sub-groups of cells representing: absent, low and high *RADAR*-RNA intensity determined by imaging flow cytometry. (h) Graphs show mean \pm SEM of three independent experiments. Two-tailed unpaired Student test was applied to determine the statistical significance. (ns, not significant; *, $p < 0.05$; **, $p < 0.01$; ***, $p < 0.001$; ****, $p < 0.0001$).

Suppl_Figure 2

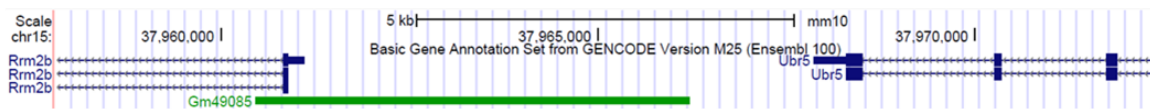


Supplementary Figure 2. The Characterization of *RADAR* Gene isoforms and Coding Potential

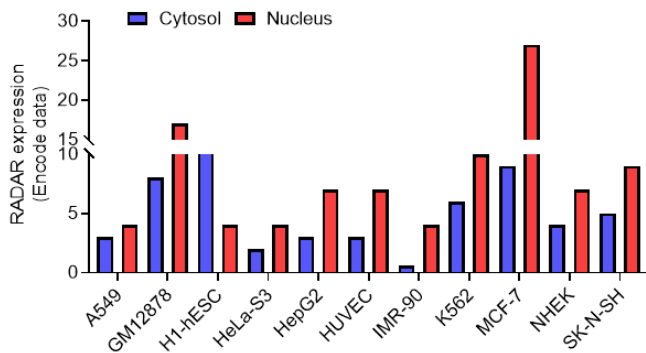
(a) Genomic locus of the lncRNA *RADAR* isoforms (LNCipedia v4.1) reports 10 isoforms and representation of the main *RADAR* transcript in this study, (b) *RADAR*'s transcript variants relative RNA level treated or not with TMZ for 24 hr determined by qRT-PCR and normalized to Human Brain Reference (HBR) RNA (c) *Agarose gel analysis of 5' and 3'-RACE-PCR products of RADAR*, Coding potential analysis of *RADAR* sequence was analyzed using Coding Potential Assessment Tool (CPAT) (d), Coding Potential Calculator (CPC) (e) and PhyloCSF (f), MALAT1 and NEAT1 served as a control non-coding gene. GAPDH and β -actin served as control coding genes, (g) Prediction of putative proteins encoded by *RADAR* using Open Reading Frame Finder (NCBI-ORF). We set minimal ORF = 90 nt for transcripts < 4 kb.

Suppl_Figure 3

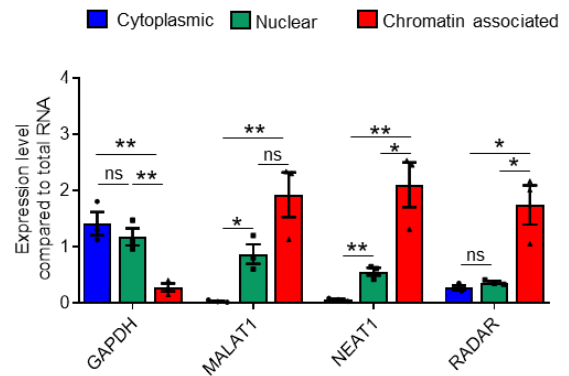
a



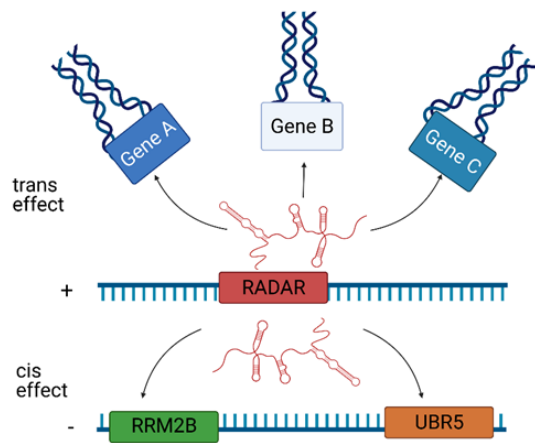
b



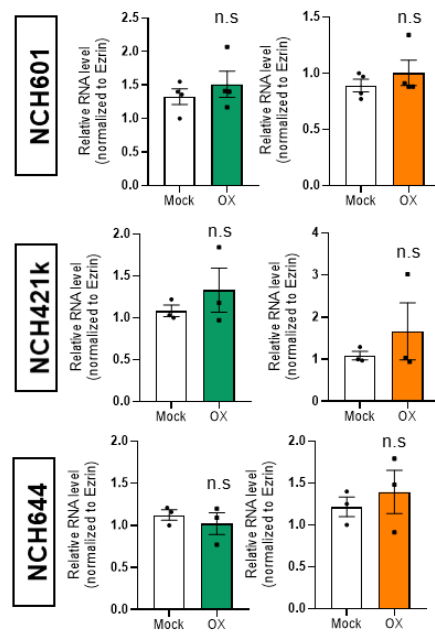
c



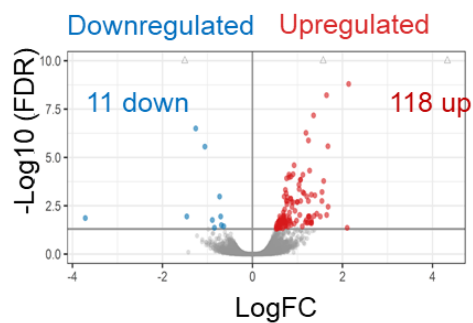
d



e



f



Supplementary Figure 3. RADAR Locus Conservation, subcellular localization and RADAR effect on gene expression

(a) The mouse genomic locus of the lncRNA Gm49085 (ENSMUST00000228937.1) spanning Rrm2b and Ubr5 genes. Exons: 1, Coding exons: 0, Transcript length: 5,748 bps. (Source: UCSC Genome Browser on Mouse Dec. 2011 (GRCm38/mm10) Assembly), (b) DATA extracted from ENCODE Project show RADAR's cytosolic and nuclear localization in different cell lines, (c) RADAR relative RNA level in the cytoplasmic, nuclear and chromatin-associated fractions isolated from NCH601 cells (TMZ-untreated) using RNA-subcellular fractionation. GAPDH used as reference mRNA control whereas MALAT1 and NEAT1 used as reference lncRNAs controls. Graphs show mean \pm SEM of three independent experiments. Two-tailed unpaired Student test was applied to determine the statistical significance. (ns, not significant; *, $p < 0.05$; **, $p < 0.01$), (d) Models depicting potential role of RADAR in *Cis* or *Trans* mechanism for the regulation of gene expression, (e) Relative RNA level for RRM2B and UBR5 in GBM cells with RADAR exogenous overexpression determined by qRT-PCR, (f) Volcano plot of differential gene expression, with fold difference between logFC normalized expression in control and RADAR exogenous overexpression ($n = 3$) plotted versus $-\log_{10}$ adjusted FDR-value. Graph shows mean \pm SEM of 3 independent experiments. The two-tailed unpaired Student test was applied to determine the statistical significance. (ns, not significant; *, $p < 0.05$; ****, $p < 0.0001$).

Figure 3

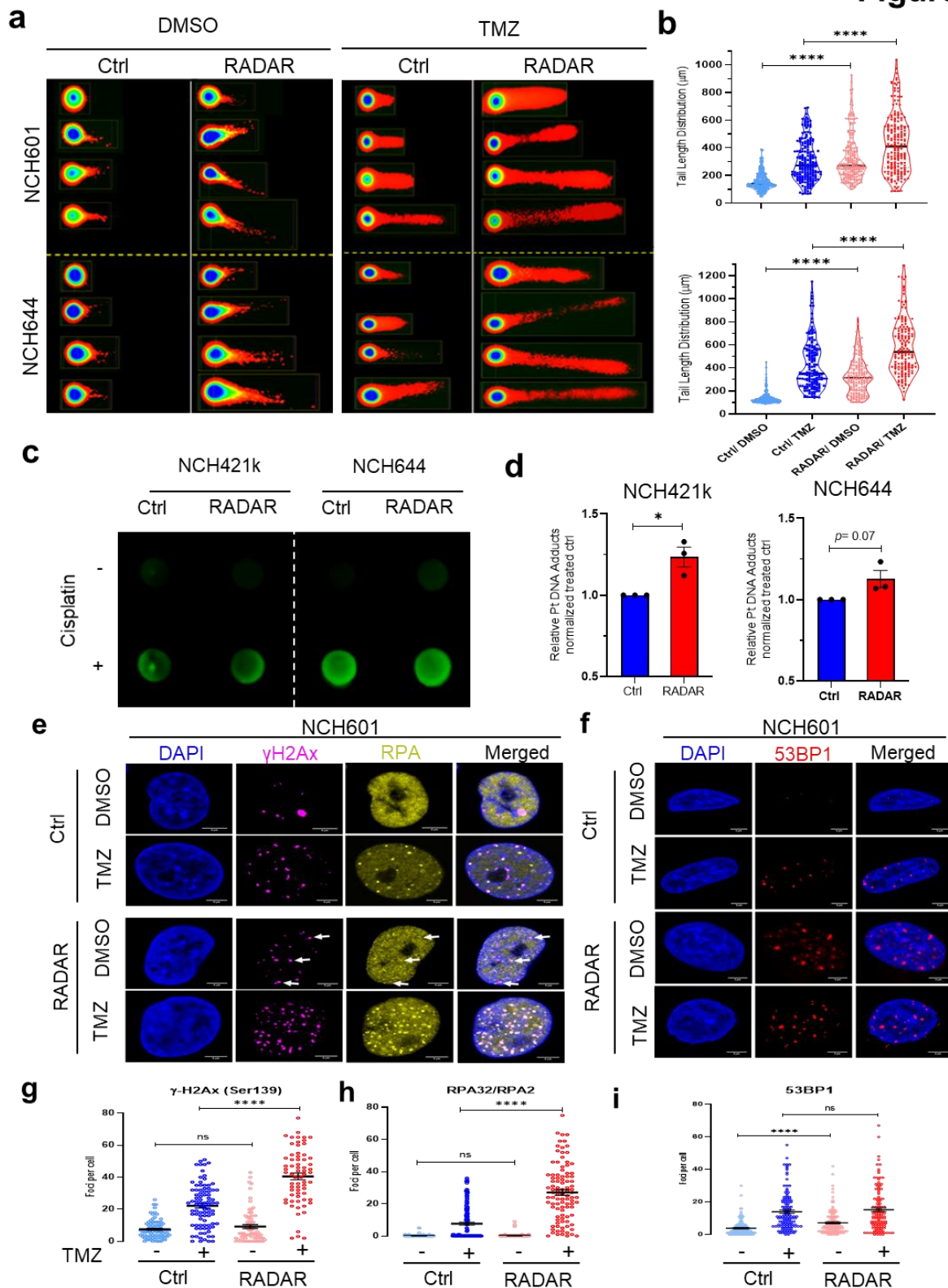
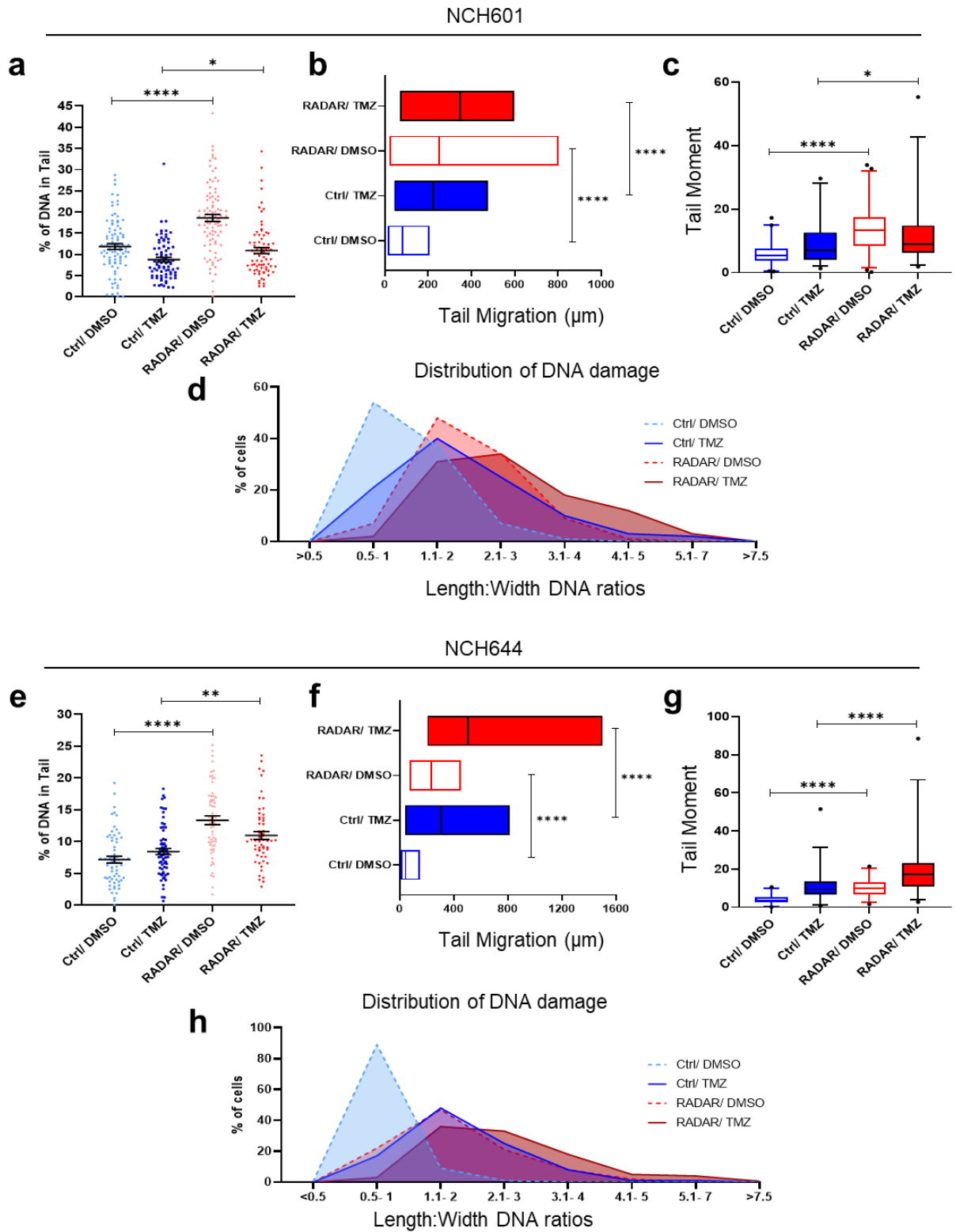


Figure 3. RADAR Potentiates DNA Damage

(a) Representative images of alkaline comet assay of GBM cells with *RADAR* exogenous overexpression treated or not with TMZ for 24 hr, (b) Tail length of GBM cells in (A) measured ($n \geq 50$ cells were analyzed for each condition per biological replicate) by Comet Assay IV software and represented with violin plot (each dot represents single cell), (c) Levels of platinum adducts detected by DNA-dot blot, the amount of gDNA loaded is 2 μ g following treatment of GBM cells with 25 μ M cisplatin for 4 hr, (d) Quantification of relative Pt-DNA adducts in (c), Graphs show mean \pm SEM of three independent experiments. The two-tailed unpaired Student test was applied to determine the statistical significance. (****, $p < 0.0001$), (e) Representative confocal images of γ -H2Ax (magenta) and RPA32/RPA2 (yellow) foci in NCH601, (f) 53BP1 foci in *RADAR* and control cells $-/+$ TMZ, DAPI (blue) was used to stain DNA, (g-i) γ -H2Ax, RPA32/RPA2, and 53BP1 foci number quantification ≥ 30 cells were analyzed for each condition per biological replicate and foci number were scored using ImageJ software and represented with dot plot (each dot represents single cell). Graphs show mean \pm SEM of 3 independent experiments. The two-tailed unpaired Student test was applied to determine the statistical significance. Scale bar (5 μ m)

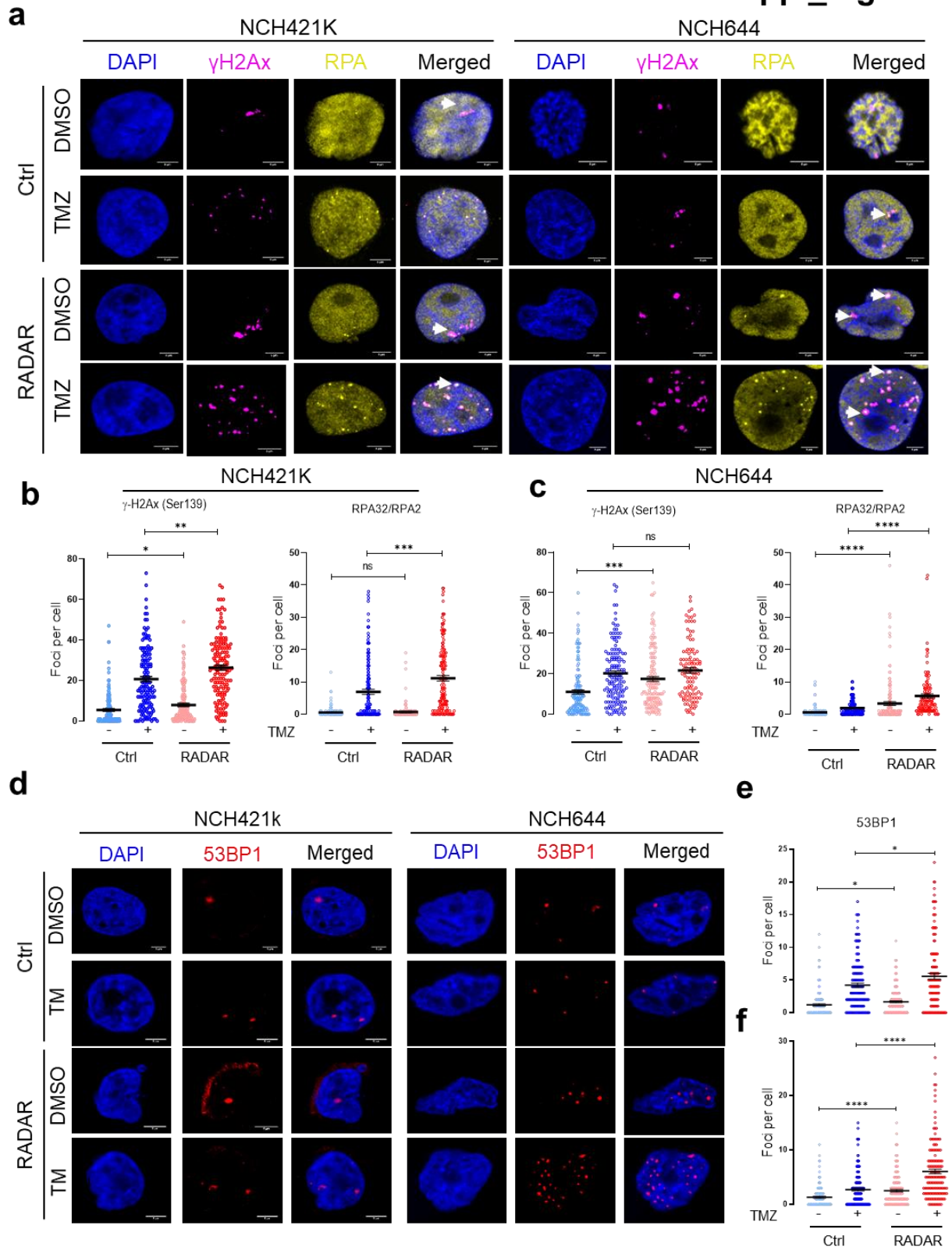
Suppl_Figure 4



Supplementary Figure 4. RADAR Potentiates DNA Damage

Analysis of the neutral comet assay on GBM cells showing the higher DNA damage caused by *RADAR* reflected by: (a,e) the percentage of DNA in tail, (b,f) tail migration, (c,g) tail moment, and (d,h) Length:Width DNA ratios. Graphs show mean \pm SEM of three independent experiments. The two-tailed unpaired Student test was applied to determine the statistical significance. (*, $p < 0.05$; **, $p < 0.01$; ****, $p < 0.0001$).

Suppl_Figure 5



Supplementary Figure 5. RADAR Overexpression Triggers Single Strand Break (SSB)

(a) Representative confocal images of γ -H2Ax (magenta), RPA32/RPA2 (yellow) foci, (d) 53BP1 foci in NCH421k and NCH644 +/- TMZ in RADAR and control cells, DAPI (blue) was used to stain DNA, (b, c, e) γ -H2Ax, RPA32/RPA2 and 53BP1 foci number quantification. At least 30 cells were analyzed for each condition per biological replicate and foci number were scored using ImageJ software and represented with dot plot (each dot represents single cell). Graphs show mean \pm SEM of 3 independent experiments. The two-tailed unpaired Student test was applied to determine the statistical significance. (ns, not significant; *, $p < 0.05$; **, $p < 0.01$; ***, $p < 0.001$; ****, $p < 0.0001$). Scale bar (5 μ m).

Figure 4

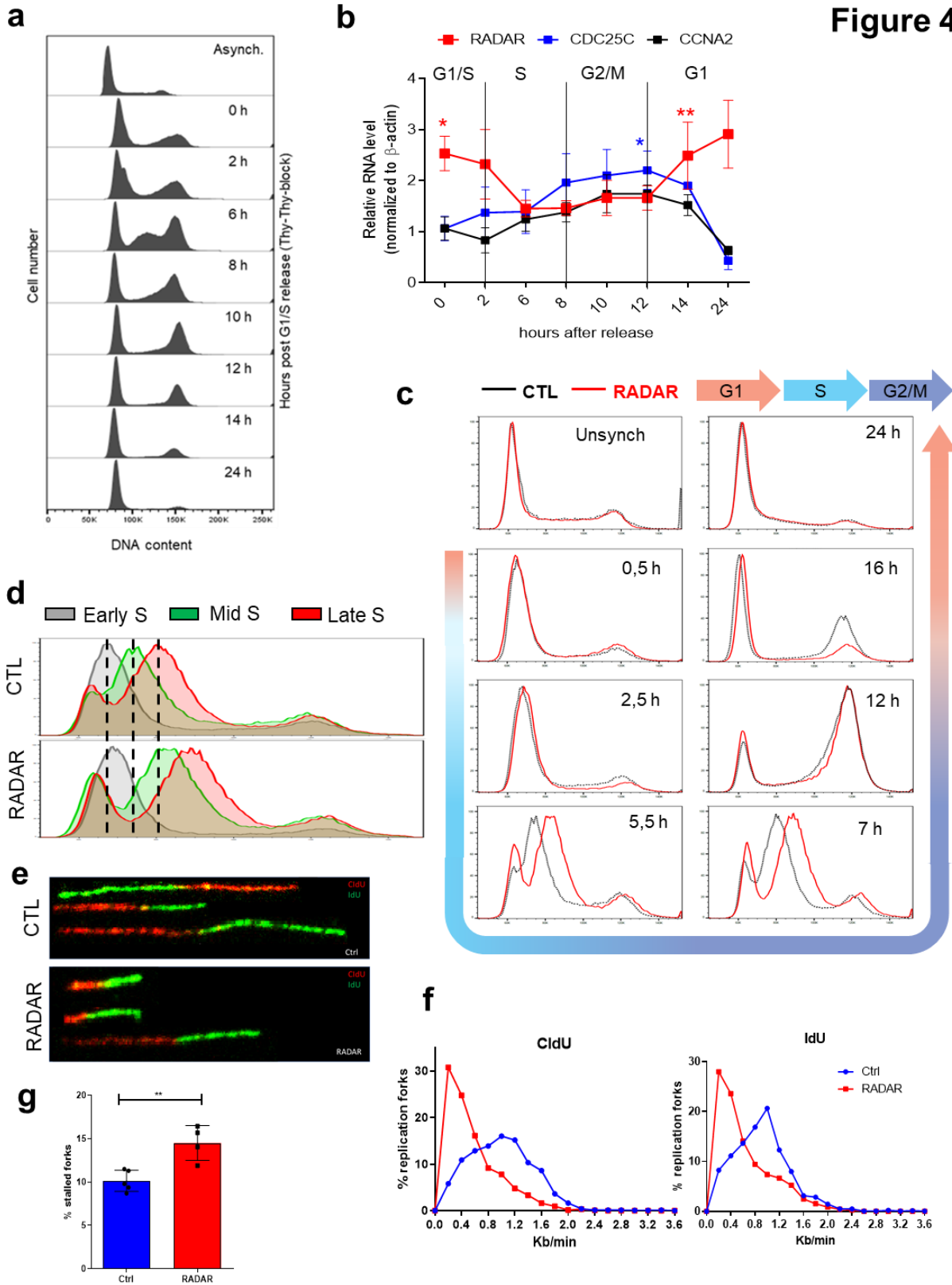
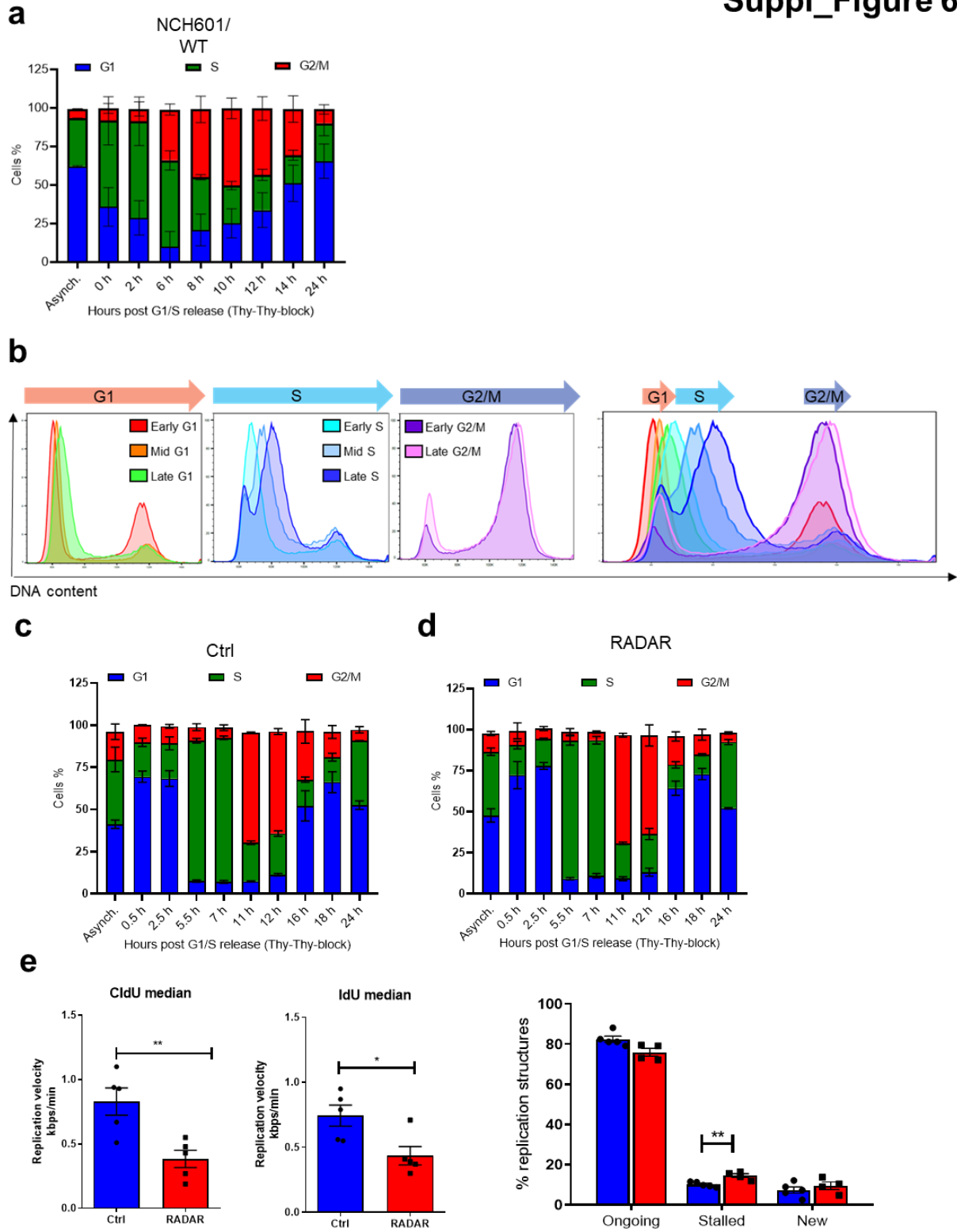


Figure 4. RADAR Expression is Cell Cycle Dependent and Affects DNA Replication

(a) G1/S synchronized NCH601 (WT) cells obtained by double thymidine block and release method (one representative experiment is shown), (b) Cells were harvested at several time points for RADAR expression analysis by qRT-PCR, CDC25C and CCNA2 were used as control G2/M reference genes, (c,d) Cell cycle analysis of G1/S synchronized GBM cells with *RADAR* exogenous overexpression obtained by double thymidine block and release method (one representative experiment is shown). Graphs show mean \pm SEM of two independent experiments. The two-tailed unpaired Student test was applied to determine the statistical significance. (*, $p < 0.05$; **, $p < 0.01$), (e) Representative immunofluorescent images showing the DNA fiber in Ctrl (upper) and RADAR (lower) following sequential pulse labeling with CldU (red) and IdU (green), (f) Quantification of DNA replication elongation rates. The DNA replication elongation rates (fork rates) were calculated as fiber length divided by CldU (upper) or IdU (lower) pulse labeling times, (g) Bar chart summarizes the quantification of stalled replication forks as a percentage of total number of replication structures.

Suppl_Figure 6



Supplementary Figure 6. RADAR Expression is Cell Cycle Dependent and Affects DNA Replication

(a) G1/S synchronized NCH601 (WT) cells obtained by double thymidine block and release method (one representative experiment is shown). Cells harvested at several time points then the synchrony of the cells was validated by flow cytometry. (b) G1/S synchronized cells obtained by double thymidine block and release method (one representative experiment is shown) for the study of cell cycle profile. Cells harvested at several time points then the synchrony of the cells was validated by flow cytometry to ensure that we successfully divided each cell cycle phase into early, mid and late (c,d) quantification of control and RADAR cells synchronized as in (a), (e) Bar chart summarizes the quantification of CldU and IdU incorporation rates (replication velocity) in Ctrl and RADAR+ GBM cells, (f) Bar chart summarizes the quantification of ongoing, stalled, and new replication forks as a percentage of total number of replication structures.

Figure 5

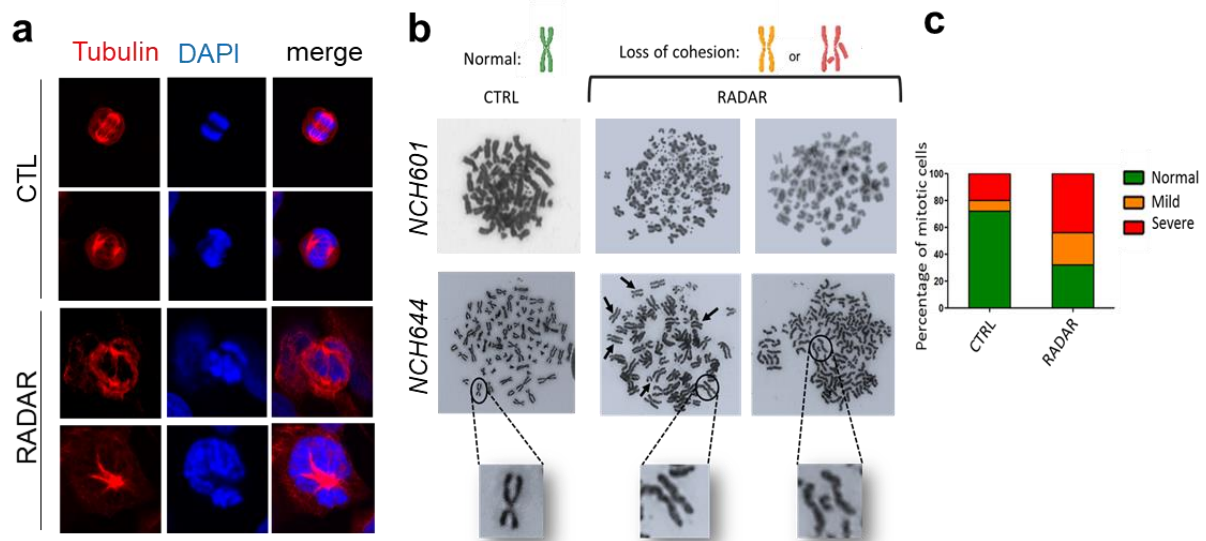


Figure 5. RADAR Overexpression Reduces DNA replication velocity rate and Causes Severe Mitotic and Sister Chromatid Cohesion Defects

(a) Representative confocal images and quantification in (E) showing mitotic defects in GBM cells with *RADAR* exogenous overexpression. Tubulin (red) and DAPI (blue) used to stain the DNA, (b) Representative images of chromosome spreads for cells synchronized in metaphase showing normal X-shaped chromosome in control cells (left) and cohesion loss or breakage in cells with *RADAR* exogenous overexpression (right), (c) Percentage of mitotic cells showing normal, mild or severe mitotic defects. ($n \geq 50$ metaphases per condition were scored).

EXTENDED DATA

1. Additional Characterization of *RADAR* Transcripts: Expression of a CircRNA Isoform

CircRNAs can be formed from lncRNAs through the non-canonical splicing (back splicing) of their introns when the 3' sequence of one exon is back-spliced and fused with the 5' sequence of the same or another exon (tail-to-head fusion) (Quinn and Chang, 2016). During our characterization of *RADAR* transcript variants by RACE-PCR, we isolated a PCR product corresponding to a transcript whose first and second exons lay within the genomic locus of *RADAR*, but contained a third exon extended ~3 kb downstream of the 3' end of *RADAR* predicted isoforms. Therefore, we investigated whether this transcript could be a circular isoform back spliced from *RADAR*. The detection of sequences matching with the back splice formation is an essential evidence of the presence of an exonic circRNA. We prepared total RNAs from GSCs and reverse transcribed to detect circRNAs by PCR. To this end, we designed a set of divergent forward and reverse primers that would amplify in outward facing directions in respect to linear sequence (Figure EX1A). In the presence of a circRNA structure, these primers become convergent and amplify in inward facing directions (Figure EX1A). We amplified with the divergent primers (Table S1) a sequence (Figure EX1B and appendix 3), which after its sequencing and mapping on the human genome was composed of 3 exons (Figure EX1C), where the 3' sequences of the third exon was back-spliced and fused with the 5' sequences of the first exon (Figure EX1D). This confirmed the existence of a back spliced exon junction (Figure EX1E and appendix 3, highlighted in light blue). Furthermore, the biogenesis of a circRNA is favored when there are complementary sequences such as the family of *Alu* repeats present in SINEs (short interspersed nuclear elements) flanking the two back-spliced exons (Figure EX1F) (Chen, 2016a). Interestingly, we identified the presence of two SINE repetitive elements (82% identical) located up- and down-stream of the back-spliced exons (Figure EX1G, red squares). Altogether, our results suggest the presence of a circRNA isoform of *RADAR*.

To rule out any false-positive results, we prepared total RNAs from NCH421k cells and subjected them to digestion by RNase R, which is able to degrade linear RNAs but not circRNAs. The degradation of linear RNA transcripts was confirmed by on-chip electrophoresis (Figure EX2A). We prepared cDNAs using a reverse gene specific primer (GSP), which anneals specifically to the circ*RADAR* isoform then followed by PCR with the same divergent primers. We obtained an amplicon with the expected size (~800 bp) (Figure EX2B). However, due to the low yields of DNA extraction from the agarose gel we were unable to further confirm the presence of the back spliced exon junction by Sanger sequencing.

Studies reported that circRNAs can be translated into small peptides in a cap-independent mechanism known as rolling circle translation, provided by the presence of a start codon and IRES-like structure for the assembly of ribosomes (Abe et al., 2015; Pamudurti et al., 2017; Schneider and Bindereif, 2017). To our knowledge, only one circRNA back-spliced from the lncRNA “*LINC-PINT*” is reported to have the possibility to code for small peptides with regulatory functions (Zhang et al., 2018). To test the possibility of circRADAR translation, we searched for an ORF and identified one that might have the ability to translate a small peptide of 49 aa (Figure EX2C). The prediction analysis showed that circRADAR may form an IRES-like structure upstream to the located ORF (Figure EX2CD). Finally, our BLAT search for a possible peptide present in nature matched the protein SGT1 homolog (SGT1_Human, UNIPROT ID: Q9Y2Z0) and the Rab5 GDP/GTP exchange factor (RABX5_Human, UNIPROT ID: Q9UJ41). Altogether, we conclude that *RADAR* is back-spliced to form a circRNA isoform that has the potential to be translated into small peptide.

2. Genetic Manipulation of GBM Cells to Modulate *RADAR* Structure and Expression

2.1. Deletion Constructs Using a Bicistronic Plasmid to determine *RADAR* functional domain

The nucleotide sequence is fundamental to the various functions of lncRNAs as it allows the direct interaction with the DNA, RNA, and proteins (Jayaraj et al., 2012; Johnsson et al., 2014; Lu et al., 2016). In order to determine *RADAR* functional domains, we transfected adherent GBM cell lines (U251 and LN229) with constructs (Figure EX3A) containing either *RADAR* third exon only (*RADAR**1) (**Appendix 4**) or *RADAR* with a partial deletion of the third exon (*RADAR**2) (**Appendix 5**). We evaluated the proliferation rate of these cells by using the IncuCyte live cell imaging. To our surprise, *RADAR**1 and *RADAR**2 transfected cells showed a strong decrease in proliferation compared to both control cells and full length *RADAR* sequence (Figure EX3B). We hypothesized that: (1) *RADAR**1 and *RADAR**2 could form a more stable secondary structure, (2) *RADAR**1 and *RADAR**2 might have less turn-over due to the lack of potential miRNA(s)-interacting sequences from the full length *RADAR*, (3) *RADAR* functional domain might be present in the 5' sequence of exon 3 as this region remained unmodified in our two constructs. Additionally, we tested whether *RADAR* is able to form G-quadruplex structures by searching for guanine tetrads within stretches of maximum length of 30 bases. Using QGRS Mapper (Kikin et al., 2006) we identified a total of 5 G-quadruplexes (Figure EX3C and Appendix 2). Interestingly, *RADAR*-exon 3 contains 3 G-quadruplexes, 2 of them are present in the nucleotide sequence embedded in the 5' end of exon 3, supporting our hypothesis that this region might contain the functional domain of *RADAR*. We conclude that the presence of *RADAR*-exon 3 is important for its function and that

the G-quadruplex formed from the sequence of this exon might participate to its molecular structure and function. However, this requires further investigations.

2.2. CRISPR-dCAS9 Approach for *RADAR* Functional Studies

To validate the biological effect of *RADAR*, we generated GSCs constitutively expressing CRISPR-dCAS9 fused with either transcription repressor (CRISPRi) (Figure EX4A) or activator (CRISPRa) (Figure EX4B) targeting the *RADAR* promoter region, and we evaluated *RADAR* gene expression by RT-qPCR. Unfortunately, none of our designed sgRNAs for CRISPRi was able to significantly repress *RADAR* expression. In contrast, we were able to successfully reach a significant induction of *RADAR* expression with most of our designed sgRNAs for CRISPRa. Next we checked for sgRNAs off-targeting or effects on the neighboring genes (*RRM2B* and *UBR5*). We found that *UBR5* expression remained unchanged with no alteration in both CRISPRi (Figure EX4C) and CRISPRa (Figure EX4D) systems. *RRM2B* expression was not affected by CRISPRi (Figure EX4E), but was significantly activated by CRISPRa (Figure EX3F). This can likely be explained by the fact that *RADAR* and *RRM2B* genes are transcribed divergently from the same promoter region. Because our efforts to obtain successful *RADAR* downregulation or induction without affecting the neighboring genes were unsuccessful so far, we were unable to proceed in validating *RADAR*'s biological effect. We propose to downregulate *RADAR* by other alternative mechanisms such as knockout via the insertion of an early polyA transcription stop signal or knockdown with an antisense oligonucleotide (ASO) strategy.

3. The Evaluation of *RADAR* Effect *In-vivo*

To evaluate the functional role of *RADAR in-vivo*, mock control and *RADAR* overexpressing NCH421k cells were intracranially implanted into the brain of female nude mice (Figure EX5A). Tumor volumes were measured by MRI once a week and calculated starting from when the first tumor began to appear until a total of 4 weeks (Figure EX5A). Mice were sacrificed at the appearance of neurological or behavioral abnormalities. Mock control and *RADAR* overexpressing groups showed similar brain tumor volume (Figure EX5B and C). Because of similar brain tumor growth between the two groups, we hypothesized that *RADAR* effect might be better seen following TMZ treatment as *RADAR* was shown to increase chemosensitivity to DNA damaging agents *in-vitro*. To this end, we selected NCH644 cells (mock and *RADAR* overexpression) to test *RADAR* effect on tumor response in animals receiving TMZ treatment. We selected these cells because they are positive for MGMT and resistant to TMZ and they can be easily detected by MRI. Two weeks following the intracranial implantation of cells, the mice groups received either TMZ (400 mg/kg in 10% DMSO) or DMSO alone as a vehicle via oral gavage daily. Tumor volumes were measured by MRI twice a week and calculated starting from when the first tumor appeared until the neurological or behavioral abnormalities (Figure

EX6A). Mice implanted with NCH644 cells overexpressing *RADAR* showed similar tumor volume compared to control mice group (Figure EX6B and C).

Extended_Figure 1

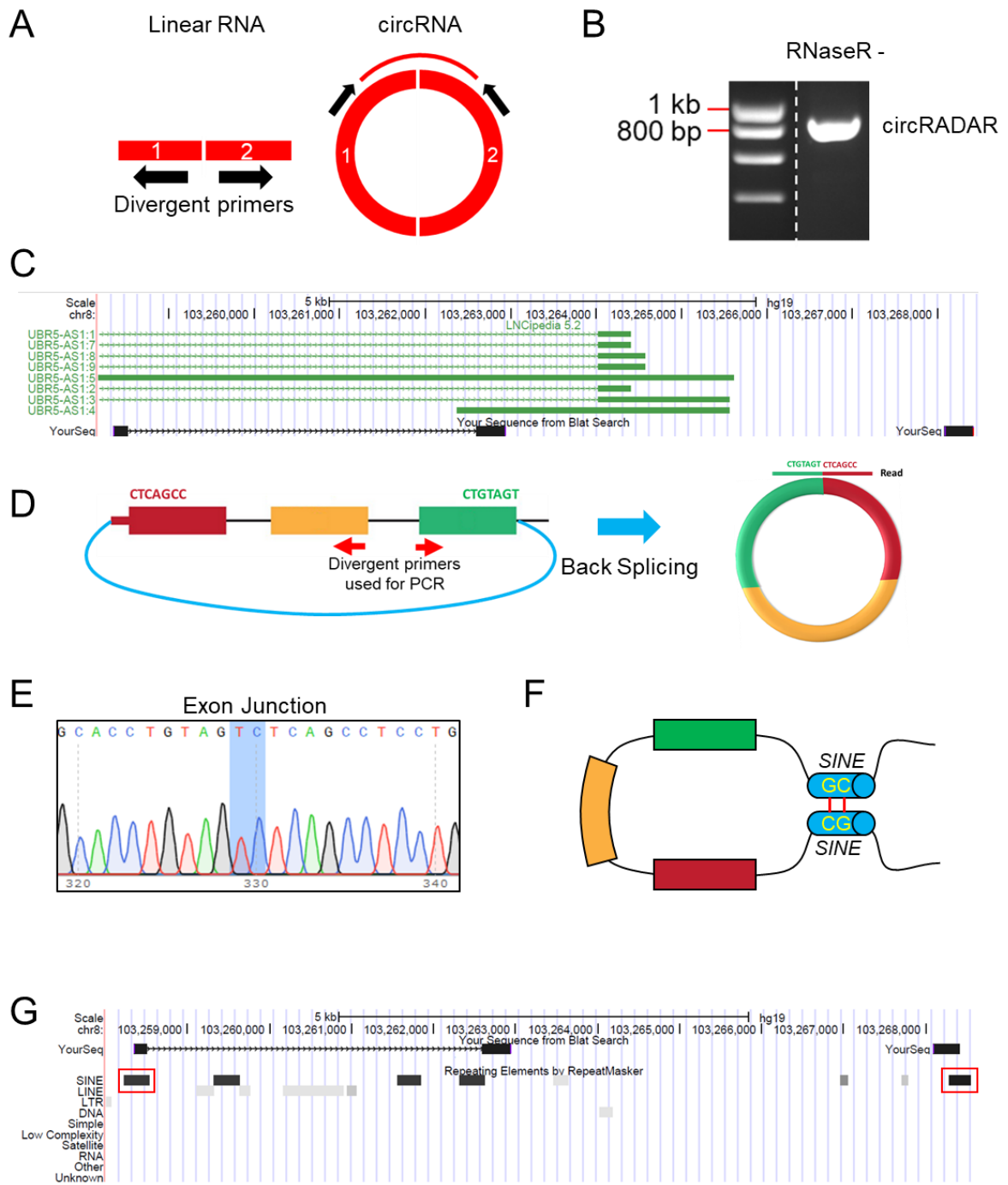


Figure EX1. RADAR produces a circRNA isoform.

(A) An illustration of PCR assay to detect the presence of circRNA. Divergent primers that would amplify in opposite directions with respect to gDNA become properly inward facing and produce amplicons when a backsplice connects outside sequences (Jeck and Sharpless, 2014).

(B) Agarose gel electrophoresis of the PCR product of circRADAR that amplified from cDNA prepared from a total RNA.

(C and D) The BLAT search of the sequenced PCR amplicon showing the genomic localization of circRADAR transcript.

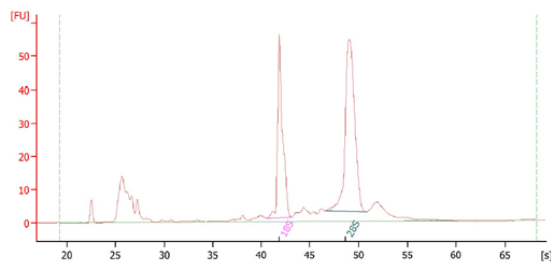
(A) Sequencing of the back spliced junction site for circRADAR.

(B) An illustration for the possible mechanism of circRADAR biogenesis.

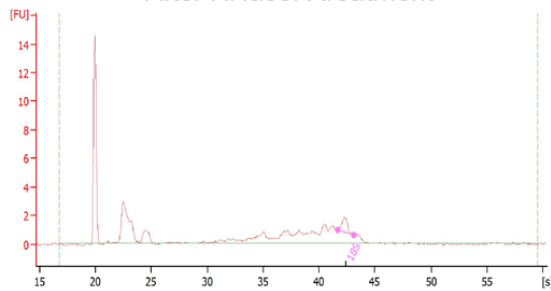
(C) The genomic locus of circRADAR showing the presence of two repetitive elements (SINE) flanking the back-spliced exons (highlighted inside red square).

Extended_Figure 2

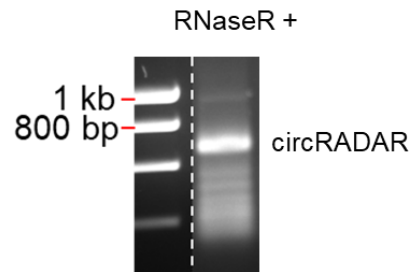
A Before RNaseR treatment



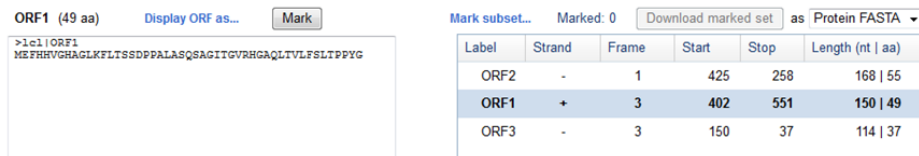
After RNaseR treatment



B



C



D

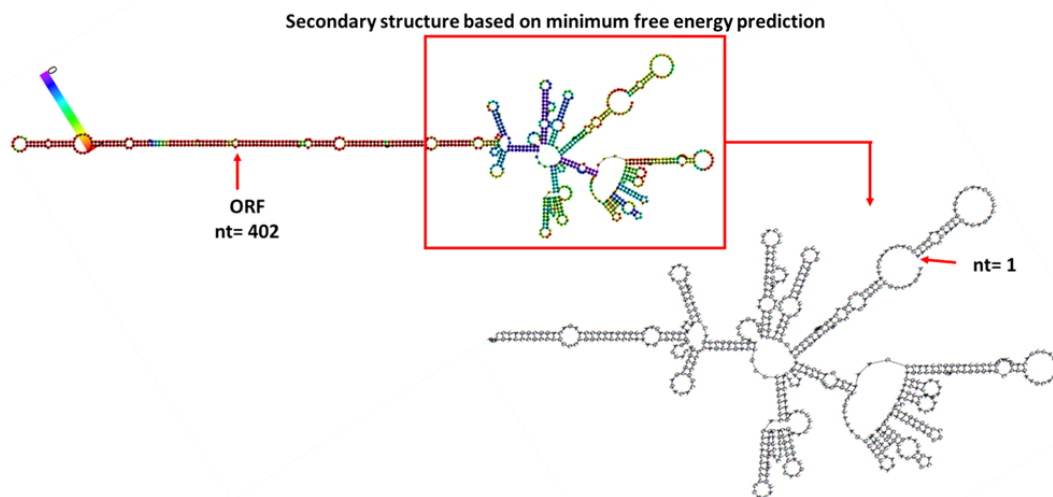


Figure EX2. RADAR produces a circRNA isoform that might be translated into small peptide.

(A) On-chip RNA electrophoresis on Agilent 2100 Bioanalyzer showing (upper) two high-molecular-weight rRNA species (28S and 18S) and therefore undegraded RNA, and (lower) RNA electrophoresis profile after RNase R treatment.

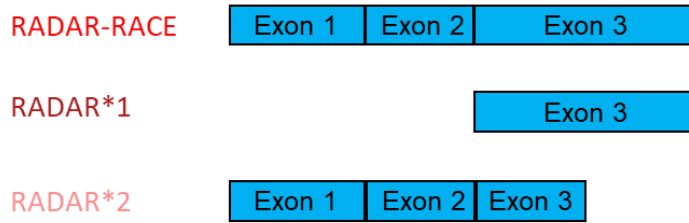
(B) Agarose gel electrophoresis of the PCR product of circRADAR that amplified from cDNA made from a total RNA treated with RNase R.

(C) The search of ORF inside circRADAR

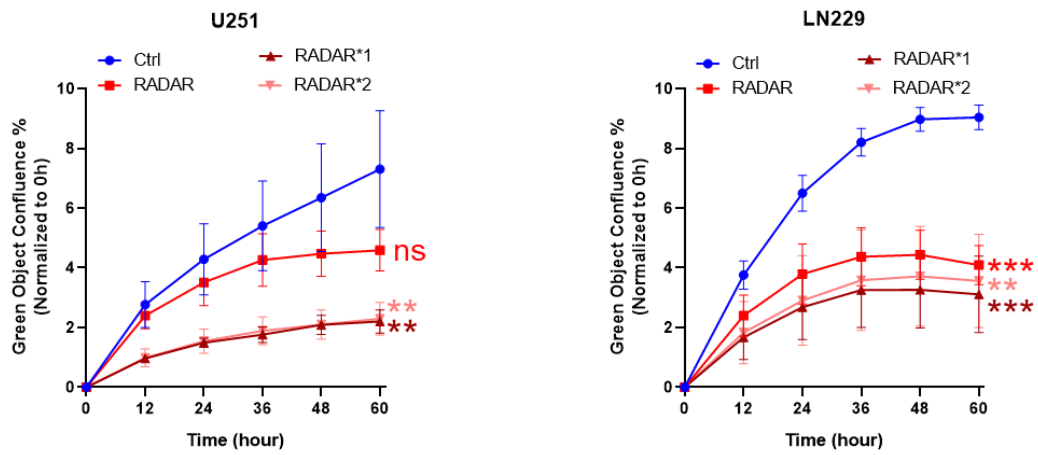
(D) The prediction analysis of the folding and secondary structure of circRADAR showing the presence of an IRES-like structure

Extended_Figure 3

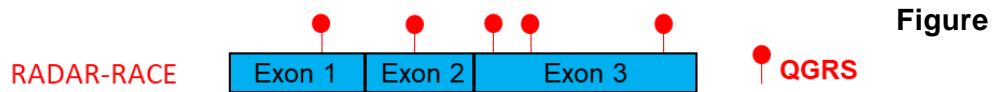
A



B



C



Figure

EX3. RADAR deletion constructs and the G-quadruplexes.

- (A) Representation of RADAR truncated constructs (RADAR*1 and RADAR*2) and the location of deleted sequences.
- (B) U251 (left) and LN229 (right) cell proliferation.
- (C) Representation of the location of G-quadruplex structures in RADAR-RACE transcript.

Figure EX4. CRISPR-dCAS9 systems for *RADAR* functional studies

(I and II) Schematic illustration of CRIPRi (I) and CRISPRa (II) strategies to evaluate *RADAR* function.

(A and B) RT-qPCR after *RADAR* promoter-targeted CRISPR-dCas9 inhibition (A) or induction (B).

(C and D) RT-qPCR to check off-targeting on the neighboring gene expression (*UBR5*) after *RADAR* promoter-targeted CRISPR-dCas9 inhibition (C) or induction (D).

(E and F) RT-qPCR to check off-targeting on the neighboring gene expression (*RRM2B*) after *RADAR* promoter-targeted CRISPR-dCas9 inhibition (E) or induction (F).

Extended_Figure 5

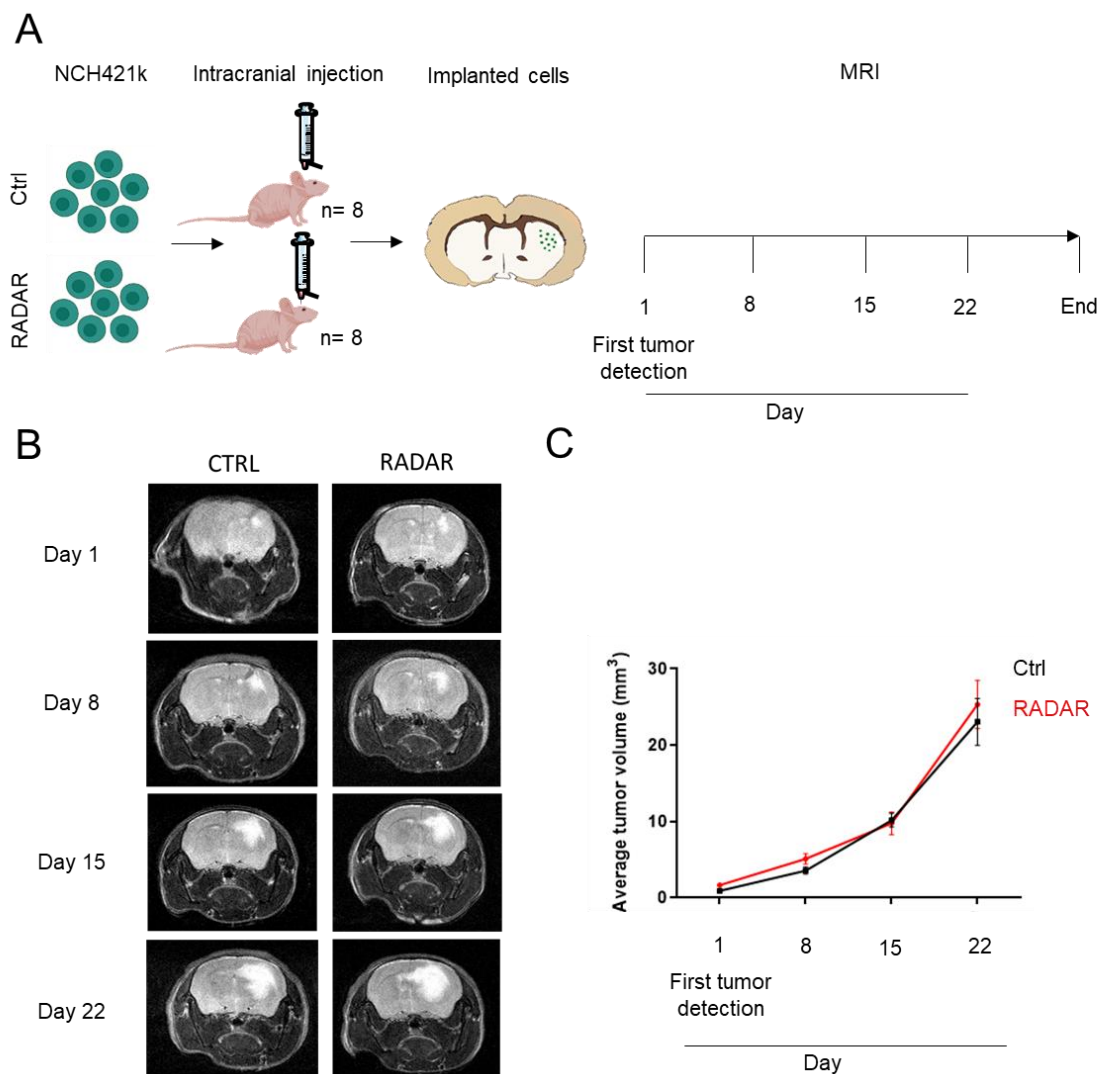


Figure EX5. The evaluation of *RADAR* effect *in-vivo*

(A) Schematic of *in-vivo* experiment. Tumor volume was analyzed by MRI.

(B) Representative images of MRI T2-weighted scan.

(C) Tumor volume over time. Mice we scanned once per week.

Extended_Figure 6

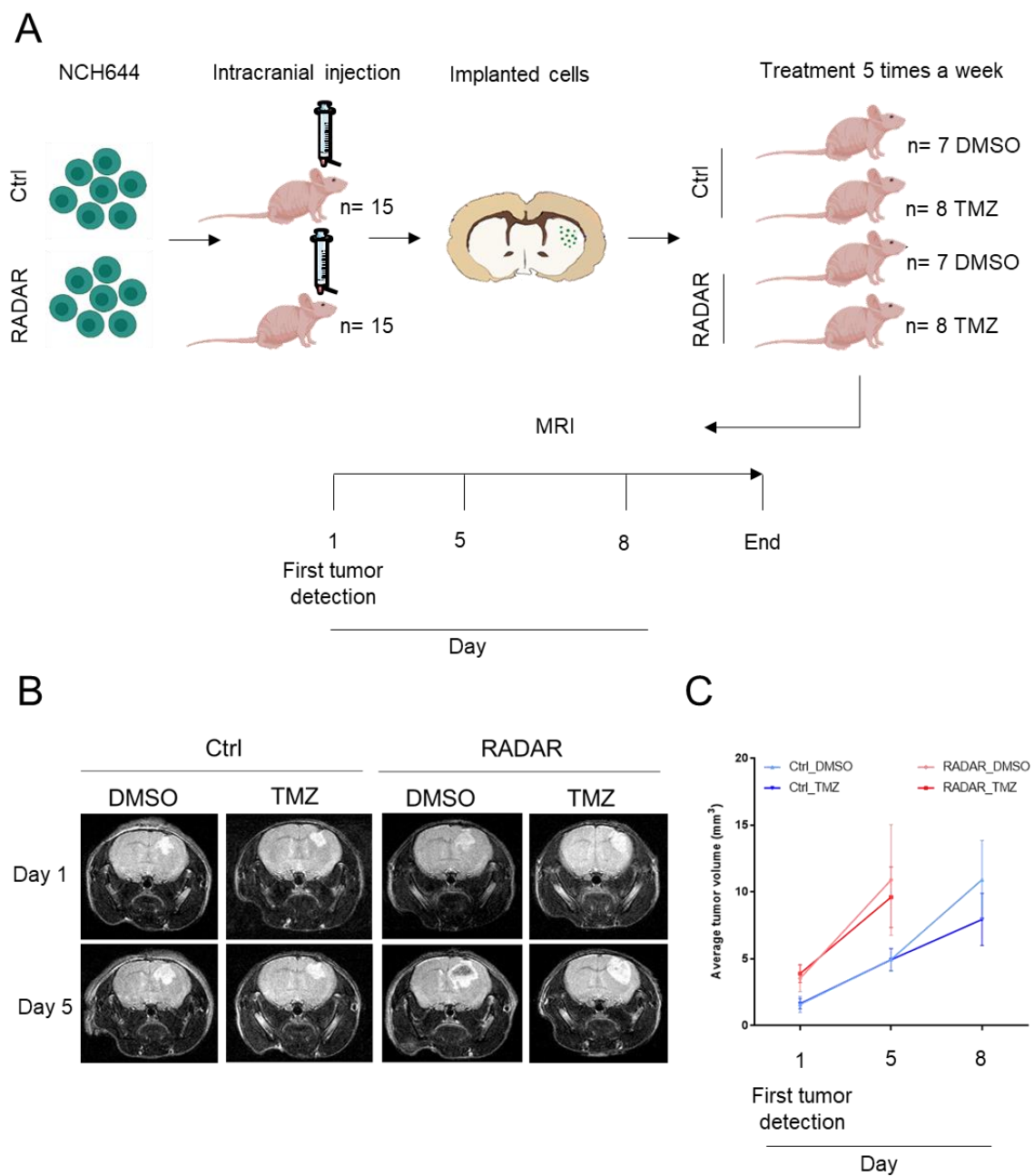


Figure EX6. The evaluation of RADAR effect *in-vivo* after Temozolomide treatment

- (A) Schematic of *in-vivo* experiment and treatment. Tumor volume was analyzed by MRI.
 (B) Representative images of MRI T2-weighted scan.
 (C) Tumor volume over time. Mice were scanned twice per week.

CHAPTER 6

DISCUSSION AND CONCLUSIONS

DISCUSSION

LncRNAs are a regulatory RNA class with important biological functions and frequently deregulated in cancer including glioblastoma (GBM). However, our knowledge of lncRNA contribution to tumor cell proliferation, survival and resistance to therapy is still minimal in view of the large number of annotated lncRNA transcripts. Therefore, a better understanding of lncRNAs biology and their involvement in pathogenesis may provide new options for exploiting lncRNAs in the treatment of disease.

Thus, the aim of this thesis was to investigate lncRNA-mediated regulation of GBM response to the DNA alkylating agent temozolomide (TMZ). For this purpose, we explored whether TMZ treatment could affect the GBM transcriptional response and we identified several lncRNA candidates deregulated upon TMZ treatment. To further probe the function of these genes, we focused on one of the top lncRNA candidates identified from transcriptomic analysis. Since this lncRNA gene “*ENSG000246263* or *RADAR*” has not been previously characterized and investigated in biological terms, we performed multiple functional studies to address several questions:

- 1- What are the mechanisms of its expression regulation?
- 2- Does this lncRNA gene have a role in regulating GBM response to chemotherapy?
- 3- What is the cellular effect resulting from its overexpression or knockdown?
- 4- What is the molecular mechanism of this lncRNA?
- 5- Can we benefit from this lncRNA to manipulate tumor growth and sensitivity *in-vivo*?

Hence, in this work we highlighted that TMZ can induce transcriptional changes in GBM cells, which form a network to modulate GBM response to therapy. Additionally, we confirmed that perturbation in lncRNA expression play a major role in fundamental cellular processes to regulate GBM chemosensitivity to TMZ

1. Role of transcriptional regulatory loops containing lncRNAs

We showed that an acute TMZ dose triggers alterations in the transcriptome of GBM cells, specifically in TMZ-sensitive cell line. *In-silico* analysis of the differentially expressed genes revealed gene regulatory networks composed of mRNAs, miRNAs, and lncRNAs. These results are in line with other studies showing that cells respond to external stimuli and alterations associated with disease to establish RNA-RNA interactions which coordinate gene expression and result in a cellular response and cell fate decisions (Cai et al., 2020; Guil and Esteller, 2015; Miotto et al., 2019). Competitive endogenous RNAs (ceRNAs) including miRNAs and lncRNAs are essential intrinsic regulatory components in the cell. ceRNAs interact with each other and with mRNAs via sequence-specific binding sites to establish a regulatory circuit modulating gene expression and biological processes. For instance, the YY1

transcription factor activates the expression of the oncogenic lncRNA *SNHG9* in GBM (Chen et al., 2019). *SNHG9* enhances cell proliferation by sequestering miR199a-5p, which leads to Wnt2 expression upregulation in GBM cells (Zhang et al., 2019a). Hence, we propose that the RNA transcriptional loops revealed by TMZ treatment, may present crosstalk circuits between different classes of RNA transcripts to regulate GBM sensitivity to TMZ. The analysis of the regulatory network predicted interactions between key regulators including miRNAs such as “miR 19-a” and TFs such as “*MYC*, *TCF12*, *EGR1*, *HEY1*, *TFAP2A*”. These RNAs are important for glioma proliferation, invasion, and chemoresistance (Gaetani et al., 2010; Labreche et al., 2015; Sakakini et al., 2016; Sun et al., 2017; Wang et al., 2018). The analysis by qPCR of some of these regulators did not show major differences upon treatment or overexpression of one lncRNA candidate. It could be that these regulators are present in tight relationship with each other in a single network, and the dysregulation of one regulator can be neutralized by other compensatory RNA-RNA interactions, especially that the identified TFs also interact with each other. Another reason could be due to that our regulatory network is based on systems-level interaction prediction, which so far extracting gene interactions through this approach is still challenging and does not include tissue specific expression interactions. Another computational challenge is the lack of the proper algorithm to apply for different modeling and analysis steps, especially when ncRNA transcripts are included in these analyses because of the relatively poor accuracy in ncRNA annotations between databases (Fritah et al., 2014).

Nevertheless, our transcriptional regulatory loop provides an RNA-interactome map which can be used as a reference to predict transcripts that might be involved in biological processes. Indeed, miR 19-a is highly upregulated in glioma and regulates cell proliferation, via modulating β -catenin/TCF4 transcription activity and by targeting *RUNX3* mRNA (Sun et al., 2017). The transcription factor *EGR1* enhances GBM cell proliferation and self-renewal by positively regulating the expression of growth-stimulatory genes including *GLI1*, *GLI2*, and *PDGFA* (Sakakini et al., 2016). Additionally, we successfully isolated several lncRNAs with putative roles in cell cycle, DNA replication and DDR. These lncRNAs include transcripts such as *TP53TG1*, *GAS6-AS1*, and *ENSG000246263*, which are also predicted to have an important value as prognostic marker for GBM patient survival. The lncRNA *TP53TG1* is a tumor suppressor and crucial regulator of P53 in response to DNA damage. *TP53TG1* protects P53 from degradation by preventing the nuclear localization of the YBX1 protein, which activates the transcription of *PI3K* that is responsible for mediating P53 degradation (Diaz-Lagares et al., 2016). In non-small cell lung cancer (NSCLC), the expression of the lncRNA *GAS6-AS1* is downregulated, negatively correlated with metastasis, and its low expression is associated with poor disease prognosis (Han et al., 2013). Moreover, *GAS6-AS1* by stabilizing its sense mRNA

GAS6 can affect gastric cancer progression (Zhang et al., 2019b). Altogether, we conclude that the lncRNA candidates, which are identified in our regulatory circuit are considered potential regulators of GBM response to TMZ with relevance to cancer. Therefore, functional studies on these lncRNA candidates can be valuable to uncover their role in GBM biology and response to therapy.

2. *RADAR* expression regulation and induction upon DNA damaging drug treatment

In order to determine the functional relevance of lncRNA candidates in GBM and the regulation of response to TMZ, we focused on a novel lncRNA gene (*ENSG000246263*). We assessed its involvement in regulating GBM cell chemosensitivity to TMZ together with deciphering its molecular mechanism in DNA damage and repair. The lncRNA “ENSG000246263” was subsequently characterized at the cellular and molecular function as part of this thesis. The lncRNA “*ENSG000246263* or *UBR5-AS1*”, which is reported in this thesis as *RADAR* (RNA Associated with DNA DAmage and Replication) is upregulated in sensitive and semi-sensitive GBM cells upon TMZ treatment. As our analysis of the regulatory RNA loop revealed by the RNA-seq suggested an upregulation of several TFs together with *RADAR* upon TMZ treatment, we hypothesize that some of these TFs including TCF12, EGR1, and/ or MYC could be responsible for the activation of *RADAR* transcription. In fact, the promoter region of *RADAR* (data not shown) shows DNA binding motifs that have high affinity to interact with these TFs. Moreover, ChIP-seq experiments performed by the ENCODE project also support that these TFs are binding to the promoter region of *RADAR*. Thus, we speculate that TCF12, EGR1, and/ or MYC could be the TFs responsible for *RADAR* transcription activation upon TMZ treatment (**Figure 17A**). Since *RADAR* was not induced in GBM resistant cells, one hypothesis to explain the differential expression among the different cell lines could be that one of the predicted TFs of *RADAR* is transcriptionally downregulated (**Figure 17B**) or unable to effectively bind the promoter region (**Figure 17C**) as part of GBM-mediated resistance mechanism to chemotherapy. Therefore, ChIP in GBM cells (sensitive vs. resistant) can be performed to identify the TF of *RADAR* expression. Moreover, gene expression analysis and/or protein level of these TFs can be done in GBM resistant cells to assess their expression regulation. Another hypothesis of *RADAR*'s differential expression between GBM cells could be that resistant cells may have *RADAR* methylated promoter region (especially that *RADAR*'s promoter contains 2 CpG islands), which represses its expression and affects GBM cells response to therapy (**Figure 17D**). Thus, one approach to investigate this hypothesis can be performed using bisulfite sequencing on the promoter region of *RADAR* to assess the methylation level. Finally, TMZ-resistant cells may have lower expression of

RADAR as part of post-transcriptional regulation by miRNAs to modulate chemosensitivity by decreasing the levels of *RADAR* (Figure 17E).

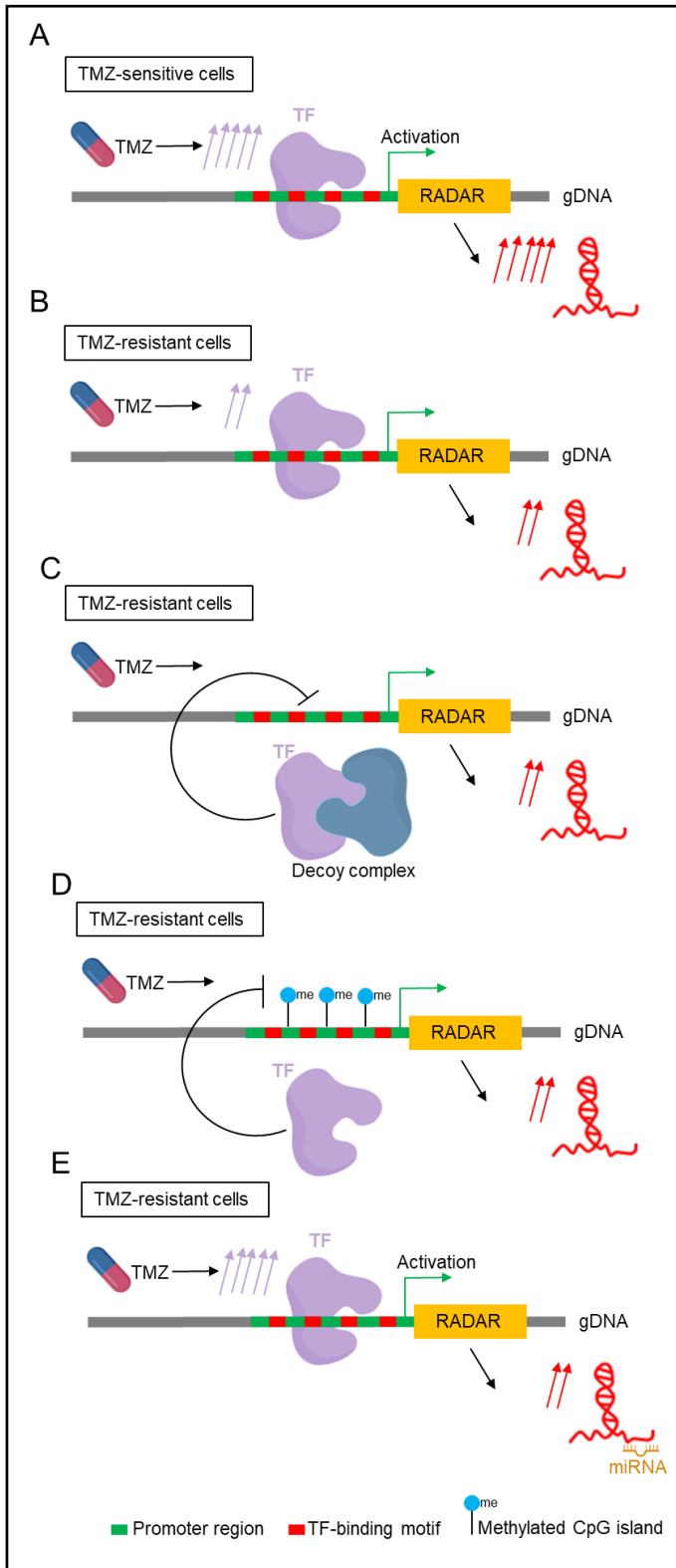


Figure 17. Model of the transcription regulation of *RADAR*. (A) In GBM-sensitive cells, the transcription factors (TF) TCF12, EGR1, and MYC are upregulated upon TMZ treatment (represented in violet). These TFs interact with DNA binding motifs (red) in the promoter region (green) of *RADAR* (red transcript) to activate its transcription upregulation. In GBM-resistant cells, *RADAR* is not induced upon TMZ possibly due to (B) low expression level of the TFs, (C) ineffective binding of the TF to the promoter region of *RADAR*, (D) methylated CpG islands of the promoter region of *RADAR*, or (E) post-transcriptional regulation by miRNA.

The upregulation of *RADAR* expression in GBM cells was not only linked to TMZ but also to the antimetabolite “ARA-C”, which interferes with DNA replication. Moreover, *RADAR* overexpression sensitized GBM cells to other DNA damaging agents including ARA-C and Cisplatin. Additionally, in a large-scale panel looking at genes correlated with treatment response in acute myeloid leukemia (AML), the high expression of *RADAR* was associated with increased AML sensitivity to ARA-C treatment (Bester et al., 2018). Thus, we speculate that *RADAR*-mediated regulation mechanism of the DDR may not only limited to GBM, but could also be extended to other types of cancer.

Altogether, we propose that *RADAR* induction is occurring in response to DNA damage caused by chemotherapeutic drug treatment and may exhibit a general mechanism under replication stress of modulating the DDR to several DNA damaging drugs. Hence, additional experiments such as irradiating GBM cells by UV could be performed to confirm the induction of *RADAR* upon DNA damage and replication stress. Additionally, to test whether the induction of *RADAR* is due to DNA damage-induced stress or it is implicated in GBM cells resistance mechanism to chemotherapy. One approach could be done by measuring the expression of *RADAR* in normal cells alone and upon inducing DNA damage through chemotherapeutic drug treatment.

3. Gene expression regulation by *RADAR*: *cis/trans* effect

LncRNAs have functions in regulating gene expression either in *cis* or *trans* mechanisms (Quinn and Chang, 2016; Ransohoff et al., 2018; Yao et al., 2019). *RADAR* is localized on chromosome 8 in opposite orientation to two protein-coding genes: *UBR5* (Ubiquitin Protein Ligase E3 Component N-Recognin 5) and *RRM2B* (Ribonucleotide Reductase Regulatory TP53 Inducible Subunit M2B). *UBR5* participates in the regulation of DDR by controlling the ubiquitination levels of H2A and H2Ax histone variants (Gudjonsson et al., 2012; Tamburri et al., 2020). Additionally, *RRM2B* affects DDR and cell cycle progression by participating in the DNA repair through P53-dependent manner and supplying the deoxy-ribonucleotides during DNA replication (Tanaka et al., 2000; Yamaguchi et al., 2001). Despite these functional implications in DDR, our results show that *RADAR* does not regulate *UBR5* and *RRM2B* gene expression in *cis*. Hence, *RADAR* effect on the regulation of DNA damage is independent of *UBR5* and *RRM2B* gene expression. Notably, antisense lncRNAs can regulate their sense mRNA levels, thereby affecting translation and protein levels. Part of the 3'-end of *RADAR* is overlapping with the 3'-end of *UBR5*. Our analysis of *UBR5* protein showed that *RADAR* is also not affecting *UBR5* mRNA stability or translation. In fact, antisense lncRNAs are not always interacting with or regulating the transcription of their sense mRNAs. For instance, the lncRNA *CONCR* (*DDX11-AS1*) is antisense to the ATP-dependent DNA helicase (*DDX11*). Similarly to *RADAR*, *CONCR* does affect neither the mRNA nor the protein level of *DDX11*,

but it acts by regulating the DDX11-ATPase activity (Marchese et al., 2016). Another study asked whether the antisense lncRNAs would regulate their sense mRNAs leading to an inverse expression correlation (Goyal et al., 2017). They focused on two pairs of mRNA-lncRNA sense-antisense transcripts during DNA damage. Although the mRNA-lncRNA transcripts were inversely correlated, there was no direct regulatory relationship between both sense and antisense transcripts (Goyal et al., 2017). In contrast, our investigation of *RADAR*'s effect on gene expression in *trans* showed that *RADAR* is able to affect the expression of genes located at distant chromosomal sites. However, gene enrichment analysis showed no statistical significance to pathways such as cell cycle or DNA damage repair. This suggests that *RADAR* might be involved in other cellular functions, by regulating gene expression either at the transcriptional or post-transcriptional level. Another hypothesis could be that *RADAR* may regulate expression of genes whose replication or transcription occur at early or late phase of the cell cycle. This would require further investigation.

4. *RADAR* has a role in regulating the DDR independently of MGMT

Resistance to TMZ is partially associated with the expression status of the MGMT repair protein (Hegi et al., 2005; Kitange et al., 2009). However, the phenotype observed in our study was solely related to *RADAR* overexpression and irrespective to the MGMT status of the cell lines. Several mechanisms other than the MGMT play a role in TMZ-acquired resistance in GBM (Erasimus et al., 2016; Johannessen and Bjerkvig, 2012). For example, MGMT-deficient glioblastomas are resistant to TMZ in a mechanism associated with XPC and CBX5 direct localization to the site of toxic lesions by DHC1-dependent mechanism to facilitate DNA repair (Yi et al., 2019). Low expression of the MMR proteins (MSH2 and MSH6) increase TMZ resistance in GBM (McFaline-Figueroa et al., 2015). The majority of TMZ-induced lesions are recognized and repaired by MGMT-independent BER mechanisms involving the DNA glycosylase (MPG) and DNA polymerase- β (pol-B) (Tang et al., 2011; Trivedi et al., 2005). Therefore, further exploration of the relationship of *RADAR* with other DNA repair mechanisms in particular MMR-driven futile cycles is required to better understand DDR regulation by *RADAR*.

Identification novel lncRNAs involved in regulating DDR and sensitivity to TMZ independently from MGMT, might offer new insights for improving therapeutic management of GBM patients with or without MGMT expression. Interestingly, several lncRNAs such as *DINO*, *ncRNACCND1*, *lincRNA p21*, *PANDA*, and *GUARDIN* are induced in response to DNA damage or replication stress and play a regulatory role in DNA repair (Hu et al., 2018; Huarte et al., 2010; Hung et al., 2011; Puvvula et al., 2014; Schmitt et al., 2016; Wang et al., 2008). RNA polymerase II can localize at the site of DNA damage to transcribe damage-induced lncRNAs (dilncRNAs) from the DSB ends, which can associate with 53BP1 and facilitate DDR activation

and DNA repair (Michellini et al., 2017). Hence, as *RADAR* overexpression resulted in increased foci of specific DNA damage markers including γ H2Ax, RPA, and 53BP1, these results support *RADAR*'s involvement in the modulation of DDR, possibly through direct binding to one of the component of DDR proteins.

5. The role of *RADAR* in cell cycle and DNA replication

Several DNA damage checkpoints together with transcriptional waves of cell cycle-related genes are responsible for controlling the level of DNA damage, cell cycle progression, and phase completion. LncRNAs are novel regulators of cell cycle checkpoints and progression either by regulating the expression of cell cycle genes such as cyclins and CDKs, or by acting on DNA damage signaling pathways (Kitagawa et al., 2013). A recent review highlighted a subset of lncRNAs with specific role in cell cycle and genome integrity (Guiducci and Stojic, 2021). Several lncRNAs such as *Gadd7*, *GAS5*, *ANRIL*, *LAST*, and *CCAT1* are expressed exclusively during G1 to regulate the expression of G1-related genes and phase transition (Guiducci and Stojic, 2021). Whereas, other lncRNAs including *CONCR* and *SUNO1* are expressed specifically in S-phase and bind with the DEAD-box helicase family proteins to modulate either their activity or promote gene transcription respectively (Guiducci and Stojic, 2021; Hao et al., 2020; Marchese et al., 2016). Our data showed that *RADAR*'s expression is cell cycle dependent with peaks corresponding to the time-points matching the late G1-early S phase of the cell cycle. This was also confirmed in an independent study that identified >200 lncRNAs with peaks of expression occurring during S-phase with *RADAR* being among the cell cycle-regulated lncRNA candidates enriched during S-phase (Yildirim et al., 2020). Interestingly, the depletion of three lncRNA candidates (*LINC00704*, *LUCAT1*, and *MIAT*) showed a delay of release into the S-phase and premature progression through the S-phase (Yildirim et al., 2020). These data suggest that *RADAR* has a potential role in the regulation of cell cycle progression during S-phase by causing premature S-phase exit with under-replicated or unrepaired DNA.

Obstacles during DNA replication and inefficient DNA repair during S-phase lead to replication stress, which is the main source of cancer genome instability (Burrell et al., 2013). Thus, obstacles if not repaired or resolved successfully, may lead to high frequency of mitotic abnormalities (Lamm et al., 2016). For example, the lncRNA *GUARDIN* in response to DNA breaks helps to maintain genome stability by preventing end-to-end fusion of the DNA (Hu et al., 2018). The downregulation of *NORAD* causes slower replication fork velocity and defects in sister chromatid segregation during M phase (Munschauer et al., 2018). Similarly, the depletion of *CONCR* affects the activity of DDX11 helicase during DNA replication resulting in sister chromatid cohesion loss (Marchese et al., 2016). On the other hand, the high expression of *Ginir* interferes with Cep112/BRCA1 complex leading to mitotic abnormalities (Panda et al.,

2018). Here, we show that *RADAR* overexpression resulted in a shorter time window of S-phase leading to a faster exit from the S-phase into G2/M. Moreover, *RADAR* caused a decreased DNA replication velocity with a higher percentage of stalled replication fork structures. Thus, we conclude that *RADAR* alters DNA replication progression and results in premature S-phase termination, with under-replicated or unrepaired DNA carried to G2/M phase resulting in higher levels of replication stress, mitotic abnormalities, and genome instability.

6. Deciphering the function of *RADAR* in normal cells, physiological conditions, and cancer

Examination of the data extracted from the ENCODE project on *RADAR*'s subcellular localization across different cell types showed that H1-hESC (human embryonic stem cells) was the only cell type that showed cytoplasmic localization of *RADAR*. LncRNA transcripts can be present in different cellular compartments, or they can shuttle between nuclear and cytoplasmic compartments to exert different molecular functions (Fico et al., 2019; Geisler and Collier, 2013). For example, *linc-ROR* is a cytoplasmic lncRNA that modulates cellular reprogramming of human induced pluripotent stem cells by controlling mRNA stability in the cytoplasm (Loewer et al., 2010). Whereas, in gastric (AGS) and colon (HT29) cancer cell lines, *linc-ROR* is in the nucleus occupying the *TESC* promoter to control its expression activation by modulating histone H3K9 methylation (Fan et al., 2015). Similarly, it is possible that *RADAR* might play a role in regulating differentiation of embryonic stem cells through its predominant cytoplasmic localization. Whereas, in the nucleus of differentiated cells it regulates DNA replication and cell cycle progression. Interestingly, earlier studies showed that mammalian ESCs have an unusual cell cycle structure characterized by a very short G1-phase and a unique mechanism of cell cycle regulation (Becker et al., 2006; Coronado et al., 2013; Savatier and Malashicheva, 2004; White and Dalton, 2005). Hence, one hypothesis of *RADAR*'s role in normal cells based on its G1/S phase expression and role in shortening S-phase could be the normalization of the cell cycle. In which, as ESCs differentiate, the cell cycle undergoes changes, such as G1-phase lengthening. Increased *RADAR* expression at late G1 might engage in the control of DNA replication velocity and S-phase shortening (**Figure 18**). Thus, *RADAR* could act as a surveillance camera to help maintain cell state and balance between cell cycle phases in healthy cells.

Given that cancer cells exhibit intrinsic DNA damage, an increased tendency of replication errors and replication stress, which further increased following the exposure to DNA damaging agents (Burrell et al., 2013; Lamm et al., 2016; Tubbs and Nussenzweig, 2017), *RADAR* may sense these abnormalities and imbalances to slow down the DNA replication speed and

regulates cell cycle progression to act as a negative regulator of DNA repair and replication, thereby avoiding the passage of toxic lesions and drastic effects to the daughter cells.

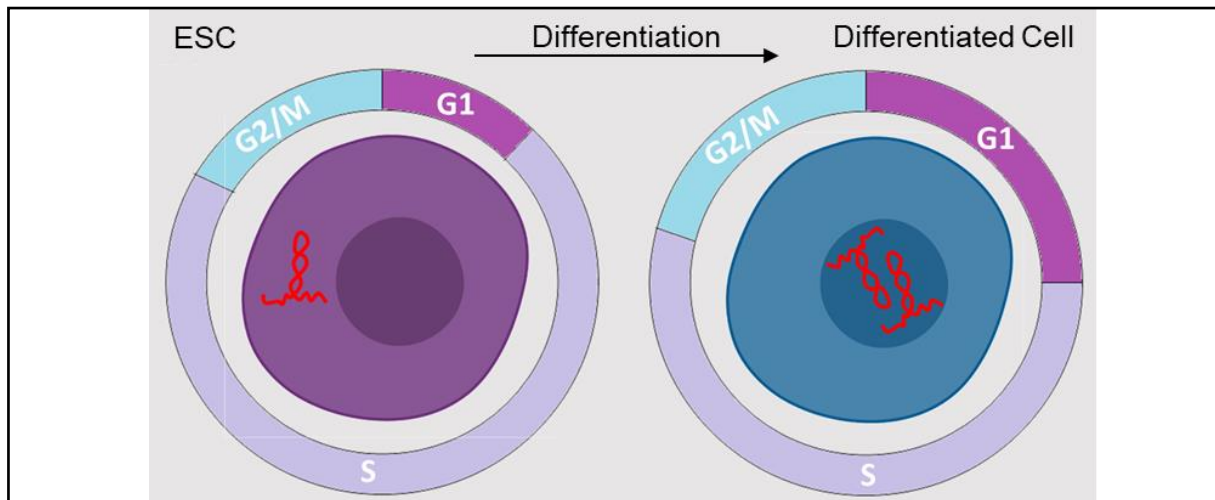


Figure 18. *RADAR*'s cellular function hypothesis in normal cells under physiological condition. *RADAR* (red) is localized in the cytoplasm of embryonic stem cell (ESC) to facilitate fast DNA replication, long S-phase to retain ESC state. Upon differentiation, *RADAR* localizes in the nucleus, slows down the DNA replication velocity, and shorten S-phase duration to help control cell cycle progression, level of DNA damage, cell state, and proliferation.

7. Distinct *in-vivo* role of *RADAR*

Novel therapeutic strategies based on targeting replication stress and enhancing the level of DNA damage by using lncRNAs such as *RADAR* may represent opportunity against cancer cells, especially in organs characterized by low proliferative index such as the brain. Indeed, if the level of S-phase damage reaches a certain threshold, this can result in DNA replication catastrophe and trigger cell death (Ovejero et al., 2020; Toledo et al., 2013). Although cancer cells can cope with such errors, they are carried into mitosis leading to mitotic abnormalities (Mankouri et al., 2013). It has been previously recommended to use a combination of DNA damaging agents targeting two different phases of the cell cycle to maximize the DNA damage and avoid alternative DDR pathways used by cancer cells to escape cell death. (Albain et al., 2008; Chilimoniuk et al., 2010; Deep and Agarwal, 2008). However, this strategy showed high toxicity and intolerance in patients. Therefore, therapies that depend on targeting the DDR as monotherapy or in combination with DNA damaging agents could represent a new approach to increase DNA damage and sensitivity of cancer cells to chemotherapy, such as for example the PARP inhibitor for the treatment of BRCA-mutated ovarian cancer (FDA, 2018; O'Connor, 2015). Therefore, we tested the effect of *RADAR* in mice transplanted intracranially with GSCs overexpressing *RADAR*. Mice with either empty or *RADAR* overexpressing cells showed similar tumor growth over time, which might be due to the inability of *RADAR* to generate alone high levels of DNA damage in the absence of a DNA damaging agent. Consequently, we repeated the same approach in combination with TMZ. Surprisingly, mice with *RADAR*

overexpressing cells with or without TMZ showed bigger tumor volume compared to the control group. Hence, *RADAR* might enhance the level of DNA damage in the presence of TMZ, leading to high levels of genomic instability and chromosomal rearrangements. However, the presence of proficient DNA repair pathways and higher levels of genomic instability caused by *RADAR in-vivo* may have tilted the balance towards tumor growth. Another possible argument could be that, the high level of DNA damage caused by *RADAR* led to edema, blood leakage, and intracranial hemorrhage in the core of the tumor, which may resulted in bigger tumor volume quantification by MRI. Of note, we faced critical technical problem during our second *in-vivo* study, in which we were unable to determine the zero time-point of tumor growth and thereby mice randomization due to faulty in MRI operation. Thus, several quality control and follow-up experiments are needed such as the measurement of *RADAR* expression at the end of the *in-vivo* study to make sure that the expression of *RADAR* is conserved, immunohistological staining to assess the proliferation index, angiogenesis, and molecular profiling to evaluate the level of genome instability.

Cancer cells must maintain a balance in the regulation of DNA damage and proficient DNA repair pathways to prevent genomic instability and mitotic abnormalities. Maximizing the level of DNA damage represents a double-edged sword that might lead to further mutations resulting in an enhanced tumor growth on the long term. Reduced GBM-sphere size as a result of *RADAR* overexpression was only seen and validated *in-vitro* upon short (24 h) and acute (500 μ M) dose of TMZ. Therefore, it would be of interest to investigate the level of genome instability in GSCs or in normal cells for longer period of time. Importantly, other studies assessing the effect of targeting the DDR by using PARP inhibitors (Olaparib and Veliparib) in normal cells harboring proficient cellular repair processes found that both drugs could induce genomic instability leading to an increase of sister chromatid exchange and chromatid aberrations, which correlated with mutagenic potential (Ito et al., 2016). Additionally, several preclinical studies evaluated the combination of TMZ with PARP inhibitor (Veliparib) for the treatment of GBM, but there were inconsistent *in-vitro* and *in-vivo* results (Barazzuol et al., 2013; Clarke et al., 2009; Tentori et al., 2014). Also, the phase II clinical trial of TMZ in combination with methoxyamine that targets APE1 (involved in base excision repair) in patients with recurrent GBM has been terminated due to the lack of adequate response and toxicity in patients (NCT02395692). As a conclusion, further investigations are needed to explore this therapeutic approach and find the optimal condition of use such as monotherapy, combination with DNA damaging agents, treatment period, dose, or delivery to patients lacking specific DDR pathways.

8. Loss-of-function strategies to evaluate the function of *RADAR*

Functional studies which are based on *RADAR* loss-of-function, are still required to validate its cellular effect and function in normal and cancer cells. However, we were facing multiple technical challenges in respect to successful lncRNA knockdown due to several reasons. The most frequently used strategies to downregulate lncRNAs are based on RNA-mediated degradation by RNA interference (RNAi), antisense oligonucleotides (ASOs), or CRISPR/dCas9 transcription repression (CRISPRi) system at the DNA level. RNA interference (RNAi) relies on the RNAi-induced silencing complex (RISC) to degrade the lncRNA of interest, however RISC-mediated RNA degradation mainly occurs in the cytoplasm and thus might not be sufficient for nuclear lncRNA transcripts such as *RADAR* (Zeng and Cullen, 2002). ASOs seem to be efficient in the nucleus because they utilize the endogenous RNase H1 enzyme (abundant in the nucleus) to degrade lncRNAs (Wu et al., 2004). However, efficient transfection using cationic-lipid reagents is difficult to achieve in GSCs. Additionally, since RNAi and ASOs methods require sequence homology to hybridize with the targeted lncRNA of interest, there is a possibility of off-target effects and crosstalk with miRNAs. Moreover, lncRNAs exist in a folded secondary structure and may not be accessible due to protein binding or hybridization with RNA or DNA. Therefore, effective knockdown of target lncRNAs can be challenging. The (CRISPRi) system may provide the best solution to downregulate lncRNAs at the DNA level (Konermann et al., 2015). CRISPRi utilizes the genetically modified Cas9 protein (dCas9) that lost its endonuclease ability to break the DNA, and is fused to the repressor domain Krüppel associated box (KRAB). Hence, CRISPRi can be guided by sgRNA targeting the promoter region of the lncRNA of interest to suppress its transcription. Despite our attempts to use this strategy, we did not achieve effective gene knockdown due to the low efficiency of the CRISPRi system to repress the genes differentially regulated across cell cycle phases (Sanson et al., 2018). Another limitation is the particular genomic localization of *RADAR*, which shares the same promoter region with the *RRM2B* gene (divergent transcription) and the risk of off-target effect.

9. Uncovering the molecular mechanism and direct target of *RADAR*

The precise molecular mechanism of how *RADAR* performs its function in regulating DNA damage and cell cycle remains to be elucidated. Studies to evaluate the cellular effect of *RADAR* and the regulation of DNA damage could be done in cells receiving ionizing radiation. In addition, uncovering the role of *RADAR* in normal cells and physiological conditions is important to fully understand the molecular mechanism of *RADAR* in cellular processes. Such studies may include the measurement of *RADAR* expression and localization in multiple normal cells including ESCs. It would be of interest to analyze the cell cycle profile and gene expression regulation of the ESCs in the presence or absence of *RADAR* to assess the effect

of *RADAR* on cell differentiation. Defining the molecular mechanism of lncRNAs requires to understand how much lncRNA nucleotide sequence and secondary structure are associated to their molecular function. lncRNAs can fold into a complex secondary structure allowing interaction with protein(s). Several algorithms and web-based software such as *catRAPID*, *RNAcAct*, and *PLAIDOH* are available to predict lncRNA-protein binding. Our extraction of the predicted *RADAR*-binding proteins (data not shown) show enrichment in pathways related to chromosome organization, cell cycle process, and DNA metabolic process. Unfortunately, our preliminary attempts using lncRNA-pulldown to identify and validate *RADAR*-binding proteins were not fruitful due to lack of specificity in our control conditions. In addition, as lncRNA-pulldown assays require the incubation of *in-vitro* transcribed and biotinylated lncRNA of interest with cell lysate in the test tube, improperly folded lncRNA due to bypassing the normal processing of endogenous RNAs within the cell, may capture non-physiological lncRNA-proteins interactions. Therefore, to overcome these problems we are currently adopting a newly developed in-cell method for the unbiased identification of lncRNA-protein interaction named *incPRINT* (Graindorge et al., 2019). The *incPRINT* method (**Figure 19**) is based on the dual transfection of HEK293T cells stably expressing a NanoLuc luciferase-MS2CP with vectors encoding MS2-tagged-lncRNA of interest and FLAG-tagged protein candidates in a 96-well plate. Protein candidates with its interacting lncRNA are then immuno-captured by anti-FLAG antibody. Finally, the lncRNA-protein complex can be detected and quantified by using NanoLuc luciferase assay and second anti-FLAG antibody coupled to horseradish peroxidase (HRP) respectively (Graindorge et al., 2019).

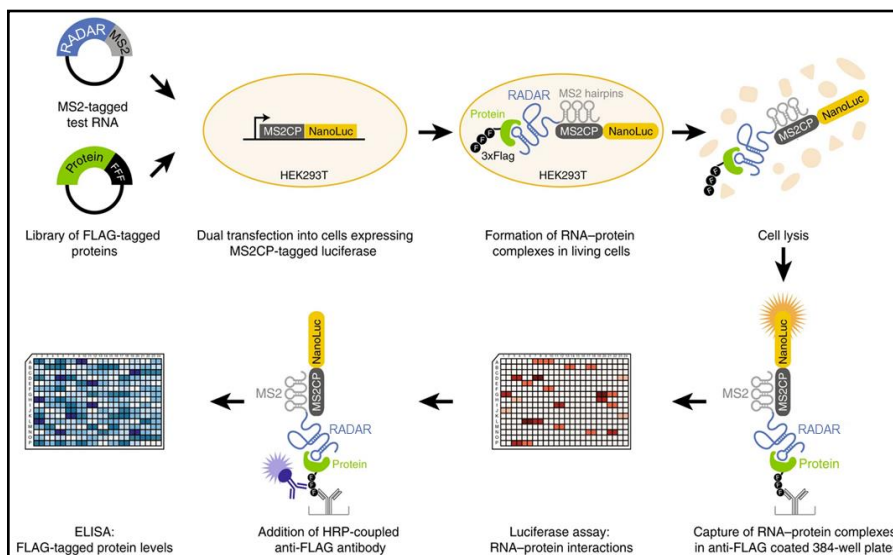


Figure 19. *incPRINT* method for the identification of *RADAR*-protein partners. HEK293T cells are stably expressing a NanoLuc luciferase-MS2CP protein and transfected with dual plasmids encoding for *RADAR*-MS2 and FLAG-tagged protein candidate. Cells are lysed and *RADAR*-protein complex is immuno-purified using anti-FLAG antibody. *RADAR* protein complex

is then detected by NanoLuc luciferase. ELISA assay then will be used to evaluate the specificity and levels of the FLAG-tagged candidate proteins using a second anti-FLAG antibody coupled to horseradish peroxidase (HRP). Adapted from (Graindorge et al., 2019).

10. Structural motifs and RADAR functional domain

The nucleotide sequence of lncRNAs are the key determinant for their interaction with DNA or proteins. Two web-tools have been published recently which can be used to predict putative Quadruplex forming G-Rich Sequences (QGRS) in nucleotide sequences (QGRS Mapper) or cluster lncRNAs with putatively related functions (KEEPER) based on similar *k*-mer content (short nucleotide sequences responsible for protein binding) (Kikin et al., 2006; Kirk et al., 2018). Our comparison of *RADAR* sequence to several known DNA- and protein-binding lncRNAs (data not shown), showed that *RADAR* clusters together with several cis-repressive lncRNAs such as *XIST*, *TSIX*, *ANRIL*, *THRIL*, and *SOX2-OT* due to high abundance of AU-rich *k*-mer content. Given that these lncRNAs have functions related to gene expression regulation via modulating the 3D nuclear structure, we suggest that *RADAR* might be involved in similar mechanisms. This is supported by our findings showing the ability of *RADAR* to alter gene expression in *trans*. Hence, we propose to perform experiments such as ATAC-seq to assess genome-wide chromatin accessibility upon *RADAR* overexpression and by combining these results with our RNA-seq data, we may be able to link chromatin state with cell cycle phases or to assess *RADAR*'s ability to preferentially regulate the expression of genes which are transcribed at a specific cell cycle phase.

QGRS structure formation is facilitated by the presence of guanine (G)-rich sequences within the RNA transcript and are stabilized by metal cations enabling interactions with proteins and DNA (Jayaraj et al., 2012). Examples of lncRNAs with potential QGRS are *MALAT1*, *XIST*, and *NEAT1* (Kwok et al., 2016; Yang et al., 2018). So far, the functional relevance of QGRS formation is reported only in three lncRNAs *NEAT1*, *GSEC*, and *REG1CP* (Matsumura et al., 2017; Simko et al., 2020; Yari et al., 2019). QGRS in *NEAT1* is important for its interaction with NONO protein, enabling paraspeckle formation and stabilization (Simko et al., 2020). In *GSEC*, QGRS allows the interaction with DHX36 protein for the regulation of gene expression (Matsumura et al., 2017). Finally, QGRS in *REG1CP* enables DNA:RNA hybrids (R-loop) for the assembly and recruitment of the FANCD1 to the *REG3A* core promoter to activate its transcription (Yari et al., 2019). Upon analysis of the nucleotide sequence of *RADAR*, we identified 5 QGRS motifs. Taking into consideration the association of *RADAR* with chromatin and its effect on DNA replication together with stalled replication forks, we speculate that QGRS in *RADAR* might facilitate R-loop formation responsible for increased DNA replication stress and high DNA damage due to R-loop-replication fork collision. Taking together, we propose that *RADAR* may act by one or several of the following mechanisms (**Figure 20**):

1. Regulating the enzyme(s) activity of the DNA replication machinery.
2. Serving as a decoy for protein(s) involved in DNA replication or DDR.

3. Forming RNA:DNA hybrids during DNA replication (R-loop), or interfering with R-loop resolution during DNA replication.

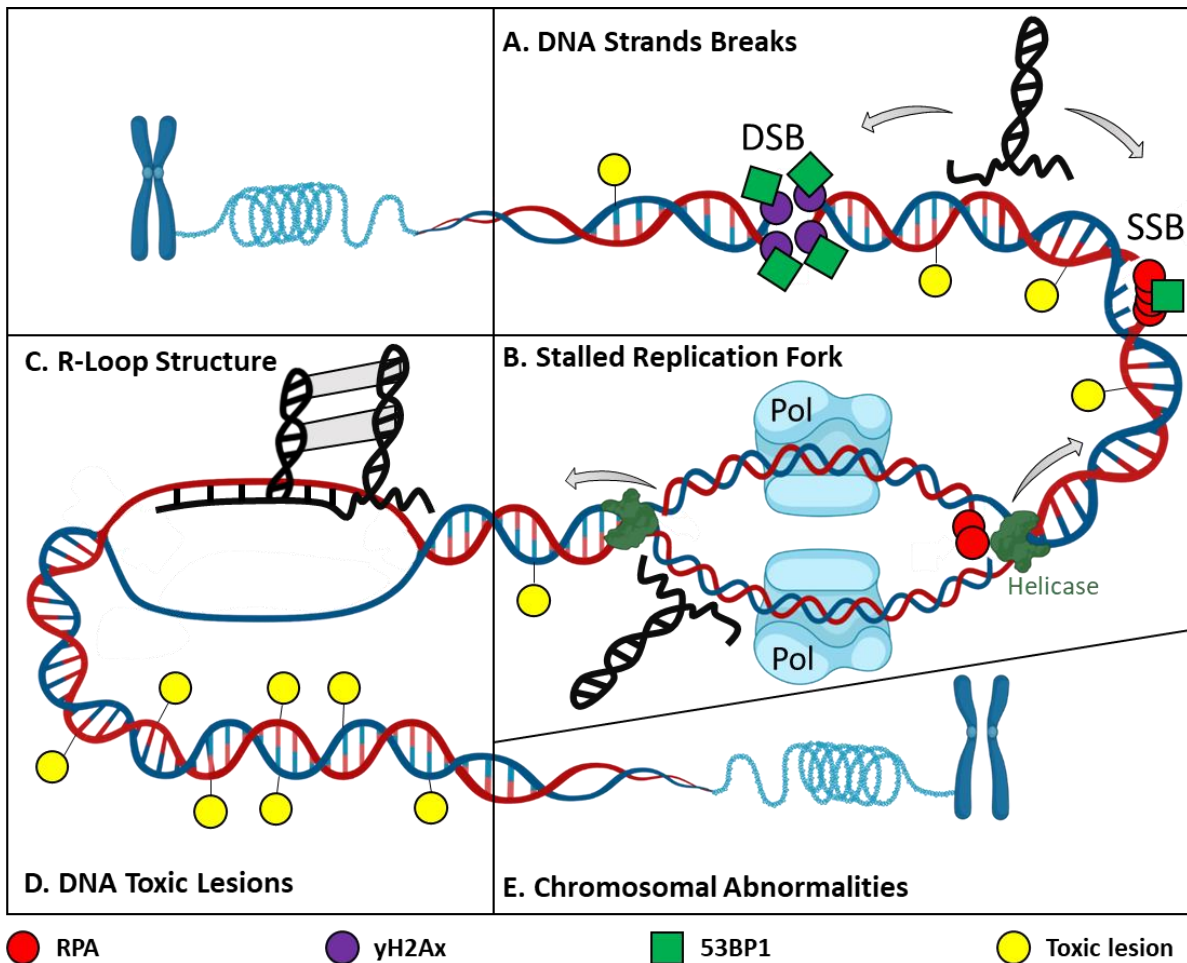


Figure 20. The proposed molecular mechanisms of *RADAR* regulation of DNA damage and its consequences on genome instability. (A) *RADAR* interacts with/ regulates the activity of component(s) of DDR to enhance DNA damage and strand break. (B) *RADAR* interferes with the DNA replication machinery and causes stalled replication fork. (C) *RADAR* forms DNA:RNA triplex, or prevents R-loop structure resolution during DNA replication, which increases replication stress due to R-loop-replication fork collision. As a result *RADAR* leads to higher accumulation of DNA toxic lesions (D) and DNA damage causing chromosomal breakage and sister chromatid cohesion loss (E). DSB: double-strand break, SSB: single-strand break, Pol: DNA polymerase.

CONCLUSIONS

LncRNAs represent hitherto an underestimated class of molecules involved in novel epigenetic mechanisms contributing to carcinogenesis and resistance to therapy. While the number of lncRNA transcripts is still rising, only a handful of lncRNAs are well characterized and functionally studied in diseases. In cancer, several lncRNAs such as *H19*, *MALAT1*, and *HOTAIR* are described to orchestrate gene expression. However, little is known about the role of lncRNAs in GBM and role in regulating response to temozolomide (TMZ).

The work of this thesis aimed to investigate the role of lncRNAs in GBM biology, using patient-derived GBM cells as a primary disease model. We here addressed two fundamental aspects comprising: 1) the elucidation of the effect of TMZ treatment on the RNA transcriptome, especially lncRNAs in GSCs; and 2) the functional characterization of a novel lncRNA in GBM. The findings presented herein reinforce the premise that lncRNAs are an integral part of transcriptional regulatory loops in close relationship with other regulatory RNAs to affect cellular response to therapy. Moreover, we further support that changes in lncRNA expression have strong effects on DNA damage regulation, cell cycle, and therapeutic outcomes in GBM. We speculate that our findings may be generalized to other cancer types, DNA damaging drugs, and possibly to rare hereditary diseases with defects in DNA repair such as Fanconi anemia, ataxia telangiectasia, xeroderma pigmentosum, Bloom Syndrome, and Cockayne syndrome.

In summary, the work of this thesis uncovered a novel human lncRNA gene named *RADAR* (RNA Associated with DNA DAmage and Replication), which has a direct role in regulating DNA damage during S-phase and affecting genome instability. Our results suggest that targeting replication stress and enhancing levels of DNA damage may enhance cancer cells' response to chemotherapy, especially in tissues with low proliferative index such as the brain. Hence, this study brings additional evidence of the important role of lncRNAs in human disease and expands our understanding of essential cellular pathways that could lead to the development of novel therapeutic strategies. Such therapeutics will be based on either directly drugging/ targeting the lncRNAs in the form of synthetic oligonucleotides or small molecules that can disrupt lncRNA-targets interaction.

CHAPTER 7

REFERENCES

REFERENCES

- Abe, N., Matsumoto, K., Nishihara, M., Nakano, Y., Shibata, A., Maruyama, H., Shuto, S., Matsuda, A., Yoshida, M., Ito, Y., *et al.* (2015). Rolling Circle Translation of Circular RNA in Living Human Cells. *Sci Rep* 5, 16435.
- Acharya, S., Wilson, T., Gradia, S., Kane, M.F., Guerrette, S., Marsischky, G.T., Kolodner, R., and Fishel, R. (1996). hMSH2 forms specific mismatch-binding complexes with hMSH3 and hMSH6. *Proc Natl Acad Sci U S A* 93, 13629-13634.
- Aguilera, A., and García-Muse, T. (2012). R loops: from transcription byproducts to threats to genome stability. *Mol Cell* 46, 115-124.
- Akhade, V.S., Pal, D., and Kanduri, C. (2017). Long Noncoding RNA: Genome Organization and Mechanism of Action. *Adv Exp Med Biol* 1008, 47-74.
- Albain, K.S., Nag, S.M., Calderillo-Ruiz, G., Jordaan, J.P., Llombart, A.C., Pluzanska, A., Rolski, J., Melemed, A.S., Reyes-Vidal, J.M., Sekhon, J.S., *et al.* (2008). Gemcitabine plus Paclitaxel versus Paclitaxel monotherapy in patients with metastatic breast cancer and prior anthracycline treatment. *J Clin Oncol* 26, 3950-3957.
- Alberts, B. (2015). *Molecular biology of the cell*, Sixth edition. edn (New York, NY: Garland Science, Taylor and Francis Group).
- Alfieri, C., Zhang, S., and Barford, D. (2017). Visualizing the complex functions and mechanisms of the anaphase promoting complex/cyclosome (APC/C). *Open Biol* 7.
- Annovazzi, L., Mellai, M., Caldera, V., Valente, G., and Schiffer, D. (2011). SOX2 expression and amplification in gliomas and glioma cell lines. *Cancer Genomics Proteomics* 8, 139-147.
- Aoki, K., Nakamura, H., Suzuki, H., Matsuo, K., Kataoka, K., Shimamura, T., Motomura, K., Ohka, F., Shiina, S., Yamamoto, T., *et al.* (2018). Prognostic relevance of genetic alterations in diffuse lower-grade gliomas. *Neuro Oncol* 20, 66-77.
- Arab, K., Park, Y.J., Lindroth, A.M., Schafer, A., Oakes, C., Weichenhan, D., Lukanova, A., Lundin, E., Risch, A., Meister, M., *et al.* (2014). Long noncoding RNA TARID directs demethylation and activation of the tumor suppressor TCF21 via GADD45A. *Mol Cell* 55, 604-614.
- Ariel, I., de Groot, N., and Hochberg, A. (2000). Imprinted H19 gene expression in embryogenesis and human cancer: the oncofetal connection. *Am J Med Genet* 91, 46-50.
- Aznaourova, M., Janga, H., Sefried, S., Kaufmann, A., Dorna, J., Volkers, S.M., Georg, P., Lechner, M., Hoppe, J., Dokel, S., *et al.* (2020). Noncoding RNA Mall1 is an integral component of the TLR4-TRIF pathway. *Proc Natl Acad Sci U S A* 117, 9042-9053.
- Azzalin, C.M., Reichenbach, P., Khoriatuli, L., Giulotto, E., and Lingner, J. (2007). Telomeric repeat containing RNA and RNA surveillance factors at mammalian chromosome ends. *Science* 318, 798-801.
- Bady, P., Sciuscio, D., Diserens, A.C., Bloch, J., van den Bent, M.J., Marosi, C., Dietrich, P.Y., Weller, M., Mariani, L., Heppner, F.L., *et al.* (2012). MGMT methylation analysis of glioblastoma on the Infinium methylation BeadChip identifies two distinct CpG regions associated with gene silencing and outcome, yielding a prediction model for comparisons across datasets, tumor grades, and CIMP-status. *Acta Neuropathol* 124, 547-560.
- Banfai, B., Jia, H., Khatun, J., Wood, E., Risk, B., Gundling, W.E., Jr., Kundaje, A., Gunawardena, H.P., Yu, Y., Xie, L., *et al.* (2012). Long noncoding RNAs are rarely translated in two human cell lines. *Genome Res* 22, 1646-1657.
- Barazzuol, L., Jena, R., Burnet, N.G., Meira, L.B., Jaynes, J.C., Kirkby, K.J., and Kirkby, N.F. (2013). Evaluation of poly (ADP-ribose) polymerase inhibitor ABT-888 combined with radiotherapy and temozolomide in glioblastoma. *Radiat Oncol* 8, 65.
- Barnum, K.J., and O'Connell, M.J. (2014). Cell cycle regulation by checkpoints. *Methods Mol Biol* 1170, 29-40.
- Becker, K.A., Ghule, P.N., Therrien, J.A., Lian, J.B., Stein, J.L., van Wijnen, A.J., and Stein, G.S. (2006). Self-renewal of human embryonic stem cells is supported by a shortened G1 cell cycle phase. *J Cell Physiol* 209, 883-893.

- Bester, A.C., Lee, J.D., Chavez, A., Lee, Y.R., Nachmani, D., Vora, S., Victor, J., Sauvageau, M., Monteleone, E., Rinn, J.L., *et al.* (2018). An Integrated Genome-wide CRISPRa Approach to Functionalize lncRNAs in Drug Resistance. *Cell* 173, 649-664.e620.
- Bhan, A., Soleimani, M., and Mandal, S.S. (2017). Long Noncoding RNA and Cancer: A New Paradigm. *Cancer Res* 77, 3965-3981.
- Bond, C.S., and Fox, A.H. (2009). Paraspeckles: nuclear bodies built on long noncoding RNA. *J Cell Biol* 186, 637-644.
- Boque-Sastre, R., Soler, M., Oliveira-Mateos, C., Portela, A., Moutinho, C., Sayols, S., Villanueva, A., Esteller, M., and Guil, S. (2015). Head-to-head antisense transcription and R-loop formation promotes transcriptional activation. *Proc Natl Acad Sci U S A* 112, 5785-5790.
- Borsani, G., Tonlorenzi, R., Simmler, M.C., Dandolo, L., Arnaud, D., Capra, V., Grompe, M., Pizzuti, A., Muzny, D., Lawrence, C., *et al.* (1991). Characterization of a murine gene expressed from the inactive X chromosome. *Nature* 351, 325-329.
- Bradshaw, A., Wickremsekera, A., Tan, S.T., Peng, L., Davis, P.F., and Itinteang, T. (2016). Cancer Stem Cell Hierarchy in Glioblastoma Multiforme. *Front Surg* 3, 21.
- Brannan, C.I., Dees, E.C., Ingram, R.S., and Tilghman, S.M. (1990). The product of the H19 gene may function as an RNA. *Mol Cell Biol* 10, 28-36.
- Brat, D.J., Aldape, K., Colman, H., Figarella-Branger, D., Fuller, G.N., Giannini, C., Holland, E.C., Jenkins, R.B., Kleinschmidt-DeMasters, B., Komori, T., *et al.* (2020). cIMPACT-NOW update 5: recommended grading criteria and terminologies for IDH-mutant astrocytomas. *Acta Neuropathol* 139, 603-608.
- Brat, D.J., Aldape, K., Colman, H., Holland, E.C., Louis, D.N., Jenkins, R.B., Kleinschmidt-DeMasters, B.K., Perry, A., Reifenberger, G., Stupp, R., *et al.* (2018). cIMPACT-NOW update 3: recommended diagnostic criteria for "Diffuse astrocytic glioma, IDH-wildtype, with molecular features of glioblastoma, WHO grade IV". *Acta Neuropathol* 136, 805-810.
- Breen, W.G., Anderson, S.K., Carrero, X.W., Brown, P.D., Ballman, K.V., O'Neill, B.P., Curran, W.J., Abrams, R.A., Laack, N.N., Levitt, R., *et al.* (2020). Final report from Intergroup NCCTG 86-72-51 (Alliance): a phase III randomized clinical trial of high-dose versus low-dose radiation for adult low-grade glioma. *Neuro Oncol* 22, 830-837.
- Brennan, C.W., Verhaak, R.G., McKenna, A., Campos, B., Nounshmehr, H., Salama, S.R., Zheng, S., Chakravarty, D., Sanborn, J.Z., Berman, S.H., *et al.* (2013). The somatic genomic landscape of glioblastoma. *Cell* 155, 462-477.
- Brockdorff, N., Ashworth, A., Kay, G.F., McCabe, V.M., Norris, D.P., Cooper, P.J., Swift, S., and Rastan, S. (1992). The product of the mouse Xist gene is a 15 kb inactive X-specific transcript containing no conserved ORF and located in the nucleus. *Cell* 71, 515-526.
- Brown, C.J., Hendrich, B.D., Rupert, J.L., Lafreniere, R.G., Xing, Y., Lawrence, J., and Willard, H.F. (1992). The human XIST gene: analysis of a 17 kb inactive X-specific RNA that contains conserved repeats and is highly localized within the nucleus. *Cell* 71, 527-542.
- Burrell, R.A., McClelland, S.E., Endesfelder, D., Groth, P., Weller, M.C., Shaikh, N., Domingo, E., Kanu, N., Dewhurst, S.M., Gronroos, E., *et al.* (2013). Replication stress links structural and numerical cancer chromosomal instability. *Nature* 494, 492-496.
- Bussemakers, M.J., van Bokhoven, A., Verhaegh, G.W., Smit, F.P., Karthaus, H.F., Schalken, J.A., Debruyne, F.M., Ru, N., and Isaacs, W.B. (1999). DD3: a new prostate-specific gene, highly overexpressed in prostate cancer. *Cancer Res* 59, 5975-5979.
- Cabili, M.N., Trapnell, C., Goff, L., Koziol, M., Tazon-Vega, B., Regev, A., and Rinn, J.L. (2011). Integrative annotation of human large intergenic noncoding RNAs reveals global properties and specific subclasses. *Genes Dev* 25, 1915-1927.
- Cabrera, A.R., Kirkpatrick, J.P., Fiveash, J.B., Shih, H.A., Koay, E.J., Lutz, S., Petit, J., Chao, S.T., Brown, P.D., Vogelbaum, M., *et al.* (2016). Radiation therapy for glioblastoma: Executive summary of an American Society for Radiation Oncology Evidence-Based Clinical Practice Guideline. *Pract Radiat Oncol* 6, 217-225.
- Cahill, D.P., Levine, K.K., Betensky, R.A., Codd, P.J., Romany, C.A., Reavie, L.B., Batchelor, T.T., Futreal, P.A., Stratton, M.R., Curry, W.T., *et al.* (2007). Loss of the mismatch repair protein MSH6 in human glioblastomas is associated with tumor progression during temozolomide treatment. *Clin Cancer Res* 13, 2038-2045.

- Cai, S., Xu, Y., Cooper, R.J., Ferkowicz, M.J., Hartwell, J.R., Pollok, K.E., and Kelley, M.R. (2005). Mitochondrial targeting of human O6-methylguanine DNA methyltransferase protects against cell killing by chemotherapeutic alkylating agents. *Cancer Res* 65, 3319-3327.
- Cai, Z., Cao, C., Ji, L., Ye, R., Wang, D., Xia, C., Wang, S., Du, Z., Hu, N., Yu, X., *et al.* (2020). RIC-seq for global in situ profiling of RNA-RNA spatial interactions. *Nature* 582, 432-437.
- Calin, G.A., and Croce, C.M. (2006). MicroRNA signatures in human cancers. *Nat Rev Cancer* 6, 857-866.
- Campos, B., Wan, F., Farhadi, M., Ernst, A., Zeppernick, F., Tagscherer, K.E., Ahmadi, R., Lohr, J., Dictus, C., Gdynia, G., *et al.* (2010). Differentiation therapy exerts antitumor effects on stem-like glioma cells. *Clin Cancer Res* 16, 2715-2728.
- Cancer Genome Atlas Research, N. (2008). Comprehensive genomic characterization defines human glioblastoma genes and core pathways. *Nature* 455, 1061-1068.
- Carlevaro-Fita, J., and Johnson, R. (2019). Global Positioning System: Understanding Long Noncoding RNAs through Subcellular Localization. *Mol Cell* 73, 869-883.
- Carninci, P., Kasukawa, T., Katayama, S., Gough, J., Frith, M.C., Maeda, N., Oyama, R., Ravasi, T., Lenhard, B., Wells, C., *et al.* (2005). The transcriptional landscape of the mammalian genome. *Science* 309, 1559-1563.
- Carruthers, R.D., Ahmed, S.U., Ramachandran, S., Strathdee, K., Kurian, K.M., Hedley, A., Gomez-Roman, N., Kalna, G., Neilson, M., Gilmour, L., *et al.* (2018). Replication Stress Drives Constitutive Activation of the DNA Damage Response and Radioresistance in Glioblastoma Stem-like Cells. *Cancer Res* 78, 5060-5071.
- Chan, H.L., and Morey, L. (2019). Emerging Roles for Polycomb-Group Proteins in Stem Cells and Cancer. *Trends Biochem Sci* 44, 688-700.
- Chaumeil, J., Le Baccon, P., Wutz, A., and Heard, E. (2006). A novel role for Xist RNA in the formation of a repressive nuclear compartment into which genes are recruited when silenced. *Genes Dev* 20, 2223-2237.
- Chen, C.K., Blanco, M., Jackson, C., Aznauryan, E., Ollikainen, N., Surka, C., Chow, A., Cerase, A., McDonel, P., and Guttman, M. (2016). Xist recruits the X chromosome to the nuclear lamina to enable chromosome-wide silencing. *Science* 354, 468-472.
- Chen, G., Cao, Y., Zhang, L., Ma, H., Shen, C., and Zhao, J. (2017). Analysis of long non-coding RNA expression profiles identifies novel lncRNA biomarkers in the tumorigenesis and malignant progression of gliomas. *Oncotarget* 8, 67744-67753.
- Chen, L., Gong, X., and Huang, M. (2019). YY1-Activated Long Noncoding RNA SNHG5 Promotes Glioblastoma Cell Proliferation Through p38/MAPK Signaling Pathway. *Cancer Biother Radiopharm* 34, 589-596.
- Chen, L.L. (2016a). The biogenesis and emerging roles of circular RNAs. *Nat Rev Mol Cell Biol* 17, 205-211.
- Chen, L.L. (2016b). Linking Long Noncoding RNA Localization and Function. *Trends Biochem Sci* 41, 761-772.
- Chen, Q., Cai, J., Wang, Q., Wang, Y., Liu, M., Yang, J., Zhou, J., Kang, C., Li, M., and Jiang, C. (2018). Long Noncoding RNA NEAT1, Regulated by the EGFR Pathway, Contributes to Glioblastoma Progression Through the WNT/beta-Catenin Pathway by Scaffolding EZH2. *Clin Cancer Res* 24, 684-695.
- Chen, R., and Wold, M.S. (2014). Replication protein A: single-stranded DNA's first responder: dynamic DNA-interactions allow replication protein A to direct single-strand DNA intermediates into different pathways for synthesis or repair. *Bioessays* 36, 1156-1161.
- Chen, W., and Schuman, E. (2016). Circular RNAs in Brain and Other Tissues: A Functional Enigma. *Trends Neurosci* 39, 597-604.
- Cheng, Z., Li, Z., Ma, K., Li, X., Tian, N., Duan, J., Xiao, X., and Wang, Y. (2017). Long Non-coding RNA XIST Promotes Glioma Tumorigenicity and Angiogenesis by Acting as a Molecular Sponge of miR-429. *J Cancer* 8, 4106-4116.
- Chilimoniuk, M., Olszewska, E., and Maksimowicz, T. (2010). [Taxan induction chemotherapy and concomitant chemoradiotherapy with cisplatin in patients with locally advanced head and neck cancer--early results]. *Pol Merkur Lekarski* 29, 357-360.

- Clamp, M., Fry, B., Kamal, M., Xie, X., Cuff, J., Lin, M.F., Kellis, M., Lindblad-Toh, K., and Lander, E.S. (2007). Distinguishing protein-coding and noncoding genes in the human genome. *Proc Natl Acad Sci U S A* *104*, 19428-19433.
- Clarke, M.J., Mulligan, E.A., Grogan, P.T., Mladek, A.C., Carlson, B.L., Schroeder, M.A., Curtin, N.J., Lou, Z., Decker, P.A., Wu, W., *et al.* (2009). Effective sensitization of temozolomide by ABT-888 is lost with development of temozolomide resistance in glioblastoma xenograft lines. *Mol Cancer Ther* *8*, 407-414.
- Collins, A.R. (2004). The comet assay for DNA damage and repair: principles, applications, and limitations. *Mol Biotechnol* *26*, 249-261.
- Conn, S.J., Pillman, K.A., Toubia, J., Conn, V.M., Salamanidis, M., Phillips, C.A., Roslan, S., Schreiber, A.W., Gregory, P.A., and Goodall, G.J. (2015). The RNA binding protein quaking regulates formation of circRNAs. *Cell* *160*, 1125-1134.
- Consortium, E.P. (2012). An integrated encyclopedia of DNA elements in the human genome. *Nature* *489*, 57-74.
- Consortium, E.P., Birney, E., Stamatoyannopoulos, J.A., Dutta, A., Guigo, R., Gingeras, T.R., Margulies, E.H., Weng, Z., Snyder, M., Dermitzakis, E.T., *et al.* (2007). Identification and analysis of functional elements in 1% of the human genome by the ENCODE pilot project. *Nature* *447*, 799-816.
- Cordaux, R., and Batzer, M.A. (2009). The impact of retrotransposons on human genome evolution. *Nat Rev Genet* *10*, 691-703.
- Coronado, D., Godet, M., Bourillot, P.Y., Tapponnier, Y., Bernat, A., Petit, M., Afanassieff, M., Markossian, S., Malashicheva, A., Iacone, R., *et al.* (2013). A short G1 phase is an intrinsic determinant of naive embryonic stem cell pluripotency. *Stem Cell Res* *10*, 118-131.
- Creamer, K.M., and Lawrence, J.B. (2017). XIST RNA: a window into the broader role of RNA in nuclear chromosome architecture. *Philos Trans R Soc Lond B Biol Sci* *372*.
- Dang, C.V. (2012). MYC on the path to cancer. *Cell* *149*, 22-35.
- Dang, L., White, D.W., Gross, S., Bennett, B.D., Bittinger, M.A., Driggers, E.M., Fantin, V.R., Jang, H.G., Jin, S., Keenan, M.C., *et al.* (2009). Cancer-associated IDH1 mutations produce 2-hydroxyglutarate. *Nature* *462*, 739-744.
- Daniel, P., Sabri, S., Chaddad, A., Meehan, B., Jean-Claude, B., Rak, J., and Abdulkarim, B.S. (2019). Temozolomide Induced Hypermutation in Glioma: Evolutionary Mechanisms and Therapeutic Opportunities. *Front Oncol* *9*, 41.
- Dasari, S., and Tchounwou, P.B. (2014). Cisplatin in cancer therapy: molecular mechanisms of action. *Eur J Pharmacol* *740*, 364-378.
- Davidovich, C., and Cech, T.R. (2015). The recruitment of chromatin modifiers by long noncoding RNAs: lessons from PRC2. *RNA* *21*, 2007-2022.
- De Boer, L., Oakes, V., Beamish, H., Giles, N., Stevens, F., Somodevilla-Torres, M., Desouza, C., and Gabrielli, B. (2008). Cyclin A/cdk2 coordinates centrosomal and nuclear mitotic events. *Oncogene* *27*, 4261-4268.
- de Hoon, M., Shin, J.W., and Carninci, P. (2015). Paradigm shifts in genomics through the FANTOM projects. *Mamm Genome* *26*, 391-402.
- de Koning, A.P., Gu, W., Castoe, T.A., Batzer, M.A., and Pollock, D.D. (2011). Repetitive elements may comprise over two-thirds of the human genome. *PLoS Genet* *7*, e1002384.
- De Magis, A., Manzo, S.G., Russo, M., Marinello, J., Morigi, R., Sordet, O., and Capranico, G. (2019). DNA damage and genome instability by G-quadruplex ligands are mediated by R loops in human cancer cells. *Proc Natl Acad Sci U S A* *116*, 816-825.
- de Souza, F.S., Franchini, L.F., and Rubinstein, M. (2013). Exaptation of transposable elements into novel cis-regulatory elements: is the evidence always strong? *Mol Biol Evol* *30*, 1239-1251.
- deCarvalho, A.C., Kim, H., Poisson, L.M., Winn, M.E., Mueller, C., Cherba, D., Koeman, J., Seth, S., Protopopov, A., Felicella, M., *et al.* (2018). Discordant inheritance of chromosomal and extrachromosomal DNA elements contributes to dynamic disease evolution in glioblastoma. *Nat Genet* *50*, 708-717.
- Deep, G., and Agarwal, R. (2008). New combination therapies with cell-cycle agents. *Curr Opin Investig Drugs* *9*, 591-604.

- Delacroix, S., Wagner, J.M., Kobayashi, M., Yamamoto, K., and Karnitz, L.M. (2007). The Rad9-Hus1-Rad1 (9-1-1) clamp activates checkpoint signaling via TopBP1. *Genes Dev* 21, 1472-1477.
- Derrien, T., Johnson, R., Bussotti, G., Tanzer, A., Djebali, S., Tilgner, H., Guernec, G., Martin, D., Merkel, A., Knowles, D.G., *et al.* (2012). The GENCODE v7 catalog of human long noncoding RNAs: analysis of their gene structure, evolution, and expression. *Genome Res* 22, 1775-1789.
- Di Gesualdo, F., Capaccioli, S., and Lulli, M. (2014). A pathophysiological view of the long non-coding RNA world. *Oncotarget* 5, 10976-10996.
- Diaz-Lagares, A., Crujeiras, A.B., Lopez-Serra, P., Soler, M., Setien, F., Goyal, A., Sandoval, J., Hashimoto, Y., Martinez-Cardus, A., Gomez, A., *et al.* (2016). Epigenetic inactivation of the p53-induced long noncoding RNA TP53 target 1 in human cancer. *Proc Natl Acad Sci U S A* 113, E7535-E7544.
- Dirkse, A., Golebiewska, A., Buder, T., Nazarov, P.V., Muller, A., Poovathingal, S., Brons, N.H.C., Leite, S., Sauvageot, N., Sarkisjan, D., *et al.* (2019). Stem cell-associated heterogeneity in Glioblastoma results from intrinsic tumor plasticity shaped by the microenvironment. *Nat Commun* 10, 1787.
- Djebali, S., Davis, C.A., Merkel, A., Dobin, A., Lassmann, T., Mortazavi, A., Tanzer, A., Lagarde, J., Lin, W., Schlesinger, F., *et al.* (2012). Landscape of transcription in human cells. *Nature* 489, 101-108.
- Du, Z., Fei, T., Verhaak, R.G.W., Su, Z., Zhang, Y., Brown, M., Chen, Y., and Liu, X.S. (2013). Integrative genomic analyses reveal clinically relevant long noncoding RNAs in human cancer. *Nature structural & molecular biology* 20, 908-913.
- Duncan, C.G., Barwick, B.G., Jin, G., Rago, C., Kapoor-Vazirani, P., Powell, D.R., Chi, J.T., Bigner, D.D., Vertino, P.M., and Yan, H. (2012). A heterozygous IDH1R132H/WT mutation induces genome-wide alterations in DNA methylation. *Genome Res* 22, 2339-2355.
- Ellis, B.C., Molloy, P.L., and Graham, L.D. (2012). CRNDE: A Long Non-Coding RNA Involved in Cancer, Neurobiology, and DEvelopment. *Front Genet* 3, 270.
- Ellison, D.W., Hawkins, C., Jones, D.T.W., Onar-Thomas, A., Pfister, S.M., Reifenberger, G., and Louis, D.N. (2019). cIMPACT-NOW update 4: diffuse gliomas characterized by MYB, MYBL1, or FGFR1 alterations or BRAF(V600E) mutation. *Acta Neuropathol* 137, 683-687.
- Erasimus, H., Gobin, M., Niclou, S., and Van Dyck, E. (2016). DNA repair mechanisms and their clinical impact in glioblastoma. *Mutat Res Rev Mutat Res* 769, 19-35.
- Faghihi, M.A., Modarresi, F., Khalil, A.M., Wood, D.E., Sahagan, B.G., Morgan, T.E., Finch, C.E., St Laurent, G., 3rd, Kenny, P.J., and Wahlestedt, C. (2008). Expression of a noncoding RNA is elevated in Alzheimer's disease and drives rapid feed-forward regulation of beta-secretase. *Nat Med* 14, 723-730.
- Faghihi, M.A., and Wahlestedt, C. (2009). Regulatory roles of natural antisense transcripts. *Nat Rev Mol Cell Biol* 10, 637-643.
- Fan, J., Xing, Y., Wen, X., Jia, R., Ni, H., He, J., Ding, X., Pan, H., Qian, G., Ge, S., *et al.* (2015). Long non-coding RNA ROR decoys gene-specific histone methylation to promote tumorigenesis. *Genome Biol* 16, 139.
- Fang, Q., Kanugula, S., and Pegg, A.E. (2005). Function of domains of human O6-alkylguanine-DNA alkyltransferase. *Biochemistry* 44, 15396-15405.
- Fatica, A., and Bozzoni, I. (2014). Long non-coding RNAs: new players in cell differentiation and development. *Nat Rev Genet* 15, 7-21.
- FDA (2018). FDA approved olaparib (LYNPARZA, AstraZeneca Pharmaceuticals LP) for the maintenance treatment of adult patients with deleterious or suspected deleterious germline or somatic BRCA-mutated (gBRCAm or sBRCAm) advanced epithelial ovarian, fallopian tube or primary peritoneal cancer who are in complete or partial response to first-line platinum-based.
- Feretaki, M., Pospisilova, M., Valador Fernandes, R., Lunardi, T., Krejci, L., and Lingner, J. (2020). RAD51-dependent recruitment of TERRA lncRNA to telomeres through R-loops. *Nature* 587, 303-308.

- Fico, A., Fiorenzano, A., Pascale, E., Patriarca, E.J., and Minchiotti, G. (2019). Long non-coding RNA in stem cell pluripotency and lineage commitment: functions and evolutionary conservation. *Cell Mol Life Sci* 76, 1459-1471.
- Figueroa, M.E., Abdel-Wahab, O., Lu, C., Ward, P.S., Patel, J., Shih, A., Li, Y., Bhagwat, N., Vasanthakumar, A., Fernandez, H.F., *et al.* (2010). Leukemic IDH1 and IDH2 mutations result in a hypermethylation phenotype, disrupt TET2 function, and impair hematopoietic differentiation. *Cancer Cell* 18, 553-567.
- Flynn, R.A., and Chang, H.Y. (2014). Long noncoding RNAs in cell-fate programming and reprogramming. *Cell Stem Cell* 14, 752-761.
- Fort, V., Khelifi, G., and Hussein, S.M.I. (2021). Long non-coding RNAs and transposable elements: A functional relationship. *Biochim Biophys Acta Mol Cell Res* 1868, 118837.
- Fritah, S., Muller, A., Jiang, W., Mitra, R., Sarmini, M., Dieterle, M., Golebiewska, A., Ye, T., Van Dyck, E., Herold-Mende, C., *et al.* (2020). Temozolomide-Induced RNA Interactome Uncovers Novel LncRNA Regulatory Loops in Glioblastoma. *Cancers (Basel)* 12.
- Fritah, S., Niclou, S.P., and Azuaje, F. (2014). Databases for lncRNAs: a comparative evaluation of emerging tools. *Rna* 20, 1655-1665.
- Frith, M.C., Bailey, T.L., Kasukawa, T., Mignone, F., Kummerfeld, S.K., Madera, M., Sunkara, S., Furuno, M., Bult, C.J., Quackenbush, J., *et al.* (2006). Discrimination of non-protein-coding transcripts from protein-coding mRNA. *RNA Biol* 3, 40-48.
- Gaetani, P., Hulleman, E., Levi, D., Quarto, M., Scorsetti, M., Helins, K., Simonelli, M., Colombo, P., and Baena y Rodriguez, R. (2010). Expression of the transcription factor HEY1 in glioblastoma: a preliminary clinical study. *Tumori* 96, 97-102.
- Gagnon, K.T., Li, L., Janowski, B.A., and Corey, D.R. (2014). Analysis of nuclear RNA interference in human cells by subcellular fractionation and Argonaute loading. *Nat Protoc* 9, 2045-2060.
- Galupa, R., Nora, E.P., Worsley-Hunt, R., Picard, C., Gard, C., van Bommel, J.G., Servant, N., Zhan, Y., El Marjou, F., Johanneau, C., *et al.* (2020). A Conserved Noncoding Locus Regulates Random Monoallelic Xist Expression across a Topological Boundary. *Mol Cell* 77, 352-367 e358.
- Gascoigne, D.K., Cheetham, S.W., Cattenoz, P.B., Clark, M.B., Amaral, P.P., Taft, R.J., Wilhelm, D., Dinger, M.E., and Mattick, J.S. (2012). Pinstripe: a suite of programs for integrating transcriptomic and proteomic datasets identifies novel proteins and improves differentiation of protein-coding and non-coding genes. *Bioinformatics* 28, 3042-3050.
- Gavet, O., and Pines, J. (2010). Progressive activation of CyclinB1-Cdk1 coordinates entry to mitosis. *Dev Cell* 18, 533-543.
- Geisler, S., and Coller, J. (2013). RNA in unexpected places: long non-coding RNA functions in diverse cellular contexts. *Nat Rev Mol Cell Biol* 14, 699-712.
- Ghosal, G., and Chen, J. (2013). DNA damage tolerance: a double-edged sword guarding the genome. *Transl Cancer Res* 2, 107-129.
- Glazar, P., Papavasileiou, P., and Rajewsky, N. (2014). circBase: a database for circular RNAs. *RNA* 20, 1666-1670.
- Goffeau, A., Barrell, B.G., Bussey, H., Davis, R.W., Dujon, B., Feldmann, H., Galibert, F., Hoheisel, J.D., Jacq, C., Johnston, M., *et al.* (1996). Life with 6000 genes. *Science* 274, 546, 563-547.
- Gong, X., and Huang, M.Y. (2020). Tumor-Suppressive Function of lncRNA-MEG3 in Glioma Cells by Regulating miR-6088/SMARCB1 Axis. *Biomed Res Int* 2020, 4309161.
- Gordon, F.E., Nutt, C.L., Cheunsuchon, P., Nakayama, Y., Provencher, K.A., Rice, K.A., Zhou, Y., Zhang, X., and Klibanski, A. (2010). Increased expression of angiogenic genes in the brains of mouse meg3-null embryos. *Endocrinology* 151, 2443-2452.
- Goyal, A., Fiskin, E., Gutschner, T., Polycarpou-Schwarz, M., Gross, M., Neugebauer, J., Gandhi, M., Caudron-Herger, M., Benes, V., and Diederichs, S. (2017). A cautionary tale of sense-antisense gene pairs: independent regulation despite inverse correlation of expression. *Nucleic Acids Res* 45, 12496-12508.

- Graf, M., Bonetti, D., Lockhart, A., Serhal, K., Kellner, V., Maicher, A., Jolivet, P., Teixeira, M.T., and Luke, B. (2017). Telomere Length Determines TERRA and R-Loop Regulation through the Cell Cycle. *Cell* 170, 72-85 e14.
- Graindorge, A., Pinheiro, I., Nawrocka, A., Mallory, A.C., Tsvetkov, P., Gil, N., Carolis, C., Buchholz, F., Ulitsky, I., Heard, E., *et al.* (2019). In-cell identification and measurement of RNA-protein interactions. *Nat Commun* 10, 5317.
- Grelet, S., Link, L.A., Howley, B., Obellianne, C., Palanisamy, V., Gangaraju, V.K., Diehl, J.A., and Howe, P.H. (2017). A regulated PNUTS mRNA to lncRNA splice switch mediates EMT and tumour progression. *Nat Cell Biol* 19, 1105-1115.
- Guarnerio, J., Bezzi, M., Jeong, J.C., Paffenholz, S.V., Berry, K., Naldini, M.M., Lo-Coco, F., Tay, Y., Beck, A.H., and Pandolfi, P.P. (2016). Oncogenic Role of Fusion-circRNAs Derived from Cancer-Associated Chromosomal Translocations. *Cell* 166, 1055-1056.
- Gudjonsson, T., Altmeyer, M., Savic, V., Toledo, L., Dinant, C., Grofte, M., Bartkova, J., Poulsen, M., Oka, Y., Bekker-Jensen, S., *et al.* (2012). TRIP12 and UBR5 suppress spreading of chromatin ubiquitylation at damaged chromosomes. *Cell* 150, 697-709.
- Guertin, D.A., Trautmann, S., and McCollum, D. (2002). Cytokinesis in eukaryotes. *Microbiol Mol Biol Rev* 66, 155-178.
- Guh, C.Y., Hsieh, Y.H., and Chu, H.P. (2020). Functions and properties of nuclear lncRNAs—from systematically mapping the interactomes of lncRNAs. *J Biomed Sci* 27, 44.
- Guiducci, G., and Stojic, L. (2021). Long Noncoding RNAs at the Crossroads of Cell Cycle and Genome Integrity. *Trends Genet.*
- Guil, S., and Esteller, M. (2015). RNA-RNA interactions in gene regulation: the coding and noncoding players. *Trends Biochem Sci* 40, 248-256.
- Gupta, R.A., Shah, N., Wang, K.C., Kim, J., Horlings, H.M., Wong, D.J., Tsai, M.C., Hung, T., Argani, P., Rinn, J.L., *et al.* (2010). Long non-coding RNA HOTAIR reprograms chromatin state to promote cancer metastasis. *Nature* 464, 1071-1076.
- Guttman, M., Amit, I., Garber, M., French, C., Lin, M.F., Feldser, D., Huarte, M., Zuk, O., Carey, B.W., Cassady, J.P., *et al.* (2009). Chromatin signature reveals over a thousand highly conserved large non-coding RNAs in mammals. *Nature* 458, 223-227.
- Hadjicharalambous, M.R., and Lindsay, M.A. (2019). Long Non-Coding RNAs and the Innate Immune Response. *Noncoding RNA* 5.
- Hall, L.L., and Lawrence, J.B. (2010). XIST RNA and architecture of the inactive X chromosome: implications for the repeat genome. *Cold Spring Harb Symp Quant Biol* 75, 345-356.
- Han, L., Kong, R., Yin, D.D., Zhang, E.B., Xu, T.P., De, W., and Shu, Y.Q. (2013). Low expression of long noncoding RNA GAS6-AS1 predicts a poor prognosis in patients with NSCLC. *Med Oncol* 30, 694.
- Han, L., Zhang, K., Shi, Z., Zhang, J., Zhu, J., Zhu, S., Zhang, A., Jia, Z., Wang, G., Yu, S., *et al.* (2012). LncRNA profile of glioblastoma reveals the potential role of lncRNAs in contributing to glioblastoma pathogenesis. *Int J Oncol* 40, 2004-2012.
- Han, M., Wang, S., Fritah, S., Wang, X., Zhou, W., Yang, N., Ni, S., Huang, B., Chen, A., Li, G., *et al.* (2020). Interfering with long non-coding RNA MIR22HG processing inhibits glioblastoma progression through suppression of Wnt/ β -catenin signalling. *Brain* 143, 512-530.
- Han, P., Li, W., Lin, C.H., Yang, J., Shang, C., Nuernberg, S.T., Jin, K.K., Xu, W., Lin, C.Y., Lin, C.J., *et al.* (2014). A long noncoding RNA protects the heart from pathological hypertrophy. *Nature* 514, 102-106.
- Hanahan, D., and Weinberg, R.A. (2000). The hallmarks of cancer. *Cell* 100, 57-70.
- Hao, Q., Zong, X., Sun, Q., Lin, Y.C., Song, Y.J., Hashemikhabir, S., Hsu, R.Y., Kamran, M., Chaudhary, R., Tripathi, V., *et al.* (2020). The S-phase-induced lncRNA SUNO1 promotes cell proliferation by controlling YAP1/Hippo signaling pathway. *Elife* 9.
- Harper, J.W., Adami, G.R., Wei, N., Keyomarsi, K., and Elledge, S.J. (1993). The p21 Cdk-interacting protein Cip1 is a potent inhibitor of G1 cyclin-dependent kinases. *Cell* 75, 805-816.
- Harrow, J., Frankish, A., Gonzalez, J.M., Tapanari, E., Diekhans, M., Kokocinski, F., Aken, B.L., Barrell, D., Zadissa, A., Searle, S., *et al.* (2012). GENCODE: the reference human genome annotation for The ENCODE Project. *Genome Res* 22, 1760-1774.

- Heard, E. (2004). Recent advances in X-chromosome inactivation. *Curr Opin Cell Biol* 16, 247-255.
- Heard, E., Clerc, P., and Avner, P. (1997). X-chromosome inactivation in mammals. *Annu Rev Genet* 31, 571-610.
- Hegi, M.E., Diserens, A.C., Gorlia, T., Hamou, M.F., de Tribolet, N., Weller, M., Kros, J.M., Hainfellner, J.A., Mason, W., Mariani, L., *et al.* (2005). MGMT gene silencing and benefit from temozolomide in glioblastoma. *N Engl J Med* 352, 997-1003.
- Hezroni, H., Koppstein, D., Schwartz, M.G., Avrutin, A., Bartel, D.P., and Ulitsky, I. (2015). Principles of long noncoding RNA evolution derived from direct comparison of transcriptomes in 17 species. *Cell Rep* 11, 1110-1122.
- Higgs, D.R. (2020). Enhancer-promoter interactions and transcription. *Nat Genet* 52, 470-471.
- Higuchi, F., Nagashima, H., Ning, J., Koerner, M.V.A., Wakimoto, H., and Cahill, D.P. (2020). Restoration of Temozolomide Sensitivity by PARP Inhibitors in Mismatch Repair Deficient Glioblastoma is Independent of Base Excision Repair. *Clin Cancer Res* 26, 1690-1699.
- Hsiao, K.Y., Lin, Y.C., Gupta, S.K., Chang, N., Yen, L., Sun, H.S., and Tsai, S.J. (2017). Noncoding Effects of Circular RNA CCDC66 Promote Colon Cancer Growth and Metastasis. *Cancer Res* 77, 2339-2350.
- Hu, W.L., Jin, L., Xu, A., Wang, Y.F., Thorne, R.F., Zhang, X.D., and Wu, M. (2018). GUARDIN is a p53-responsive long non-coding RNA that is essential for genomic stability. *Nat Cell Biol* 20, 492-502.
- Huarte, M., Guttman, M., Feldser, D., Garber, M., Koziol, M.J., Kenzelmann-Broz, D., Khalil, A.M., Zuk, O., Amit, I., Rabani, M., *et al.* (2010). A large intergenic noncoding RNA induced by p53 mediates global gene repression in the p53 response. *Cell* 142, 409-419.
- Hung, T., Wang, Y., Lin, M.F., Koegel, A.K., Kotake, Y., Grant, G.D., Horlings, H.M., Shah, N., Umbricht, C., Wang, P., *et al.* (2011). Extensive and coordinated transcription of noncoding RNAs within cell-cycle promoters. *Nat Genet* 43, 621-629.
- Hunter, C., Smith, R., Cahill, D.P., Stephens, P., Stevens, C., Teague, J., Greenman, C., Edkins, S., Bignell, G., Davies, H., *et al.* (2006). A hypermutation phenotype and somatic MSH6 mutations in recurrent human malignant gliomas after alkylator chemotherapy. *Cancer Res* 66, 3987-3991.
- Iacovoni, J.S., Caron, P., Lassadi, I., Nicolas, E., Massip, L., Trouche, D., and Legube, G. (2010). High-resolution profiling of gammaH2AX around DNA double strand breaks in the mammalian genome. *EMBO J* 29, 1446-1457.
- Ingolia, N.T., Brar, G.A., Stern-Ginossar, N., Harris, M.S., Talhouarne, G.J., Jackson, S.E., Wills, M.R., and Weissman, J.S. (2014). Ribosome profiling reveals pervasive translation outside of annotated protein-coding genes. *Cell Rep* 8, 1365-1379.
- Ito, S., Murphy, C.G., Doubrovina, E., Jasin, M., and Moynahan, M.E. (2016). PARP Inhibitors in Clinical Use Induce Genomic Instability in Normal Human Cells. *PLoS One* 11, e0159341.
- Ivanov, A., Memczak, S., Wyler, E., Torti, F., Porath, H.T., Orejuela, M.R., Piechotta, M., Levanon, E.Y., Landthaler, M., Dieterich, C., *et al.* (2015). Analysis of intron sequences reveals hallmarks of circular RNA biogenesis in animals. *Cell Rep* 10, 170-177.
- Jackson, S.P., and Bartek, J. (2009). The DNA-damage response in human biology and disease. *Nature* 461, 1071-1078.
- Jayaraj, G.G., Pandey, S., Scaria, V., and Maiti, S. (2012). Potential G-quadruplexes in the human long non-coding transcriptome. *RNA Biol* 9, 81-86.
- Jeck, W.R., and Sharpless, N.E. (2014). Detecting and characterizing circular RNAs. *Nat Biotechnol* 32, 453-461.
- Jeggari, A., Marks, D.S., and Larsson, E. (2012). miRcode: a map of putative microRNA target sites in the long non-coding transcriptome. *Bioinformatics* 28, 2062-2063.
- Jegu, T., Aeby, E., and Lee, J.T. (2017). The X chromosome in space. *Nat Rev Genet* 18, 377-389.
- Jensen, T.H., Jacquier, A., and Libri, D. (2013). Dealing with pervasive transcription. *Mol Cell* 52, 473-484.
- Ji, P., Diederichs, S., Wang, W., Boing, S., Metzger, R., Schneider, P.M., Tidow, N., Brandt, B., Buerger, H., Bulk, E., *et al.* (2003). MALAT-1, a novel noncoding RNA, and thymosin beta4

- predict metastasis and survival in early-stage non-small cell lung cancer. *Oncogene* 22, 8031-8041.
- Johannessen, T.C., and Bjerkvig, R. (2012). Molecular mechanisms of temozolomide resistance in glioblastoma multiforme. *Expert Rev Anticancer Ther* 12, 635-642.
- Johnson, R., and Guigo, R. (2014). The RIDL hypothesis: transposable elements as functional domains of long noncoding RNAs. *RNA* 20, 959-976.
- Johnsson, P., Lipovich, L., Grander, D., and Morris, K.V. (2014). Evolutionary conservation of long non-coding RNAs; sequence, structure, function. *Biochim Biophys Acta* 1840, 1063-1071.
- Kamachi, Y., and Kondoh, H. (2013). Sox proteins: regulators of cell fate specification and differentiation. *Development* 140, 4129-4144.
- Kapranov, P., Cheng, J., Dike, S., Nix, D.A., Dutttagupta, R., Willingham, A.T., Stadler, P.F., Hertel, J., Hackermuller, J., Hofacker, I.L., *et al.* (2007). RNA maps reveal new RNA classes and a possible function for pervasive transcription. *Science* 316, 1484-1488.
- Kawai, J., Shinagawa, A., Shibata, K., Yoshino, M., Itoh, M., Ishii, Y., Arakawa, T., Hara, A., Fukunishi, Y., Konno, H., *et al.* (2001). Functional annotation of a full-length mouse cDNA collection. *Nature* 409, 685-690.
- Kelley, D., and Rinn, J. (2012). Transposable elements reveal a stem cell-specific class of long noncoding RNAs. *Genome Biol* 13, R107.
- Kenneweg, F., Bang, C., Xiao, K., Boulanger, C.M., Loyer, X., Mazlan, S., Schroen, B., Hermans-Beijnsberger, S., Foinquinos, A., Hirt, M.N., *et al.* (2019). Long Noncoding RNA-Enriched Vesicles Secreted by Hypoxic Cardiomyocytes Drive Cardiac Fibrosis. *Mol Ther Nucleic Acids* 18, 363-374.
- Khalil, A.M., Guttman, M., Huarte, M., Garber, M., Raj, A., Rivea Morales, D., Thomas, K., Presser, A., Bernstein, B.E., van Oudenaarden, A., *et al.* (2009). Many human large intergenic noncoding RNAs associate with chromatin-modifying complexes and affect gene expression. *Proc Natl Acad Sci U S A* 106, 11667-11672.
- Khanduja, J.S., Calvo, I.A., Joh, R.I., Hill, I.T., and Motamedi, M. (2016). Nuclear Noncoding RNAs and Genome Stability. *Mol Cell* 63, 7-20.
- Kikin, O., D'Antonio, L., and Bagga, P.S. (2006). QGRS Mapper: a web-based server for predicting G-quadruplexes in nucleotide sequences. *Nucleic Acids Res* 34, W676-682.
- Kim, D., Perteza, G., Trapnell, C., Pimentel, H., Kelley, R., and Salzberg, S.L. (2013). TopHat2: accurate alignment of transcriptomes in the presence of insertions, deletions and gene fusions. *Genome Biol* 14, R36.
- Kim, Y.W., Lee, S., Yun, J., and Kim, A. (2015). Chromatin looping and eRNA transcription precede the transcriptional activation of gene in the beta-globin locus. *Biosci Rep* 35.
- Kino, T., Hurt, D.E., Ichijo, T., Nader, N., and Chrousos, G.P. (2010). Noncoding RNA gas5 is a growth arrest- and starvation-associated repressor of the glucocorticoid receptor. *Sci Signal* 3, ra8.
- Kirk, J.M., Kim, S.O., Inoue, K., Smola, M.J., Lee, D.M., Schertzer, M.D., Wooten, J.S., Baker, A.R., Sprague, D., Collins, D.W., *et al.* (2018). Functional classification of long non-coding RNAs by k-mer content. *Nat Genet* 50, 1474-1482.
- Kitagawa, M., Kitagawa, K., Kotake, Y., Niida, H., and Ohhata, T. (2013). Cell cycle regulation by long non-coding RNAs. *Cell Mol Life Sci* 70, 4785-4794.
- Kitange, G.J., Carlson, B.L., Schroeder, M.A., Grogan, P.T., Lamont, J.D., Decker, P.A., Wu, W., James, C.D., and Sarkaria, J.N. (2009). Induction of MGMT expression is associated with temozolomide resistance in glioblastoma xenografts. *Neuro Oncol* 11, 281-291.
- Kitao, H., Iimori, M., Kataoka, Y., Wakasa, T., Tokunaga, E., Saeki, H., Oki, E., and Maehara, Y. (2018). DNA replication stress and cancer chemotherapy. *Cancer Sci* 109, 264-271.
- Kleaveland, B., Shi, C.Y., Stefano, J., and Bartel, D.P. (2018). A Network of Noncoding Regulatory RNAs Acts in the Mammalian Brain. *Cell* 174, 350-362 e317.
- Koboldt, D.C., Steinberg, K.M., Larson, D.E., Wilson, R.K., and Mardis, E.R. (2013). The next-generation sequencing revolution and its impact on genomics. *Cell* 155, 27-38.
- Konermann, S., Brigham, M.D., Trevino, A.E., Joung, J., Abudayyeh, O.O., Barcena, C., Hsu, P.D., Habib, N., Gootenberg, J.S., Nishimasu, H., *et al.* (2015). Genome-scale transcriptional activation by an engineered CRISPR-Cas9 complex. *Nature* 517, 583-588.

- Kong, L., Zhang, Y., Ye, Z.Q., Liu, X.Q., Zhao, S.Q., Wei, L., and Gao, G. (2007). CPC: assess the protein-coding potential of transcripts using sequence features and support vector machine. *Nucleic Acids Res* 35, W345-349.
- Kopp, F., Elguindy, M.M., Yalvac, M.E., Zhang, H., Chen, B., Gillett, F.A., Lee, S., Sivakumar, S., Yu, H., Xie, Y., *et al.* (2019). PUMILIO hyperactivity drives premature aging of Norad-deficient mice. *Elife* 8.
- Kopp, F., and Mendell, J.T. (2018). Functional Classification and Experimental Dissection of Long Noncoding RNAs. *Cell* 172, 393-407.
- Kristensen, L.S., Okholm, T.L.H., Veno, M.T., and Kjems, J. (2018). Circular RNAs are abundantly expressed and upregulated during human epidermal stem cell differentiation. *RNA Biol* 15, 280-291.
- Kung, J.T., Colognori, D., and Lee, J.T. (2013). Long noncoding RNAs: past, present, and future. *Genetics* 193, 651-669.
- Kurukuti, S., Tiwari, V.K., Tavoosidana, G., Pugacheva, E., Murrell, A., Zhao, Z., Lobanenko, V., Reik, W., and Ohlsson, R. (2006). CTCF binding at the H19 imprinting control region mediates maternally inherited higher-order chromatin conformation to restrict enhancer access to Igf2. *Proc Natl Acad Sci U S A* 103, 10684-10689.
- Kwok, C.K., Marsico, G., Sahakyan, A.B., Chambers, V.S., and Balasubramanian, S. (2016). rG4-seq reveals widespread formation of G-quadruplex structures in the human transcriptome. *Nat Methods* 13, 841-844.
- LaBaer, J., Garrett, M.D., Stevenson, L.F., Slingerland, J.M., Sandhu, C., Chou, H.S., Fattaey, A., and Harlow, E. (1997). New functional activities for the p21 family of CDK inhibitors. *Genes Dev* 11, 847-862.
- Labib, K., Tercero, J.A., and Diffley, J.F. (2000). Uninterrupted MCM2-7 function required for DNA replication fork progression. *Science* 288, 1643-1647.
- Labreche, K., Simeonova, I., Kamoun, A., Gleize, V., Chubb, D., Letouze, E., Riazalhosseini, Y., Dobbins, S.E., Elarouci, N., Ducray, F., *et al.* (2015). TCF12 is mutated in anaplastic oligodendroglioma. *Nat Commun* 6, 7207.
- Lamm, N., Ben-David, U., Golan-Lev, T., Storchova, Z., Benvenisty, N., and Kerem, B. (2016). Genomic Instability in Human Pluripotent Stem Cells Arises from Replicative Stress and Chromosome Condensation Defects. *Cell Stem Cell* 18, 253-261.
- Lander, E.S., Linton, L.M., Birren, B., Nusbaum, C., Zody, M.C., Baldwin, J., Devon, K., Dewar, K., Doyle, M., FitzHugh, W., *et al.* (2001). Initial sequencing and analysis of the human genome. *Nature* 409, 860-921.
- Langston, L.D., and O'Donnell, M. (2006). DNA replication: keep moving and don't mind the gap. *Mol Cell* 23, 155-160.
- Lathia, J.D., Mack, S.C., Mulkearns-Hubert, E.E., Valentim, C.L., and Rich, J.N. (2015). Cancer stem cells in glioblastoma. *Genes Dev* 29, 1203-1217.
- Lee, H., Zhang, Z., and Krause, H.M. (2019). Long Noncoding RNAs and Repetitive Elements: Junk or Intimate Evolutionary Partners? *Trends Genet* 35, 892-902.
- Lee, S., Kopp, F., Chang, T.C., Sataluri, A., Chen, B., Sivakumar, S., Yu, H., Xie, Y., and Mendell, J.T. (2016). Noncoding RNA NORAD Regulates Genomic Stability by Sequestering PUMILIO Proteins. *Cell* 164, 69-80.
- Li, J.-H., Liu, S., Zhou, H., Qu, L.-H., and Yang, J.-H. (2014). starBase v2.0: decoding miRNA-ceRNA, miRNA-ncRNA and protein-RNA interaction networks from large-scale CLIP-Seq data. *Nucleic acids research* 42, D92-97.
- Li, Q., Dong, C., Cui, J., Wang, Y., and Hong, X. (2018). Over-expressed lncRNA HOTAIRM1 promotes tumor growth and invasion through up-regulating HOXA1 and sequestering G9a/EZH2/Dnmts away from the HOXA1 gene in glioblastoma multiforme. *J Exp Clin Cancer Res* 37, 265.
- Li, S., Teng, S., Xu, J., Su, G., Zhang, Y., Zhao, J., Zhang, S., Wang, H., Qin, W., Lu, Z.J., *et al.* (2019). Microarray is an efficient tool for circRNA profiling. *Brief Bioinform* 20, 1420-1433.
- Lim, S., and Kaldis, P. (2013). Cdks, cyclins and CKIs: roles beyond cell cycle regulation. *Development* 140, 3079-3093.

- Lin, D. (2016). Commentary on "The oestrogen receptor alpha-regulated lncRNA NEAT1 is a critical modulator of prostate cancer." Chakravarty D, Sboner A, Nair SS, Giannopoulou E, Li R, Hennig S, Mosquera JM, Pauwels J, Park K, Kossai M, MacDonald TY, Fontugne J, Erho N, Vergara IA, Ghadessi M, Davicioni E, Jenkins RB, Palanisamy N, Chen Z, Nakagawa S, Hirose T, Bander NH, Beltran H, Fox AH, Elemento O, Rubin MA, University of Washington-Urology, Seattle, WA. *Nat Commun* 2014; 5:5383. *Urol Oncol* 34, 522.
- Lin, M.F., Jungreis, I., and Kellis, M. (2011). PhyloCSF: a comparative genomics method to distinguish protein coding and non-coding regions. *Bioinformatics* 27, i275-282.
- Lin, Y.H. (2020). Crosstalk of lncRNA and Cellular Metabolism and Their Regulatory Mechanism in Cancer. *Int J Mol Sci* 21.
- Linsenmann, T., Jawork, A., Westermaier, T., Homola, G., Monoranu, C.M., Vince, G.H., Kessler, A.F., Ernestus, R.I., and Lohr, M. (2019). Tumor growth under rhGM-CSF application in an orthotopic rodent glioma model. *Oncol Lett* 17, 4843-4850.
- Liu, B., Zhou, J., Wang, C., Chi, Y., Wei, Q., Fu, Z., Lian, C., Huang, Q., Liao, C., Yang, Z., *et al.* (2020). lncRNA SOX2OT promotes temozolomide resistance by elevating SOX2 expression via ALKBH5-mediated epigenetic regulation in glioblastoma. *Cell Death Dis* 11, 384.
- Liu, J., Wang, W.M., Zhang, X.L., Du, Q.H., Li, H.G., and Zhang, Y. (2018). Effect of downregulated lncRNA NBAT1 on the biological behavior of glioblastoma cells. *Eur Rev Med Pharmacol Sci* 22, 2715-2722.
- Liu, X., Li, D., Zhang, W., Guo, M., and Zhan, Q. (2012). Long non-coding RNA gadd7 interacts with TDP-43 and regulates Cdk6 mRNA decay. *EMBO J* 31, 4415-4427.
- Loewer, S., Cabili, M.N., Guttman, M., Loh, Y.H., Thomas, K., Park, I.H., Garber, M., Curran, M., Onder, T., Agarwal, S., *et al.* (2010). Large intergenic non-coding RNA-RoR modulates reprogramming of human induced pluripotent stem cells. *Nat Genet* 42, 1113-1117.
- Lopez-Urrutia, E., Bustamante Montes, L.P., Ladron de Guevara Cervantes, D., Perez-Plasencia, C., and Campos-Parra, A.D. (2019). Crosstalk Between Long Non-coding RNAs, Micro-RNAs and mRNAs: Deciphering Molecular Mechanisms of Master Regulators in Cancer. *Front Oncol* 9, 669.
- Lord, C.J., and Ashworth, A. (2012). The DNA damage response and cancer therapy. *Nature* 481, 287-294.
- Louis, D.N., Aldape, K., Brat, D.J., Capper, D., Ellison, D.W., Hawkins, C., Paulus, W., Perry, A., Reifenberger, G., Figarella-Branger, D., *et al.* (2017a). Announcing cIMPACT-NOW: the Consortium to Inform Molecular and Practical Approaches to CNS Tumor Taxonomy. *Acta Neuropathol* 133, 1-3.
- Louis, D.N., Aldape, K., Brat, D.J., Capper, D., Ellison, D.W., Hawkins, C., Paulus, W., Perry, A., Reifenberger, G., Figarella-Branger, D., *et al.* (2017b). cIMPACT-NOW (the consortium to inform molecular and practical approaches to CNS tumor taxonomy): a new initiative in advancing nervous system tumor classification. *Brain Pathol* 27, 851-852.
- Louis, D.N., Perry, A., Reifenberger, G., von Deimling, A., Figarella-Branger, D., Cavenee, W.K., Ohgaki, H., Wiestler, O.D., Kleihues, P., and Ellison, D.W. (2016). The 2016 World Health Organization Classification of Tumors of the Central Nervous System: a summary. *Acta Neuropathol* 131, 803-820.
- Louis, D.N., Wesseling, P., Aldape, K., Brat, D.J., Capper, D., Cree, I.A., Eberhart, C., Figarella-Branger, D., Fouladi, M., Fuller, G.N., *et al.* (2020). cIMPACT-NOW update 6: new entity and diagnostic principle recommendations of the cIMPACT-Utrecht meeting on future CNS tumor classification and grading. *Brain Pathol* 30, 844-856.
- Lu, C., Wei, Y., Wang, X., Zhang, Z., Yin, J., Li, W., Chen, L., Lyu, X., Shi, Z., Yan, W., *et al.* (2020). DNA-methylation-mediated activating of lncRNA SNHG12 promotes temozolomide resistance in glioblastoma. *Mol Cancer* 19, 28.
- Lu, Z., Zhang, Q.C., Lee, B., Flynn, R.A., Smith, M.A., Robinson, J.T., Davidovich, C., Gooding, A.R., Goodrich, K.J., Mattick, J.S., *et al.* (2016). RNA Duplex Map in Living Cells Reveals Higher-Order Transcriptome Structure. *Cell* 165, 1267-1279.
- Lubelsky, Y., and Ulitsky, I. (2018). Sequences enriched in Alu repeats drive nuclear localization of long RNAs in human cells. *Nature* 555, 107-111.

- Ma, L., Bajic, V.B., and Zhang, Z. (2013). On the classification of long non-coding RNAs. *RNA Biol* 10, 925-933.
- Ma, L., Cao, J., Liu, L., Du, Q., Li, Z., Zou, D., Bajic, V.B., and Zhang, Z. (2019). LncBook: a curated knowledgebase of human long non-coding RNAs. *Nucleic Acids Res* 47, 2699.
- Malumbres, M., and Barbacid, M. (2001). To cycle or not to cycle: a critical decision in cancer. *Nat Rev Cancer* 1, 222-231.
- Mankouri, H.W., Huttner, D., and Hickson, I.D. (2013). How unfinished business from S-phase affects mitosis and beyond. *EMBO J* 32, 2661-2671.
- Mao, Y.S., Zhang, B., and Spector, D.L. (2011). Biogenesis and function of nuclear bodies. *Trends Genet* 27, 295-306.
- Marchese, F.P., Grossi, E., Marin-Bejar, O., Bharti, S.K., Raimondi, I., Gonzalez, J., Martinez-Herrera, D.J., Athie, A., Amadoz, A., Brosh, R.M., Jr., *et al.* (2016). A Long Noncoding RNA Regulates Sister Chromatid Cohesion. *Mol Cell* 63, 397-407.
- Marvin, M.C., Clauder-Munster, S., Walker, S.C., Sarkeshik, A., Yates, J.R., 3rd, Steinmetz, L.M., and Engelke, D.R. (2011). Accumulation of noncoding RNA due to an RNase P defect in *Saccharomyces cerevisiae*. *RNA* 17, 1441-1450.
- Maston, G.A., Evans, S.K., and Green, M.R. (2006). Transcriptional regulatory elements in the human genome. *Annu Rev Genomics Hum Genet* 7, 29-59.
- Matsumura, K., Kawasaki, Y., Miyamoto, M., Kamoshida, Y., Nakamura, J., Negishi, L., Suda, S., and Akiyama, T. (2017). The novel G-quadruplex-containing long non-coding RNA GSEC antagonizes DHX36 and modulates colon cancer cell migration. *Oncogene* 36, 1191-1199.
- Mattick, J.S. (2001). Non-coding RNAs: the architects of eukaryotic complexity. *EMBO Rep* 2, 986-991.
- Mattick, J.S., Taft, R.J., and Faulkner, G.J. (2010). A global view of genomic information--moving beyond the gene and the master regulator. *Trends Genet* 26, 21-28.
- Mazor, G., Levin, L., Picard, D., Ahmadov, U., Caren, H., Borkhardt, A., Reifenberger, G., Leprivier, G., Remke, M., and Rotblat, B. (2019). The lncRNA TP73-AS1 is linked to aggressiveness in glioblastoma and promotes temozolomide resistance in glioblastoma cancer stem cells. *Cell Death Dis* 10, 246.
- McFaline-Figueroa, J.L., Braun, C.J., Stanciu, M., Nagel, Z.D., Mazzucato, P., Sangaraju, D., Cerniauskas, E., Barford, K., Vargas, A., Chen, Y., *et al.* (2015). Minor Changes in Expression of the Mismatch Repair Protein MSH2 Exert a Major Impact on Glioblastoma Response to Temozolomide. *Cancer Res* 75, 3127-3138.
- McHugh, C.A., Chen, C.K., Chow, A., Surka, C.F., Tran, C., McDonel, P., Pandya-Jones, A., Blanco, M., Burghard, C., Moradian, A., *et al.* (2015). The Xist lncRNA interacts directly with SHARP to silence transcription through HDAC3. *Nature* 521, 232-236.
- Mercer, T.R., Dinger, M.E., Sunken, S.M., Mehler, M.F., and Mattick, J.S. (2008). Specific expression of long noncoding RNAs in the mouse brain. *Proc Natl Acad Sci U S A* 105, 716-721.
- Michelini, F., Pitchiaya, S., Vitelli, V., Sharma, S., Gioia, U., Pessina, F., Cabrini, M., Wang, Y., Capozzo, I., Iannelli, F., *et al.* (2017). Damage-induced lncRNAs control the DNA damage response through interaction with DDRNAs at individual double-strand breaks. *Nat Cell Biol* 19, 1400-1411.
- Miotto, M., Marinari, E., and De Martino, A. (2019). Competing endogenous RNA crosstalk at system level. *PLoS Comput Biol* 15, e1007474.
- Mirza-Aghazadeh-Attari, M., Mohammadzadeh, A., Yousefi, B., Mihanfar, A., Karimian, A., and Majidinia, M. (2019). 53BP1: A key player of DNA damage response with critical functions in cancer. *DNA Repair (Amst)* 73, 110-119.
- Moen, E.L., Stark, A.L., Zhang, W., Dolan, M.E., and Godley, L.A. (2014). The role of gene body cytosine modifications in MGMT expression and sensitivity to temozolomide. *Mol Cancer Ther* 13, 1334-1344.
- Mohammad, F., Mondal, T., Guseva, N., Pandey, G.K., and Kanduri, C. (2010). Kcnq1ot1 noncoding RNA mediates transcriptional gene silencing by interacting with Dnmt1. *Development* 137, 2493-2499.

- Molinari, M. (2000). Cell cycle checkpoints and their inactivation in human cancer. *Cell Prolif* 33, 261-274.
- Motamedi, M.R., Verdel, A., Colmenares, S.U., Gerber, S.A., Gygi, S.P., and Moazed, D. (2004). Two RNAi complexes, RITS and RDRC, physically interact and localize to noncoding centromeric RNAs. *Cell* 119, 789-802.
- Munschauer, M., Nguyen, C.T., Sirokman, K., Hartigan, C.R., Hogstrom, L., Engreitz, J.M., Ulirsch, J.C., Fulco, C.P., Subramanian, V., Chen, J., *et al.* (2018). The NORAD lncRNA assembles a topoisomerase complex critical for genome stability. *Nature* 561, 132-136.
- Murat, A., Migliavacca, E., Gorlia, T., Lambiv, W.L., Shay, T., Hamou, M.F., de Tribolet, N., Regli, L., Wick, W., Kouwenhoven, M.C., *et al.* (2008). Stem cell-related "self-renewal" signature and high epidermal growth factor receptor expression associated with resistance to concomitant chemoradiotherapy in glioblastoma. *J Clin Oncol* 26, 3015-3024.
- Nakada, M., Furuta, T., Hayashi, Y., Minamoto, T., and Hamada, J. (2012). The strategy for enhancing temozolomide against malignant glioma. *Front Oncol* 2, 98.
- Newlands, E.S., Stevens, M.F., Wedge, S.R., Wheelhouse, R.T., and Brock, C. (1997). Temozolomide: a review of its discovery, chemical properties, pre-clinical development and clinical trials. *Cancer Treat Rev* 23, 35-61.
- Ng, S.Y., Bogu, G.K., Soh, B.S., and Stanton, L.W. (2013). The long noncoding RNA RMST interacts with SOX2 to regulate neurogenesis. *Mol Cell* 51, 349-359.
- Nieminuszczy, J., Schwab, R.A., and Niedzwiedz, W. (2016). The DNA fibre technique - tracking helicases at work. *Methods* 108, 92-98.
- Nishikawa, T., Ota, T., and Isogai, T. (2000). Prediction whether a human cDNA sequence contains initiation codon by combining statistical information and similarity with protein sequences. *Bioinformatics* 16, 960-967.
- O'Brien, K., Breyne, K., Ughetto, S., Laurent, L.C., and Breakefield, X.O. (2020). RNA delivery by extracellular vesicles in mammalian cells and its applications. *Nat Rev Mol Cell Biol* 21, 585-606.
- O'Connor, M.J. (2015). Targeting the DNA Damage Response in Cancer. *Mol Cell* 60, 547-560.
- Ohgaki, H., and Kleihues, P. (2005). Epidemiology and etiology of gliomas. *Acta Neuropathol* 109, 93-108.
- Olive, P.L., and Banath, J.P. (2006). The comet assay: a method to measure DNA damage in individual cells. *Nat Protoc* 1, 23-29.
- Omuro, A., Beal, K., Gutin, P., Karimi, S., Correa, D.D., Kaley, T.J., DeAngelis, L.M., Chan, T.A., Gavrilovic, I.T., Nolan, C., *et al.* (2014). Phase II study of bevacizumab, temozolomide, and hypofractionated stereotactic radiotherapy for newly diagnosed glioblastoma. *Clin Cancer Res* 20, 5023-5031.
- Ostrom, Q.T., Cioffi, G., Gittleman, H., Patil, N., Waite, K., Kruchko, C., and Barnholtz-Sloan, J.S. (2019). CBTRUS Statistical Report: Primary Brain and Other Central Nervous System Tumors Diagnosed in the United States in 2012-2016. *Neuro Oncol* 21, v1-v100.
- Ovejero, S., Bueno, A., and Sacristan, M.P. (2020). Working on Genomic Stability: From the S-Phase to Mitosis. *Genes (Basel)* 11.
- Pamudurti, N.R., Bartok, O., Jens, M., Ashwal-Fluss, R., Stottmeister, C., Ruhe, L., Hanan, M., Wyler, E., Perez-Hernandez, D., Ramberger, E., *et al.* (2017). Translation of CircRNAs. *Mol Cell* 66, 9-21 e27.
- Panda, S., Setia, M., Kaur, N., Shepal, V., Arora, V., Singh, D.K., Mondal, A., Teli, A., Tathode, M., Gajula, R., *et al.* (2018). Noncoding RNA Ginir functions as an oncogene by associating with centrosomal proteins. *PLoS Biol* 16, e2004204.
- Pandey, G.K., Mitra, S., Subhash, S., Hertwig, F., Kanduri, M., Mishra, K., Fransson, S., Ganeshram, A., Mondal, T., Bandaru, S., *et al.* (2014). The risk-associated long noncoding RNA NBAT-1 controls neuroblastoma progression by regulating cell proliferation and neuronal differentiation. *Cancer Cell* 26, 722-737.
- Piwecka, M., Glazar, P., Hernandez-Miranda, L.R., Memczak, S., Wolf, S.A., Rybak-Wolf, A., Filipchyk, A., Klironomos, F., Cerda Jara, C.A., Fenske, P., *et al.* (2017). Loss of a mammalian circular RNA locus causes miRNA deregulation and affects brain function. *Science* 357.

- Plasschaert, R.N., Vigneau, S., Tempera, I., Gupta, R., Maksimoska, J., Everett, L., Davuluri, R., Mamorstein, R., Lieberman, P.M., Schultz, D., *et al.* (2014). CTCF binding site sequence differences are associated with unique regulatory and functional trends during embryonic stem cell differentiation. *Nucleic Acids Res* *42*, 774-789.
- Pombo, A., and Dillon, N. (2015). Three-dimensional genome architecture: players and mechanisms. *Nat Rev Mol Cell Biol* *16*, 245-257.
- Postepska-Igielska, A., Giwojna, A., Gasri-Plotnitsky, L., Schmitt, N., Dold, A., Ginsberg, D., and Grummt, I. (2015). LncRNA Khps1 Regulates Expression of the Proto-oncogene SPHK1 via Triplex-Mediated Changes in Chromatin Structure. *Mol Cell* *60*, 626-636.
- Posti, J.P., Bori, M., Kauko, T., Sankinen, M., Nordberg, J., Rahi, M., Frantzen, J., Vuorinen, V., and Sipila, J.O. (2015). Presenting symptoms of glioma in adults. *Acta Neurol Scand* *131*, 88-93.
- Pramono, A.A., Rather, G.M., Herman, H., Lestari, K., and Bertino, J.R. (2020). NAD- and NADPH-Contributing Enzymes as Therapeutic Targets in Cancer: An Overview. *Biomolecules* *10*.
- Press, R.H., Shafer, S.L., Jiang, R., Buchwald, Z.S., Abugideiri, M., Tian, S., Morgan, T.M., Behera, M., Sengupta, S., Voloschin, A.D., *et al.* (2020). Optimal timing of chemoradiotherapy after surgical resection of glioblastoma: Stratification by validated prognostic classification. *Cancer* *126*, 3255-3264.
- Prolla, T.A., Baker, S.M., Harris, A.C., Tsao, J.L., Yao, X., Bronner, C.E., Zheng, B., Gordon, M., Reneker, J., Arnheim, N., *et al.* (1998). Tumour susceptibility and spontaneous mutation in mice deficient in Mlh1, Pms1 and Pms2 DNA mismatch repair. *Nat Genet* *18*, 276-279.
- Puvvula, P.K., Desetty, R.D., Pineau, P., Marchio, A., Moon, A., Dejean, A., and Bischof, O. (2014). Long noncoding RNA PANDA and scaffold-attachment-factor SAFA control senescence entry and exit. *Nat Commun* *5*, 5323.
- Qu, S., Yang, X., Li, X., Wang, J., Gao, Y., Shang, R., Sun, W., Dou, K., and Li, H. (2015). Circular RNA: A new star of noncoding RNAs. *Cancer Lett* *365*, 141-148.
- Quinn, J.A., Desjardins, A., Weingart, J., Brem, H., Dolan, M.E., Delaney, S.M., Vredenburgh, J., Rich, J., Friedman, A.H., Reardon, D.A., *et al.* (2005). Phase I trial of temozolomide plus O6-benzylguanine for patients with recurrent or progressive malignant glioma. *J Clin Oncol* *23*, 7178-7187.
- Quinn, J.A., Jiang, S.X., Reardon, D.A., Desjardins, A., Vredenburgh, J.J., Rich, J.N., Gururangan, S., Friedman, A.H., Bigner, D.D., Sampson, J.H., *et al.* (2009). Phase II trial of temozolomide plus o6-benzylguanine in adults with recurrent, temozolomide-resistant malignant glioma. *J Clin Oncol* *27*, 1262-1267.
- Quinn, J.J., and Chang, H.Y. (2016). Unique features of long non-coding RNA biogenesis and function. *Nat Rev Genet* *17*, 47-62.
- Quinn, J.J., Zhang, Q.C., Georgiev, P., Ilik, I.A., Akhtar, A., and Chang, H.Y. (2016). Rapid evolutionary turnover underlies conserved lncRNA-genome interactions. *Genes Dev* *30*, 191-207.
- Quinodoz, S.A., Ollikainen, N., Tabak, B., Palla, A., Schmidt, J.M., Detmar, E., Lai, M.M., Shishkin, A.A., Bhat, P., Takei, Y., *et al.* (2018). Higher-Order Inter-chromosomal Hubs Shape 3D Genome Organization in the Nucleus. *Cell* *174*, 744-757 e724.
- Rackham, O., Shearwood, A.M., Mercer, T.R., Davies, S.M., Mattick, J.S., and Filipovska, A. (2011). Long noncoding RNAs are generated from the mitochondrial genome and regulated by nuclear-encoded proteins. *RNA* *17*, 2085-2093.
- Rai, R., Banerjee, M., Wong, D.H., McCullagh, E., Gupta, A., Tripathi, S., Riquelme, E., Jangir, R., Yadav, S., Raja, M., *et al.* (2016). Temozolomide analogs with improved brain/plasma ratios - Exploring the possibility of enhancing the therapeutic index of temozolomide. *Bioorg Med Chem Lett* *26*, 5103-5109.
- Ramilowski, J.A., Yip, C.W., Agrawal, S., Chang, J.C., Ciani, Y., Kulakovskiy, I.V., Mendez, M., Ooi, J.L.C., Ouyang, J.F., Parkinson, N., *et al.* (2020). Functional annotation of human long noncoding RNAs via molecular phenotyping. *Genome Res* *30*, 1060-1072.
- Ransohoff, J.D., Wei, Y., and Khavari, P.A. (2018). The functions and unique features of long intergenic non-coding RNA. *Nat Rev Mol Cell Biol* *19*, 143-157.

- Ranson, M., Middleton, M.R., Bridgewater, J., Lee, S.M., Dawson, M., Jowle, D., Halbert, G., Waller, S., McGrath, H., Gumbrell, L., *et al.* (2006). Lomeguatrib, a potent inhibitor of O6-alkylguanine-DNA-alkyltransferase: phase I safety, pharmacodynamic, and pharmacokinetic trial and evaluation in combination with temozolomide in patients with advanced solid tumors. *Clin Cancer Res* 12, 1577-1584.
- Rashid, F., Shah, A., and Shan, G. (2016). Long Non-coding RNAs in the Cytoplasm. *Genomics Proteomics Bioinformatics* 14, 73-80.
- Rebucci, M., and Michiels, C. (2013). Molecular aspects of cancer cell resistance to chemotherapy. *Biochem Pharmacol* 85, 1219-1226.
- Ren, J., Ding, L., Zhang, D., Shi, G., Xu, Q., Shen, S., Wang, Y., Wang, T., and Hou, Y. (2018). Carcinoma-associated fibroblasts promote the stemness and chemoresistance of colorectal cancer by transferring exosomal lncRNA H19. *Theranostics* 8, 3932-3948.
- Reon, B.J., Anaya, J., Zhang, Y., Mandell, J., Purow, B., Abounader, R., and Dutta, A. (2016). Expression of lncRNAs in Low-Grade Gliomas and Glioblastoma Multiforme: An In Silico Analysis. *PLoS Med* 13, e1002192.
- Richardson, K.A., Vega, T.P., Richardson, F.C., Moore, C.L., Rohloff, J.C., Tomkinson, B., Bendele, R.A., and Kuchta, R.D. (2004). Polymerization of the triphosphates of AraC, 2',2'-difluorodeoxycytidine (dFdC) and OSI-7836 (T-araC) by human DNA polymerase alpha and DNA primase. *Biochem Pharmacol* 68, 2337-2346.
- Rinn, J., and Guttman, M. (2014). RNA Function. RNA and dynamic nuclear organization. *Science* 345, 1240-1241.
- Romero-Pozuelo, J., Figlia, G., Kaya, O., Martin-Villalba, A., and Teleman, A.A. (2020). Cdk4 and Cdk6 Couple the Cell-Cycle Machinery to Cell Growth via mTORC1. *Cell Rep* 31, 107504.
- Roos, W.P., Batista, L.F., Naumann, S.C., Wick, W., Weller, M., Menck, C.F., and Kaina, B. (2007). Apoptosis in malignant glioma cells triggered by the temozolomide-induced DNA lesion O6-methylguanine. *Oncogene* 26, 186-197.
- Sakakini, N., Turchi, L., Bergon, A., Holota, H., Rekima, S., Lopez, F., Paquis, P., Almairac, F., Fontaine, D., Baeza-Kallee, N., *et al.* (2016). A Positive Feed-forward Loop Associating EGR1 and PDGFA Promotes Proliferation and Self-renewal in Glioblastoma Stem Cells. *J Biol Chem* 291, 10684-10699.
- Salzman, J., Chen, R.E., Olsen, M.N., Wang, P.L., and Brown, P.O. (2013). Cell-type specific features of circular RNA expression. *PLoS Genet* 9, e1003777.
- Sanborn, J.Z., Salama, S.R., Grifford, M., Brennan, C.W., Mikkelsen, T., Jhanwar, S., Katzman, S., Chin, L., and Haussler, D. (2013). Double minute chromosomes in glioblastoma multiforme are revealed by precise reconstruction of oncogenic amplicons. *Cancer Res* 73, 6036-6045.
- Sanson, K.R., Hanna, R.E., Hegde, M., Donovan, K.F., Strand, C., Sullender, M.E., Vaimberg, E.W., Goodale, A., Root, D.E., Piccioni, F., *et al.* (2018). Optimized libraries for CRISPR-Cas9 genetic screens with multiple modalities. *Nat Commun* 9, 5416.
- Savatier, P., and Malashicheva, A. (2004). 5 - Cell-Cycle Control in Embryonic Stem Cells. In *Handbook of Stem Cells*, R. Lanza, J. Gearhart, B. Hogan, D. Melton, R. Pedersen, J. Thomson, and M. West, eds. (Burlington: Academic Press), pp. 53-62.
- Schertzer, M.D., Bracerros, K.C.A., Starmer, J., Cherney, R.E., Lee, D.M., Salazar, G., Justice, M., Bischoff, S.R., Cowley, D.O., Ariel, P., *et al.* (2019). lncRNA-Induced Spread of Polycomb Controlled by Genome Architecture, RNA Abundance, and CpG Island DNA. *Mol Cell* 75, 523-537 e510.
- Schilsky, R.L., Dolan, M.E., Bertucci, D., Ewesuedo, R.B., Vogelzang, N.J., Mani, S., Wilson, L.R., and Ratain, M.J. (2000). Phase I clinical and pharmacological study of O6-benzylguanine followed by carmustine in patients with advanced cancer. *Clin Cancer Res* 6, 3025-3031.
- Schmitt, A.M., and Chang, H.Y. (2016). Long Noncoding RNAs in Cancer Pathways. *Cancer Cell* 29, 452-463.
- Schmitt, A.M., Garcia, J.T., Hung, T., Flynn, R.A., Shen, Y., Qu, K., Payumo, A.Y., Peres-da-Silva, A., Broz, D.K., Baum, R., *et al.* (2016). An inducible long noncoding RNA amplifies DNA damage signaling. *Nat Genet* 48, 1370-1376.

- Schneider, T., and Bindereif, A. (2017). Circular RNAs: Coding or noncoding? *Cell Res* 27, 724-725.
- Schoenfelder, S., and Fraser, P. (2019). Long-range enhancer-promoter contacts in gene expression control. *Nat Rev Genet* 20, 437-455.
- Scully, R., Panday, A., Elango, R., and Willis, N.A. (2019). DNA double-strand break repair-pathway choice in somatic mammalian cells. *Nat Rev Mol Cell Biol* 20, 698-714.
- Sharma, V., Khurana, S., Kubben, N., Abdelmohsen, K., Oberdoerffer, P., Gorospe, M., and Misteli, T. (2015). A BRCA1-interacting lncRNA regulates homologous recombination. *EMBO Rep* 16, 1520-1534.
- Sherr, C.J., Beach, D., and Shapiro, G.I. (2016). Targeting CDK4 and CDK6: From Discovery to Therapy. *Cancer Discov* 6, 353-367.
- Shukla, C.J., McCorkindale, A.L., Gerhardinger, C., Korthauer, K.D., Cabili, M.N., Shechner, D.M., Irizarry, R.A., Maass, P.G., and Rinn, J.L. (2018). High-throughput identification of RNA nuclear enrichment sequences. *EMBO J* 37.
- Simko, E.A.J., Liu, H., Zhang, T., Velasquez, A., Teli, S., Haeusler, A.R., and Wang, J. (2020). G-quadruplexes offer a conserved structural motif for NONO recruitment to NEAT1 architectural lncRNA. *Nucleic Acids Res* 48, 7421-7438.
- Skourti-Stathaki, K., and Proudfoot, N.J. (2014). A double-edged sword: R loops as threats to genome integrity and powerful regulators of gene expression. *Genes Dev* 28, 1384-1396.
- Sleeth, K.M., Sorensen, C.S., Issaeva, N., Dziegielewska, J., Bartek, J., and Helleday, T. (2007). RPA mediates recombination repair during replication stress and is displaced from DNA by checkpoint signalling in human cells. *J Mol Biol* 373, 38-47.
- Soh, K.T., and Wallace, P.K. (2018). RNA Flow Cytometry Using the Branched DNA Technique. *Methods Mol Biol* 1678, 49-77.
- St Laurent, G., Shtokalo, D., Dong, B., Tackett, M.R., Fan, X., Lazorthes, S., Nicolas, E., Sang, N., Triche, T.J., McCaffrey, T.A., *et al.* (2013). lincRNAs controlled by retroviral elements are a hallmark of pluripotency and cancer. *Genome Biol* 14, R73.
- Stackhouse, C.T., Gillespie, G.Y., and Willey, C.D. (2020). Exploring the Roles of lncRNAs in GBM Pathophysiology and Their Therapeutic Potential. *Cells* 9.
- Stillman, B. (2008). DNA polymerases at the replication fork in eukaryotes. *Mol Cell* 30, 259-260.
- Stupp, R., Mason, W.P., van den Bent, M.J., Weller, M., Fisher, B., Taphoorn, M.J., Belanger, K., Brandes, A.A., Marosi, C., Bogdahn, U., *et al.* (2005). Radiotherapy plus concomitant and adjuvant temozolomide for glioblastoma. *N Engl J Med* 352, 987-996.
- Su, M., Wang, H., Wang, W., Wang, Y., Ouyang, L., Pan, C., Xia, L., Cao, D., and Liao, Q. (2018). lncRNAs in DNA damage response and repair in cancer cells. *Acta Biochim Biophys Sin (Shanghai)* 50, 433-439.
- Sulli, G., Di Micco, R., and d'Adda di Fagagna, F. (2012). Crosstalk between chromatin state and DNA damage response in cellular senescence and cancer. *Nat Rev Cancer* 12, 709-720.
- Sun, J., Jia, Z., Li, B., Zhang, A., Wang, G., Pu, P., Chen, Z., Wang, Z., and Yang, W. (2017). MiR-19 regulates the proliferation and invasion of glioma by RUNX3 via beta-catenin/Tcf-4 signaling. *Oncotarget* 8, 110785-110796.
- Szczesniak, M.W., and Makalowska, I. (2016). lncRNA-RNA Interactions across the Human Transcriptome. *PLoS One* 11, e0150353.
- Tamburri, S., Lavarone, E., Fernandez-Perez, D., Conway, E., Zanotti, M., Manganaro, D., and Pasini, D. (2020). Histone H2AK119 Mono-Ubiquitination Is Essential for Polycomb-Mediated Transcriptional Repression. *Mol Cell* 77, 840-856 e845.
- Tamimi, A.F., and Juweid, M. (2017). Epidemiology and Outcome of Glioblastoma. In *Glioblastoma*, S. De Vleeschouwer, ed. (Brisbane (AU)).
- Tanaka, H., Arakawa, H., Yamaguchi, T., Shiraishi, K., Fukuda, S., Matsui, K., Takei, Y., and Nakamura, Y. (2000). A ribonucleotide reductase gene involved in a p53-dependent cell-cycle checkpoint for DNA damage. *Nature* 404, 42-49.
- Tang, J.B., Svilar, D., Trivedi, R.N., Wang, X.H., Goellner, E.M., Moore, B., Hamilton, R.L., Banze, L.A., Brown, A.R., and Sobol, R.W. (2011). N-methylpurine DNA glycosylase and DNA

- polymerase beta modulate BER inhibitor potentiation of glioma cells to temozolomide. *Neuro Oncol* 13, 471-486.
- Tedeschi, P.M., Lin, H., Gounder, M., Kerrigan, J.E., Abali, E.E., Scotto, K., and Bertino, J.R. (2015). Suppression of Cytosolic NADPH Pool by Thionicotinamide Increases Oxidative Stress and Synergizes with Chemotherapy. *Mol Pharmacol* 88, 720-727.
- Tentori, L., Ricci-Vitiani, L., Muzi, A., Ciccarone, F., Pelacchi, F., Calabrese, R., Runci, D., Pallini, R., Caiafa, P., and Graziani, G. (2014). Pharmacological inhibition of poly(ADP-ribose) polymerase-1 modulates resistance of human glioblastoma stem cells to temozolomide. *BMC Cancer* 14, 151.
- Teschendorff, A.E., Lee, S.H., Jones, A., Fiegl, H., Kalwa, M., Wagner, W., Chindera, K., Evans, I., Dubeau, L., Orjalo, A., *et al.* (2015). HOTAIR and its surrogate DNA methylation signature indicate carboplatin resistance in ovarian cancer. *Genome Med* 7, 108.
- Tichon, A., Gil, N., Lubelsky, Y., Havkin Solomon, T., Lemze, D., Itzkovitz, S., Stern-Ginossar, N., and Ulitsky, I. (2016). A conserved abundant cytoplasmic long noncoding RNA modulates repression by Pumilio proteins in human cells. *Nat Commun* 7, 12209.
- Toledo, L.I., Altmeyer, M., Rask, M.B., Lukas, C., Larsen, D.H., Povlsen, L.K., Bekker-Jensen, S., Mailand, N., Bartek, J., and Lukas, J. (2013). ATR prohibits replication catastrophe by preventing global exhaustion of RPA. *Cell* 155, 1088-1103.
- Touat-Todeschini, L., Shichino, Y., Danguin, M., Thierry-Mieg, N., Gilquin, B., Hiriart, E., Sachidanandam, R., Lambert, E., Brettschneider, J., Reuter, M., *et al.* (2017). Selective termination of lncRNA transcription promotes heterochromatin silencing and cell differentiation. *EMBO J* 36, 2626-2641.
- Tripathi, V., Ellis, J.D., Shen, Z., Song, D.Y., Pan, Q., Watt, A.T., Freier, S.M., Bennett, C.F., Sharma, A., Bubulya, P.A., *et al.* (2010). The nuclear-retained noncoding RNA MALAT1 regulates alternative splicing by modulating SR splicing factor phosphorylation. *Mol Cell* 39, 925-938.
- Tripathi, V., Shen, Z., Chakraborty, A., Giri, S., Freier, S.M., Wu, X., Zhang, Y., Gorospe, M., Prasanth, S.G., Lal, A., *et al.* (2013). Long noncoding RNA MALAT1 controls cell cycle progression by regulating the expression of oncogenic transcription factor B-MYB. *PLoS Genet* 9, e1003368.
- Trivedi, R.N., Almeida, K.H., Fornsaglio, J.L., Schamus, S., and Sobol, R.W. (2005). The role of base excision repair in the sensitivity and resistance to temozolomide-mediated cell death. *Cancer Res* 65, 6394-6400.
- Tseng, Y.Y., Moriarity, B.S., Gong, W., Akiyama, R., Tiwari, A., Kawakami, H., Ronning, P., Reuland, B., Guenther, K., Beadnell, T.C., *et al.* (2014). PVT1 dependence in cancer with MYC copy-number increase. *Nature* 512, 82-86.
- Tubbs, A., and Nussenzweig, A. (2017). Endogenous DNA Damage as a Source of Genomic Instability in Cancer. *Cell* 168, 644-656.
- Turcan, S., Rohle, D., Goenka, A., Walsh, L.A., Fang, F., Yilmaz, E., Campos, C., Fabius, A.W., Lu, C., Ward, P.S., *et al.* (2012). IDH1 mutation is sufficient to establish the glioma hypermethylator phenotype. *Nature* 483, 479-483.
- Turner, K.M., Deshpande, V., Beyter, D., Koga, T., Rusert, J., Lee, C., Li, B., Arden, K., Ren, B., Nathanson, D.A., *et al.* (2017). Extrachromosomal oncogene amplification drives tumour evolution and genetic heterogeneity. *Nature* 543, 122-125.
- Ulitsky, I., and Bartel, D.P. (2013). lincRNAs: genomics, evolution, and mechanisms. *Cell* 154, 26-46.
- Ulitsky, I., Shkumatava, A., Jan, C.H., Sive, H., and Bartel, D.P. (2011). Conserved function of lincRNAs in vertebrate embryonic development despite rapid sequence evolution. *Cell* 147, 1537-1550.
- Urbanska, K., Sokolowska, J., Szmids, M., and Sysa, P. (2014). Glioblastoma multiforme - an overview. *Contemp Oncol (Pozn)* 18, 307-312.
- Valdiglesias, V., Giunta, S., Fenech, M., Neri, M., and Bonassi, S. (2013). gammaH2AX as a marker of DNA double strand breaks and genomic instability in human population studies. *Mutat Res* 753, 24-40.

- van Thuijl, H.F., Mazor, T., Johnson, B.E., Fouse, S.D., Aihara, K., Hong, C., Malmstrom, A., Hallbeck, M., Heimans, J.J., Kloezeman, J.J., *et al.* (2015). Evolution of DNA repair defects during malignant progression of low-grade gliomas after temozolomide treatment. *Acta Neuropathol* 129, 597-607.
- Vance, K.W., Sansom, S.N., Lee, S., Chalei, V., Kong, L., Cooper, S.E., Oliver, P.L., and Ponting, C.P. (2014). The long non-coding RNA Paupar regulates the expression of both local and distal genes. *EMBO J* 33, 296-311.
- Venter, J.C., Adams, M.D., Myers, E.W., Li, P.W., Mural, R.J., Sutton, G.G., Smith, H.O., Yandell, M., Evans, C.A., Holt, R.A., *et al.* (2001). The sequence of the human genome. *Science* 291, 1304-1351.
- Verdel, A., Jia, S., Gerber, S., Sugiyama, T., Gygi, S., Grewal, S.I., and Moazed, D. (2004). RNAi-mediated targeting of heterochromatin by the RITS complex. *Science* 303, 672-676.
- Verhaak, R.G., Hoadley, K.A., Purdom, E., Wang, V., Qi, Y., Wilkerson, M.D., Miller, C.R., Ding, L., Golub, T., Mesirov, J.P., *et al.* (2010). Integrated genomic analysis identifies clinically relevant subtypes of glioblastoma characterized by abnormalities in PDGFRA, IDH1, EGFR, and NF1. *Cancer Cell* 17, 98-110.
- Viel, T., Monfared, P., Schelhaas, S., Fricke, I.B., Kuhlmann, M.T., Fraefel, C., and Jacobs, A.H. (2013). Optimizing glioblastoma temozolomide chemotherapy employing lentiviral-based anti-MGMT shRNA technology. *Mol Ther* 21, 570-579.
- Villa, A., Snyder, E.Y., Vescovi, A., and Martinez-Serrano, A. (2000). Establishment and properties of a growth factor-dependent, perpetual neural stem cell line from the human CNS. *Exp Neurol* 161, 67-84.
- Wade, J.T., and Grainger, D.C. (2014). Pervasive transcription: illuminating the dark matter of bacterial transcriptomes. *Nat Rev Microbiol* 12, 647-653.
- Walter, J., and Newport, J. (2000). Initiation of eukaryotic DNA replication: origin unwinding and sequential chromatin association of Cdc45, RPA, and DNA polymerase alpha. *Mol Cell* 5, 617-627.
- Wang, L., Park, H.J., Dasari, S., Wang, S., Kocher, J.P., and Li, W. (2013a). CPAT: Coding-Potential Assessment Tool using an alignment-free logistic regression model. *Nucleic Acids Res* 41, e74.
- Wang, P., Ren, Z., and Sun, P. (2012). Overexpression of the long non-coding RNA MEG3 impairs in vitro glioma cell proliferation. *J Cell Biochem* 113, 1868-1874.
- Wang, P., Xue, Y., Han, Y., Lin, L., Wu, C., Xu, S., Jiang, Z., Xu, J., Liu, Q., and Cao, X. (2014a). The STAT3-binding long noncoding RNA lnc-DC controls human dendritic cell differentiation. *Science* 344, 310-313.
- Wang, P.L., Bao, Y., Yee, M.C., Barrett, S.P., Hogan, G.J., Olsen, M.N., Dinneny, J.R., Brown, P.O., and Salzman, J. (2014b). Circular RNA is expressed across the eukaryotic tree of life. *PLoS One* 9, e90859.
- Wang, S., Xia, P., Ye, B., Huang, G., Liu, J., and Fan, Z. (2013b). Transient activation of autophagy via Sox2-mediated suppression of mTOR is an important early step in reprogramming to pluripotency. *Cell Stem Cell* 13, 617-625.
- Wang, W., Han, S., Gao, W., Feng, Y., Li, K., and Wu, D. (2020). Long Noncoding RNA KCNQ1OT1 Confers Gliomas Resistance to Temozolomide and Enhances Cell Growth by Retrieving PIM1 From miR-761. *Cell Mol Neurobiol*.
- Wang, W., Zhang, A., Hao, Y., Wang, G., and Jia, Z. (2018). The emerging role of miR-19 in glioma. *J Cell Mol Med* 22, 4611-4616.
- Wang, X., Arai, S., Song, X., Reichart, D., Du, K., Pascual, G., Tempst, P., Rosenfeld, M.G., Glass, C.K., and Kurokawa, R. (2008). Induced ncRNAs allosterically modify RNA-binding proteins in cis to inhibit transcription. *Nature* 454, 126-130.
- Wang, Y., Wang, Y., Li, J., Zhang, Y., Yin, H., and Han, B. (2015). CRNDE, a long-noncoding RNA, promotes glioma cell growth and invasion through mTOR signaling. *Cancer Lett* 367, 122-128.
- Wapinski, O., and Chang, H.Y. (2011). Long noncoding RNAs and human disease. *Trends Cell Biol* 21, 354-361.

- Weller, M., van den Bent, M., Preusser, M., Le Rhun, E., Tonn, J.C., Minniti, G., Bendszus, M., Balana, C., Chinot, O., Dirven, L., *et al.* (2020). EANO guidelines on the diagnosis and treatment of diffuse gliomas of adulthood. *Nat Rev Clin Oncol*.
- White, J., and Dalton, S. (2005). Cell cycle control of embryonic stem cells. *Stem Cell Rev* 1, 131-138.
- Wick, W., Meisner, C., Hentschel, B., Platten, M., Schilling, A., Wiestler, B., Sabel, M.C., Koeppen, S., Ketter, R., Weiler, M., *et al.* (2013). Prognostic or predictive value of MGMT promoter methylation in gliomas depends on IDH1 mutation. *Neurology* 81, 1515-1522.
- Wick, W., Weller, M., van den Bent, M., Sanson, M., Weiler, M., von Deimling, A., Plass, C., Hegi, M., Platten, M., and Reifenberger, G. (2014). MGMT testing--the challenges for biomarker-based glioma treatment. *Nat Rev Neurol* 10, 372-385.
- Wu, H., Lima, W.F., Zhang, H., Fan, A., Sun, H., and Crooke, S.T. (2004). Determination of the role of the human RNase H1 in the pharmacology of DNA-like antisense drugs. *J Biol Chem* 279, 17181-17189.
- Xiang, J.F., Yin, Q.F., Chen, T., Zhang, Y., Zhang, X.O., Wu, Z., Zhang, S., Wang, H.B., Ge, J., Lu, X., *et al.* (2014). Human colorectal cancer-specific CCAT1-L lncRNA regulates long-range chromatin interactions at the MYC locus. *Cell Res* 24, 513-531.
- Xing, Y.H., Yao, R.W., Zhang, Y., Guo, C.J., Jiang, S., Xu, G., Dong, R., Yang, L., and Chen, L.L. (2017). SLERT Regulates DDX21 Rings Associated with Pol I Transcription. *Cell* 169, 664-678 e616.
- Xu, H., Guo, S., Li, W., and Yu, P. (2015). The circular RNA Cdr1as, via miR-7 and its targets, regulates insulin transcription and secretion in islet cells. *Sci Rep* 5, 12453.
- Xu, W., Yang, H., Liu, Y., Yang, Y., Wang, P., Kim, S.H., Ito, S., Yang, C., Wang, P., Xiao, M.T., *et al.* (2011). Oncometabolite 2-hydroxyglutarate is a competitive inhibitor of alpha-ketoglutarate-dependent dioxygenases. *Cancer Cell* 19, 17-30.
- Yamaguchi, T., Matsuda, K., Sagiya, Y., Iwadate, M., Fujino, M.A., Nakamura, Y., and Arakawa, H. (2001). p53R2-dependent pathway for DNA synthesis in a p53-regulated cell cycle checkpoint. *Cancer Res* 61, 8256-8262.
- Yan, W., Zhang, W., You, G., Zhang, J., Han, L., Bao, Z., Wang, Y., Liu, Y., Jiang, C., Kang, C., *et al.* (2012). Molecular classification of gliomas based on whole genome gene expression: a systematic report of 225 samples from the Chinese Glioma Cooperative Group. *Neuro Oncol* 14, 1432-1440.
- Yan, Y., Xu, Z., Chen, X., Wang, X., Zeng, S., Zhao, Z., Qian, L., Li, Z., Wei, J., Huo, L., *et al.* (2019). Novel Function of lncRNA ADAMTS9-AS2 in Promoting Temozolomide Resistance in Glioblastoma via Upregulating the FUS/MDM2 Ubiquitination Axis. *Front Cell Dev Biol* 7, 217.
- Yang, J.-H., Li, J.-H., Jiang, S., Zhou, H., and Qu, L.-H. (2013). ChIPBase: a database for decoding the transcriptional regulation of long non-coding RNA and microRNA genes from ChIP-Seq data. *Nucleic acids research* 41, D177-187.
- Yang, S.Y., Lejault, P., Chevrier, S., Boidot, R., Robertson, A.G., Wong, J.M.Y., and Monchaud, D. (2018). Transcriptome-wide identification of transient RNA G-quadruplexes in human cells. *Nat Commun* 9, 4730.
- Yang, Y.G., and Qi, Y. (2015). RNA-directed repair of DNA double-strand breaks. *DNA Repair (Amst)* 32, 82-85.
- Yao, R.W., Wang, Y., and Chen, L.L. (2019). Cellular functions of long noncoding RNAs. *Nat Cell Biol* 21, 542-551.
- Yari, H., Jin, L., Teng, L., Wang, Y., Wu, Y., Liu, G.Z., Gao, W., Liang, J., Xi, Y., Feng, Y.C., *et al.* (2019). lncRNA REG1CP promotes tumorigenesis through an enhancer complex to recruit FANCD1 helicase for REG3A transcription. *Nat Commun* 10, 5334.
- Yi, G.Z., Huang, G., Guo, M., Zhang, X., Wang, H., Deng, S., Li, Y., Xiang, W., Chen, Z., Pan, J., *et al.* (2019). Acquired temozolomide resistance in MGMT-deficient glioblastoma cells is associated with regulation of DNA repair by DHC2. *Brain* 142, 2352-2366.
- Yildirim, O., Izgu, E.C., Damle, M., Chalei, V., Ji, F., Sadreyev, R.I., Szostak, J.W., and Kingston, R.E. (2020). S-phase Enriched Non-coding RNAs Regulate Gene Expression and Cell Cycle Progression. *Cell Rep* 31, 107629.

- Yoon, J.H., Abdelmohsen, K., Srikantan, S., Yang, X., Martindale, J.L., De, S., Huarte, M., Zhan, M., Becker, K.G., and Gorospe, M. (2012). LincRNA-p21 suppresses target mRNA translation. *Mol Cell* 47, 648-655.
- Yoshimoto, K., Mizoguchi, M., Hata, N., Murata, H., Hatae, R., Amano, T., Nakamizo, A., and Sasaki, T. (2012). Complex DNA repair pathways as possible therapeutic targets to overcome temozolomide resistance in glioblastoma. *Front Oncol* 2, 186.
- Yu, C.Y., and Kuo, H.C. (2019). The emerging roles and functions of circular RNAs and their generation. *J Biomed Sci* 26, 29.
- Zampetaki, A., Albrecht, A., and Steinhofel, K. (2018). Long Non-coding RNA Structure and Function: Is There a Link? *Front Physiol* 9, 1201.
- Zeman, M.K., and Cimprich, K.A. (2014). Causes and consequences of replication stress. *Nat Cell Biol* 16, 2-9.
- Zeng, Y., and Cullen, B.R. (2002). RNA interference in human cells is restricted to the cytoplasm. *RNA* 8, 855-860.
- Zhang, B., Gunawardane, L., Niazi, F., Jahanbani, F., Chen, X., and Valadkhan, S. (2014). A novel RNA motif mediates the strict nuclear localization of a long noncoding RNA. *Mol Cell Biol* 34, 2318-2329.
- Zhang, H., Qin, D., Jiang, Z., and Zhang, J. (2019a). SNHG9/miR-199a-5p/Wnt2 Axis Regulates Cell Growth and Aerobic Glycolysis in Glioblastoma. *J Neuropathol Exp Neurol* 78, 939-948.
- Zhang, J., Baran, J., Cros, A., Guberman, J.M., Haider, S., Hsu, J., Liang, Y., Rivkin, E., Wang, J., Whitty, B., *et al.* (2011). International Cancer Genome Consortium Data Portal--a one-stop shop for cancer genomics data. *Database (Oxford)* 2011, bar026.
- Zhang, J., Stevens, M.F., and Bradshaw, T.D. (2012a). Temozolomide: mechanisms of action, repair and resistance. *Curr Mol Pharmacol* 5, 102-114.
- Zhang, J.X., Han, L., Bao, Z.S., Wang, Y.Y., Chen, L.Y., Yan, W., Yu, S.Z., Pu, P.Y., Liu, N., You, Y.P., *et al.* (2013). HOTAIR, a cell cycle-associated long noncoding RNA and a strong predictor of survival, is preferentially expressed in classical and mesenchymal glioma. *Neuro Oncol* 15, 1595-1603.
- Zhang, M., Zhao, K., Xu, X., Yang, Y., Yan, S., Wei, P., Liu, H., Xu, J., Xiao, F., Zhou, H., *et al.* (2018). A peptide encoded by circular form of LINC-PINT suppresses oncogenic transcriptional elongation in glioblastoma. *Nat Commun* 9, 4475.
- Zhang, P., Dong, Q., Zhu, H., Li, S., Shi, L., and Chen, X. (2019b). Long non-coding antisense RNA GAS6-AS1 supports gastric cancer progression via increasing GAS6 expression. *Gene* 696, 1-9.
- Zhang, S., and Guo, W. (2019). Long noncoding RNA MEG3 suppresses the growth of glioma cells by regulating the miR965p/MTSS1 signaling pathway. *Mol Med Rep* 20, 4215-4225.
- Zhang, X., Kiang, K.M., Zhang, G.P., and Leung, G.K. (2015a). Long Non-Coding RNAs Dysregulation and Function in Glioblastoma Stem Cells. *Noncoding RNA* 1, 69-86.
- Zhang, X., Sun, S., Pu, J.K., Tsang, A.C., Lee, D., Man, V.O., Lui, W.M., Wong, S.T., and Leung, G.K. (2012b). Long non-coding RNA expression profiles predict clinical phenotypes in glioma. *Neurobiol Dis* 48, 1-8.
- Zhang, X.W., Bu, P., Liu, L., Zhang, X.Z., and Li, J. (2015b). Overexpression of long non-coding RNA PVT1 in gastric cancer cells promotes the development of multidrug resistance. *Biochem Biophys Res Commun* 462, 227-232.
- Zhao, J., Sun, B.K., Erwin, J.A., Song, J.J., and Lee, J.T. (2008). Polycomb proteins targeted by a short repeat RNA to the mouse X chromosome. *Science* 322, 750-756.
- Zhou, Y., Zhang, X., and Klibanski, A. (2012). MEG3 noncoding RNA: a tumor suppressor. *J Mol Endocrinol* 48, R45-53.
- Zhu, H.R., Yu, X.N., Zhang, G.C., Shi, X., Bilegsaikhan, E., Guo, H.Y., Liu, L.L., Cai, Y., Song, G.Q., Liu, T.T., *et al.* (2019). Comprehensive analysis of long noncoding RNAmessenger RNAmicroRNA coexpression network identifies cell cyclereLATED lncRNA in hepatocellular carcinoma. *Int J Mol Med* 44, 1844-1854.

Zhu, J., Liu, S., Ye, F., Shen, Y., Tie, Y., Zhu, J., Wei, L., Jin, Y., Fu, H., Wu, Y., *et al.* (2015). Long Noncoding RNA MEG3 Interacts with p53 Protein and Regulates Partial p53 Target Genes in Hepatoma Cells. *PLoS One* 10, e0139790.

CHAPTER 8

APPENDICES

Appendix 1: 5'-RADAR-RACE-PCR-Sequence

GCCCGGCTTTCCACTGAGGGACGCCCCCTGCTCTGGACTGCTTAGCCTACTCCAGCTG
GCCCCACCTCACCTCATCGGCCCGCCTCCTCCGCTCGCCCACTCCGGGCGCCCACT
CCTGAGGAGCTATCCCAGAGTCCGCGCGGCCTCGCCTTCCCGGCCCGCTCACCACCC
CGCCTCGTCCCACCTCGCCTCGCCCTCCCCGGGCTCTAGCCACTTGGTGCGGCAGGT
GTCCTGCAGGCCGGCTCGAGATTCCCGAGCTCGCCCTCGTGGTGTTCAGGAACACGA
GTCTCGCTCGGGCACCAGGCTGGAGTGCAGTGGCACGGTCTCGGCTTACTACAACCTC
CGCCTTCCGGATTCAAGTGATTCTGCTGCCTCAGCCTCCCGAATAGCTGGGATTACAGT
GTTTCAGAATCACCTGGGATGATCTGCATGAAGATTCTGGCCTCCACCAAAGACTTAC
TGAATCAGAAAGGAGGCAAGAGGATGAGGAATGCTTAAGAATCTGCATTAACAACTTT
ACAAATGAATCTTACAACATACAGAAGCATGGAACTACTGCCTCAAGGGATTATCTCAA
CTTGAGTTTAAACATAGGAATTGCTGACTACCTTTAAAATGTAAAATAGTATCTTTATGG
GAGGGATGTTGTTTGGGGGCAGCTACTAAATAGTAAATCATTCTTTAAAATACCCTCT
CAAGTCTGCCCCAGTTATCCATTTTACTGGATAGTCTTGGTATCCAGATGATTTAGGGAA
AAAAATAGTAGTAACTCTGAAAACACTCAGTAAAGTTCATTCTTGGTCTTCTCTTCC
TAAATTTGTTTTCAATTGTTAGATTTAAACACTAAACAAGACCAAAGAGAACTTTATTTTA
CATGTCTTTATTTTACATTTAGAACCGTTTTATGATTTACTTAAAAAAAAAATCTTTTACTA
TTATTAGAAGTATTTTTTAACCAAATCTTGATTTAGGAAGACTTAAGACATTGTGCATTA
TTTTAAATATTTTCATTTAGTAATTTAAAATAAATTCACAATTAGGGTTTCAAATGTC
CTAATCATATCTAGTTTGTCTCATTTAATATTTTATCAATCCCATCATGTGCATACAGAG
GTTAAGGTGATGTATAAATTTATATCTTTCAAACACATTGATGCTAATCAGCTCTTGATC
TAATTACTATTTTATTTATTCAGAAATAGCATTAGACATAAAAACCAATGTCTCACTTTGT
AAAATAACCTTTGGCTAATTTACACACATCTAATACAGCGTGTTATATAAGTTTTAAGTAA
TACAATGAGTCACTACTATCATTAGTTTTAAATATTTTATGTTAACAGGGCTGAGAAT
ATCATGTGGTTCAGTCTTCTGAAGGAAGTTATATAATAAAAGCATAGTGCCTTTGAACAT
GAAGACTATCCTCAAGGCCAGAAATCCTACAAAGGAACTGAAAGGAGAGATTCCAGAGA
ATTGCTCTCCTCATTTTTAATATGTAAAGTGACTGTTTTAAGTCACTTCATTGAAGACTTA
AGGAAGAAAACAGTGTTATTATGCCACTGAATAAAGCTACTTAAACCAGAGTAATTTTGG
GATATTAATCCTAGGCTACATAATTAATAGGTCATCAAAACAAAACCTGTCAGTTATTAG
GTGTAAGTTAACTTCTATGCCAAGTAAGGGGTCACACTTCACTTCCCCCATTTGTAAAA
TGAAAAGGTGGCCAGGCCAGTGCCATTTAGGATTCTCTGCTAACTGTAAAATGTGGACT
GATTTTCTTCTGTTTCTTATAGTCCAGGTGTATATAAACTTCCAGTTCTTTAAGTCAAAT
TTTATGCACATAACCATGTCAGTGTATTGCCCTTAGTTTTAAAATGTACAACACTACATAAT
AAAACTATTGTTTCTTC

Appendix 2: G-quadruplex structures present in the 5'-RADAR-RACE-PCR-Sequence

(GCCCCGGCTTTCCACTGAGGGACGCCCCCTGCTCTGGACTGCTTAGCCTACTCCAGCT
 GGCCCCACCTCACCTCATCGGCCCGCCTCCTCCGCTCGCCCACTCCGGGCGCCAC
 TCCTGAGGAGCTATCCAGAGTCCGCGCGGCCTCGCCTTCCGGCCCGCTCACCACC
 CCGCCTCGTCCCACCTCGCCTCGCCCTCCCCGGGCTCTAGCCACTT**GGTGCGGCAGG**
TGTCCTGCAGGCCGGCTCGAGATTCCCGAGCTCGCCCTCGTGGTGTTCAGGAACAC
 GAGTCTCGCTCGGGCACCAGGCT**GGAGTGCAGTGGCACGGTCTCGG**CTTACTACAAC
 CTCCGCCTTCCGATTCAAGTATTCTGCTGCCTCAGCCTCCGAATAGCTGGGATTA
CAG)TGTTTCAGAATCACCTGGGATGATCTGCATGAAGATTCTGGCCTCCACCAAAG
 ACTTACTGAATCAGAAA**GGAGGCAAGAGGATGAGG**AATGCTTAAGAATCTGCATTAA
 CAACTTTACAAATGAATCTTACAACATACAGAAGCATGGAACTACTGCCTCAAGGGA
 TTATCTCAACTTGAGTTTAAACATAGGAATTGCTGACTACCTTTAAAATGTAAAAATAGTA
 TCTTTAT**GGGAGGGATGTTGTTTGGGGG**CAGCTACTAAATAGTGAATCATTCTTTAA
 AATACCCTCTCAAGTCTGCCCCAGTTATCCATTTTACTGGATAGTCTTGGTATCCAGAT
 GATTTAGGGAAAAAATAGTAGTAC(AACTCTGAAAACACTCAGTAAAGTTCATTCT
 TGGTCTTCTCTTCTAAATTTGTTTTCAATTGTTAGATTTAAACACTAAACAAGACCAA
 AGAGAACTTTATTTTACATGTCTTTATTTTACATTTAGAACCGTTTTATGATTTACTTAAAA
 AAAAAATCTTTTACTATTATTAGAAGTATTTTTTAAACCAAATCTTGATTTAGGAAGACT
 TAAGACATTGTGCATTATTTTAAATATTTTCATTTAGTAACTATTTAAAAATAAATTCAC
 AATTAGGGTTTCAAATGTCTAATCATATCTAGTTTGTTCATTTAATATTTTATCAAT
 CCCATCATGTGCATACAGAGGTTAAGGTGATGTATAAATTTTATATCTTTCAAACACAT
 TGATGCTAATCAGCTCTTGATCTAATTAATTTTATTTTATTCAGAAATAGCATTTAGAC
 ATAAAAACCAATGTCTCACTTTGTAAAATAACCTTTGGCTAATTTACACACATCTAATA
 CAGCGTGTATATAAGTTTTAAGTAATACAATGAGTCACTACTATCATTAGTTTTAAAT
 ATTTTTAGTGTTAACAGGGCTGAGAATATCATGTGGTTCAGTCTTCTGAAGGAAGTTAT
 ATAATAAAGCATAGTGCCTTTGAACATGAAGACTATCCTCAAGGCCAGAAATCCTAC
 AAAGGAACTGAAAGGAGAGATTCCAGAGAATTGCTCTCCTCATTTTTAATATGTAAG
 TGACTGTTTTAAGTCACTTCATTGAAGACTTAAGGAAGAAAACAGTGTTATTATGCCAC
 TGAATAAAGCTACTTAAACCAGAGTAATTTTGGGATATTAATCCTAGGCTACATAATTA
 ATAGGTCATCAAAACAAAACCTGTCAGTTATTAGGTGTAAGTTAACTTCCTATGCCAA
 GTAAGGGGTCACACTTCACTTCCCCCATTGTAAAATGAAAA**GGTGGCCAGGCCAGTGCC**
CATTTAGGATTCTCTGCTAACTGTAAAATGTGGACTGATTTTCTTCTGTTTCTTATAGTCC
 AGGTGTATATAAACTTCCAGTCTTTAAGTCAAATTTTTATGCACATAACCATGTCAG
 TGTATTGCCCTTAGTTTAAAAATGTACAACACTACATAAATAAAAATATTGTTTCTTC)

NNNNN 1st exon

NNNNN 2nd exon

NNNNN 3rd exon

NNNNN QGRS

ID	Position	Length	QGRS	G-Score
1	218	22	<u>GGTGCGGCAGGTGTCCTGCAGG</u>	14
2	309	23	<u>GGAGTGCAGTGGCACGGTCTCGG</u>	16
3	475	18	<u>GGAGGCAAGAGGATGAGG</u>	17
4	642	21	<u>GGGAGGGATGTTGTTTGGGGG</u>	13
5	1745	25	<u>GGTGGCCAGGCCAGTGCCATTTAGG</u>	9

RADAR*1: (1st and 2nd)exon deletion (QGRS= 1+2)

RADAR*2: (3rd) exon partial deletion (QGRS= 5)

Appendix 3: CircRNA sequence

AACCCTAAACATAGATTTTCAATAAGAGTTTAAGGTTACAAACTAAAGCTGTTGACAGG
AAATTTTGAGGTCTTTATAGAAGGAGATTTTCTTTTTCTAAGATTGAGTCACTAGCAAAT
TTTTCTTTCAGTAGAAGGCAGAACTCATGAGATTTAAGTTGGCTGACTGGACTGAGGAA
ATACTGGTTTAAAAACGGCAGAATTGGGAGGCCAAGACAGGCGGATCATGAGGTCAGG
AAATCGAGATCATCCAGGCTAACATGGTGAACCCTGTCTCTACTAAAAATACAAAAAAT
TAGCCAGGCGTGGTGGCAGGCACCTGTAGTCAGCCTCCTGAGTAGCTGAGCCTACA
GGCACACACCACCATGTCCAGCTAATTTTTGTATTTTTGTAGAGATGGAGTTTCACCATG
TTGGCCATGCTGGTCTCAAATTCTTGACCTCAAGTGATCCGCCTGCCCTGGCCTCCCAA
AGTGCTGGGATTACAGGCGTGAGACACGGCGCCAGTTGACTGTTTTGTTTTCACTCAC
TCCTCCATATGGGTAGTTGAGGATCACTATGACTGTTTTATGTAGGCAGAATTTTAAAG
AAAACAACATAAATTTAGATATTTGTTCCGTAAGTTACTAAAAAGTAAATATATTAAGG
TGATTGTCACATAAGCCTTCCAATCACAGTGCCTGTGATTTTCATTAGACAAAAGTGAACA
TATAAAATGTAGTTGGCTACCTGGGAGCCTGAAGCACTTTATTTACAGATACTTTCTTA
GGGCTAACTCAAACACATCTAATCAGAACCATGCCATAAGCTTGCCAGAA

TC Back-spliced exonic junction

Appendix 4: Nucleotide sequence of RADAR*1 (1st and 2nd exons deletion)

TGTTTCAGAATCACCTGGGATGATCTGCATGAAGATTCCTGGCCTCCACCAAAGACTTA
CTGAATCAGAAAGGAGGCAAGAGGATGAGGAATGCTTAAGAATCTGCATTAACAACTT
TACAAATGAATCTTACAACATACAGAAGCATGGAACTACTGCCTCAAGGGATTATCTCA
ACTTGAGTTTAAACATAGGAATTGCTGACTACCTTTAAAATGTAAAAATAGTATCTTTATG
GGAGGGATGTTGTTTGGGGGCAGCTACTAAATAGTGAAATCATTCCCTTTAAAATACCCTC
TCAAGTCTGCCCCAGTTATCCATTTTACTGGATAGTCTTGGTATCCAGATGATTTAGGGA
AAAAAATAGTAGTAGCAAACCTCTGAAAACACTCAGTAAAGTTCATTCTTGGTCTTCTCTTC
CTAAATTTGTTTTCAATTGTTAGATTTAAACACTAAACAAGACCAAAAAGAGAACTTTATTTT
ACATGTCTTTATTTTACATTTAGAACCGTTTTATGATTTACTTAAAAAAAAAATCTTTTACT
ATTATTAGAAGTATTTTTTAAACCAAATCTTGATTTAGGAAGACTTAAGACATTGTGCATT
ATTTTAAATATTTTCATTTAGTAATTTAAAATAAATTCACAATTAGGGTTTTCAAATGT
CCTAATCATATCTAGTTTGTCTCATTAAATATTTTATCAATCCCATCATGTGCATACAGA
GGTTAAGGTGATGTATAAATTTTATATCTTTCAAACACATTGATGCTAATCAGCTCTTGAT
CTAATTACTATTTTCAATTTATCAGAAATAGCATTTAGACATAAAAACCAATGTCTCACTTTG
TAAAATAACCTTTGGCTAATTTACACACATCTAATACAGCGTGTTATATAAGTTTTAAGTA
ATACAATGAGTCACTACTATCATTTCAGTTTTTAAATATTTTTAGTGTTAACAGGGCTGAGAA
TATCATGTGGTTCAGTCTTCTGAAGGAAGTTATATAATAAAGCATAGTGCCTTTGAACA
TGAAGACTATCCTCAAGGCCAGAAATCCTACAAAGGAACTGAAAGGAGAGATTCCAGAG
AATTGCTCTCCTCATTTTTAATATGTAAAGTGACTGTTTTAAGTCACTTCATTGAAGACTT
AAGGAAGAAAACAGTGTTATTATGCCACTGAATAAAGCTACTTAAACCAGAGTAATTTTG
GGATATTAATCCTAGGCTACATAATTAATAGGTCATCAAAACAAAACCTGTGAGTTATTA
GGTGTAAAGTTAACTTCCTATGCCAAGTAAGGGGTCACACTTCACTTCCCCCATTTGTAAA
ATGAAAAGGTGGCCAGGCCAGTGCCATTTAGGATTCTCTGCTAACTGTAAAATGTGGAC
TGATTTTCTTCTGTTTCTTATAGTCCAGGTGTATATAAACTTCCAGTTCTTTAAGTCAAAT
TTTTATGCACATAACCATGTCAGTGTATTGCCCTTAGTTTTAAAATGTACAACACTACATAAA
TAAAACTATTGTTTCTTC

Appendix 5: Nucleotide sequence of RADAR*2 (3' partial deletion from 3rd exon)

CGCCCGGCTTTCCACTGAGGGACGCCCCCTGCTCTGGACTGCTTAGCCTACTCCAGCT
GGCCCCACCTCACCTCATCGGCCCGCCTCCTCCGCTCGCCCACTCCGGGCGCCAC
TCCTGAGGAGCTATCCCAGAGTCCGCGCGGCCTCGCCTTCCCGGCCCGCTCACACC
CCGCCTCGTCCCACCTCGCCTCGCCCTCCCCGGGCTCTAGCCACTTGGTGCGGCAGG
TGCCTGCAGGCCGGCTCGAGATTCCCGAGCTCGCCCTCGTGGTGTTCAGGAACACG
AGTCTCGCTCGGGCACCAGGCTGGAGTGCAGTGGCACGGTCTCGGCTTACTACAACCT
CCGCCTTCCGGATTCAAGTGATTCTGCTGCCTCAGCCTCCCGAATAGCTGGGATTACAG
TGTTTCAGAATCACCTGGGATGATCTGCATGAAGATTCCTGGCCTCCACCAAAGACTTA
CTGAATCAGAAAGGAGGCAAGAGGATGAGGAATGCTTAAGAATCTGCATTAACAACTT
TACAAATGAATCTTACAACATACAGAAGCATGGAACTACTGCCTCAAGGGATTATCTCA
ACTTGAGTTTAAACATAGGAATTGCTGACTACCTTTAAAATGTAAAAATAGTATCTTTATG
GGAGGGATGTTGTTTGGGGGCAGCTACTAAATAGTGAAATCATTCTTTAAATACCCTC
TCAAGTCTGCCCCAGTTATCCATTTTACTGGATAGTCTTGGTATCCAGATGATTTAGGGA
AAAAAATAGTAGTAGCA

END OF THESIS
